


UNIVERSITA' DEGLI STUDI DI MESSINA

DIPARTIMENTO DI SCIENZE CHIMICHE, BIOLOGICHE, FARMACEUTICHE E AMBIENTALI

PhD Thesis in Applied Biology and Experimental Medicine

XXXVII cycle

Vincenza Casella

Revealing the Biosynthetic Potential of Marine Microorganisms: Production of Novel Biosurfactants, Siderophores and Antimicrobials for Biotechnological Applications

Tutor
Prof. Nunziacarla Spanò

Co-tutor
Dr. Donatella de Pascale
Dr. Fortunato Palma Esposito

PhD Coordinator
Prof. Emanuela Esposito

PhD Candidate
Vincenza Casella
ID: 537903

Academic Year 2023-2024

CONTENTS

Abstract

Blue Biotechnology focuses on the use of marine microorganisms and their secondary metabolites to address global challenges such as antibiotic resistance, climate change and environmental sustainability. Natural products are attracting increasing interest for their unique properties and therapeutic potential, with applications ranging from medicine to environmental protection. In particular, marine extremophilic bacteria represent an under-explored source for the discovery of novel bioactive metabolites due to their ability to thrive in extreme environmental conditions such as high salinity, elevated pressure, extreme temperatures, high UV irradiation, and low-nutrient environments. Their metabolic diversity is driven by biosynthetic gene clusters (BGCs) that regulate compound production. Among relevant bio-based products, biosurfactants represent a viable alternative to synthetic surfactants, as they are secreted molecules that reduce interfacial liquid tension, endowed with multiple bioactivities and a high level of biodegradability. Siderophores, iron-chelating agents, support microbial survival and hold significant potential in bioremediation and developing strategies to combat antimicrobial resistance (AMR). Furthermore, antimicrobial compounds derived from marine extremophiles are increasingly recognized for their ability to treat infections caused by multidrug-resistant pathogens. This PhD research contributes to exploring the biosynthetic potential of marine extremophilic bacteria (deep-sea, halophilic and tropical bacteria) by combining functional screening, genome analysis and chemical characterization of relevant metabolites. In particular, in three main chapters, this PhD project I) reveals the NRPS biosynthesis of novel nobilamide molecules along with known surfactins produced by a deep-sea *Bacillus* sp. BCP32, with antimicrobial activity against MDR bacteria, II) identifies new aquachelin siderophores and their previously unknown biosynthetic gene cluster (BGC) from a marine *Halomonas* and III) describes the isolation and

characterization of two novel coral-associated microorganisms (CAMs) displaying potent antimicrobial, antioxidant and UV protectant properties.

Introduction

1.1 Marine Habitat and Extreme Environments

The oceans and seas form a single global ocean, interconnected by a complex system of currents, covering 70% of the Earth's surface and representing over 95% of the biosphere's volume. The immense depth of the oceans, more than 11,000 meters, hosts a remarkable biodiversity, with species distributed differently in the water column, based on factors such as depth, salinity, and light availability [1,2]. The marine environment is a highly complex ecosystem; therefore, it is crucial to recognize that life thrives in all areas, from the surface to the deepest regions. Marine biodiversity is the richest on Earth and remains largely unexplored, as evidenced by the frequent discoveries of new marine species compared to terrestrial ones [3,4]. Over the past decade, there has been growing interest in studying extreme environments to isolate novel extremophilic microorganisms and analyze their metabolites which have significant potential for advancing bio-based economies [5–7].

The definition of an extreme ecosystem is complex and depends on chemical, biological, and physical characteristics that push the limits of life. An environment can be considered extreme due to particularly harsh conditions, such as extreme temperatures, unusual pH, high pressure, high salinity, lack of oxygen, or absence of light [6,8]. Moreover, ocean temperatures have risen significantly in recent years, including in the deep seafloor. This warming may alter the flow of carbon from the surface to deep-sea ecosystems, affecting microbial biodiversity, which may develop adaptive strategies in response to changes in ocean productivity [9–11].

The deep sea, which includes waters and depths below 200 meters, is one of the most extreme, remote, and unexplored biomes in the biosphere, comprising more than two-thirds of the ocean volume [11,12]. These extreme environments are characterized by the absence of light, an average depth of around 4200 meters,

temperatures below 4 °C, and a hydrostatic pressure of around 40 MPa [13]. These conditions pose one of the greatest challenges to the survival of life. However, over the past decades, exploration of the depths has led to discovering peculiar and highly diverse habitats, including hydrothermal springs, cold seeps, mud volcanoes, and anoxic hypersaline basins [11,14]. These ecosystems further push the limits of life, revealing the incredible adaptive capacity of extremophile organisms. An emblematic example of the complexity of the deep are the oceanic trenches, deep depressions formed by the subduction of tectonic plates. These environments reach depths of over 10,000 meters, where pressure exceeds 1,100 bar and temperatures are close to freezing. Despite these conditions, the sediments that accumulate in these areas are home to metabolically active microbial communities. These microorganisms survive and play a crucial role in nutrient recycling, contributing to the global carbon and nitrogen cycles [11,15]. Another characteristic of a deep-sea environment is hydrothermal vents, located along ocean ridges where magma rises through the Earth's crust. Here, seawater is heated to 400°C and enriched with heavy metals and gases such as hydrogen sulphide. This extreme environment is the cradle of unique ecosystems supported by chemoautotrophic bacteria, which can use chemical energy to produce organic matter. Such microorganisms form the basis of complex food webs that include specialized organisms, demonstrating that life can evolve independently of sunlight [16]. Hypersaline anoxic basins (DHABs), discovered in the depths of the Mediterranean and Red Seas, are another example of extreme adaptations. These basins, characterized by up to 30% higher salinity than seawater and a complete lack of oxygen, are home to unique microbial communities [17]. Bacteria living in these environments have developed strategies to withstand high pressure and hypersalinity and have shown exceptional metabolic versatility and adaptability [14].

In polar environments life challenges equally harsh conditions. The Arctic and Antarctic represent 14% of the total biosphere and must endure several stresses, including dehydration, osmotic stress, low biochemical activity, limited nutrients, harmful UVB radiation, and extreme light. Antarctica, separated from the other continents by the Southern Ocean, Antarctica is almost 98% covered by the Antarctic ice sheet, an area of 14 million square kilometers, with winter temperatures can drop to -80°C [18]. Despite the scarcity of resources and harsh climatic conditions, the region hosts a wide variety of extremophiles. Prokaryotes are the main component of biomass and play a key role in biogeochemical cycles and the mineralization of pollutants [19]. However, Antarctica is threatened by the introduction of contaminants such as heavy metals, antibiotics and pesticides, which are carried by atmospheric currents and human activities, and which threaten its purity and ecological balance. Also, the Arctic has a similarly extreme environment, with temperatures ranging from -80°C to 15°C and high osmotic pressure. Here, a frozen sea and permafrost make survival even more difficult [20].

However, the effects of climate change could drastically alter these ecosystems. Rising temperatures, decreasing dissolved oxygen and ocean acidification predicted for the coming decades threaten to upset the delicate ecological equilibrium of the deep sea, negatively affecting the growth and survival of organisms adapted to extreme conditions [13]. Habitats that are sensitive to climate change are transitional environments, such as coral reefs, which are rich and complex marine ecosystems where the warm, nutrient-rich waters of the coastal zone meet the deeper marine environment [21]. Coral reefs are essential to marine biodiversity, providing shelter, food and habitat for many species. However, their ability to maintain this ecological balance depends on the health of the corals, which are extremely sensitive to environmental changes [22]. The warmer waters and acidification can alter the symbiotic balance between corals

and their photosynthetic endosymbionts, the *Symbiodinium* dinoflagellates, which are vital to their survival. In addition, coral reefs are threatened by disease, pollution and other local pressures that further reduce their resilience. Recent studies have highlighted the importance of the coral microbiome, composed of bacteria, protists and other microorganisms, the balance of which could significantly influence the health and adaptability of coral reefs to increasingly harsh environmental conditions [23,24].

1.2 Exthremophilic Bacteria (Thermophiles, Psychrophiles, Halophiles)

"Extremophiles" can be defined as organisms that thrive under conditions very different from those found in standard habitats. These organisms are also categorized as extremotolerant, capable of surviving in such environments, from the poles to the ocean depths, even to the stratosphere [3,25]. While eukaryotes struggle to survive in such harsh gradients, prokaryotes, including Bacteria and Archaea, have evolved remarkable metabolic processes that enable them to endure and thrive in extreme environments [6,26]. Consequently, these extremophiles possess unique capabilities, including the production of secondary metabolites with properties that are hugely different from their terrestrial counterparts [25,27]. Temperature and pressure are key factors modulating bacterial physiology, changing the conformation of macromolecules and affecting the efficiency of metabolic reactions. To maintain internal stability in the face of extreme conditions, these organisms rely on homeostasis, a process that enables them to regulate their internal environments despite external stressors [3,28]. They are grouped into categories according to the specific environmental conditions they can endure, like thermophiles (high temperatures), psychrophiles (low temperatures), halophiles (high salt concentrations), acidophiles, and alkalophiles (acidic or alkaline pH levels), anaerobes (anaerobic conditions), piezophiles (high pressures),

polyextremophiles (UV radiation, and combinations of these conditions) [4]. During the last millennium, numerous studies have highlighted the biotechnological importance of marine extremophiles, a still under-explored source of secondary metabolites [5,29–32]. Their rich genetic diversity allows the production of stable and efficient enzymes, lipids and biomolecules with significant potential for commercial applications in both the pharmaceutical and industrial fields, opening up new perspectives for biotechnological innovation [33,34]. In fact, polyextremophiles demonstrate exceptional biochemical adaptability, making them key players in advancing biotechnology and promoting environmental sustainability.

Thermophiles

Thermophiles are heat-loving microorganisms that thrive at mesophilic temperatures, typically above 45°C. In pure culture, the highest known temperature limit for life is 122 °C, from the genus *Pyrococcus* used in research to understand extremophilic life and enzyme stability [28,35,36]. Found in environments such as deep-sea hydrothermal vents, volcanic hot springs, and compost, thermophiles are adapted to extreme heat, due to a range of specialized adaptations. The cell membranes of thermophilic bacteria have specialized lipids, like saturated fatty acids and ether-linked lipids, that maintain stability and fluidity at high temperatures[37]. They produce heat-stable proteins and enzymes through increased hydrophobic interactions, salt bridges, and disulfide bonds [38]. They also have a higher G+C content in their tRNA and DNA, contributing to RNA structure stability and enhancing thermal resilience. A notable example is Taq polymerase from *Thermus aquaticus*, which is crucial for DNA amplification in PCR [39]. Additionally, thermophilic enzymes are used in industries for processes like cellulose breakdown in biofuel production and waste treatment. Likewise, these bacteria produce molecular chaperones, such as

heat shock proteins, which help stabilize and refold proteins under thermal stress, preventing aggregation and ensuring proper protein function.

Psychrophiles

Frozen environments such as icy lakes, glaciers, and the deep-sea harbor cold-adapted organisms known as psychrophiles. These microorganisms thrive in temperatures ranging from −20°C to +10°C by making crucial cellular adaptations to withstand the cold [40]. The term 'psychrophile' reflects their affinity for cold, derived from Greek words meaning 'cold' and 'to love'[25]. These organisms are genetically equipped to withstand cold stress, producing enzymes with high catalytic efficiency that remain functional at low temperatures, and their cytosol adapts to prevent damage from freezing [34]. Psychrophiles also generate antifreeze proteins, with flexible structures that prevent rigidity and protect cellular components from damage caused by cold temperatures, which are utilized as cryoprotectants in food technology. In particular, Cold Shock Proteins (CSPs) are used for moderate cold, and Cold Acclimation Proteins (CAPs) are used for extreme cold. CSPs are activated under milder cold conditions, while CAPs are produced in response to severe cold at 4 °C [41]. These adaptations help them combat oxidative stress and maintain membrane fluidity in cold conditions fluidity [42]. They also exhibit increased gene activity related to membrane biogenesis, fatty acid synthesis, and desaturation, which enhances their survival and function in cold environments [43]. Their bioactive metabolites had anti-inflammatory, anticancer, antibacterial, and antioxidant properties, making them valuable for biotechnological applications. Psychrophilic enzymes are utilized in various applications where low temperatures are advantageous, including in the formulation of cold-water detergents, food preservation processes, and the production of chemicals and pharmaceuticals that require low-temperature conditions [44].

Halophiles

Halophiles are microorganisms that thrive in highly saline environments, such as salt flats, saline lakes, and salt mines, where salt concentrations range from 1.5% to over 30%. They are classified based on salt tolerance: weak (1–3%), moderate (3–15%), and extreme (15–30%) [45]. Halophiles use two main strategies to survive these harsh conditions. One strategy involves accumulating and synthesizing compatible solutes like glycerol or potassium ions, which stabilize cellular structures and help the organisms withstand high salt concentrations, dehydration, heat, and cold. The other strategy, known as the salt-in-cytoplasm approach, involves concentrating inorganic ions (mainly KCl) inside the cells while expelling sodium ions (NaCl) to balance osmotic pressure [33,46]. To maintain osmotic balance, halophiles also possess specialized cellular membranes with unique lipids that ensure stability and fluidity in hypertonic environments. Haloclines, or microbial 'hotspots,' are characterized by the presence of active microbial populations and unique bacterial species [47,48]. The analysis of sediments from environments such as Discovery Deep and Atlantis II has identified various microbial groups, including Proteobacteria, Actinobacteria, Deferribacteres and Euryarchaeota. Genera such as *Pseudoalteromonas, Halomonas* and *Pseudomonas* are particularly widespread, indicating a mixed microbial composition of halophiles and halotolerants. They are interesting for their ecological and evolutionary implications, as well as their ability to produce bioactive molecules and enzymes with potential industrial and biotechnological applications [49,50]. Also, halophiles are particularly suited to carotenoid production due to their high salt tolerance, which minimizes contamination and allows effective cultivation without requiring sterile conditions. As a result, they are highly sought after by the pharmaceutical industry because of the antioxidant, antitumor, and immunomodulatory properties of these pigments [51,52]. Furthermore, halophiles have useful

properties for biotechnology, such as their ability to use seawater and mixed substrates, grow in high pH environments, and possess negatively charged enzymes [53]. These include applications in detergent formulations, where high-salt environments are common, and in the production of biochemicals and pharmaceuticals, where enzyme stability in saline conditions is advantageous. Finally, the use of biogenic nanoparticles (NPs) derived from halobacteria offers a sustainable solution for heavy-metal bioremediation, thanks to their natural metal resistance mechanisms, including enzymatic detoxification, metal precipitation and energy-dependent efflux system [54,55].

1.3 Marine Bacterial Bioactive Compounds and their Involvement in the Blue Biotechnologies

The field of marine biotechnology, often referred to as "blue biotechnology," has emerged as a significant area of scientific and industrial interest, driven by the untapped potential of marine resources for biotechnological applications [56–59]. Often described as the "century of the ocean," the 21st century has seen an explosion in the exploration of marine environments, thanks to advancements in genomics, synthetic microbiology, and bioinformatics [60–62]. These technologies are accelerating the discovery of new marine microorganisms and bioactive compounds, opening new avenues for industrial applications, particularly in pharmaceuticals, cosmetics, and environmental solutions [5,56,63–65].

Marine microorganisms, including bacteria and cyanobacteria, are a particularly rich source of bioactive compounds, which are small molecules produced by organisms to perform critical ecological functions such as defense, competition for resources, and interspecies communication [66,67]. These secondary metabolites, with molecular weights under 3000 Da, are increasingly recognized for their unique and complex chemical structures, making them valuable in drug discovery [68]. The potential of marine bacteria is enormous, as they can produce

compounds that exhibit a range of biological activities, such as anticancer, antibiotic, antiviral, antimalarial, antioxidative, antifungal and anti-inflammatory properties [69–71]. The exploration of marine natural products (MNPs) has unveiled an impressive diversity of bioactive compounds (Figure 1). Reviews by Blunt et al. [72] and Carroll et al. [71] documented the extensive literature on marine natural products up to 2017, highlighting the growing body of knowledge about biologically active metabolites derived from marine microorganisms. As marine environments continue to be explored, new bioactive compounds are discovered, with an average of over 1,000 new metabolites discovered annually. Currently, over 40,000 marine natural products (MNPs) have been isolated from marine environments, as recorded in the MarinLit database (https://marinlit.rsc.org/). More than half of these have come from marine microorganisms, highlighting their role as a promising source for new drug discovery.

The pharmaceutical industry has already begun to capitalize on these compounds [63,73]. One prominent example is trabectedin (Yondelis®), the first marine-derived anticancer drug approved in the European Union, which was originally isolated from the Caribbean tunicate *Ecteinascida turbinate* [74,75]. Additionally, salinosporamide A (Marizomib®), a compound extracted from the marine bacterium *Salinospora tropica*, is currently in clinical trials for the treatment of multiple myeloma [76]. Other promising compounds, such as Thiocoraline, a depsipeptide from *Micromonospora* sp., have also shown significant anticancer potential by inhibiting DNA polymerase-α [77].

Beyond pharmaceuticals, marine bioactive compounds are increasingly being used in the cosmetics industry, with marine-derived ingredients now incorporated into various skincare products [32]. The demand for cosmeceuticals, cosmetic products that offer therapeutic benefits, has seen rapid growth, with marine-derived compounds such as peptides and terpenoids being utilized for

their anti-aging, antioxidant, and skin-healing properties [5,32]. In fact, the market for marine-derived cosmeceuticals reached $13 billion in 2011 in the U.S. alone [78].

Marine bioactive compounds also have considerable potential in environmental remediation. Marine microorganisms play a key role in the breakdown of pollutants and can be used for bioremediation processes to clean up contaminated coastal and marine environments [55,79]. This underscores the dual potential of marine biotechnology to address environmental challenges while also providing valuable bio-based products [57].

The growing interest in marine biotechnology is reflected in the significant economic contributions of the blue bioeconomy. In 2018, the sector generated over €750 billion in turnover, creating nearly 5 million jobs (European Commission, 2019- *Roadmap for the Blue Bioeconomy*). Projections indicate that in 2026 the blue biotechnology market will be valued at $6.4 billion, with ocean-based industries outpacing global economic growth by 2030 [58]. Exploring marine environments and harnessing marine microorganisms for biotechnological innovations hold immense potential for economic, environmental, and societal benefits.

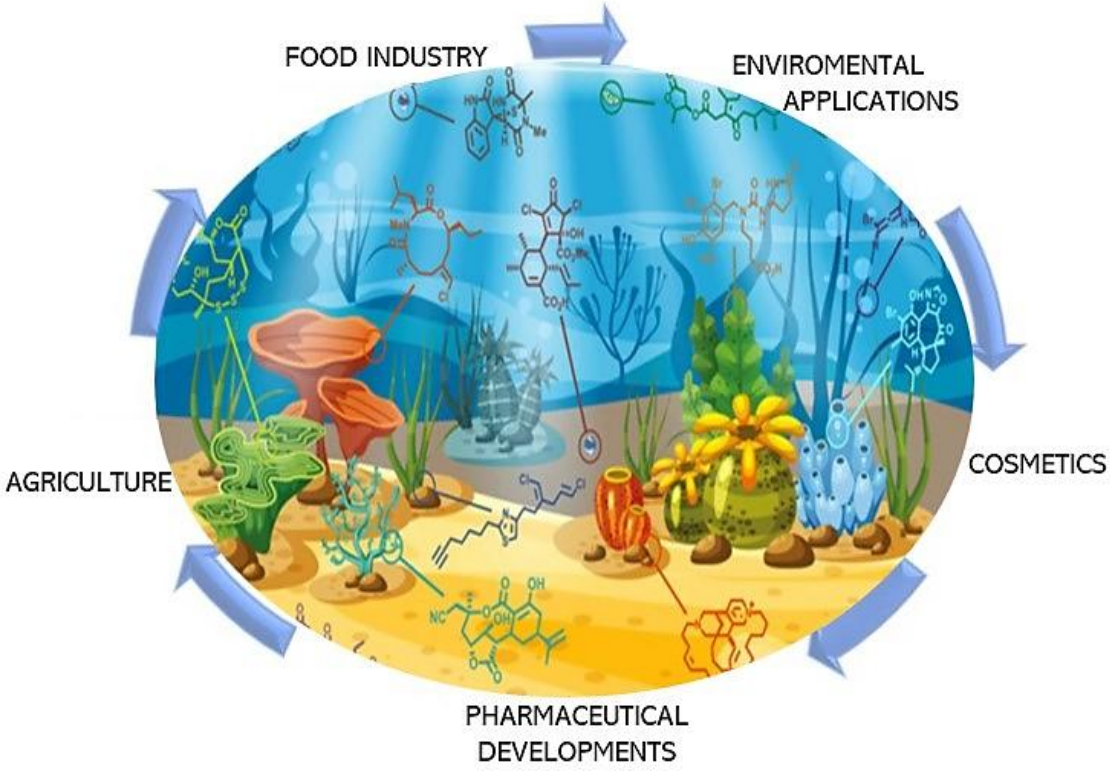

Figure 1. Graphical representation of MNPs and their biotechnological applications.

1.3.1 Marine Biosurfactants

Marine bacteria have developed the ability to produce a range of metabolites, including biosurfactants (BSs), which are essential for their interactions with materials that do not dissolve in water. These BSs enable marine bacteria to adsorb, emulsify, wet, disperse, or solubilize substances that are water-insoluble, helping them thrive in complex and extreme marine environments [80,81]. Biosurfactants are highly valued due to their biodegradability, low toxicity, and ability to be produced from renewable, cost-effective substrates. This makes them an eco-friendly alternative to synthetic chemical surfactants, particularly for industrial and environmental applications [82,83]. Biosurfactants (BSs) are amphiphilic compounds produced by bacteria and other microorganisms, composed of both hydrophilic/polar portion (water-attracting such as acids, peptides, or carbohydrates) and hydrophobic/non.-polar portion (water-

repelling like hydrocarbon chains or fatty acids) components [79,84,85]. Thanks to their dual nature, these compounds are able to reduce surface and interfacial tension, having the ability to self-assemble and form micelles and microemulsions between different phases, facilitating processes like emulsification, solubilization, cleansing, and dispersion [85]. Usually, they are produced extracellularly, but they can also be part of the cell membrane, depending on the organism and environmental conditions. These compounds facilitate key functions such as motility, cell-to-cell interaction, cellular differentiation, adhesion to substrates, protection against toxic elements, and high ionic strength [86]. BSs can be classified based on their molecular weight, cell secretion type (intracellular, extracellular, or cell-associated), ionic charge (anionic, cationic, non-ionic, or neutral), and chemical structure. Based on their molecular weight, biosurfactants are grouped into low-molecular-weight types, including glycolipids and lipopeptides (500 and 1500 Da), and high-molecular-weight types, known as bioemulsifiers, which consist of polysaccharides, lipopolysaccharides, proteins, or lipoproteins, which efficiently stabilize emulsions without altering surface tension [79,80]. Marine biosurfactants stand out for their remarkable effectiveness in extreme conditions, such as high salinity, wide temperature ranges, and varying pH levels, where synthetic surfactants often fail [44,87]. They are highly effective and remarkably efficient, achieving significant reductions in surface tension with much lower concentrations than synthetic alternatives [82]. This efficiency is reflected in their low critical micelle concentrations (CMCs), which indicate the point at which surfactant molecules begin forming micelles. For example, certain marine biosurfactants can reduce water's surface tension from 72 to 35 mN/m and decrease the interfacial tension between water and non-polar liquids, such as n-hexadecane, from 40 to 1 mN/m [88,89]. The production of biosurfactants is influenced by the composition of the fermentation medium, including factors such as carbon, nitrogen, metal ions, and

other additives [90–92]. Among these, the carbon source has a particularly strong impact on the type and quantity of biosurfactants produced [93]. Research has shown that glucose-based media tend to produce biosurfactants with superior antimicrobial and anticancer properties compared to substrates like glycerol, starch, or sucrose [94,95]. The two most studied classes, glycolipids and lipopeptides, are known for their high production yields and wide application potential, while Fatty acids represent the simplest amphiphilic class of metabolites. For instance, the marine Gammaproteobacterium *Cobetia* sp. which secretes linear 3-hydroxy fatty acids [96].

Glycolipids are the best-studied microbial biosurfactants that consist of a carbohydrate attached to aliphatic acids or hydroxyaliphatic acids through ether or ester bonds. The carbohydrate portion can include sugars such as rhamnose, mannose, glucose, galactose, galactose sulfate, or glucuronic acid. Sophorolipids, mannosylerythritol lipids (MELs), trehalose lipids, and rhamnolipids are well-known glycolipids that have proven efficient in large-scale production., For example, *Pseudomonas aeruginosa*, a known producer of rhamnolipids, has also been isolated from marine environments, which shows promise for industrial [97,98]. Also produced by *Streptomyces, Burkholderia* spp. and *Saccharomyces* species [99,100]. While *Mycobacterium*, *Nocardia*, and *Rhodococcus* species are known for producing Trehalose lipids, these involve mycolic acids attached to the disaccharide trehalose [101,102].

Lipopeptides are a type of biosurfactant that combines a peptide chain with a lipid tail, offering a unique combination of properties. These compounds are predominantly produced by bacteria from the Actinobacteria and Firmicutes phyla. In particular, marine Firmicutes, such as *Bacillus* species, are known to produce well-known lipopeptides like surfactins, fengycins, and iturins, which are highly valued for their surfactant properties. These cyclic lipopeptides have a peptide backbone made up of seven amino acids (iturins and surfactins) or ten

amino acids (fengycins), attached to a β-hydroxy or β-amino fatty acid [65]. The fatty acid chains vary in length, from C-10 to C-16 for surfactins, C-14 to C-17 for iturins, and C-14 to C-18 for fengycins. Each lipopeptide family is further divided based on the specific amino acid positions in the peptide ring [103].

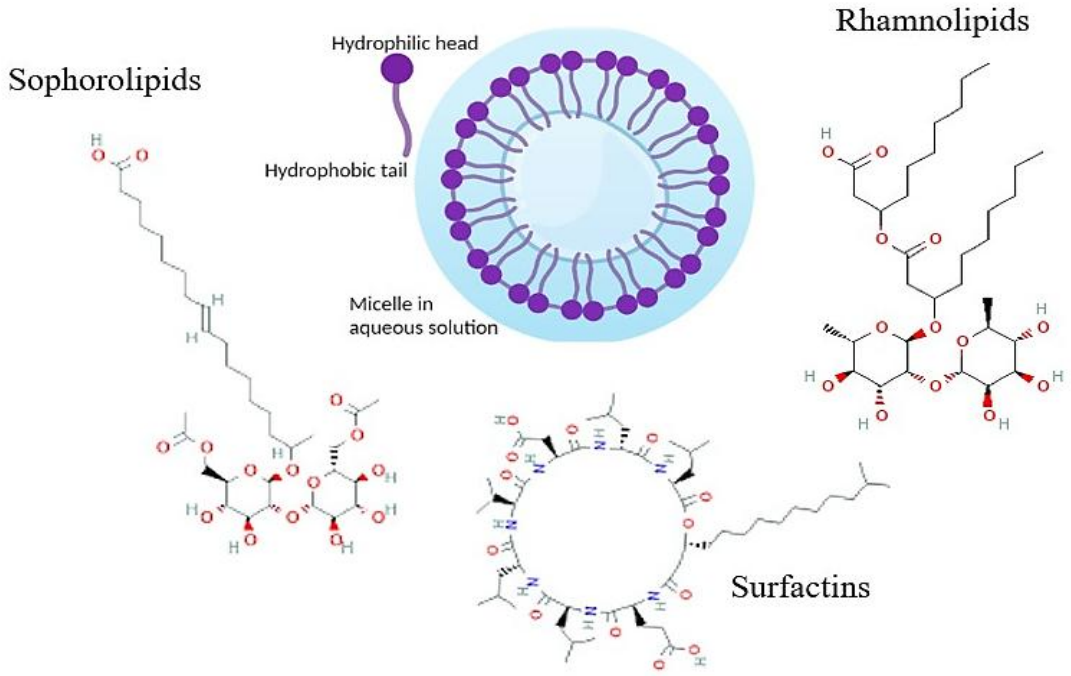

Figure 2. Structure of biosurfactants and well-known types of Glycolipids and Lipopeptides classes.

One of the most notable examples of a cyclic lipopeptide is surfactin, a versatile biosurfactant produced by various *Bacillus* strains, especially during the stationary growth phase when nutrients and oxygen are limited [104]. Surfactin is a macrolide lipopeptide with a molecular weight of 1,036 Da and an amphipathic structure, meaning it has both hydrophilic and hydrophobic components. This structure allows surfactin to interact with cell membranes in complex ways, leading to its antimicrobial, antifungal, antiviral, anti-inflammatory, and even anticancer activities [105,106]. Its mechanism of action is largely due to the hydrophobic interaction between the fatty acid chain and lipid bilayers, enabling it to penetrate the membrane while the peptide component

binds to polar lipid heads [89]. This interaction can disrupt membranes, form micelles, or produce detergent-like effects, depending on the concentration. This interaction can lead to membrane disruption, micelle formation, or even detergent-like effects depending on the concentration. Surfactin's effectiveness as a biosurfactant is evident from its (CMC) is notably low, with values of 9.4 μM in a 200 mM $NaHCO_3$ solution at pH 8.7 and 7.5 μM in a solution with 10 mM Tris and 10 mM NaCl at pH 8.5, demonstrating its ability to reduce surface tension at very low concentrations significantly. This exceptional performance underscores its superiority over many synthetic detergents [107–109].

1.3.1.1 Biosurfactant Screening Methods

The assessment of biosurfactants (BSs) production and interfacial activity is crucial for identifying potential candidates for various applications, particularly in bioremediation and industrial processes. Several methods are employed for screening biosurfactant (BS) and bioemulsifier production, assessing key properties. Here there is a summary of the common techniques:

Hemolysis Assay

The hemolytic activity assay is a widely used method for identifying microorganisms that produce biosurfactants with hemolytic properties. It was first discovered by Bernheimer and Avigad (1970), who observed that surfactin, a biosurfactant produced by *Bacillus subtilis*, lysed red blood cells [110]. The test involves culturing microbes on blood agar plates (5% blood and incubating at 25-45 °C for 24-48 h) and looking for a clear zone around colonies, which indicates red blood cell lysis. While the assay is useful, it has limitations, as only a small percentage of hemolytic strains produce biosurfactants, and false positives or negatives can occur due to unrelated enzyme activities [111,112]. Despite this, it remains a reliable initial screening tool for biosurfactant production.

Drop Collapse Technique

This technique, developed by Jain et al. (1999) is widely used for its simplicity and rapid results in detecting biosurfactant-producing cultures [113]. In this test, a drop of culture supernatant is placed on a hydrophobic surface, and in the presence of biosurfactants, the oil droplet expands or collapses due to reduced interfacial tension. In the absence of surfactants, the droplet remains stable as polar water molecules are repelled by the hydrophobic nature of the surface [114]. This method is sensitive to surfactant activity and can test multiple cultures simultaneously.

Oil Spreading Assay

The oil spread test evaluates the production of biosurfactants based on their ability to displace oil from the surface of water [112,115]. The procedure involves adding 50 mL of distilled water to a Petri dish, followed by the addition of 100 μL of crude oil to form a thin layer on the water surface. Then, 10 μL of the culture filtrate is added to the center of the oil film, and the clear zone formed by the displacement of oil is observed. The diameter of this clear zone reflects the biosurfactant emulsifying properties and it is directly proportional to the concentration of biosurfactant, providing a quantitative measure of surfactant activity. Furthermore, it is especially advantageous for initial screening.

Emulsification Activity (Emulsification Index - EI-24)

The emulsification capacity assay measures a biosurfactant's ability to form and stabilize emulsions. The standard protocol involves a 1:1 or 1:2 ratio between culture filtrate and oil, followed by vigorous vortexing for 1–2 minutes to form an emulsion. After 24 hours, the height of the emulsion layer is measured, and the emulsification index (E24) is calculated [116,117]. This assay evaluates biosurfactant performance in various industrial applications, though emulsification may not always reflect surface activity [118].

CTAB Agar Plate Assay

The agar method with CTAB (Cetyltrimethylammonium Bromide) is a semi-quantitative technique used to detect specifically anionic surfactants produced by microorganisms. Developed by Siegmund and Wagner, this method involves growing microorganisms on agar plates with light blue mineral salts containing CTAB, a cationic surfactant, and methylene blue, a basic dye [119]. When the microorganisms secrete anionic surfactants, they form a dark blue, insoluble ion pair with CTAB and methylene blue, which appears as a blue halo surrounding the colonies. The sensitivity of the CTAB test can be increased by introducing small wells into the agar gel. However, CTAB can be toxic to some microorganisms and inhibit their growth, limiting the test's applicability [120]. Additionally, not all anionic surfactants can be detected by this method, and it remains specific to anionic biosurfactants. An improvement of this method is that also possible to use it to test culture supernatants or extracts.

1.3.1.2 Biotechnological applications of biosurfactants

As consumer demand for safer, eco-friendly products continues to rise, biosurfactants are expected to play a critical role in shaping future industrial applications, driving innovation, and offering greener alternatives to traditional chemical-based ingredients. BSs offer superior performance with lower toxicity and better biodegradability, in line with global sustainability goals [108]. However, their production is still expensive, and further research is needed to improve their scalability and cost-effectiveness. The market for biosurfactants is expected to grow by 5% from 2023 to 2032, reaching over USD 8 billion. Demand is increasing in sectors such as personal care, household cleaning and healthcare [121]. In 2023, biosurfactants held 45% of the household cleaning market. The personal care sector is growing strongly, with a compound annual growth rate (CAGR) of 6.3%, driven by increasing demand for natural and eco-friendly

products [122]. In addition, the value of biosurfactants, particularly in drug delivery systems, was recognized during the COVID-19 pandemic due to increased hospital admissions and accelerated development of new drugs.

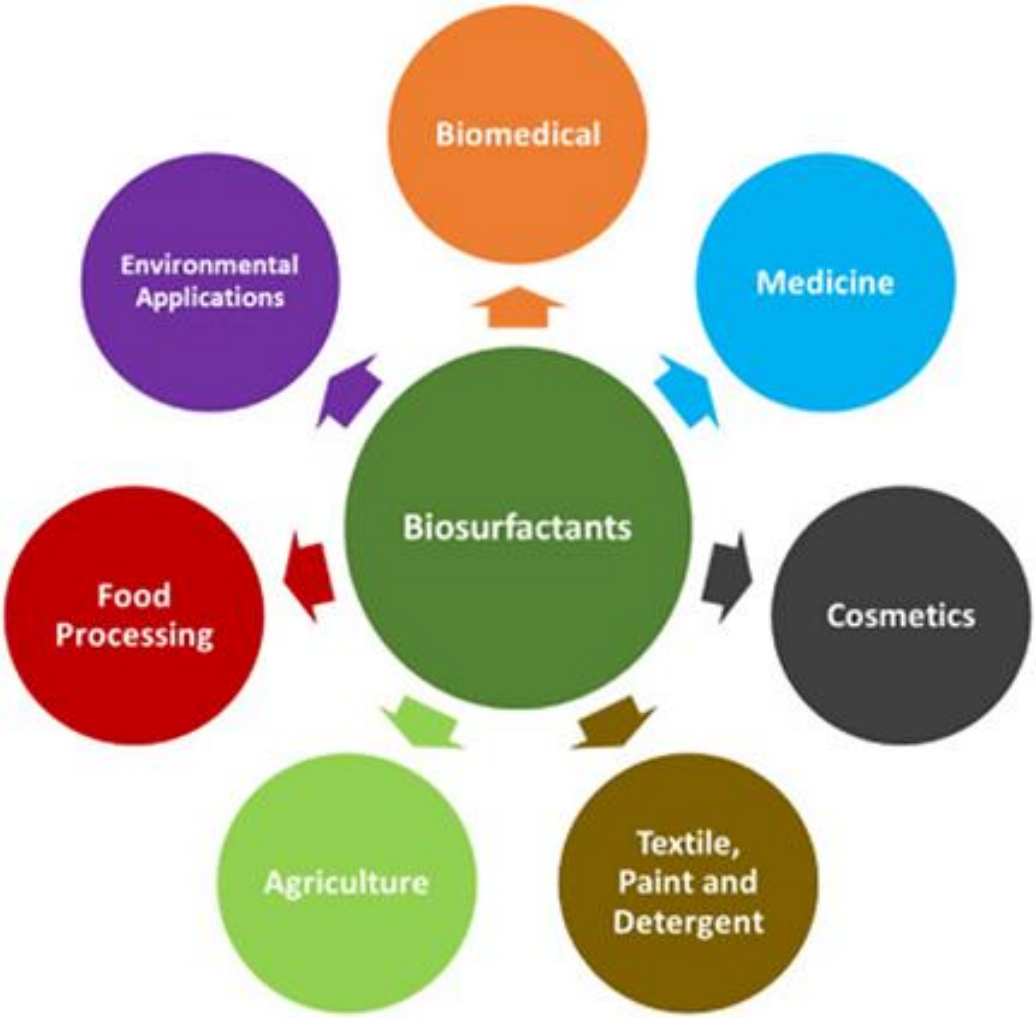

Figure 3. Biosurfactants industrial applications [123].

BSs in Bioremediation of Heavy Metal and Hydrocarbon Pollution

One of the most relevant applications of biosurfactants concerns the bioremediation of hydrocarbon pollutants and heavy metals. Petroleum-derived hydrocarbons, a major source of environmental pollution, are difficult to degrade due to their low solubility in water [79]. However, some microorganisms, such as hydrocarboclastic bacteria (e.g. *Alcanivorax, Cycloclasticus and Marinobacter*), are able to utilize oil as a carbon source. These bacteria, often dominant during oil

spills, produce biosurfactants that enhance the solubilization of hydrocarbons, making these contaminants more bioavailable and easily degradable [55,124]. In this context, biosurfactants act as both emulsifiers and bioemulsifiers, facilitating the bioremediation process, which has proven effective even under difficult conditions, such as low temperatures or the presence of compounds that are difficult to degrade, such as polycyclic aromatic hydrocarbons (PAHs) [125]. For example, rhamnolipid, produced by *Pseudomonas aeruginosa*, has demonstrated an effective ability to remove contaminants such as cadmium and lead from soil while also showing the ability to preserve soil quality and support microbial activity [126]. Moreover, biosurfactants have been utilized in microbial-enhanced oil recovery (MEOR) to increase oil extraction efficiency, making them a key player in the energy sector as well. In some studies, biosurfactants like rhamnolipids and surfactin have demonstrated recovery rates exceeding 90%, with some reaching 100% oil recovery [127]. Although the potential is promising, large-scale production of biosurfactants for bioremediation applications still faces challenges related to cost and scalability.

BSs in the Detergent and cosmetic Industry

Biosurfactants, due to their ability to emulsify, cleanse and foam, have proven very effective in detergents and personal care products. These compounds, which boast similar characteristics to synthetic surfactants, such as high stability and biodegradability, are used in household and industrial detergents, but also in skin care products [83,128]. For example, lipopeptides produced by *Bacillus subtilis* SPB1 have shown greater efficiency in removing vegetable oil and coffee stains than conventional detergents [129]. Furthermore, biosurfactants such as surfactants and rhamnolipids are used in cosmetic products for their non-irritating properties and ability to promote emulsification, solubilization, and foam formation. Their application also extends to gentle skin cleansers, shampoos and hair care products, with the need for more natural and low-

toxicity products increasing [130]. Furthermore, Beyond their functional benefits, biosurfactants contribute antimicrobial properties, adding value to hygiene and skincare products [131].

BSs in Medicinal and Pharmaceutical Industry

Biosurfactants are increasingly used in the medicinal and pharmaceutical fields, primarily for their antimicrobial, anti-adhesive, and enzyme-inhibiting properties. In the medical field, particularly lipopeptides like surfactin from *Bacillus subtilis*, play a significant role in biomedical applications due to their ability to disrupt cell membranes, increasing permeability and leading to cell lysis [109,132]. Other antimicrobial BSs like daptomycin, viscosin, and rhamnolipids, also have potent antimicrobial properties against pathogenic bacteria, including antibiotic-resistant strains such as methicillin-resistant *Staphylococcus aureus* (MRSA). Ramnolipids and surfactin also showed the potential to improve the efficacy of antibiotics by facilitating their penetration through bacterial cell walls [98,133–135]. In addition to antimicrobial applications, biosurfactants are also being investigated for their anti-inflammatory and anti-cancer properties, with studies suggesting that surfactin induces apoptosis in breast cancer cells, while other studies have found a beneficial effect in the treatment of inflammatory bowel disease[136–138]. Moreover, it also shows anti-biofilm effects, addressing persistent infections caused by biofilms, which protect pathogenic bacteria from immune responses and antibiotics. Biosurfactants destabilize microbial communities by inhibiting biofilm formation and interfering with quorum sensing, making them more vulnerable to treatment [139,140].

BSs in the Food Industry

Biosurfactants are being increasingly utilized in the food industry to enhance the quality and longevity of food products, due to consumer demand for sustainably sourced, plant-based, and healthier alternatives has surged [103,121,141].

Biosurfactants (BSs), derived from microorganisms with Generally Regarded as Safe (GRAS) status, and play a versatile role in food formulations, not only by reducing surface and interfacial tension to stabilize emulsions, making them suitable for a wide range of applications in baked goods, ice cream, sauces, and flavored oils. Notably, rhamnolipid is used to improve the stability and texture of doughs [142]. Another biosurfactant produced by *Enterobacter cloacae* is used to enhance the viscosity of acidic food products containing citric acid [143]. Moreover, biosurfactants have shown antimicrobial properties that are advantageous for maintaining food safety. By preventing the adhesion of pathogenic bacteria such as *Salmonella* and *Listeria monocytogenes*, biosurfactants help mitigate the risk of contamination and deterioration in food products [143–146].

BSs in Agricultural Applications

Biosurfactants are also gaining traction in agriculture, particularly as replacements for synthetic surfactants in agrochemical formulations. Their application supports green chemistry by reducing the environmental and health risks associated with conventional chemical surfactants. Rhamnolipid and lipopeptide biosurfactants have been identified for their ability to improve soil quality and serve as bioremediation agents for hydrophobic organic pollutants and heavy metals in contaminated environments [142].

1.3.2 Marine Siderophores

In the ocean, the concentration of iron varies between 0.01 and 2 nM, whereas marine microbes require iron levels in the micromolar range. Given the scarcity of iron in marine environments, particularly in its soluble form (Fe^{3+}), marine bacteria must possess mechanisms to solubilize and transport this essential nutrient [147–150]. Despite the natural solubility of Fe^{3+} being as low as 10^{-17} M, bacteria have developed the ability to extract iron from insoluble precipitates to

meet their energy and growth demands [150–152]. Siderophores have been identified as essential growth factors for bacteria, with over 500 siderophores discovered and 270 of these with defined structures. Siderophores (SID), meaning "iron carriers," are small iron-chelator molecules (200–2000 Da) secreted by marine bacteria, particularly in poor-iron environments, making them available for microbial uptake [148,153]. The affinity of siderophores for Fe^{3+} can vary significantly, with association constants ranging from 10^{12} to 10^{52}, reflecting their strength in binding iron [148,154]. To date, over 500 siderophores have been discovered, with 270 having defined structures [152,154]. The first siderophores discovered, such as myobactin and ferrochrome, were considered by researchers as growth factors by introducing siderophore-producing organisms into iron-deficient media [147]. Siderophores can generally be classified into four categories based on the type of ligand they use to coordinate Fe^{3+}: catecholate, hydroxamate, carboxylate and mixed types.

Catechol siderophores such as enterobactin, are particularly notable for their exceptional affinity for Fe III, driven by 2,3-dihydroxybenzamide motifs. Naturally produced by Gram-negative Enterobacteriaceae like *Escherichia coli* and *Salmonella typhimurium*, enterobactin is a tri-catechol siderophore, exhibits the highest known affinity for iron (Ka = 10^{52}) [155,156]. An example of a novel siderophore derived from the marine bacterium is nigribactin from *Vibrio nigripulchritudo*, which shares structural similarities with vibriobactin [157].

Hydroxamate Hydroxamate-type siderophores, particularly acyl peptidic variants, feature a nonpolar fatty acid tail and are commonly produced by marine bacteria like alcaligin *Alcaligenes denitrificans* by and desferrioxamine produced by *Streptomyces* spp; they also form stable iron complexes crucial for acquiring iron in limited environments [158]. For example, *Marinobacter* sp. DS40M6 that producs marinobactins [159].

Carboxylate types have carboxylate groups derivatives of citric acid are carboxylates, such as for example, staphyloferrin A produced by *Staphylococcus* species [156]. The unusual marine siderophore Vibrioferrin from *Vibrio* spp., a bis-α-hydroxycarboxylate, has one co-ordinating group from α-ketoglutarate and another from citrate [160]. Moreover, Achromobactin, produced by *Pseudomonas syringae* pv. syringae, is a tris-α-hydroxycarboxylate in which the coordinating groups come from α-ketoglutarate and citric acid [161].

Mixed-types siderophores, like pyoverdine from *Pseudomonas* spp., combine catecholate and other chelating groups, enabling efficient iron capture and binding of additional elements. Pyoverdine also fluoresces green-yellow under iron-deficient conditions due to its chromophore group. Similarly, pyochelin forms stable iron complexes, facilitating iron uptake and showcasing the versatility of mixed-ligand siderophores [162–164].

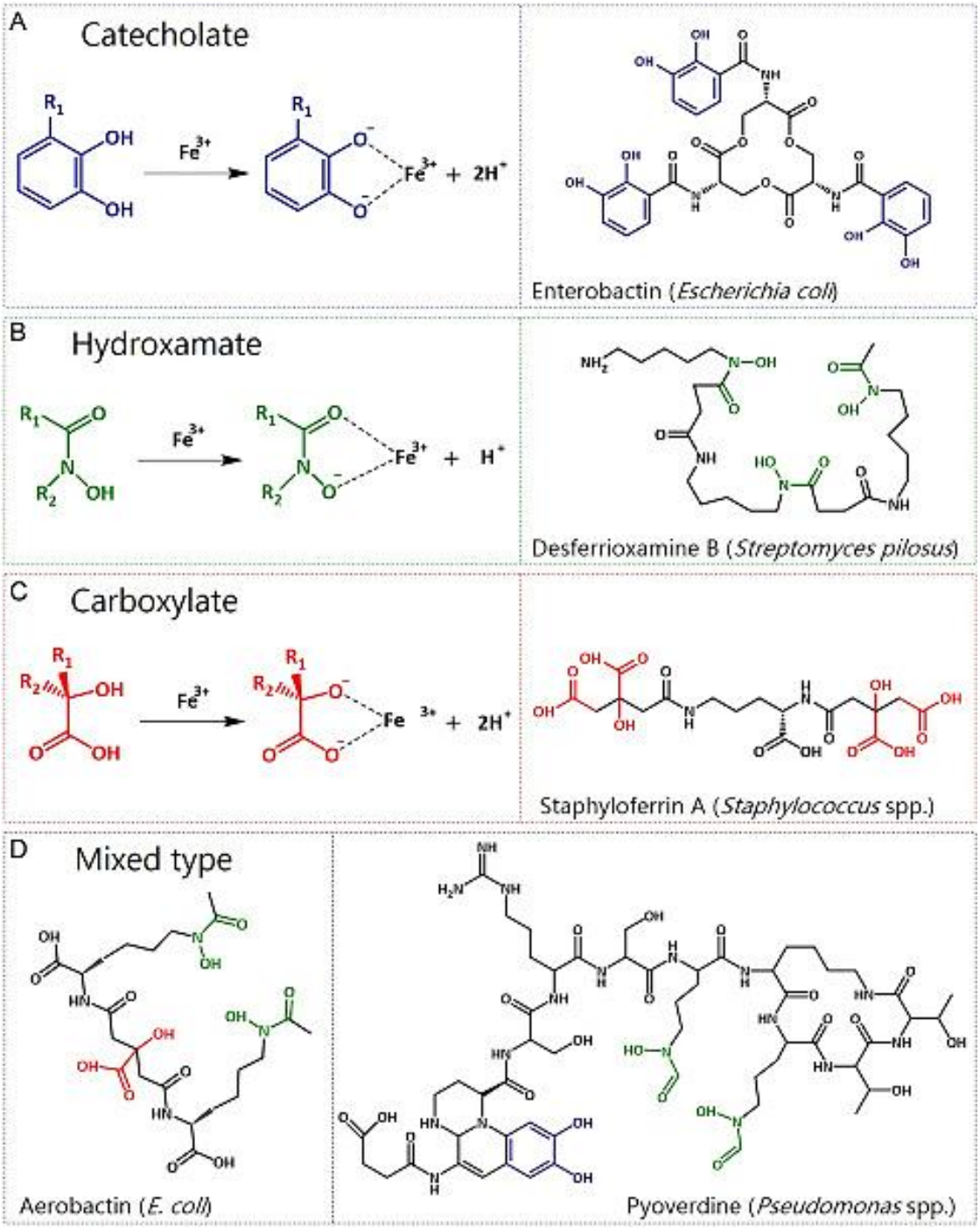

Figure 4. The most common iron-binding moieties found in microbial siderophores and examples. (A) Catecholate, (B) hydroxamate, and (C) carboxylate. Some siderophores present a combination of iron-binding moieties and are known as mixed-type siderophores [165].

Among them, another significative class is represented by amphiphilic siderophores produced mainly by marine bacteria. Both polar and non-polar components form them. The polar group is the binding site for iron and is attached to one or two fatty acid chains [150,151,159,166,167]. Another common

structural feature is the presence of an α-hydroxy carboxylic acid moiety, usually in the form of β-hydroxy aspartic acid or citric acid, which gives them photochemical reactivity. When exposed to light, ferric amphiphilic siderophores form photoproduced complexes with fatty acids and ferric iron, which are important in maintaining ferrous iron in the oceans [167,168]. The structure of amphiphilic siderophores varies depending on the length and polarity of the fatty acids. Siderophores such as amphibactins and moanachelins are hydrophobic, with long fatty acid chains (C16-C18), whereas loihichelins or aquachelins are more hydrophilic, with shorter chains and larger polar groups [151,166,169,170]. These differences influence the extraction method, with the former being obtained from the cell pellet and the latter from the supernatant. A key characteristic of amphiphilic siderophores is their ability to self-assemble into micelles and vesicles when iron is bound. When the concentration of amphiphilic siderophore exceeds the CMC (critical micelle concentration), and is not bound to iron, micelles are formed. If ferric iron (Fe III) is introduced into the solution, the size of the micelles reduces. Additionally, adding more iron can lead to a transition from micelles to vesicles [166]. This process has been observed in studies on marinobactins and has implications for biotechnology and pharmacology [159].

Siderophores are particularly useful when iron is concentrated in specific areas, such as mineral particles, and bacteria are not nearby. They help dissolve and distribute the iron more evenly, making it accessible to bacteria. These molecules, once secreted, can spread far from their producers, benefiting other bacteria or organisms rather than the original cells [149,154]. This cooperative behavior is common in bacterial biofilms, where secreted siderophores often help neighboring cells rather than the ones that produced them. In fact, the production of siderophores is considered a form of cooperation, as these molecules can be shared and support the lives of other individuals [153]. In addition, bacterial cells

usually grow in aggregates, such as biofilms adhered to surfaces and therefore secreted siderophores are not necessarily used by the cells themselves. Studies on siderophores are mainly based on controlled laboratory experiments where iron availability is regulated. In these settings, siderophore concentrations in the medium typically range from micromolar (μM) to millimolar (mM) during liquid fermentations [151]. Siderophore secretion is an energy-dependent process mediated by various efflux pumps. In Gram-negative bacteria, siderophores bind to specific receptors in the outer membrane, are transported into the periplasm, and then into the cytosol with the help of the TonB complex and ATP-binding cassette transporters. In contrast, Gram-positive bacteria lack an outer membrane and import siderophores directly through ATP-binding cassette transporters in the cell membrane. After iron release, siderophores may either be recycled or hydrolyzed to release the iron. Their production, release, and uptake are tightly regulated to maintain iron balance within the cell. The main regulator, Fur (ferric uptake regulator), controls this process by repressing siderophore synthesis and activating related proteins [152,154].

1.3.2.1 Siderophores Screening Methods

Various techniques have been developed to identify different types of siderophores based on their biological and functional properties.

CAS assay

The chrome azurol S (CAS) assay is a colorimetric method, created by Schwyn and Neilands. The assay operates on the principle of competition for iron between the siderophore and the CAS dye, causing a color change from blue to orange. While widely used for its sensitivity and quantitative potential, the CAS assay has limitations due to its non-specificity and the presence of HDTMA (hexadecyltrimethylammonium bromide), which can inhibit microbial growth at high concentrations [171,172]. To address the limitations of the CAS method,

several variants have been developed, such the CAS-Agar Plate Assay, which allows for the detection of siderophores produced by Gram-positive fungi and bacteria, reducing dye toxicity and improving medium stability [171,173]. In addition, this method can also be used by assaying the cell-free supernatant of the culture or crude extracts. The liquid CAS assay, a more widely used version, is sensitive and quantitative but is limited to chemically defined media, as it is interfered with by yellowish components in complex culture media and biological fluids. New quantitative siderophore tests are being developed, combining methods from both plate and liquid assays to improve accuracy. In the liquid CAS assay, the color change from blue to yellow occurs as siderophores chelate iron from the CAS dye. Absorbance is measured at 630 nm, and siderophore activity is expressed as a relative absorbance ratio [174]. The O-CAS assay, also known as "Overlaid CAS", allows for the simultaneous detection of multiple siderophore-producing microorganisms by optimizing the soil composition to enhance the growth of Gram-positive bacteria and fungi [175]. The Layer Plate CAS Assay employs DDAPS, a less toxic surfactant than HDTMA, while maintaining comparable results to the traditional method.

Arnow test

It is a colorimetric method used to detect catecholate-type siderophores in microbial cultures. The procedure involves treating the sample with ferric chloride ($FeCl_3$) and sodium hydroxide (NaOH), producing a reddish-brown color if catecholate siderophores are present [176].

Csaky test

This test identifies hydroxamate-type siderophores. This test requires adding a mixture of ferric chloride and hydroxylamine hydrochloride to the sample, where a reddish color indicates the presence of hydroxamate siderophores through iron chelation. While, the Tetrazolium test [177] is utilized to assess the production of hydroxamate siderophores. This method is based on the ability of

siderophores to reduce tetrazolium compounds, resulting in the development of a red color, which indicates the presence of siderophores [178].

1.3.2.2 Biotechnological applications of siderophores

Siderophore research has shown a significant growth trend over the last two decades. The number of articles published has doubled from an average of 16.6 per year between 2004 and 2013 to 32.2 between 2014 and 2023. This increase highlights the growing interest in their practical applications, particularly in bioremediation and antimicrobial therapies [179]. In 2019, the largest increase in research will be in microbiological and ecological studies. The main areas of research focus on the role of siderophores in combating antibiotic resistance, fungal pathogenicity and improving environmental remediation [180]. Indeed, beyond their ecological roles, SIDs are being explored for several potential applications.

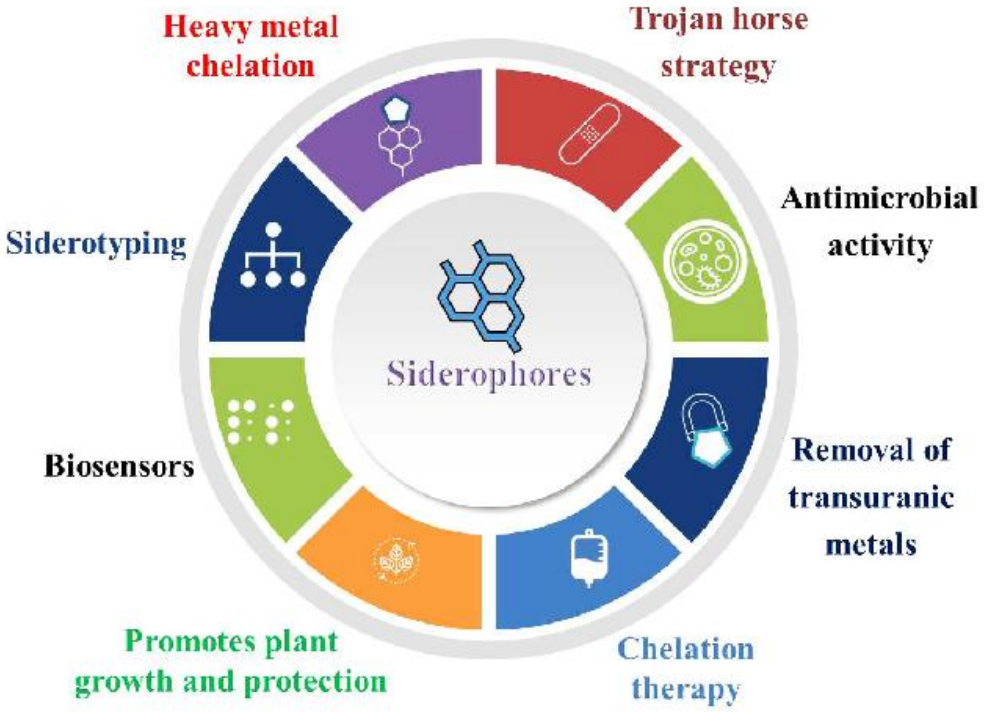

Figure 5. Siderophores industrial applications [181].

SIDs in Agriculture

Siderophores (SIDs) are valuable in agriculture due to their ability to enhance plant growth and health by improving iron bioavailability in soils [152,172]. Iron is an essential micronutrient for plants, participating in crucial processes such as chlorophyll production and redox reactions. However, plants require only trace amounts of soluble iron, whereas microorganisms need much higher concentrations. Certain bacteria, such as *Pseudomonas* species and other endophytes, produce siderophores that facilitate iron uptake, indirectly boosting plant growth [182]. This property positions these microorganisms as effective plant-growth-promoting agents, contributing to enhanced crop productivity and ecosystem stability. By increasing iron solubility in the rhizosphere, siderophore-producing bacteria help mitigate iron deficiencies that can otherwise reduce agricultural yields and quality [172].

SIDs as Biosensors

In biosensing, siderophore-based biosensors and nanosensors serve as powerful tools for detecting various compounds, including metal ions, antibiotics, pesticides, and microorganisms with high precision and sensitivity also their cost-effective. Biosensors combine a biological recognition element, such as a siderophore, with a transducer to generate quantifiable signals based on analyte concentration. These biosensors biosensors have been used for environmental monitoring, to assess the presence of contaminants like heavy metals, and in agricultural applications to track pesticide residues. Additionally, they play a crucial role in detecting antibiotic resistance and monitoring microbial populations in various settings [183–185]. For example, fluorescent siderophores like pyoverdines are particularly effective for constructing optical biosensors that monitor iron bioavailability in soils, ocean waters, and other environments [186].

SIDs in pharmaceutical Industry

Siderophores have emerged as powerful tools in medicine for addressing challenges such as antibiotic resistance, cancer, and parasitic diseases. These compounds utilize their natural iron-scavenging properties to deliver therapeutic agents into cells, often bypassing mechanisms of resistance or targeting iron-dependent cellular pathways [149,187,188]. In combating antibiotic resistance, siderophores act as "Trojan horses", which leverages siderophores as carriers to deliver drugs directly to pathogenic microbes, improving targeting precision while reducing the use of pesticides. In medicine, this approach addresses the challenges of selectively permeable cell membranes by conjugating siderophores with antibiotics to create sideromycins [189,190]. The conjugate comprises three components: the siderophore (for iron binding), the drug (for antibacterial activity), and a linker (to connect the two and regulate drug release). These compounds exploit the microbes' iron uptake systems to transport the drug into pathogen cells, enhancing therapeutic effectiveness [189,190]. This strategy is particularly effective against Gram-negative bacteria, whose outer membrane often blocks conventional drugs. Examples include Cefiderocol, a cephalosporin-catechol conjugate in advanced clinical trials, and synthetic siderophore-antibiotic conjugates like beta-lactam-siderophores, which have demonstrated strong activity against pathogens like *E. coli* and *Acinetobacter baumannii* [191]. In cancer treatment, the iron dependency of tumor cells makes them susceptible to siderophore-based iron chelation therapies, such as deferasirox[192]. Compounds like deferoxamine (DFO), initially used for iron overload conditions, have shown potential against neuroblastoma and leukemia by reducing oxidative stress and disrupting iron metabolism [144,193]. Additionally, bacterial siderophores like enterobactin have been found to arrest cancer cell proliferation by targeting intracellular iron stores and reducing reactive oxygen species [155,194].

SIDs in Bioremediation of Heavy Metal and Hydrocarbon Pollution

Siderophores (SIDs) are increasingly recognized for their role in bioremediation, particularly in the management of heavy metal and hydrocarbon contamination. Metals such as copper, cobalt, zinc, and chromium, while essential for many biochemical processes, can become toxic at high concentrations due to industrial activities, posing significant risks to human health and the environment. Unlike organic pollutants, heavy metals cannot be fully degraded but can be transformed into more soluble and mobile forms through complexation with siderophores, enhancing their removal from contaminated sites [154,195]. The effectiveness of siderophores in this process depends on several factors, such as the nature of the ligands and the type of metal involved [196]. For example, pyoverdine has a strong affinity for metals like zinc, copper, and manganese, while its affinity for iron is even stronger. Siderophores like deferoxamine B can also chelate metals like cobalt, facilitating their removal, especially in environments with high pH levels [197]. Siderophores are also valuable in marine environments, where they help in the bioremediation of oil spills. Marine bacteria, such as *Marinobacter hydrocarbonoclasticus*, produce petrobactin, a siderophore that aids in oil degradation [198]. Similarly, siderophores like ochrobactine, produced by bacteria in response to oil spills, can also help in the cleanup of hydrocarbons [168].

1.3.3 Marine Antimicrobials

The discovery of antibiotics has largely focused on terrestrial microorganisms, such as *Actinobacteria* and *Penicillium*. However, since the 1980s, this approach has led to diminishing returns, rediscovering known compounds [199,200]. This stagnation is concerning, especially as antibiotic resistance (AMR) has become a global health crisis. AMR, responsible for 1.3 million deaths annually, is driven by genetic mutations and the misuse of antibiotics [201]. By 2050, AMR could

cause up to 10 million deaths per year [202]. Acquired resistance spreads through horizontal gene transfer, where bacteria exchange resistance genes via transformation, transduction, or conjugation, leading to multidrug-resistant strains [203–205]. Key resistance mechanisms include the absence of antibiotic targets, enzyme production to deactivate antibiotics, changes in membrane permeability, and efflux pumps expelling antibiotics [203,206]. For instance, *Staphylococcus aureus* develops resistance by acquiring the *mecA* gene, which alters penicillin-binding proteins, reducing penicillin effectiveness [133,207]. In response to this growing crisis, the need for new antibiotics with novel mechanisms of action has never been more urgent. Marine bacteria, which thrive in extreme environments, have developed unique bioactive compounds, such as peptides, polyketides, and non-ribosomal peptides, that have unique structures and mechanisms of action, making them promising candidates for overcoming AMR that could provide innovative solutions for combating AMR [67,208–210]. For instance, polyketides like erythromycin and vancomycin show activity against a broad range of pathogens [207,211]. Additionally, marine antimicrobial peptides (AMPs), which are small, amphiphilic polypeptides, have demonstrated potent activity by disrupting bacterial membranes through electrostatic interactions [67,135,205]. These peptides are particularly valuable because their mechanisms of action make it harder for bacteria to develop resistance [212]. Also, some AMPs have been observed to inhibit DNA and protein synthesis within target cells [203]. Among the various types of AMPs, cyclic peptides are of particular interest. These peptides, which are synthesized by non-ribosomal peptide synthetases (NRPS), possess stable chemical bonds and can include lipopeptides, glycopeptides, and depsipeptides [213,214]. Their ability to target bacterial membranes and inhibit vital cellular processes makes them strong candidates for antibiotic development. For example, daptomycin, a cyclic lipopeptide approved by the FDA, is effective against Gram-positive bacteria

[134,139,215]. Moreover, the combination of marine-derived antimicrobials with novel delivery strategies, like using siderophores to transport drugs into bacterial cells, offers further potential. Cyclic peptides are also less prone to resistance due to their unique structural features, making them a promising alternative to conventional antibiotics [190,216]. Recent scientific studies have demonstrated that the primary groups of bacteria exhibiting antimicrobial activity are Actinobacteria, Firmicutes, and Proteobacteria [201,205]. These groups account for over 93% of the articles published in the past twenty-five years, with *Actinobacteria* being of particular significance as they are responsible for the production of 90% of the antibiotics currently in use [132]. A variety of chemical compounds, including fijimicins and linamycins derived from Actinobacteria, as well as macrolactins derived from *Bacillus*, have been identified as playing a crucial role in this field [67,135,212,217].

1.3.3.1 Antimicrobial Screening Methods

Agar diffusion method

The agar disk-diffusion method (ADM), developed in 1940, remains one of the most widely used techniques for antimicrobial susceptibility testing in clinical microbiology, endorsed by the Clinical and Laboratory Standards Institute (CLSI) [218]. In this method, a standardized microbial inoculum is spread on an agar plate, and filter paper disks containing an antimicrobial agent are placed on the surface. As the agent diffuses, it creates a concentration gradient that inhibits microbial growth, with the inhibition zone measured to determine its effectiveness. Variants like the Agar Well Diffusion method are also used, where a sample is applied to wells or discs in the agar, forming a zone of inhibition if the compound is active [219].

Broth dilution methods

The dilution methods are widely used to determine the Minimum Inhibitory Concentration (MIC) of antimicrobial agents, defined as the smallest

concentration of an antimicrobial agent that prevents visible growth, usually expressed in μg/mL or mg/L [220]. In the broth dilution method, antimicrobial agents are serially diluted in a liquid growth medium in a 96-well microtitration plate and a bacterial culture suspension, typically at a concentration of 1.5×10^8 CFU/ml, is added to the wells medium at each dilution. After inoculation, the cultures are incubated at 37 °C and the resulting turbidity is observed to assess the efficacy of the antimicrobial agent. While these methods provide high accuracy, they are more complex and time-consuming, limiting their widespread clinical use [218].

1.3.3.2. Biotechnological applications of antimicrobials

Marine-derived antimicrobials have significant biotechnological applications due to their potential to address the increasing threat of antimicrobial resistance (AMR) and their broad range of biological activities.

AMPs in Pharmaceutical Industry

In medical settings, these compounds represent a promising frontier in combating infections, especially those linked to biofilms and multidrug-resistant pathogens. These compounds have shown exceptional efficacy in preventing biofilm formation on medical devices, such as catheters, implants, and wound dressings, reducing the risk of associated infections [220,221]. AMPs work through diverse mechanisms, including disrupting extracellular biofilm matrices, inhibiting bacterial quorum sensing—essential for microbial communication—and targeting resilient microbial populations, such as antibiotic-resistant "persister" cells that often evade traditional treatments [222] Genera like *Streptomyces* and *Nocardiopsis,* are well-known for producing antimicrobial molecules that effectively combat resistant pathogens like *S. aureus* and *S. epidermidis*, offering solutions for infections associated with biofilm formation on medical devices and chronic wounds [223]. Moreover, their ability

to act synergistically with existing antimicrobial drugs enhances their overall effectiveness, offering a potent solution to tackle multidrug-resistant infections. Other marine-derived antimicrobials, demonstrate diverse mechanisms of action. For instance Chromomycins bind to DNA, disrupting bacterial replication, while Napyradiomycins and Marinomycins exhibit potent antibacterial activities against resilient strains [224–226]

Innovative advancements, such as antimicrobial peptide–polymer conjugates, have further improved the stability, bioavailability, and therapeutic efficacy of these compounds. These conjugates merge the natural antimicrobial potency of AMPs with the structural versatility of polymers, paving the way for enhanced infection control and therapeutic delivery [227]. Additionally Liposomal and solid lipid nanoparticle (SLN) delivery systems are promising approaches in the transport of AMPs. These systems are designed to improve the bioavailability and efficacy of AMPs, especially in the face of challenging infections caused by both Gram-positive and Gram-negative bacteria [227].

In addition to their antimicrobial properties, AMPs have also other bioactivities. Anti-inflammatory peptides, such as those inhibiting NF-κB or MAPK pathways, reduce the release of inflammatory mediators and cytokines, helping to manage conditions like arthritis [228]. Anti-diabetic peptides, including those that activate glucagon-like peptide-1 (GLP-1) receptors, assist in regulating blood sugar levels and enhancing insulin sensitivity [229]. Furthermore, certain peptides exhibit anticancer activity by inducing apoptosis or necrosis in cancer cells. For instance, tritrpticin and its analogs have shown toxicity towards tumor cells [230].

AMPs in Aquaculture

In modern aquaculture, infectious diseases pose a significant challenge, driven by high population densities and stressful farming conditions. As an alternative, antimicrobial peptides (AMPs) have emerged as a promising and sustainable

solution to prevent and treat infections in fish [231]. In addition to their antimicrobial properties, AMPs exhibit immunomodulatory effects, enhancing both innate and adaptive immune responses. They also play a key role in reducing oxidative stress through their antioxidant activity, which is particularly important in aquaculture, where stress can severely impact fish health.

AMPs in Cosmetic Industry

In the cosmetic industry, marine antimicrobials are increasingly incorporated into skincare products to target acne-causing bacteria and other dermatological infections [232]. Studies on coral-associated *Streptomyces* sp. have identified tirandamycin derivatives that effectively target bacteria such as *Streptococcus agalactiae* and *S. aureus*, highlighting their potential in treating acne-related and other bacterial infections [233]. They also serve as natural preservatives, enhancing product safety by reducing reliance on synthetic chemicals.

AMPs in Agriculture and Food

AMPs are increasingly being explored as natural food preservatives due to their ability to inhibit bacteria and fungi, offering a safer alternative to synthetic preservatives. For example, nisin, a bacteriocin produced by *Lactococcus lactis*, is widely used to preserve food and is recognized as safe by the FDA [234]. AMPs also show potential in active packaging solutions, such as combining ε-poly-L-lysine with starch biofilms to prevent mold growth on food [235]. In agriculture, AMPs like antifungal peptides (AFPs) have demonstrated effectiveness in controlling plant diseases caused by fungi, such as *Aspergillus flavus* on corn and peanuts, and *Penicillium digitatum* on citrus fruits [236]. However, the widespread use of AMPs in food and agriculture faces challenges, including high costs, particularly for transportation and preservation of perishable goods.

AMPs in Environmental Industry

In environmental applications, these compounds are used as biofilm control and biofouling prevention. In marine environments, these compounds help inhibit the growth of fouling organisms like barnacles and algae on underwater structures such as ships and pipelines. This significantly reduces maintenance costs and environmental impacts, as it reduces the need for regular cleaning and harsh chemicals [237]. Moreover, these antimicrobial agents are incorporated into water treatment systems to improve microbial control, preventing biofilm formation and enhancing the efficiency of water purification processes. Beyond this, research is advancing the development of antimicrobial biomaterials and biomedical devices with antibacterial and antibiofouling properties. Multifunctional antimicrobial surfaces, including antibacterial metal surfaces created through methods like magnetron sputtering, are also being explored for their potential to combat microbial growth and biofilm formation across various sectors [237]. These developments contribute to better maintenance practices and more sustainable technologies.

1.4 Barriers in MNPs Discovery

The field of NPs discovery from marine bacteria is increasingly driven by the vast and largely unexplored microbial diversity of the oceans. Marine bacteria offer a unique opportunity for the development of new bioactive compounds [220]. However, discovering these compounds presents numerous challenges, as demonstrated by the increasing frequency of the rediscovery of known compounds. The traditional process of marine drug discovery extracting, isolating, and purifying bioactive products through bioassays remains slow, labor-intensive, and inefficient, with no guaranteed success [239,240]. Marine natural product discovery faces a several important barriers that limit its potential.

One of the main difficulties is access to the hostile marine environment. For a long time, research was limited to coastlines and sea surface, while deep-sea exploration remains underdeveloped, with only a tiny fraction (0.001%) of the deep sea comprehensively studied for biodiversity [1,13]. Moreover, the collection of marine resources must be balanced with environmental sustainability, as marine ecosystems are increasingly protected by stringent regulations [12].

Another challenge lies in the fact that over 99% of marine bacteria cannot be cultured using conventional laboratory methods [241]. This phenomenon, known as the "great plate count anomaly," complicates the identification and cultivation of potential bioactive compound producers [242]. Many microorganisms that are isolated end up in a viable but non-culturable state (VBNC), making them difficult to study and exploit for natural product discovery. Even when culturing is possible, replicating the specific environmental conditions required for bioactive secondary metabolite production is often impractical in the lab [243–245].

Moreover, marine microorganisms frequently live in symbiosis with other organisms, such as sponges and corals [246]. These symbiotic relationships further complicate the discovery of new bioactive compounds, as the microbial products often depend on these intricate associations [243,247]. Additionally, slow-growing species from nutrient-poor environments are often outcompeted by fast-growing bacteria, limiting our ability to isolate these valuable organisms [248].

Even when bacteria can be cultured, another barrier arises: many secondary metabolites remain "silent" under standard laboratory conditions due to inactive biosynthetic gene clusters (BGCs) [249]. This means that even though a microorganism may have the genetic capability to produce bioactive compounds, the compounds may not be detected unless specific environmental conditions

trigger the expression of the relevant genes [250]. Additionally, the process of extracting natural compounds from marine sources is complicated by low yields and the complexity of identifying bioactive compounds among other chemicals in the sample. Identifying bioactive compounds is an expensive and resource-intensive process. It can take months and cost up to $50,000 per isolate. One way to optimize this process is by rapidly identifying compounds that have already been discovered, enabling researchers to focus resources on more promising leads [251].

1.5 Overcoming barriers

To unlock the vast biosynthetic potential of marine microorganisms, several strategies have been developed, overcoming the barriers that once hindered exploration of the deep ocean. Consequently, the probability of discovering novel natural compounds with various applications can be enhanced.

1.5.1 Advanced technologies to gain access to the unexplored ocean environment and life

The ocean, once a "deep secret," has only recently become accessible to scientific exploration, thanks to advancements such as scuba diving, submersibles, and remotely operated vehicles (ROVs) [252,253]. These technologies have facilitated sampling at great depths, revealing a previously unknown diversity of life. For example, the ROVs developed by Galloway et al., capable of gently collecting marine microorganisms from depths of 100 to 170 meters, has significantly enhanced marine bioprospecting efforts [2,254]. However, traditional methods of isolating and cultivating marine microbial species continue to present challenges, especially with regard to rare and more uncultured bacteria. Several studies have revealed a wealth of bioactive compounds from rare actinobacteria in under-explored marine environments, highlighting the need for innovative isolation methods [255,256]. Infact, traditional culture media often favour fast-growing

bacteria, but new techniques such as diluted media and longer incubation times have been successful in isolating slow-growing species [248,257]. Furthermore, the use of diluted media, longer incubation times and modifications to standard agar preparations, such as the use of gellan gum or separate autoclaving of medium components, enabled the isolation of slow-growing bacteria and previously uncultured species [258]. For instance, Choi et al. (2005) demonstrated that relatively simple cultivation techniques enabled the isolation of previously uncultured bacterial taxa from the phyla Bacteroidetes and Proteobacteria [259]. The "dilution to extinction" method has been effective in isolating rare bacteria by diluting samples to allow individual colonies to grow [260]. This technique has been crucial for isolating species like SAR11 [261]. Moreover, several approaches are used to entry into the “uncultured majority”. They allow to mimic the habitat of the specific microorganism, such as the diffusion chamber system, and the subsequent I-chip method, that allow in situ cultivation of previously unculturable strains [262,263]. The iChip enabled the discovery of teixobactin, a novel antibiotic from the previously uncultured *Eleftheria terrae* [264]. Later, MacIntyre et al. adapted the iChip for marine environments, isolating a new species from the sponge *Xestospongia muta* [265]. Additionally, methods like the I-tip focus on isolating symbiotic microorganisms, using micropipette tips filled with agar and microbeads that are placed directly on the host-organism [266].

1.5.2 Unveil potential novel BGCs

MNPs are often encoded by biosynthetic gene clusters (BGCs), which have a modular structure, with specific genes for the biosynthesis of each compound clustered in the genome. Marine bacteria use multienzyme complexes to conduct multistage biosynthetic processes, resulting in the production of metabolites. The products of BGCs are subdivided into several classes, such as polyketides (PKS), ribosomally synthesised and post-translationally modified peptides (RiPP, which

include lantipeptides, lasso peptides, glycopeptides and others), terpenes, alkaloids and saccharides and non-ribosomal peptides (NRPS). The biosynthesis of these products varies depending on the substrates and enzymes involved [62,213,246]. In particular, the production of these compounds is guided by the NRPS enzyme system. The NRPS are multi-modular enzymes that synthesise peptides with diverse structures. This is achieved by the enzyme recognising, activating, modifying and linking amino acids. The structural diversity of nonribosomal peptides confers significant biological activity. NRPS enzymes are composed of modules, composed by three or more domains and each module performs a specific function [213]. The adenylation domain (A) recognizes and activates specific substrates using ATP, forming an acyl-AMP intermediate (Figure 6). This activated substrate is then transferred to the phosphopantetheine (ppant) arm of the PCP domain or (T) through a transesterification reaction. The thiolation domain (T) equipped with a CoA-derived ppant cofactor, shuttles the substrate to the C domain. The condensation domain (C) catalyzes peptide bond formation by facilitating nucleophilic attack of the α-amino group of the acceptor substrate on the activated α-carboxy group of the donor substrate. This modular process is repeated in a co-linear fashion, with the sequence of modules determining the peptide's structure [213,267,268]. The thioesterase (Te) domain (Te) the final peptide through hydrolysis or macrocyclization, completing the synthesis process. Substrate specificity in NRPS is governed by the A domain, which selects its cognate substrate based on the amino acid residues lining its binding pocket. This specificity is described by the "Stachelhaus code," a sequence motif that correlates with substrate preference [269]. The modular nature of NRPS allows for immense structural variability in their products. Additional tailoring domains, such as epimerization (E) domains and methyltransferase (MT) domains, a further enhancing peptide diversity and function. The first one catalyzes the conversion of L-amino acid residues to D-

amino acids. This modification is often essential for NRPs to adopt specific conformations, which are critical for their biological activities, such as antibiotic efficacy [270]; the second one transfers a methyl group to the substrate, that could influence the chemical properties and biological activity of the peptide, further expanding its potential applications. The heterocyclization domain (Cy) is also crucial, ensuring proper peptide synthesis and modification [213,267].

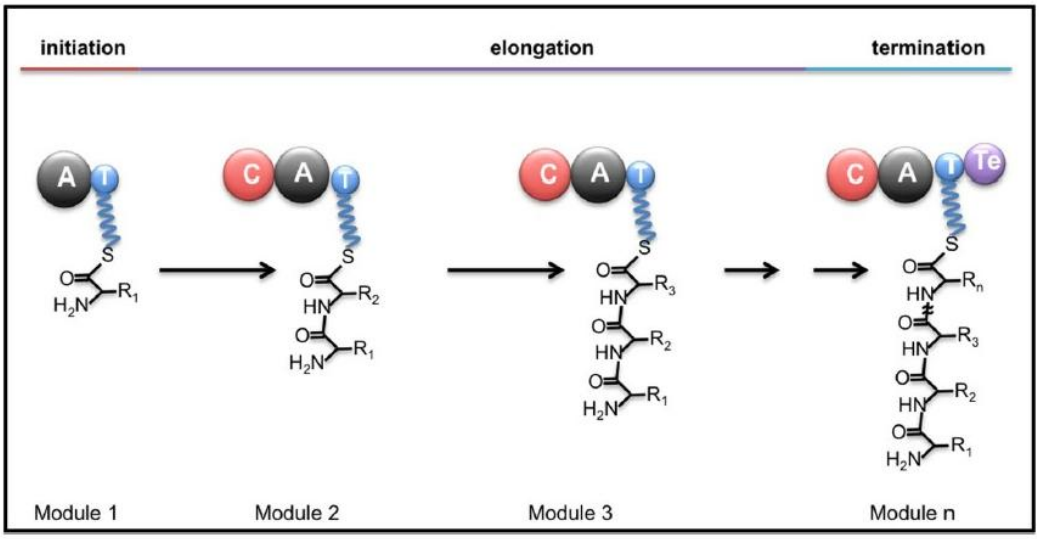

Figure 6. Non-ribosomal peptide synthesis (NRPS). Adenylation domain (A), Condensation domain (C), Thiolation domain (T) with Peptidyl Carrier Protein (PCP), Termination domain (TE).

1.5.2.1 Culture-independent approach:

Advances in marine microbial genomics, particularly through meta-omics techniques like metagenomics and metaproteomics, has allowed the study of marine microorganisms without their cultivation, overcoming the limitations of traditional techniques [271]. Projects such as Global Ocean Sampling (GOS) have greatly expanded the marine genetic landscape, revealing that over 50% of the protein sequences discovered were previously unknown [272]. This has led to a better understanding of microbial biodiversity and the discovery of new genes and biosynthetic pathways. Genome mining, particularly targeted approaches, are valuable tool for the identification of biosynthetic gene clusters (BGCs)

responsible for the production of secondary metabolites, such as antibiotics and other bioactive compounds [62,273–275]. Thanks to several bioinformatics tools such as antiSMASH [276,277], GECCO [278], DeepBGC [279], EvoMining [280] and PRISM 4 [281], it is possible to and analyze various biosynthetic pathways, offering predictions on the chemical structures of metabolites. based on genetic data. These methods allow for targeted discovery of compounds like non-ribosomal peptides (NRPs) and polyketides (PKS), which have significant potential novel bioactivities [62,213,246]. Therefore, Initiatives like the Minimum Information about a Biosynthetic Gene Cluster (MIBiG) [282] allows genomic dereplication by comparing newly discovered BGCs by sequence homology with genes involved in the production of known natural compounds (Bachmann, Van Lanen, & Baltz 2014). Ultimately, omics technologies and metabolic engineering have significantly improved the modification of metabolic pathways, leading to better production of specific compounds, particularly in industrial fermentation processes, through the application of recombinant DNA technologies [271,283]. The refinement of the techniques of cloning and heterologous gene has opened the way for new tools in the synthetic biology field [284,285]. These innovations create new opportunities for natural product discovery by enabling the overexpression of activator genes and the inactivation of transcriptional repressors.

1.5.2.2 Culture-dependent approach: OSMAC strategy

Among the strategies used to activate cryptic microbial biosynthetic gene clusters (BGCs), the One Strain - Many Compounds (OSMAC) approach has emerged as one of the most successful [286–288]. This strategy highlights how a single microbial species can produce a diverse range of metabolites when different cultivation parameters, such as nutrient concentration, temperature, pH, osmotic conditions, aeration and the addition of specific inducers (e.g. metals, vitamins),

are altered [95,289]. In addition to modifying cultivation parameters, the OSMAC strategy includes the addition of small molecules in the culture media, such as chemical elicitors, which influence gene expression at the transcriptional level [287], also heavy metals, nickel and β-glucans are recognised as common elicitors, but DNA methyltransferase (DNMT) and histone deacetylase (HDAC) inhibitors, such as 5-Azacytidine and SAHA, have also been successfully used to remodel the epigenetic profile of microbial metabolomes, thereby increasing chemical diversity and activating silent biosynthetic pathways [290,291]. Some studies have shown that antibiotics at sub-inhibitory concentrations induce transcriptional changes in bacteria [155,292]. Another promising strategy for activating 'silent' BGCs is co-cultivation, where two or more microorganisms are grown together. This method can be seen as an extension of OSMAC and often leads to enhanced production of known compounds or the discovery of previously cryptic metabolites that may not be detected in axenic cultures. Co-culturing microorganisms leads to a variety of interactions, such as competition for resources, exchange of signalling molecules (quorum sensing) and biofilm formation, all of which mimic natural ecosystems. These interactions can stimulate the production of metabolites that would otherwise remain dormant in isolated cultures [293]. Co-culture strategies also include innovations such as shared liquid media, solid-liquid interfaces (bead entrapment), spatial arrangements and microfluidic systems to promote beneficial interactions between microorganisms [294,295].

1.5.3 Fast Dereplication and Metabolomics

In the discovery of microbial natural products (MNPs), dereplication plays a crucial role in quickly identifying known bioactive compounds and avoiding redundant discoveries [240,275]. This process involves the comparison of new compounds against existing databases to determine whether they have already

been identified. The most effective dereplication techniques combine high-performance liquid chromatography (HPLC) with tandem mass spectrometry (MS/MS). This combination allows researchers to separate multiple compounds within a sample and identify them based on their molecular mass. High-resolution mass spectrometry (HRMS) provides precise mass data, while MS/MS further refines structural analysis by examining fragmentation patterns of metabolites [275]. Furthermore, Nuclear magnetic resonance (NMR) has also evolved, enabling the prediction of stereochemical relationships and the rapid determination of metabolite connectivity using chemical shift models [275]. Advanced software such as Sirius and MS-FINDER allow in silico analysis of MS/MS data, making it easy to identify known molecules without the need to compare them with spectral libraries [296]. One of the challenges in dereplication is the large volume of data generated during analysis. Computational tools, like MZ mine, are used to pre-process raw LC-MS/MS data, filtering features based on isotope patterns and retention times, which are then uploaded to platforms like GNPS (Global Natural Products Social). This platform provides access to over 80,000 MS/MS spectra, generating a feature-based molecular network (FBMN), highlighting chemical relationships between metabolites detected in an extract based on similar fragmentation patterns [297,298]. After These networks are visualized using software like Cytoscape, aiding in the efficient identification of metabolites [299]. In addition, through new bioinformatics tools such as Dereplicator+ [300] , CSI:FingerID [301] and RODEO [273], it is possible to compare the fragmentation spectra of the compounds present in a sample with those of known products deposited in the databases.

Metabolomics, positioned downstream in the "omics" cascade, focuses on the comprehensive analysis of metabolites, bridging the gap between genomics and natural product chemistry [271]. The integration of metabolomics with genomics and genetic engineering has led to the emergence of metabologenomics, a field

combining metabolic and genomic analysis to expedite the discovery of new natural product [302]. Metabolomics utilizes both targeted and untargeted approaches [271,303]. Targeted methods focus on known metabolites, using prior knowledge to perform quantitative analyses and track changes in specific compounds. This is supported by metabolite libraries for tailored analysis [304]. Conversely, untargeted approaches aim to identify as many metabolites as possible, producing large datasets that require annotation and identification, often through databases like METLIN [305]. Techniques like NMR, GC-MS, and LC-MS are commonly used, and their integration broadens the scope of metabolomic studies, enabling the discovery of new metabolites and enhancing the analysis of metabolic profiles [306].

Conclusions

The findings presented above underscore the vast and largely untapped potential of marine ecosystems as reservoirs for biotechnological innovations. Extremophilic bacteria have evolved remarkable metabolic pathways to thrive under extreme conditions, enabling them to produce structurally diverse and biologically active compounds. These include antibiotics, anticancer, biosurfactants, and siderophores, which hold promise for applications in medicine, agriculture, and environmental conservation. However, substantial challenges remain, particularly in accessing extreme marine habitats, overcoming the "great plate count anomaly," and activating silent biosynthetic gene clusters (BGCs). Advances in cultivation-independent techniques, genome mining, the development of advanced screening techniques and metabolic engineering have significantly expanded our ability to discover and harness new marine natural products offering promising solutions to overcome the current barriers. By integrating interdisciplinary approaches, this research highlights the importance of exploring unexplored marine environments.

References

1. Sogin, M.L.; Morrison, H.G.; Huber, J.A.; Welch, D.M.; Huse, S.M.; Neal, P.R.; Arrieta, J.M.; Herndl, G.J. Microbial Diversity in the Deep Sea and the Underexplored "Rare Biosphere." *Proceedings of the National Academy of Sciences* **2006**, *103*, 12115–12120, doi:10.1073/pnas.0605127103.
2. Danovaro, R.; Aronson, J.; Cimino, R.; Gambi, C.; Snelgrove, P.V.R.; Van Dover, C. Marine Ecosystem Restoration in a Changing Ocean. *Restoration Ecology* **2021**, *29*, e13432, doi:10.1111/rec.13432.
3. Canganella, F.; Wiegel, J. Extremophiles: From Abyssal to Terrestrial Ecosystems and Possibly Beyond. *Naturwissenschaften* **2011**, *98*, 253–279, doi:10.1007/s00114-011-0775-2.
4. Capece, M.C.; Clark, E.; Saleh, J.K.; Halford, D.; Heinl, N.; Hoskins, S.; Rothschild, L.J. Polyextremophiles and the Constraints for Terrestrial Habitability. In *Polyextremophiles: Life Under Multiple Forms of Stress*; Seckbach, J., Oren, A., Stan-Lotter, H., Eds.; Springer Netherlands: Dordrecht, 2013; pp. 3–59 ISBN 978-94-007-6488-0.
5. Raddadi, N.; Cherif, A.; Daffonchio, D.; Neifar, M.; Fava, F. Biotechnological Applications of Extremophiles, Extremozymes and Extremolytes. *Appl Microbiol Biotechnol* **2015**, *99*, 7907–7913, doi:10.1007/s00253-015-6874-9.
6. Merino, N.; Aronson, H.S.; Bojanova, D.P.; Feyhl-Buska, J.; Wong, M.L.; Zhang, S.; Giovannelli, D. Living at the Extremes: Extremophiles and the Limits of Life in a Planetary Context. *Front Microbiol* **2019**, *10*, 780, doi:10.3389/fmicb.2019.00780.
7. Giordano, D. Bioactive Molecules from Extreme Environments. *Marine Drugs* **2020**, *18*, 640, doi:10.3390/md18120640.
8. Merlino, G.; Barozzi, A.; Michoud, G.; Ngugi, D.K.; Daffonchio, D. Microbial Ecology of Deep-Sea Hypersaline Anoxic Basins. *FEMS Microbiology Ecology* **2018**, *94*, fiy085, doi:10.1093/femsec/fiy085.
9. Teske, A.; Sørensen, K.B. Uncultured Archaea in Deep Marine Subsurface Sediments: Have We Caught Them All? *The ISME Journal* **2008**, *2*, 3–18, doi:10.1038/ismej.2007.90.
10. Glover, A. Measuring Up the Deep. *BioScience* **2011**, *61*, 327–328, doi:10.1525/bio.2011.61.4.17.
11. Du, M.; Peng, X.; Zhang, H.; Ye, C.; Dasgupta, S.; Li, J.; Li, J.; Liu, S.; Xu, H.; Chen, C.; et al. Geology, Environment, and Life in the Deepest Part of the World's Oceans. *Innovation* **2021**, *2*, doi:10.1016/j.xinn.2021.100109.
12. Ramirez-Llodra, E.; Brandt, A.; Danovaro, R.; De Mol, B.; Escobar, E.; German, C.R.; Levin, L.A.; Martinez Arbizu, P.; Menot, L.; Buhl-Mortensen, P.; et al. Deep, Diverse and Definitely Different: Unique Attributes of the World's Largest Ecosystem. *Biogeosciences* **2010**, *7*, 2851–2899, doi:10.5194/bg-7-2851-2010.
13. Danovaro, R.; Corinaldesi, C.; Dell'Anno, A.; Snelgrove, P.V.R. The Deep-Sea under Global Change. *Current Biology* **2017**, *27*, R461–R465, doi:10.1016/j.cub.2017.02.046.
14. Varrella, S.; Tangherlini, M.; Corinaldesi, C. Deep Hypersaline Anoxic Basins as Untapped Reservoir of Polyextremophilic Prokaryotes of Biotechnological Interest. *Marine Drugs* **2020**, *18*, 91, doi:10.3390/md18020091.
15. Wang, F.; Zhang, Y.; Jing, H.; Liu, H. Spatial Variation and Metabolic Diversity of Microbial Communities in the Surface Sediments of the Mariana Trench. *Front Microbiol* **2022**, *13*, 1051999, doi:10.3389/fmicb.2022.1051999.
16. Rizzo, C.; Arcadi, E.; Calogero, R.; Sciutteri, V.; Consoli, P.; Esposito, V.; Canese, S.; Andaloro, F.; Romeo, T. Ecological and Biotechnological Relevance of Mediterranean Hydrothermal Vent Systems. *Minerals* **2022**, *12*, 251, doi:10.3390/min12020251.
17. Sass, A.M.; Sass, H.; Coolen, M.J.L.; Cypionka, H.; Overmann, J. Microbial Communities in the Chemocline of a Hypersaline Deep-Sea Basin (Urania Basin, Mediterranean Sea). *Applied and Environmental Microbiology* **2001**, *67*, 5392–5402, doi:10.1128/AEM.67.12.5392-5402.2001.
18. Convey, P.; Gibson, J.A.E.; Hillenbrand, C.-D.; Hodgson, D.A.; Pugh, P.J.A.; Smellie, J.L.; Stevens, M.I. Antarctic Terrestrial Life – Challenging the History of the Frozen Continent? *Biological Reviews* **2008**, *83*, 103–117, doi:10.1111/j.1469-185X.2008.00034.x.
19. Bargagli, R. Environmental Contamination in Antarctic Ecosystems. *Science of The Total Environment* **2008**, *400*, 212–226, doi:10.1016/j.scitotenv.2008.06.062.
20. Bratchkova, A.; Ivanova, V. Bioactive Metabolites Produced by Microorganisms Collected in Antarctica and the Arctic. *Biotechnology & Biotechnological Equipment* **2011**, *25*, 1–7, doi:10.5504/BBEQ.2011.0116.
21. Mora, C.; Graham, N.A.J.; Nyström, M. Ecological Limitations to the Resilience of Coral Reefs. *Coral Reefs* **2016**, *35*, 1271–1280, doi:10.1007/s00338-016-1479-z.

22. Ainsworth, T.D.; Gates, R.D. Corals' Microbial Sentinels. *Science* **2016**, *352*, 1518–1519, doi:10.1126/science.aad9957.
23. Sweet, M.J.; Bulling, M.T. On the Importance of the Microbiome and Pathobiome in Coral Health and Disease. *Front. Mar. Sci.* **2017**, *4*, doi:10.3389/fmars.2017.00009.
24. Ainsworth, T.D.; Fordyce, A.J.; Camp, E.F. The Other Microeukaryotes of the Coral Reef Microbiome. *Trends in Microbiology* **2017**, *25*, 980–991, doi:10.1016/j.tim.2017.06.007.
25. Rabari, A.; Ruparelia, J.; Jha, Dr.C. Extremophiles: Subsistence of an Extreme Nature Enthusiast. In; 2021 ISBN 978-1-79989-146-8.
26. Hagström, Å.; Pommier, T.; Rohwer, F.; Simu, K.; Stolte, W.; Svensson, D.; Zweifel, U.L. Use of 16S Ribosomal DNA for Delineation of Marine Bacterioplankton Species. *Applied and Environmental Microbiology* **2002**, *68*, 3628–3633, doi:10.1128/AEM.68.7.3628-3633.2002.
27. Huber, H.; Hohn, M.J.; Rachel, R.; Fuchs, T.; Wimmer, V.C.; Stetter, K.O. A New Phylum of Archaea Represented by a Nanosized Hyperthermophilic Symbiont. *Nature* **2002**, *417*, 63–67, doi:10.1038/417063a.
28. Somayaji, A.; Dhanjal, C.R.; Lingamsetty, R.; Vinayagam, R.; Selvaraj, R.; Varadavenkatesan, T.; Govarthanan, M. An Insight into the Mechanisms of Homeostasis in Extremophiles. *Microbiological Research* **2022**, *263*, 127115, doi:10.1016/j.micres.2022.127115.
29. Ksouri, R.; Ksouri, W.M.; Jallali, I.; Debez, A.; Magné, C.; Hiroko, I.; Abdelly, C. Medicinal Halophytes: Potent Source of Health Promoting Biomolecules with Medical, Nutraceutical and Food Applications. *Critical Reviews in Biotechnology* **2012**, *32*, 289–326, doi:10.3109/07388551.2011.630647.
30. Sathyanarayana Reddy, G.; Chattopadhyay, M.K.; Shivaji, S. Biodiversity, Adaptation and Biotechnological Importance of Bacteria Occurring in Cold Climates. In *Biotechnology of Extremophiles: Advances and Challenges*; Rampelotto, P.H., Ed.; Springer International Publishing: Cham, 2016; pp. 47–81 ISBN 978-3-319-13521-2.
31. Chattopadhyay, M.K.; Reddy, G.S.; Shivaji, S. Psychrophilic Bacteria: Biodiversity, Molecular Basis of Cold Adaptation and Biotechnological Implications. *Current Biotechnology 3*, 100–116, doi:10.2174/2211550113026660039.
32. Corinaldesi, C.; Barone, G.; Marcellini, F.; Dell'Anno, A.; Danovaro, R. Marine Microbial-Derived Molecules and Their Potential Use in Cosmeceutical and Cosmetic Products. *Marine Drugs* **2017**, *15*, 118, doi:10.3390/md15040118.
33. Poli, A.; Finore, I.; Romano, I.; Gioiello, A.; Lama, L.; Nicolaus, B. Microbial Diversity in Extreme Marine Habitats and Their Biomolecules. *Microorganisms* **2017**, *5*, 25, doi:10.3390/microorganisms5020025.
34. Dumorné, K.; Severe, R. Marine Enzymes and Their Industrial and Biotechnological Applications. *Minerva Biotecnol* **2018**, *30*, doi:10.23736/S1120-4826.18.02442-4.
35. Zillig, W.; Holz, I.; Klenk, H.-P.; Trent, J.; Wunderl, S.; Janekovic, D.; Imsel, E.; Haas, B. *Pyrococcus Woesei*, Sp. Nov., an Ultra-Thermophilic Marine Archaebacterium, Representing a Novel Order, *Thermococcales*. *Systematic and Applied Microbiology* **1987**, *9*, 62–70, doi:10.1016/S0723-2020(87)80057-7.
36. Panda, A.K.; Bisht, S.S.; De Mandal, S.; Kumar, N.S. Chapter 13 - Microbial Diversity of Thermophiles Through the Lens of Next Generation Sequencing. In *Microbial Diversity in the Genomic Era*; Das, S., Dash, H.R., Eds.; Academic Press, 2019; pp. 217–226 ISBN 978-0-12-814849-5.
37. Kohli, I.; Joshi, N.C.; Mohapatra, S.; Varma, A. Extremophile - An Adaptive Strategy for Extreme Conditions and Applications. *Curr Genomics* **2020**, *21*, 96–110, doi:10.2174/1389202921666200401105908.
38. Laemthong, T.; Lewis, A.M.; Crosby, J.R.; Bing, R.G.; Schneider, W.H.; Willard, D.J.; Counts, J.A.; Kelly, R.M. Chapter 2 - Enzymes from Extremely Thermophilic Bacteria and Archaea: Current Status and Future Prospects. In *Extremozymes and Their Industrial Applications*; Arora, N.K., Agnihotri, S., Mishra, J., Eds.; Academic Press, 2022; pp. 41–84 ISBN 978-0-323-90274-8.
39. Brock, T.D.; Freeze, H. Thermus Aquaticus Gen. n. and Sp. n., a Nonsporulating Extreme Thermophile. *Journal of Bacteriology* **1969**, *98*, 289–297, doi:10.1128/jb.98.1.289-297.1969.
40. Moyer, C.L.; Eric Collins, R.; Morita, R.Y. Psychrophiles and Psychrotrophs. In *Reference Module in Life Sciences*; Elsevier, 2017 ISBN 978-0-12-809633-8.
41. Reed, C.J.; Lewis, H.; Trejo, E.; Winston, V.; Evilia, C. Protein Adaptations in Archaeal Extremophiles. *Archaea* **2013**, *2013*, 373275, doi:10.1155/2013/373275.
42. Collins, T.; Margesin, R. Psychrophilic Lifestyles: Mechanisms of Adaptation and Biotechnological Tools. *Appl Microbiol Biotechnol* **2019**, *103*, 2857–2871, doi:10.1007/s00253-019-09659-5.

43. Cavicchioli, R. On the Concept of a Psychrophile. *The ISME Journal* **2016**, *10*, 793–795, doi:10.1038/ismej.2015.160.
44. Perfumo, A.; Banat, I.M.; Marchant, R. Going Green and Cold: Biosurfactants from Low-Temperature Environments to Biotechnology Applications. *Trends in Biotechnology* **2018**, *36*, 277–289, doi:10.1016/j.tibtech.2017.10.016.
45. Liu, C.; Baffoe, D.K.; Zhan, Y.; Zhang, M.; Li, Y.; Zhang, G. Halophile, an Essential Platform for Bioproduction. *Journal of Microbiological Methods* **2019**, *166*, 105704, doi:10.1016/j.mimet.2019.105704.
46. Gunde-Cimerman, N.; Plemenitaš, A.; Oren, A. Strategies of Adaptation of Microorganisms of the Three Domains of Life to High Salt Concentrations. *FEMS Microbiology Reviews* **2018**, *42*, 353–375, doi:10.1093/femsre/fuy009.
47. Yakimov, M.M.; La Cono, V.; Denaro, R.; D'Auria, G.; Decembrini, F.; Timmis, K.N.; Golyshin, P.N.; Giuliano, L. Primary Producing Prokaryotic Communities of Brine, Interface and Seawater above the Halocline of Deep Anoxic Lake L'Atalante, Eastern Mediterranean Sea. *ISME J* **2007**, *1*, 743–755, doi:10.1038/ismej.2007.83.
48. Pachiadaki, M.G.; Yakimov, M.M.; LaCono, V.; Leadbetter, E.; Edgcomb, V. Unveiling Microbial Activities along the Halocline of Thetis, a Deep-Sea Hypersaline Anoxic Basin. *ISME J* **2014**, *8*, 2478–2489, doi:10.1038/ismej.2014.100.
49. Siam, R.; Mustafa, G.A.; Sharaf, H.; Moustafa, A.; Ramadan, A.R.; Antunes, A.; Bajic, V.B.; Stingl, U.; Marsis, N.G.R.; Coolen, M.J.L.; et al. Unique Prokaryotic Consortia in Geochemically Distinct Sediments from Red Sea Atlantis II and Discovery Deep Brine Pools. *PLOS ONE* **2012**, *7*, e42872, doi:10.1371/journal.pone.0042872.
50. Ziko, L.; Saqr, A.-H.A.; Ouf, A.; Gimpel, M.; Aziz, R.K.; Neubauer, P.; Siam, R. Antibacterial and Anticancer Activities of Orphan Biosynthetic Gene Clusters from Atlantis II Red Sea Brine Pool. *Microbial Cell Factories* **2019**, *18*, 56, doi:10.1186/s12934-019-1103-3.
51. Waditee-Sirisattha, R.; Kageyama, H.; Takabe, T.; Waditee-Sirisattha, R.; Kageyama, H.; Takabe, T. Halophilic Microorganism Resources and Their Applications in Industrial and Environmental Biotechnology. *AIMSMICRO* **2016**, *2*, 42–54, doi:10.3934/microbiol.2016.1.42.
52. Dutta, B.; Bandopadhyay, R. Biotechnological Potentials of Halophilic Microorganisms and Their Impact on Mankind. *Beni-Suef University Journal of Basic and Applied Sciences* **2022**, *11*, 75, doi:10.1186/s43088-022-00252-w.
53. Mokashe, N.; Chaudhari, B.; Patil, U. Operative Utility of Salt-Stable Proteases of Halophilic and Halotolerant Bacteria in the Biotechnology Sector. *International Journal of Biological Macromolecules* **2018**, *117*, 493–522, doi:10.1016/j.ijbiomac.2018.05.217.
54. Diba, H.; Cohan, R.A.; Salimian, M.; Mirjani, R.; Soleimani, M.; Khodabakhsh, F. Isolation and Characterization of Halophilic Bacteria with the Ability of Heavy Metal Bioremediation and Nanoparticle Synthesis from Khara Salt Lake in Iran. *Arch Microbiol* **2021**, *203*, 3893–3903, doi:10.1007/s00203-021-02380-w.
55. Sun, J.; He, X.; Le, Y.; Al-Tohamy, R.; Ali, S.S. Potential Applications of Extremophilic Bacteria in the Bioremediation of Extreme Environments Contaminated with Heavy Metals. *J Environ Manage* **2024**, *352*, 120081, doi:10.1016/j.jenvman.2024.120081.
56. Hurst, D.; Børresen, T.; Almesjö, L.; Raedemaecker, F.; Bergseth, S. *Marine Biotechnology Strategic Research and Innovation Roadmap - Insights to the Future Direction of European Marine Biotechnology*; 2016; ISBN 978-94-92043-27-6.
57. Barre, S.L.; Bates, S.S. *Blue Biotechnology: Production and Use of Marine Molecules*; John Wiley & Sons, 2018; ISBN 978-3-527-34138-2.
58. Rayner, R.; Jolly, C.; Gouldman, C. Ocean Observing and the Blue Economy. *Front. Mar. Sci.* **2019**, *6*, doi:10.3389/fmars.2019.00330.
59. Rotter, A.; Barbier, M.; Bertoni, F.; Bones, A.M.; Cancela, M.L.; Carlsson, J.; Carvalho, M.F.; Cegłowska, M.; Chirivella-Martorell, J.; Conk Dalay, M.; et al. The Essentials of Marine Biotechnology. *Front. Mar. Sci.* **2021**, *8*, doi:10.3389/fmars.2021.629629.
60. Liu, F.; Huang, Y.; Zhang, L.; Li, G. Marine Environmental Pollution, Aquatic Products Trade and Marine Fishery Economy——An Empirical Analysis Based on Simultaneous Equation Model. *Ocean & Coastal Management* **2022**, *222*, 106096, doi:10.1016/j.ocecoaman.2022.106096.
61. Pereira, R.; Oliveira, J.; Sousa, M. Bioinformatics and Computational Tools for Next-Generation Sequencing Analysis in Clinical Genetics. *Journal of Clinical Medicine* **2020**, *9*, 132, doi:10.3390/jcm9010132.

62. Wang, Y.; Zhao, Y.; Bollas, A.; Wang, Y.; Au, K.F. Nanopore Sequencing Technology, Bioinformatics and Applications. *Nat Biotechnol* **2021**, *39*, 1348–1365, doi:10.1038/s41587-021-01108-x.
63. Khalifa, S.A.M.; Elias, N.; Farag, M.A.; Chen, L.; Saeed, A.; Hegazy, M.-E.F.; Moustafa, M.S.; Abd El-Wahed, A.; Al-Mousawi, S.M.; Musharraf, S.G.; et al. Marine Natural Products: A Source of Novel Anticancer Drugs. *Marine Drugs* **2019**, *17*, 491, doi:10.3390/md17090491.
64. Daniotti, S.; Re, I. Marine Biotechnology: Challenges and Development Market Trends for the Enhancement of Biotic Resources in Industrial Pharmaceutical and Food Applications. A Statistical Analysis of Scientific Literature and Business Models. *Marine Drugs* **2021**, *19*, 61, doi:10.3390/md19020061.
65. Huang, L.; Ling, X.; Peng, S.; Tan, M.; Yan, L.; Liang, Y.; Li, G.; Li, K. A Marine Lipopeptides-Producing Bacillus Amyloliquefaciens HY2-1 with a Broad-Spectrum Antifungal and Antibacterial Activity and Its Fermentation Kinetics Study. *World J Microbiol Biotechnol* **2023**, *39*, 196, doi:10.1007/s11274-023-03643-y.
66. Andryukov, B.; Mikhailov, V.; Besednova, N. The Biotechnological Potential of Secondary Metabolites from Marine Bacteria. *Journal of Marine Science and Engineering* **2019**, *7*, 176, doi:10.3390/jmse7060176.
67. Srinivasan, R.; Kannappan, A.; Shi, C.; Lin, X. Marine Bacterial Secondary Metabolites: A Treasure House for Structurally Unique and Effective Antimicrobial Compounds. *Marine Drugs* **2021**, *19*, 530, doi:10.3390/md19100530.
68. Fouillaud, M.; Dufossé, L. Microbial Secondary Metabolism and Biotechnology. *Microorganisms* **2022**, *10*, 123, doi:10.3390/microorganisms10010123.
69. Shinde, P.; Banerjee, P.; Mandhare, A. Marine Natural Products as Source of New Drugs: A Patent Review (2015–2018). *Expert Opinion on Therapeutic Patents* **2019**, *29*, 283–309, doi:10.1080/13543776.2019.1598972.
70. Rosic, N.N. Recent Advances in the Discovery of Novel Marine Natural Products and Mycosporine-like Amino Acid UV-Absorbing Compounds. *Appl Microbiol Biotechnol* **2021**, *105*, 7053–7067, doi:10.1007/s00253-021-11467-9.
71. Carroll, A.R.; Copp, B.R.; Davis, R.A.; Keyzers, R.A.; Prinsep, M.R. Marine Natural Products. *Nat Prod Rep* **2022**, *39*, 1122–1171, doi:10.1039/d1np00076d.
72. Blunt, J.W.; Carroll, A.R.; Copp, B.R.; Davis, R.A.; Keyzers, R.A.; Prinsep, M.R. Marine Natural Products. *Nat. Prod. Rep.* **2018**, *35*, 8–53, doi:10.1039/C7NP00052A.
73. Banday, A.H.; Azha, N. ul; Farooq, R.; Sheikh, S.A.; Ganie, M.A.; Parray, M.N.; Mushtaq, H.; Hameed, I.; Lone, M.A. Exploring the Potential of Marine Natural Products in Drug Development: A Comprehensive Review. *Phytochemistry Letters* **2024**, *59*, 124–135, doi:10.1016/j.phytol.2024.01.001.
74. Rinehart, K.L.; Holt, T.G.; Fregeau, N.L.; Stroh, J.G.; Keifer, P.A.; Sun, F.; Li, L.H.; Martin, D.G. Ecteinascidins 729, 743, 745, 759A, 759B, and 770: Potent Antitumor Agents from the Caribbean Tunicate Ecteinascidia Turbinata. *J. Org. Chem.* **1990**, *55*, 4512–4515, doi:10.1021/jo00302a007.
75. D'Incalci, M.; Badri, N.; Galmarini, C.M.; Allavena, P. Trabectedin, a Drug Acting on Both Cancer Cells and the Tumour Microenvironment. *Br J Cancer* **2014**, *111*, 646–650, doi:10.1038/bjc.2014.149.
76. Feling, R.H.; Buchanan, G.O.; Mincer, T.J.; Kauffman, C.A.; Jensen, P.R.; Fenical, W. Salinosporamide A: A Highly Cytotoxic Proteasome Inhibitor from a Novel Microbial Source, a Marine Bacterium of the New Genus Salinospora. *Angewandte Chemie International Edition* **2003**, *42*, 355–357, doi:10.1002/anie.200390115.
77. Sparidans, R.W.; Henrar, R.E.C.; Jimeno, J.M.; Faircloth, G.; Floriano, P.; Beijnen, J.H. Bioanalysis of Thiocoraline, a New Marine Antitumoral Depsipeptide, in Plasma by High-Performance Liquid Chromatography and Fluorescence Detection. *Journal of Chromatography B: Biomedical Sciences and Applications* **1999**, *726*, 255–260, doi:10.1016/S0378-4347(99)00062-6.
78. Martins, A.; Vieira, H.; Gaspar, H.; Santos, S. Marketed Marine Natural Products in the Pharmaceutical and Cosmeceutical Industries: Tips for Success. *Marine Drugs* **2014**, *12*, 1066–1101, doi:10.3390/md12021066.
79. Desai, R.; Vyas, T.K. Role of Biosurfactants Produced by Marine Microbes in Bioremediation. In *Marine Surfactants*; CRC Press, 2022 ISBN 978-1-00-330746-4.
80. Kubicki, S.; Bollinger, A.; Katzke, N.; Jaeger, K.-E.; Loeschcke, A.; Thies, S. Marine Biosurfactants: Biosynthesis, Structural Diversity and Biotechnological Applications. *Marine Drugs* **2019**, *17*, 408, doi:10.3390/md17070408.

81. Ali, N.; Pang, Z.; Wang, F.; Xu, B.; El-Seedi, H.R. Lipopeptide Biosurfactants from Bacillus Spp.: Types, Production, Biological Activities, and Applications in Food. *Journal of Food Quality* **2022**, *2022*, 3930112, doi:10.1155/2022/3930112.
82. Jahan, R.; Bodratti, A.M.; Tsianou, M.; Alexandridis, P. Biosurfactants, Natural Alternatives to Synthetic Surfactants: Physicochemical Properties and Applications. *Advances in Colloid and Interface Science* **2020**, *275*, 102061, doi:10.1016/j.cis.2019.102061.
83. Madankar, C.S.; Meshram, A. Review on Classification, Physicochemical Properties and Applications of Microbial Surfactants. *Tenside Surfactants Detergents* **2022**, *59*, 1–16, doi:10.1515/tsd-2021-2353.
84. Ron, E.Z.; Rosenberg, E. Natural Roles of Biosurfactants. *Environ Microbiol* **2001**, *3*, 229–236, doi:10.1046/j.1462-2920.2001.00190.x.
85. Kumar, A.; Singh, S.K.; Kant, C.; Verma, H.; Kumar, D.; Singh, P.P.; Modi, A.; Droby, S.; Kesawat, M.S.; Alavilli, H.; et al. Microbial Biosurfactant: A New Frontier for Sustainable Agriculture and Pharmaceutical Industries. *Antioxidants* **2021**, *10*, 1472, doi:10.3390/antiox10091472.
86. Van Hamme, J.D.; Singh, A.; Ward, O.P. Physiological Aspects: Part 1 in a Series of Papers Devoted to Surfactants in Microbiology and Biotechnology. *Biotechnology Advances* **2006**, *24*, 604–620, doi:10.1016/j.biotechadv.2006.08.001.
87. Darvishi, P.; Ayatollahi, S.; Mowla, D.; Niazi, A. Biosurfactant Production under Extreme Environmental Conditions by an Efficient Microbial Consortium, ERCPPI-2. *Colloids and Surfaces B: Biointerfaces* **2011**, *84*, 292–300, doi:10.1016/j.colsurfb.2011.01.011.
88. Bezerra, K.G.O.; Rufino, R.D.; Luna, J.M.; Sarubbo, L.A. Saponins and Microbial Biosurfactants: Potential Raw Materials for the Formulation of Cosmetics. *Biotechnology Progress* **2018**, *34*, 1482–1493, doi:10.1002/btpr.2682.
89. Esmaeili, H.; Mousavi, S.M.; Hashemi, S.A.; Lai, C.W.; Chiang, W.-H.; Bahrani, S. Chapter 7 - Application of Biosurfactants in the Removal of Oil from Emulsion. In *Green Sustainable Process for Chemical and Environmental Engineering and Science*; Inamuddin, Adetunji, C.O., Eds.; Elsevier, 2021; pp. 107–127 ISBN 978-0-12-822696-4.
90. Vecino, X.; Rodríguez-López, L.; Gudiña, E.J.; Cruz, J.M.; Moldes, A.B.; Rodrigues, L.R. Vineyard Pruning Waste as an Alternative Carbon Source to Produce Novel Biosurfactants by *Lactobacillus Paracasei*. *Journal of Industrial and Engineering Chemistry* **2017**, *55*, 40–49, doi:10.1016/j.jiec.2017.06.014.
91. Gomaa, E.Z.; El-Meihy, R.M. Bacterial Biosurfactant from Citrobacter Freundii MG812314.1 as a Bioremoval Tool of Heavy Metals from Wastewater. *Bull Natl Res Cent* **2019**, *43*, 69, doi:10.1186/s42269-019-0088-8.
92. Solanki, J.D.; Patel, D.T.; Patel, K.C.; Nataraj, M. Chapter 10 - Production of Biosurfactants Using Agroindustrial Wastes as Substrates. In *Green Sustainable Process for Chemical and Environmental Engineering and Science*; Inamuddin, Adetunji, C.O., Eds.; Elsevier, 2021; pp. 185–210 ISBN 978-0-12-822696-4.
93. Banat, I.M.; Satpute, S.K.; Cameotra, S.S.; Patil, R.; Nyayanit, N.V. Cost Effective Technologies and Renewable Substrates for Biosurfactants' Production. *Frontiers in Microbiology* **2014**, *5*, doi:10.3389/fmicb.2014.00697.
94. Ramalingam, V.; Varunkumar, K.; Ravikumar, V.; Rajaram, R. Production and Structure Elucidation of Anticancer Potential Surfactin from Marine Actinomycete *Micromonospora Marina*. *Process Biochemistry* **2019**, *78*, 169–177, doi:10.1016/j.procbio.2019.01.002.
95. Palma Esposito, F.; Giugliano, R.; Della Sala, G.; Vitale, G.A.; Buonocore, C.; Ausuri, J.; Galasso, C.; Coppola, D.; Franci, G.; Galdiero, M.; et al. Combining OSMAC Approach and Untargeted Metabolomics for the Identification of New Glycolipids with Potent Antiviral Activity Produced by a Marine Rhodococcus. *Int J Mol Sci* **2021**, *22*, 9055, doi:10.3390/ijms22169055.
96. Ibacache-Quiroga, C.; Ojeda, J.; Espinoza-Vergara, G.; Olivero, P.; Cuellar, M.; Dinamarca, M.A. The Hydrocarbon-Degrading Marine Bacterium Obetia Sp. Strain MM1IDA2H-1 Produces a Biosurfactant That Interferes with Quorum Sensing of Fish Pathogens by Signal Hijacking. *Microbial Biotechnology* **2013**, *6*, 394–405, doi:10.1111/1751-7915.12016.
97. Twigg, M.S.; Tripathi, L.; Zompra, A.; Salek, K.; Irorere, V.U.; Gutierrez, T.; Spyroulias, G.A.; Marchant, R.; Banat, I.M. Identification and Characterisation of Short Chain Rhamnolipid Production in a Previously Uninvestigated, Non-Pathogenic Marine Pseudomonad. *Appl Microbiol Biotechnol* **2018**, *102*, 8537–8549, doi:10.1007/s00253-018-9202-3.
98. Buonocore, C.; Giugliano, R.; Della Sala, G.; Palma Esposito, F.; Tedesco, P.; Folliero, V.; Galdiero, M.; Franci, G.; de Pascale, D. Evaluation of Antimicrobial Properties and Potential Applications of

Pseudomonas Gessardii M15 Rhamnolipids towards Multiresistant Staphylococcus Aureus. *Pharmaceutics* **2023**, *15*, 700, doi:10.3390/pharmaceutics15020700.

99. Abdel-Mawgoud, A.M.; Lépine, F.; Déziel, E. Rhamnolipids: Diversity of Structures, Microbial Origins and Roles. *Appl Microbiol Biotechnol* **2010**, *86*, 1323–1336, doi:10.1007/s00253-010-2498-2.
100. Wittgens, A.; Santiago-Schuebel, B.; Henkel, M.; Tiso, T.; Blank, L.M.; Hausmann, R.; Hofmann, D.; Wilhelm, S.; Jaeger, K.-E.; Rosenau, F. Heterologous Production of Long-Chain Rhamnolipids from Burkholderia Glumae in Pseudomonas Putida—a Step Forward to Tailor-Made Rhamnolipids. *Appl Microbiol Biotechnol* **2018**, *102*, 1229–1239, doi:10.1007/s00253-017-8702-x.
101. Janek, T.; Krasowska, A.; Czyżnikowska, Ż.; Łukaszewicz, M. Trehalose Lipid Biosurfactant Reduces Adhesion of Microbial Pathogens to Polystyrene and Silicone Surfaces: An Experimental and Computational Approach. *Front. Microbiol.* **2018**, *9*, doi:10.3389/fmicb.2018.02441.
102. Henkel, M.; Hausmann, R. Chapter 2 - Diversity and Classification of Microbial Surfactants. In *Biobased Surfactants (Second Edition)*; Hayes, D.G., Solaiman, D.K.Y., Ashby, R.D., Eds.; AOCS Press, 2019; pp. 41–63 ISBN 978-0-12-812705-6.
103. Ali, N.; Pang, Z.; Wang, F.; Xu, B.; El-Seedi, H.R. Lipopeptide Biosurfactants from Bacillus Spp.: Types, Production, Biological Activities, and Applications in Food. *Journal of Food Quality* **2022**, *2022*, 3930112, doi:10.1155/2022/3930112.
104. Arima, K.; Kakinuma, A.; Tamura, G. Surfactin, a Crystalline Peptidelipid Surfactant Produced by Bacillus<math><mtext>Bacillus</Mtext></Math>subtilis<math><mtext>subtilis</Mtext></Math>: Isolation, Characterization and Its Inhibition of Fibrin Clot Formation. *Biochemical and Biophysical Research Communications* **1968**, *31*, 488–494, doi:10.1016/0006-291X(68)90503-2.
105. Anestopoulos, I.; Kiousi, D.-E.; Klavaris, A.; Maijo, M.; Serpico, A.; Suarez, A.; Sanchez, G.; Salek, K.; Chasapi, S.A.; Zompra, A.A.; et al. Marine-Derived Surface Active Agents: Health-Promoting Properties and Blue Biotechnology-Based Applications. *Biomolecules* **2020**, *10*, 885, doi:10.3390/biom10060885.
106. Ding, W.; Li, Y.; Chen, M.; Chen, R.; Tian, X.; Yin, H.; Zhang, S. Structures and Antitumor Activities of Ten New and Twenty Known Surfactins from the Deep-Sea Bacterium *Limimaricola* Sp. SCSIO 53532. *Bioorganic Chemistry* **2022**, *120*, 105589, doi:10.1016/j.bioorg.2021.105589.
107. Ma, Z.; Zhang, S.; Zhang, S.; Wu, G.; Shao, Y.; Mi, Q.; Liang, J.; Sun, K.; Hu, J. Isolation and Characterization of a New Cyclic Lipopeptide Surfactin from a Marine-Derived Bacillus Velezensis SH-B74. *J Antibiot* **2020**, *73*, 863–867, doi:10.1038/s41429-020-0347-9.
108. Farias, C.B.B.; Almeida, F.C.G.; Silva, I.A.; Souza, T.C.; Meira, H.M.; Soares da Silva, R. de C.F.; Luna, J.M.; Santos, V.A.; Converti, A.; Banat, I.M.; et al. Production of Green Surfactants: Market Prospects. *Electronic Journal of Biotechnology* **2021**, *51*, 28–39, doi:10.1016/j.ejbt.2021.02.002.
109. Xiao, S.; Chen, N.; Chai, Z.; Zhou, M.; Xiao, C.; Zhao, S.; Yang, X. Secondary Metabolites from Marine-Derived Bacillus: A Comprehensive Review of Origins, Structures, and Bioactivities. *Marine Drugs* **2022**, *20*, 567, doi:10.3390/md20090567.
110. Bernheimer, A.W.; Avigad, L.S. Nature and Properties of a Cytolytic Agent Produced by Bacillus Subtilis. *Microbiology* **1970**, *61*, 361–369, doi:10.1099/00221287-61-3-361.
111. Carrillo, P.G.; Mardaraz, C.; Pitta-Alvarez, S.I.; Giulietti, A.M. Isolation and Selection of Biosurfactant-Producing Bacteria. *World J Microbiol Biotechnol* **1996**, *12*, 82–84, doi:10.1007/BF00327807.
112. Youssef, N.H.; Duncan, K.E.; Nagle, D.P.; Savage, K.N.; Knapp, R.M.; McInerney, M.J. Comparison of Methods to Detect Biosurfactant Production by Diverse Microorganisms. *Journal of Microbiological Methods* **2004**, *56*, 339–347, doi:10.1016/j.mimet.2003.11.001.
113. Jain, D.K.; Collins-Thompson, D.L.; Lee, H.; Trevors, J.T. A Drop-Collapsing Test for Screening Surfactant-Producing Microorganisms. *Journal of Microbiological Methods* **1991**, *13*, 271–279, doi:10.1016/0167-7012(91)90064-W.
114. Płaza, G.A.; Zjawiony, I.; Banat, I.M. Use of Different Methods for Detection of Thermophilic Biosurfactant-Producing Bacteria from Hydrocarbon-Contaminated and Bioremediated Soils. *Journal of Petroleum Science and Engineering* **2006**, *50*, 71–77, doi:10.1016/j.petrol.2005.10.005.
115. Morikawa, M.; Hirata, Y.; Imanaka, T. A Study on the Structure–Function Relationship of Lipopeptide Biosurfactants. *Biochimica et Biophysica Acta (BBA) - Molecular and Cell Biology of Lipids* **2000**, *1488*, 211–218, doi:10.1016/S1388-1981(00)00124-4.
116. Bosch, P.; Robert, M.; Mercade, M.; Espuny, M.; Parra, J.; Guinea, J. Surface Active Compounds on Microbial Cultures. *Tenside Surfactants Detergents* **1988**, *25*, 208–211, doi:10.1515/tsd-1988-250402.

117. Willumsen, P.A.; Karlson, U. Screening of Bacteria, Isolated from PAH-Contaminated Soils, for Production of Biosurfactants and Bioemulsifiers. *Biodegradation* **1996**, *7*, 415–423, doi:10.1007/BF00056425.
118. Christova, N.; Tuleva, B.; Lalchev, Z.; Jordanova, A.; Jordanov, B. Rhamnolipid Biosurfactants Produced by Renibacterium Salmoninarum 27BN During Growth on N-Hexadecane. *Zeitschrift für Naturforschung C* **2004**, *59*, 70–74, doi:10.1515/znc-2004-1-215.
119. Siegmund, I.; Wagner, F. New Method for Detecting Rhamnolipids Excreted byPseudomonas Species during Growth on Mineral Agar. *Biotechnol Tech* **1991**, *5*, 265–268, doi:10.1007/BF02438660.
120. Gunther, N.W.; Nuñez, A.; Fett, W.; Solaiman, D.K.Y. Production of Rhamnolipids by Pseudomonas Chlororaphis, a Nonpathogenic Bacterium. *Applied and Environmental Microbiology* **2005**, *71*, 2288–2293, doi:10.1128/AEM.71.5.2288-2293.2005.
121. Sarubbo, L.A.; Silva, M. da G.C.; Durval, I.J.B.; Bezerra, K.G.O.; Ribeiro, B.G.; Silva, I.A.; Twigg, M.S.; Banat, I.M. Biosurfactants: Production, Properties, Applications, Trends, and General Perspectives. *Biochemical Engineering Journal* **2022**, *181*, 108377, doi:10.1016/j.bej.2022.108377.
122. Nagtode, V.S.; Cardoza, C.; Yasin, H.K.A.; Mali, S.N.; Tambe, S.M.; Roy, P.; Singh, K.; Goel, A.; Amin, P.D.; Thorat, B.R.; et al. Green Surfactants (Biosurfactants): A Petroleum-Free Substitute for Sustainability—Comparison, Applications, Market, and Future Prospects. *ACS Omega* **2023**, *8*, 11674–11699, doi:10.1021/acsomega.3c00591.
123. Ingsel, T.; de Souza, F.M.; Gupta, R.K. Chapter 25 - Biosurfactants for Industrial Applications. In *Green Sustainable Process for Chemical and Environmental Engineering and Science*; Inamuddin, Adetunji, C.O., Ahamed, M.I., Eds.; Academic Press, 2022; pp. 467–493 ISBN 978-0-323-85146-6.
124. Yakimov, M.M.; Timmis, K.N.; Golyshin, P.N. Obligate Oil-Degrading Marine Bacteria. *Current Opinion in Biotechnology* **2007**, *18*, 257–266, doi:10.1016/j.copbio.2007.04.006.
125. Deng, M.-C.; Li, J.; Liang, F.-R.; Yi, M.; Xu, X.-M.; Yuan, J.-P.; Peng, J.; Wu, C.-F.; Wang, J.-H. Isolation and Characterization of a Novel Hydrocarbon-Degrading Bacterium Achromobacter Sp. HZ01 from the Crude Oil-Contaminated Seawater at the Daya Bay, Southern China. *Mar Pollut Bull* **2014**, *83*, 79–86, doi:10.1016/j.marpolbul.2014.04.018.
126. Ramasamy, S.P.; Sundararajan, P.; Pallikondaperumal, M.; Karuppiah, P.; Kayarohanam, S.; Arumugam, N.; Wong, L.S.; Djearamane, S. Copper and Chromium Binding by *Pseudomonas Aeruginosa* Strain PA01 for Implications of Heavy Metal Detoxification and Soil Remediation: A Computational Approach. *Journal of King Saud University - Science* **2024**, *36*, 103552, doi:10.1016/j.jksus.2024.103552.
127. Khire, J.M. Bacterial Biosurfactants, and Their Role in Microbial Enhanced Oil Recovery (MEOR). In *Biosurfactants*; Sen, R., Ed.; Springer: New York, NY, 2010; pp. 146–157 ISBN 978-1-4419-5979-9.
128. Nasser, M.; Sharma, M.; Kaur, G. Advances in the Production of Biosurfactants as Green Ingredients in Home and Personal Care Products. *Front. Chem.* **2024**, *12*, doi:10.3389/fchem.2024.1382547.
129. Bouassida, M.; Fourati, N.; Ghazala, I.; Ellouze-Chaabouni, S.; Ghribi, D. Potential Application of Bacillus Subtilis SPB1 Biosurfactants in Laundry Detergent Formulations: Compatibility Study with Detergent Ingredients and Washing Performance. *Engineering in Life Sciences* **2018**, *18*, 70–77, doi:10.1002/elsc.201700152.
130. Fei, D.; Zhou, G.-W.; Yu, Z.-Q.; Gang, H.-Z.; Liu, J.-F.; Yang, S.-Z.; Ye, R.-Q.; Mu, B.-Z. Low-Toxic and Nonirritant Biosurfactant Surfactin and Its Performances in Detergent Formulations. *Journal of Surfactants and Detergents* **2020**, *23*, 109–118, doi:10.1002/jsde.12356.
131. Morita, T.; Fukuoka, T.; Imura, T.; Kitamoto, D. Production of Mannosylerythritol Lipids and Their Application in Cosmetics. *Appl Microbiol Biotechnol* **2013**, *97*, 4691–4700, doi:10.1007/s00253-013-4858-1.
132. Stincone, P.; Brandelli, A. Marine Bacteria as Source of Antimicrobial Compounds. *Critical Reviews in Biotechnology* **2020**, *40*, 306–319, doi:10.1080/07388551.2019.1710457.
133. Lowy, F.D. Antimicrobial Resistance: The Example of Staphylococcus Aureus. *J Clin Invest* **2003**, *111*, 1265–1273, doi:10.1172/JCI18535.
134. Ng, I.-S.; Ye, C.; Zhang, Z.; Lu, Y.; Jing, K. Daptomycin Antibiotic Production Processes in Fed-Batch Fermentation by Streptomyces Roseosporus NRRL11379 with Precursor Effect and Medium Optimization. *Bioprocess Biosyst Eng* **2014**, *37*, 415–423, doi:10.1007/s00449-013-1007-2.
135. Ribeiro, R.; Pinto, E.; Fernandes, C.; Sousa, E. Marine Cyclic Peptides: Antimicrobial Activity and Synthetic Strategies. *Mar Drugs* **2022**, *20*, 397, doi:10.3390/md20060397.
136. Subramaniam, M.D.; Venkatesan, D.; Iyer, M.; Subbarayan, S.; Govindasami, V.; Roy, A.; Narayanasamy, A.; Kamalakannan, S.; Gopalakrishnan, A.V.; Thangarasu, R.; et al. Biosurfactants

and Anti-Inflammatory Activity: A Potential New Approach towards COVID-19. *Curr Opin Environ Sci Health* **2020**, *17*, 72–81, doi:10.1016/j.coesh.2020.09.002.
137. Imtiaz, S.; Bashir, M.; Banoo, S.; Ahamed, M.I.; Anwar, N. Chapter 26 - Antitumor and Anticancer Activity of Biosurfactant. In *Green Sustainable Process for Chemical and Environmental Engineering and Science*; Inamuddin, Adetunji, C.O., Ahamed, M.I., Eds.; Academic Press, 2022; pp. 495–513 ISBN 978-0-323-85146-6.
138. Wang, X.; An, J.; Cao, T.; Guo, M.; Han, F. Application of Biosurfactants in Medical Sciences. *Molecules* **2024**, *29*, 2606, doi:10.3390/molecules29112606.
139. Mishra, B.; Lushnikova, T.; Wang, G. Small Lipopeptides Possess Anti-Biofilm Capability Comparable to Daptomycin and Vancomycin. *RSC Adv* **2015**, *5*, 59758–59769, doi:10.1039/C5RA07896B.
140. Diaz De Rienzo, M.A.; Stevenson, P.S.; Marchant, R.; Banat, I.M. Effect of Biosurfactants on Pseudomonas Aeruginosa and Staphylococcus Aureus Biofilms in a BioFlux Channel. *Appl Microbiol Biotechnol* **2016**, *100*, 5773–5779, doi:10.1007/s00253-016-7310-5.
141. Baptista, R.C.; Horita, C.N.; Sant'Ana, A.S. Natural Products with Preservative Properties for Enhancing the Microbiological Safety and Extending the Shelf-Life of Seafood: A Review. *Food Research International* **2020**, *127*, 108762, doi:10.1016/j.foodres.2019.108762.
142. Mnif, I.; Ghribi, D. Glycolipid Biosurfactants: Main Properties and Potential Applications in Agriculture and Food Industry. *Journal of the Science of Food and Agriculture* **2016**, *96*, 4310–4320, doi:10.1002/jsfa.7759.
143. Nitschke, M.; Costa, S.G.V.A.O. Biosurfactants in Food Industry. *Trends in Food Science & Technology* **2007**, *18*, 252–259, doi:10.1016/j.tifs.2007.01.002.
144. Molina-González, D.; Alonso-Calleja, C.; Alonso-Hernando, A.; Capita, R. Effect of Sub-Lethal Concentrations of Biocides on the Susceptibility to Antibiotics of Multi-Drug Resistant *Salmonella Enterica* Strains. *Food Control* **2014**, *40*, 329–334, doi:10.1016/j.foodcont.2013.11.046.
145. Olaimat, A.N.; Al-Holy, M.A.; Shahbaz, H.M.; Al-Nabulsi, A.A.; Abu Ghoush, M.H.; Osaili, T.M.; Ayyash, M.M.; Holley, R.A. Emergence of Antibiotic Resistance in Listeria Monocytogenes Isolated from Food Products: A Comprehensive Review. *Compr Rev Food Sci Food Saf* **2018**, *17*, 1277–1292, doi:10.1111/1541-4337.12387.
146. Osek, J.; Lachtara, B.; Wieczorek, K. Listeria Monocytogenes – How This Pathogen Survives in Food-Production Environments? *Front. Microbiol.* **2022**, *13*, doi:10.3389/fmicb.2022.866462.
147. Garibaldi, J.A.; Neilands, J.B. Formation of Iron-Binding Compounds by Micro-Organisms. *Nature* **1956**, *177*, 526–527, doi:10.1038/177526a0.
148. Neilands, J.B. Siderophores. *Archives of Biochemistry and Biophysics* **1993**, *302*, 1–3, doi:10.1006/abbi.1993.1172.
149. Prabhakar, P.K. Bacterial Siderophores and Their Potential Applications: A Review. *Current Molecular Pharmacology* **2020**, *13*, 295–305, doi:10.2174/1874467213666200518094445.
150. Butler, A. Marine Microbial Siderophores: Reactivity and Structural Diversity. *The chemist* **2022**.
151. Zhang, G.; Amin, S.A.; Küpper, F.C.; Holt, P.D.; Carrano, C.J.; Butler, A. Ferric Stability Constants of Representative Marine Siderophores: Marinobactins, Aquachelins, and Petrobactin. *Inorg. Chem.* **2009**, *48*, 11466–11473, doi:10.1021/ic901739m.
152. Timofeeva, A.M.; Galyamova, M.R.; Sedykh, S.E. Bacterial Siderophores: Classification, Biosynthesis, Perspectives of Use in Agriculture. *Plants* **2022**, *11*, 3065, doi:10.3390/plants11223065.
153. Kramer, J.; Özkaya, Ö.; Kümmerli, R. Bacterial Siderophores in Community and Host Interactions. *Nat Rev Microbiol* **2020**, *18*, 152–163, doi:10.1038/s41579-019-0284-4.
154. Ahmed, E.; Holmström, S.J.M. Siderophores in Environmental Research: Roles and Applications. *Microbial Biotechnology* **2014**, *7*, 196–208, doi:10.1111/1751-7915.12117.
155. Raymond, K.N.; Dertz, E.A.; Kim, S.S. Enterobactin: An Archetype for Microbial Iron Transport. *Proceedings of the National Academy of Sciences* **2003**, *100*, 3584–3588, doi:10.1073/pnas.0630018100.
156. Saha, M.; Sarkar, S.; Sarkar, B.; Sharma, B.K.; Bhattacharjee, S.; Tribedi, P. Microbial Siderophores and Their Potential Applications: A Review. *Environ Sci Pollut Res* **2016**, *23*, 3984–3999, doi:10.1007/s11356-015-4294-0.
157. Nielsen, A.; Mansson, M.; Wietz, M.; Varming, A.N.; Phipps, R.K.; Larsen, T.O.; Gram, L.; Ingmer, H. Nigribactin, a Novel Siderophore from Vibrio Nigripulchritudo, Modulates Staphylococcus Aureus Virulence Gene Expression. *Mar Drugs* **2012**, *10*, 2584–2595, doi:10.3390/md10112584.

158. Mawji, E.; Gledhill, M.; Milton, J.A.; Tarran, G.A.; Ussher, S.; Thompson, A.; Wolff, G.A.; Worsfold, P.J.; Achterberg, E.P. Hydroxamate Siderophores: Occurrence and Importance in the Atlantic Ocean. *Environ. Sci. Technol.* **2008**, *42*, 8675–8680, doi:10.1021/es801884r.
159. Martinez, J.S.; Butler, A. Marine Amphiphilic Siderophores: Marinobactin Structure, Uptake, and Microbial Partitioning. *Journal of Inorganic Biochemistry* **2007**, *101*, 1692–1698, doi:10.1016/j.jinorgbio.2007.07.007.
160. Amin, S.A.; Green, D.H.; Küpper, F.C.; Carrano, C.J. Vibrioferrin, an Unusual Marine Siderophore: Iron Binding, Photochemistry, and Biological Implications. *Inorg. Chem.* **2009**, *48*, 11451–11458, doi:10.1021/ic9016883.
161. Berti, A.D.; Thomas, M.G. Analysis of Achromobactin Biosynthesis by Pseudomonas Syringae Pv. Syringae B728a. *J Bacteriol* **2009**, *191*, 4594–4604, doi:10.1128/JB.00457-09.
162. Visca, P.; Imperi, F.; Lamont, I. Visca P, Imperi F, Lamont I.. Pyoverdine Siderophores: From Biogenesis to Biosignificance. Trends Microbiol 15: 22-30. *Trends in microbiology* **2007**, *15*, 22–30, doi:10.1016/j.tim.2006.11.004.
163. Brandel, J.; Humbert, N.; Elhabiri, M.; Schalk, I.J.; Mislin, G.L.A.; Albrecht-Gary, A.-M. Pyochelin, a Siderophore of Pseudomonas Aeruginosa: Physicochemical Characterization of the Iron(III), Copper(II) and Zinc(II) Complexes. *Dalton Trans.* **2012**, *41*, 2820–2834, doi:10.1039/C1DT11804H.
164. Adler, C.; Corbalán, N.S.; Seyedsayamdost, M.R.; Pomares, M.F.; Cristóbal, R.E. de; Clardy, J.; Kolter, R.; Vincent, P.A. Catecholate Siderophores Protect Bacteria from Pyochelin Toxicity. *PLOS ONE* **2012**, *7*, e46754, doi:10.1371/journal.pone.0046754.
165. Albelda-Berenguer, M.; Monachon, M.; Joseph, E. Chapter Five - Siderophores: From Natural Roles to Potential Applications. In *Advances in Applied Microbiology*; Gadd, G.M., Sariaslani, S., Eds.; Academic Press, 2019; Vol. 106, pp. 193–225.
166. Martinez, J.S.; Zhang, G.P.; Holt, P.D.; Jung, H.-T.; Carrano, C.J.; Haygood, M.G.; Butler, A. Self-Assembling Amphiphilic Siderophores from Marine Bacteria. *Science* **2000**, *287*, 1245–1247, doi:10.1126/science.287.5456.1245.
167. Butler, A.; Harder, T.; Ostrowski, A.D.; Carrano, C.J. Photoactive Siderophores: Structure, Function and Biology. *Journal of Inorganic Biochemistry* **2021**, *221*, 111457, doi:10.1016/j.jinorgbio.2021.111457.
168. Gauglitz, J.M.; Zhou, H.; Butler, A. A Suite of Citrate-Derived Siderophores from a Marine *Vibrio* Species Isolated Following the Deepwater Horizon Oil Spill. *Journal of Inorganic Biochemistry* **2012**, *107*, 90–95, doi:10.1016/j.jinorgbio.2011.10.013.
169. Homann, V.V.; Sandy, M.; Tincu, J.A.; Templeton, A.S.; Tebo, B.M.; Butler, A. Loihichelins A−F, a Suite of Amphiphilic Siderophores Produced by the Marine Bacterium Halomonas LOB-5. *J. Nat. Prod.* **2009**, *72*, 884–888, doi:10.1021/np800640h.
170. Gauglitz, J.M.; Butler, A. Amino Acid Variability in the Peptide Composition of a Suite of Amphiphilic Peptide Siderophores from an Open Ocean Vibrio Species. *J Biol Inorg Chem* **2013**, *18*, 489–497, doi:10.1007/s00775-013-0995-3.
171. Schwyn, B.; Neilands, J.B. Universal Chemical Assay for the Detection and Determination of Siderophores. *Anal Biochem* **1987**, *160*, 47–56, doi:10.1016/0003-2697(87)90612-9.
172. Ghosh, S.K.; Bera, T.; Chakrabarty, A.M. Microbial Siderophore – A Boon to Agricultural Sciences. *Biological Control* **2020**, *144*, 104214, doi:10.1016/j.biocontrol.2020.104214.
173. Milagres, A.M.; Machuca, A.; Napoleão, D. Detection of Siderophore Production from Several Fungi and Bacteria by a Modification of Chrome Azurol S (CAS) Agar Plate Assay. *J Microbiol Methods* **1999**, *37*, 1–6, doi:10.1016/s0167-7012(99)00028-7.
174. Shin, S.H.; Lim, Y.; Lee, S.E.; Yang, N.W.; Rhee, J.H. CAS Agar Diffusion Assay for the Measurement of Siderophores in Biological Fluids. *Journal of Microbiological Methods* **2001**, *44*, 89–95, doi:10.1016/S0167-7012(00)00229-3.
175. Pérez-Miranda, S.; Cabirol, N.; George-Téllez, R.; Zamudio-Rivera, L.S.; Fernández, F.J. O-CAS, a Fast and Universal Method for Siderophore Detection. *J Microbiol Methods* **2007**, *70*, 127–131, doi:10.1016/j.mimet.2007.03.023.
176. Arnow, L.E. COLORIMETRIC DETERMINATION OF THE COMPONENTS OF 3,4-DIHYDROXYPHENYLALANINETYROSINE MIXTURES. *Journal of Biological Chemistry* **1937**, *118*, 531–537, doi:10.1016/S0021-9258(18)74509-2.
177. Hu, X.; Boyer, G.L. Siderophore-Mediated Aluminum Uptake by Bacillus Megaterium ATCC 19213. *Applied and Environmental Microbiology* **1996**, *62*, 4044–4048, doi:10.1128/aem.62.11.4044-4048.1996.

178. Csáky, T.Z.; O., H.; Thomas, R.; Lång (Loukamo), S.; Elli, T.; Aarne, T. On the Estimation of Bound Hydroxylamine in Biological Materials. *Acta Chemica Scandinavica* **1948**, *2*, 450–454, doi:10.3891/acta.chem.scand.02-0450.
179. Khan, A.; Singh, P.; Srivastava, A. Synthesis, Nature and Utility of Universal Iron Chelator – Siderophore: A Review. *Microbiological Research* **2018**, *212–213*, 103–111, doi:10.1016/j.micres.2017.10.012.
180. Xie, B.; Wei, X.; Wan, C.; Zhao, W.; Song, R.; Xin, S.; Song, K. Exploring the Biological Pathways of Siderophores and Their Multidisciplinary Applications: A Comprehensive Review. *Molecules* **2024**, *29*, 2318, doi:10.3390/molecules29102318.
181. Marine Actinomycetes Siderophores: Types, High Throughput Characterization Techniques, Applications, and Their Association with Nanotechnology: A Comprehensive Review. *NanoWorld J* **2024**, *10*, doi:10.17756/nwj.2024-130.
182. Gao, B.; Chai, X.; Huang, Y.; Wang, X.; Han, Z.; Xu, X.; Wu, T.; Zhang, X.; Wang, Y. Siderophore Production in Pseudomonas SP. Strain SP3 Enhances Iron Acquisition in Apple Rootstock. *Journal of Applied Microbiology* **2022**, *133*, 720–732, doi:10.1111/jam.15591.
183. Gupta, V.; Saharan, K.; Kumar, L.; Gupta, R.; Sahai, V.; Mittal, A. Spectrophotometric Ferric Ion Biosensor from Pseudomonas Fluorescens Culture. *Biotechnology and Bioengineering* **2008**, *100*, 284–296, doi:10.1002/bit.21754.
184. Doorneweerd, D.D.; Henne, W.A.; Reifenberger, R.G.; Low, P.S. Selective Capture and Identification of Pathogenic Bacteria Using an Immobilized Siderophore. *Langmuir* **2010**, *26*, 15424–15429, doi:10.1021/la101962w.
185. Pawar, M.K.; Tayade, K.C.; Sahoo, S.K.; Mahulikar, P.P.; Kuwar, A.S.; Chaudhari, B.L. Selective Ciprofloxacin Antibiotic Detection by Fluorescent Siderophore Pyoverdin. *Biosensors and Bioelectronics* **2016**, *81*, 274–279, doi:10.1016/j.bios.2016.03.003.
186. Chiadò, A.; Varani, L.; Bosco, F.; Marmo, L. Opening Study on the Development of a New Biosensor for Metal Toxicity Based on Pseudomonas Fluorescens Pyoverdine. *Biosensors* **2013**, *3*, 385–399, doi:10.3390/bios3040385.
187. Khasheii, B.; Mahmoodi, P.; Mohammadzadeh, A. Siderophores: Importance in Bacterial Pathogenesis and Applications in Medicine and Industry. *Microbiological Research* **2021**, *250*, 126790, doi:10.1016/j.micres.2021.126790.
188. Fan, D.; Fang, Q. Siderophores for Medical Applications: Imaging, Sensors, and Therapeutics. *International Journal of Pharmaceutics* **2021**, *597*, 120306, doi:10.1016/j.ijpharm.2021.120306.
189. Möllmann, U.; Heinisch, L.; Bauernfeind, A.; Köhler, T.; Ankel-Fuchs, D. Siderophores as Drug Delivery Agents: Application of the "Trojan Horse" Strategy. *Biometals* **2009**, *22*, 615–624, doi:10.1007/s10534-009-9219-2.
190. Gumienna-Kontecka, E.; Carver, P.L. Building a Trojan Horse: Siderophore-Drug Conjugates for the Treatment of Infectious Diseases. *Met Ions Life Sci* **2019**, *19*, /books/9783110527872/9783110527872-013/9783110527872-013.xml, doi:10.1515/9783110527872-013.
191. Zhanel, G.G.; Golden, A.R.; Zelenitsky, S.; Wiebe, K.; Lawrence, C.K.; Adam, H.J.; Idowu, T.; Domalaon, R.; Schweizer, F.; Zhanel, M.A.; et al. Cefiderocol: A Siderophore Cephalosporin with Activity Against Carbapenem-Resistant and Multidrug-Resistant Gram-Negative Bacilli. *Drugs* **2019**, *79*, 271–289, doi:10.1007/s40265-019-1055-2.
192. Steinbrueck, A.; Sedgwick, A.C.; Han, H.-H.; Zhao, M.Y.; Sen, S.; Huang, D.-Y.; Zang, Y.; Li, J.; He, X.-P.; Sessler, J.L. In Vitro Studies of Deferasirox Derivatives as Potential Organelle-Targeting Traceable Anti-Cancer Therapeutics. *Chem. Commun.* **2021**, *57*, 5678–5681, doi:10.1039/D0CC08156F.
193. Komoto, K.; Nomoto, T.; El Muttaqien, S.; Takemoto, H.; Matsui, M.; Miura, Y.; Nishiyama, N. Iron Chelation Cancer Therapy Using Hydrophilic Block Copolymers Conjugated with Deferoxamine. *Cancer Science* **2021**, *112*, 410–421, doi:10.1111/cas.14607.
194. Saha, P.; Yeoh, B.S.; Xiao, X.; Golonka, R.M.; Kumarasamy, S.; Vijay-Kumar, M. Enterobactin, an Iron Chelating Bacterial Siderophore, Arrests Cancer Cell Proliferation. *Biochemical Pharmacology* **2019**, *168*, 71–81, doi:10.1016/j.bcp.2019.06.017.
195. Roskova, Z.; Skarohlid, R.; McGachy, L. Siderophores: An Alternative Bioremediation Strategy? *Science of The Total Environment* **2022**, *819*, 153144, doi:10.1016/j.scitotenv.2022.153144.
196. Hofmann, M.; Retamal-Morales, G.; Tischler, D. Metal Binding Ability of Microbial Natural Metal Chelators and Potential Applications. *Nat. Prod. Rep.* **2020**, *37*, 1262–1283, doi:10.1039/C9NP00058E.
197. Bellotti, D.; Remelli, M. Deferoxamine B: A Natural, Excellent and Versatile Metal Chelator. *Molecules* **2021**, *26*, 3255, doi:10.3390/molecules26113255.

198. Hickford, S.J.H.; Küpper, F.C.; Zhang, G.; Carrano, C.J.; Blunt, J.W.; Butler, A. Petrobactin Sulfonate, a New Siderophore Produced by the Marine Bacterium Marinobacter Hydrocarbonoclasticus. *J. Nat. Prod.* **2004**, *67*, 1897–1899, doi:10.1021/np049823i.
199. Brown, E.D.; Wright, G.D. Antibacterial Drug Discovery in the Resistance Era. *Nature* **2016**, *529*, 336–343, doi:10.1038/nature17042.
200. Schneider, Y.K. Bacterial Natural Product Drug Discovery for New Antibiotics: Strategies for Tackling the Problem of Antibiotic Resistance by Efficient Bioprospecting. *Antibiotics* **2021**, *10*, 842, doi:10.3390/antibiotics10070842.
201. Van Boeckel, T.P.; Pires, J.; Silvester, R.; Zhao, C.; Song, J.; Criscuolo, N.G.; Gilbert, M.; Bonhoeffer, S.; Laxminarayan, R. Global Trends in Antimicrobial Resistance in Animals in Low- and Middle-Income Countries. *Science* **2019**, *365*, eaaw1944, doi:10.1126/science.aaw1944.
202. Rice, L.B. Federal Funding for the Study of Antimicrobial Resistance in Nosocomial Pathogens: No ESKAPE. *The Journal of Infectious Diseases* **2008**, *197*, 1079–1081, doi:10.1086/533452.
203. Andersson, D.I.; Hughes, D.; Kubicek-Sutherland, J.Z. Mechanisms and Consequences of Bacterial Resistance to Antimicrobial Peptides. *Drug Resist Updat* **2016**, *26*, 43–57, doi:10.1016/j.drup.2016.04.002.
204. Kapoor, G.; Saigal, S.; Elongavan, A. Action and Resistance Mechanisms of Antibiotics: A Guide for Clinicians. *J Anaesthesiol Clin Pharmacol* **2017**, *33*, 300–305, doi:10.4103/joacp.JOACP_349_15.
205. Xuan, J.; Feng, W.; Wang, J.; Wang, R.; Zhang, B.; Bo, L.; Chen, Z.-S.; Yang, H.; Sun, L. Antimicrobial Peptides for Combating Drug-Resistant Bacterial Infections. *Drug Resistance Updates* **2023**, *68*, 100954, doi:10.1016/j.drup.2023.100954.
206. Jubair, N.; Rajagopal, M.; Chinnappan, S.; Abdullah, N.B.; Fatima, A. Review on the Antibacterial Mechanism of Plant-Derived Compounds against Multidrug-Resistant Bacteria (MDR). *Evidence-Based Complementary and Alternative Medicine* **2021**, *2021*, 3663315, doi:10.1155/2021/3663315.
207. Hiramatsu, K.; Hanaki, H.; Ino, T.; Yabuta, K.; Oguri, T.; Tenover, F.C. Methicillin-Resistant Staphylococcus Aureus Clinical Strain with Reduced Vancomycin Susceptibility. *Journal of Antimicrobial Chemotherapy* **1997**, *40*, 135–136, doi:10.1093/jac/40.1.135.
208. Uma, G.; Babu, M.M.; Prakash, V.S.G.; Nisha, S.J.; Citarasu, T. Nature and Bioprospecting of Haloalkaliphilics: A Review. *World J Microbiol Biotechnol* **2020**, *36*, 66, doi:10.1007/s11274-020-02841-2.
209. Tendulkar, S.; Hattiholi, A.; Chavadar, M.; Dodamani, S. Psychrophiles: A Journey of Hope. *J Biosci* **2021**, *46*, 64, doi:10.1007/s12038-021-00180-4.
210. Baranova, A.A.; Alferova, V.A.; Korshun, V.A.; Tyurin, A.P. Antibiotics from Extremophilic Micromycetes. *Russ J Bioorg Chem* **2020**, *46*, 903–971, doi:10.1134/S1068162020060023.
211. Gardete, S.; Tomasz, A. Mechanisms of Vancomycin Resistance in Staphylococcus Aureus. *J Clin Invest* **2014**, *124*, 2836–2840, doi:10.1172/JCI68834.
212. Falanga, A.; Lombardi, L.; Franci, G.; Vitiello, M.; Iovene, M.R.; Morelli, G.; Galdiero, M.; Galdiero, S. Marine Antimicrobial Peptides: Nature Provides Templates for the Design of Novel Compounds against Pathogenic Bacteria. *International Journal of Molecular Sciences* **2016**, *17*, 785, doi:10.3390/ijms17050785.
213. Agrawal, S.; Acharya, D.; Adholeya, A.; Barrow, C.J.; Deshmukh, S.K. Nonribosomal Peptides from Marine Microbes and Their Antimicrobial and Anticancer Potential. *Front. Pharmacol.* **2017**, *8*, doi:10.3389/fphar.2017.00828.
214. Zeng, M.; Tao, J.; Xu, S.; Bai, X.; Zhang, H. Marine Organisms as a Prolific Source of Bioactive Depsipeptides. *Marine Drugs* **2023**, *21*, 120, doi:10.3390/md21020120.
215. Adamu, Y.; Puig-Asensio, M.; Dabo, B.; Schweizer, M.L. Comparative Effectiveness of Daptomycin versus Vancomycin among Patients with Methicillin-Resistant Staphylococcus Aureus (MRSA) Bloodstream Infections: A Systematic Literature Review and Meta-Analysis. *PLOS ONE* **2024**, *19*, e0293423, doi:10.1371/journal.pone.0293423.
216. Han, S.; Zaniewski, R.P.; Marr, E.S.; Lacey, B.M.; Tomaras, A.P.; Evdokimov, A.; Miller, J.R.; Shanmugasundaram, V. Structural Basis for Effectiveness of Siderophore-Conjugated Monocarbams against Clinically Relevant Strains of Pseudomonas Aeruginosa. *Proc Natl Acad Sci U S A* **2010**, *107*, 22002–22007, doi:10.1073/pnas.1013092107.
217. Chen, X.; Lu, Y.; Shan, M.; Zhao, H.; Lu, Z.; Lu, Y. A Mini-Review: Mechanism of Antimicrobial Action and Application of Surfactin. *World J Microbiol Biotechnol* **2022**, *38*, 143, doi:10.1007/s11274-022-03323-3.

218. Wiegand, I.; Hilpert, K.; Hancock, R.E.W. Agar and Broth Dilution Methods to Determine the Minimal Inhibitory Concentration (MIC) of Antimicrobial Substances. *Nat Protoc* **2008**, *3*, 163–175, doi:10.1038/nprot.2007.521.
219. Mirtaghi, S.M.; Nejad, P.T.; Masoumeh Mazandarani, M.; Livani, F.; Bagheri, H. Evaluation of Antibacterial Activity of Urtica Dioica L. Leaf Ethanolic Extract Using Agar Well Diffusion and Disc Diffusion Methods. | EBSCOhost Available online: https://openurl.ebsco.com/contentitem/doi:10.18869%2Facadpub.mlj.10.5.15?sid=ebsco:plink:crawler&id=ebsco:doi:10.18869%2Facadpub.mlj.10.5.15 (accessed on 2 December 2024).
220. Sinha, S.; Vohora, D. Chapter 2 - Drug Discovery and Development: An Overview. In *Pharmaceutical Medicine and Translational Clinical Research*; Vohora, D., Singh, G., Eds.; Academic Press: Boston, 2018; pp. 19–32 ISBN 978-0-12-802103-3.
221. Shang, D.; Han, X.; Du, W.; Kou, Z.; Jiang, F. Trp-Containing Antibacterial Peptides Impair Quorum Sensing and Biofilm Development in Multidrug-Resistant Pseudomonas Aeruginosa and Exhibit Synergistic Effects With Antibiotics. *Front. Microbiol.* **2021**, *12*, doi:10.3389/fmicb.2021.611009.
222. Sun, H.; Hong, Y.; Xi, Y.; Zou, Y.; Gao, J.; Du, J. Synthesis, Self-Assembly, and Biomedical Applications of Antimicrobial Peptide–Polymer Conjugates. *Biomacromolecules* **2018**, *19*, 1701–1720, doi:10.1021/acs.biomac.8b00208.
223. Lim, H.-J.; An, J.S.; Bae, E.S.; Cho, E.; Hwang, S.; Nam, S.-J.; Oh, K.-B.; Lee, S.K.; Oh, D.-C. Ligiamycins A and B, Decalin-Amino-Maleimides from the Co-Culture of Streptomyces Sp. and Achromobacter Sp. Isolated from the Marine Wharf Roach, Ligia Exotica. *Marine Drugs* **2022**, *20*, 83, doi:10.3390/md20020083.
224. Kwon, H.C.; Kauffman, C.A.; Jensen, P.R.; Fenical, W. Marinomycins A−D, Antitumor-Antibiotics of a New Structure Class from a Marine Actinomycete of the Recently Discovered Genus "Marinispora." *J. Am. Chem. Soc.* **2006**, *128*, 1622–1632, doi:10.1021/ja0558948.
225. Lacret, R.; Pérez-Victoria, I.; Oves-Costales, D.; De la Cruz, M.; Domingo, E.; Martín, J.; Díaz, C.; Vicente, F.; Genilloud, O.; Reyes, F. MDN-0170, a New Napyradiomycin from Streptomyces Sp. Strain CA-271078. *Marine Drugs* **2016**, *14*, 188, doi:10.3390/md14100188.
226. Cho, E.; Kwon, O.-S.; Chung, B.; Lee, J.; Sun, J.; Shin, J.; Oh, K.-B. Antibacterial Activity of Chromomycins from a Marine-Derived Streptomyces Microflavus. *Marine Drugs* **2020**, *18*, 522, doi:10.3390/md18100522.
227. van Gent, M.E.; Ali, M.; Nibbering, P.H.; Kłodzińska, S.N. Current Advances in Lipid and Polymeric Antimicrobial Peptide Delivery Systems and Coatings for the Prevention and Treatment of Bacterial Infections. *Pharmaceutics* **2021**, *13*, 1840, doi:10.3390/pharmaceutics13111840.
228. Gao, R.; Shu, W.; Shen, Y.; Sun, Q.; Bai, F.; Wang, J.; Li, D.; Li, Y.; Jin, W.; Yuan, L. Sturgeon Protein-Derived Peptides Exert Anti-Inflammatory Effects in LPS-Stimulated RAW264.7 Macrophages via the MAPK Pathway. *Journal of Functional Foods* **2020**, *72*, 104044, doi:10.1016/j.jff.2020.104044.
229. Marya; Khan, H.; Nabavi, S.M.; Habtemariam, S. Anti-Diabetic Potential of Peptides: Future Prospects as Therapeutic Agents. *Life Sciences* **2018**, *193*, 153–158, doi:10.1016/j.lfs.2017.10.025.
230. Arias, M.; Haney, E.F.; Hilchie, A.L.; Corcoran, J.A.; Hyndman, M.E.; Hancock, R.E.W.; Vogel, H.J. Selective Anticancer Activity of Synthetic Peptides Derived from the Host Defence Peptide Tritrpticin. *Biochimica et Biophysica Acta (BBA) - Biomembranes* **2020**, *1862*, 183228, doi:10.1016/j.bbamem.2020.183228.
231. León, R.; Ruiz, M.; Valero, Y.; Cárdenas, C.; Guzman, F.; Vila, M.; Cuesta, A. Exploring Small Cationic Peptides of Different Origin as Potential Antimicrobial Agents in Aquaculture. *Fish & Shellfish Immunology* **2020**, *98*, 720–727, doi:10.1016/j.fsi.2019.11.019.
232. De La Hoz-Romo, M.C.; Díaz, L.; Villamil, L. Marine Actinobacteria a New Source of Antibacterial Metabolites to Treat Acne Vulgaris Disease—A Systematic Literature Review. *Antibiotics* **2022**, *11*, 965, doi:10.3390/antibiotics11070965.
233. Cong, Z.; Huang, X.; Liu, Y.; Liu, Y.; Wang, P.; Liao, S.; Yang, B.; Zhou, X.; Huang, D.; Wang, J. Cytotoxic Anthracycline and Antibacterial Tirandamycin Analogues from a Marine-Derived Streptomyces Sp. SCSIO 41399. *J Antibiot* **2019**, *72*, 45–49, doi:10.1038/s41429-018-0103-6.
234. Khan, I.; Oh, D.-H. Integration of Nisin into Nanoparticles for Application in Foods. *Innovative Food Science & Emerging Technologies* **2016**, *34*, 376–384, doi:10.1016/j.ifset.2015.12.013.
235. Luz, C.; Calpe, J.; Saladino, F.; Luciano, F.B.; Fernandez-Franzón, M.; Mañes, J.; Meca, G. Antimicrobial Packaging Based on ε-Polylysine Bioactive Film for the Control of Mycotoxigenic Fungi in Vitro and in Bread. *Journal of Food Processing and Preservation* **2018**, *42*, e13370, doi:10.1111/jfpp.13370.

236. da Silva Malheiros, P.; Daroit, D.J.; Brandelli, A. Food Applications of Liposome-Encapsulated Antimicrobial Peptides. *Trends in Food Science & Technology* **2010**, *21*, 284–292, doi:10.1016/j.tifs.2010.03.003.
237. Babutan, I.; Lucaci, A.-D.; Botiz, I. Antimicrobial Polymeric Structures Assembled on Surfaces. *Polymers* **2021**, *13*, 1552, doi:10.3390/polym13101552.
238. Kowalska-Krochmal, B.; Dudek-Wicher, R. The Minimum Inhibitory Concentration of Antibiotics: Methods, Interpretation, Clinical Relevance. *Pathogens* **2021**, *10*, 165, doi:10.3390/pathogens10020165.
239. Koehn, F.E.; Carter, G.T. The Evolving Role of Natural Products in Drug Discovery. *Nat Rev Drug Discov* **2005**, *4*, 206–220, doi:10.1038/nrd1657.
240. Luo, Y.; Cobb, R.E.; Zhao, H. Recent Advances in Natural Product Discovery. *Current Opinion in Biotechnology* **2014**, *30*, 230–237, doi:10.1016/j.copbio.2014.09.002.
241. Stewart, E.J. Growing Unculturable Bacteria. *Journal of Bacteriology* **2012**, *194*, 4151–4160, doi:10.1128/jb.00345-12.
242. Staley, J.T.; Konopka, A. Measurement of in Situ Activities of Nonphotosynthetic Microorganisms in Aquatic and Terrestrial Habitats. *Annu Rev Microbiol* **1985**, *39*, 321–346, doi:10.1146/annurev.mi.39.100185.001541.
243. Lewis, K.; Epstein, S.; D'Onofrio, A.; Ling, L.L. Uncultured Microorganisms as a Source of Secondary Metabolites. *J Antibiot* **2010**, *63*, 468–476, doi:10.1038/ja.2010.87.
244. Fakruddin, Md.; Mannan, K.S.B.; Andrews, S. Viable but Nonculturable Bacteria: Food Safety and Public Health Perspective. *ISRN Microbiol* **2013**, *2013*, 703813, doi:10.1155/2013/703813.
245. Lewis, W.H.; Tahon, G.; Geesink, P.; Sousa, D.Z.; Ettema, T.J.G. Innovations to Culturing the Uncultured Microbial Majority. *Nat Rev Microbiol* **2021**, *19*, 225–240, doi:10.1038/s41579-020-00458-8.
246. Tammam, M.A.; El-Demerdash, A. Pederins, Mycalamides, Onnamides and Theopederins: Distinctive Polyketide Families with Intriguing Therapeutic Potentialities. *Current Research in Biotechnology* **2023**, *6*, 100145, doi:10.1016/j.crbiot.2023.100145.
247. Niehs, S.P.; Dose, B.; Scherlach, K.; Roth, M.; Hertweck, C. Genomics-Driven Discovery of a Symbiont-Specific Cyclopeptide from Bacteria Residing in the Rice Seedling Blight Fungus. *ChemBioChem* **2018**, *19*, 2167–2172, doi:10.1002/cbic.201800400.
248. Kato, S.; Yamagishi, A.; Daimon, S.; Kawasaki, K.; Tamaki, H.; Kitagawa, W.; Abe, A.; Tanaka, M.; Sone, T.; Asano, K.; et al. Isolation of Previously Uncultured Slow-Growing Bacteria by Using a Simple Modification in the Preparation of Agar Media. *Applied and Environmental Microbiology* **2018**, *84*, e00807-18, doi:10.1128/AEM.00807-18.
249. Rutledge, P.J.; Challis, G.L. Discovery of Microbial Natural Products by Activation of Silent Biosynthetic Gene Clusters. *Nat Rev Microbiol* **2015**, *13*, 509–523, doi:10.1038/nrmicro3496.
250. Tomm, H.A.; Ucciferri, L.; Ross, A.C. Advances in Microbial Culturing Conditions to Activate Silent Biosynthetic Gene Clusters for Novel Metabolite Production. *J Ind Microbiol Biotechnol* **2019**, *46*, 1381–1400, doi:10.1007/s10295-019-02198-y.
251. Dias, D.A.; Urban, S.; Roessner, U. A Historical Overview of Natural Products in Drug Discovery. *Metabolites* **2012**, *2*, 303–336, doi:10.3390/metabo2020303.
252. Joochim, C.; Phadungthin, R.; Srikitsuwan, S. Design and Development of a Remotely Operated Underwater Vehicle. In Proceedings of the 2015 16th International Conference on Research and Education in Mechatronics (REM); November 2015; pp. 148–153.
253. Kiriiri, G.K.; Njogu, P.M.; Mwangi, A.N. Exploring Different Approaches to Improve the Success of Drug Discovery and Development Projects: A Review. *Futur J Pharm Sci* **2020**, *6*, 27, doi:10.1186/s43094-020-00047-9.
254. Sverdrup-Thygeson, J.; Kelasidi, E.; Pettersen, K.Y.; Gravdahl, J.T. The Underwater Swimming Manipulator—A Bioinspired Solution for Subsea Operations. *IEEE Journal of Oceanic Engineering* **2018**, *43*, 402–417, doi:10.1109/JOE.2017.2768108.
255. Dhakal, D.; Pokhrel, A.R.; Shrestha, B.; Sohng, J.K. Marine Rare Actinobacteria: Isolation, Characterization, and Strategies for Harnessing Bioactive Compounds. *Front. Microbiol.* **2017**, *8*, doi:10.3389/fmicb.2017.01106.
256. Hu, D.; Sun, C.; Jin, T.; Fan, G.; Mok, K.M.; Li, K.; Lee, S.M.-Y. Exploring the Potential of Antibiotic Production From Rare Actinobacteria by Whole-Genome Sequencing and Guided MS/MS Analysis. *Front. Microbiol.* **2020**, *11*, doi:10.3389/fmicb.2020.01540.
257. Vartoukian, S.R.; Palmer, R.M.; Wade, W.G. Strategies for Culture of 'Unculturable' Bacteria. *FEMS Microbiology Letters* **2010**, *309*, 1–7, doi:10.1111/j.1574-6968.2010.02000.x.

258. Bonnet, M.; Lagier, J.C.; Raoult, D.; Khelaifia, S. Bacterial Culture through Selective and Non-Selective Conditions: The Evolution of Culture Media in Clinical Microbiology. *New Microbes and New Infections* **2020**, *34*, 100622, doi:10.1016/j.nmni.2019.100622.
259. Choi, E.J.; Nam, S.-J.; Paul, L.; Beatty, D.; Kauffman, C.A.; Jensen, P.R.; Fenical, W. Previously Uncultured Marine Bacteria Linked to Novel Alkaloid Production. *Chemistry & Biology* **2015**, *22*, 1270–1279, doi:10.1016/j.chembiol.2015.07.014.
260. Aakra, Å.; Utåker, J.B.; Nes, I.F.; Bakken, L.R. An Evaluated Improvement of the Extinction Dilution Method for Isolation of Ammonia-Oxidizing Bacteria. *Journal of Microbiological Methods* **1999**, *39*, 23–31, doi:10.1016/S0167-7012(99)00094-9.
261. Rappé, M.S.; Connon, S.A.; Vergin, K.L.; Giovannoni, S.J. Cultivation of the Ubiquitous SAR11 Marine Bacterioplankton Clade. *Nature* **2002**, *418*, 630–633, doi:10.1038/nature00917.
262. Kaeberlein, T.; Lewis, K.; Epstein, S.S. Isolating "Uncultivable" Microorganisms in Pure Culture in a Simulated Natural Environment. *Science* **2002**, *296*, 1127–1129, doi:10.1126/science.1070633.
263. Nichols, D.; Cahoon, N.; Trakhtenberg, E.M.; Pham, L.; Mehta, A.; Belanger, A.; Kanigan, T.; Lewis, K.; Epstein, S.S. Use of Ichip for High-Throughput In Situ Cultivation of "Uncultivable" Microbial Species. *Appl Environ Microbiol* **2010**, *76*, 2445–2450, doi:10.1128/AEM.01754-09.
264. Piddock, L.J.V. Teixobactin, the First of a New Class of Antibiotics Discovered by iChip Technology? *J Antimicrob Chemother* **2015**, *70*, 2679–2680, doi:10.1093/jac/dkv175.
265. MacIntyre, L.W.; Charles, M.J.; Haltli, B.A.; Marchbank, D.H.; Kerr, R.G. An Ichip-Domesticated Sponge Bacterium Produces an N-Acyltyrosine Bearing an α-Methyl Substituent. *Org. Lett.* **2019**, *21*, 7768–7771, doi:10.1021/acs.orglett.9b02710.
266. Jung, D.; Seo, E.-Y.; Epstein, S.S.; Joung, Y.; Han, J.; Parfenova, V.V.; Belykh, O.I.; Gladkikh, A.S.; Ahn, T.S. Application of a New Cultivation Technology, I-Tip, for Studying Microbial Diversity in Freshwater Sponges of Lake Baikal, Russia. *FEMS Microbiology Ecology* **2014**, *90*, 417–423, doi:10.1111/1574-6941.12399.
267. Iacovelli, R.; Bovenberg, R.A.L.; Driessen, A.J.M. Nonribosomal Peptide Synthetases and Their Biotechnological Potential in *Penicillium Rubens*. *Journal of Industrial Microbiology and Biotechnology* **2021**, *48*, kuab045, doi:10.1093/jimb/kuab045.
268. Chen, H.; Zhong, L.; Zhou, H.; Bai, X.; Sun, T.; Wang, X.; Zhao, Y.; Ji, X.; Tu, Q.; Zhang, Y.; et al. Biosynthesis and Engineering of the Nonribosomal Peptides with a C-Terminal Putrescine. *Nat Commun* **2023**, *14*, 6619, doi:10.1038/s41467-023-42387-z.
269. Stachelhaus, T.; Mootz, H.D.; Marahiel, M.A. The Specificity-Conferring Code of Adenylation Domains in Nonribosomal Peptide Synthetases. *Chem Biol* **1999**, *6*, 493–505, doi:10.1016/S1074-5521(99)80082-9.
270. Kawai, Y.; Ishii, Y.; Arakawa, K.; Uemura, K.; Saitoh, B.; Nishimura, J.; Kitazawa, H.; Yamazaki, Y.; Tateno, Y.; Itoh, T.; et al. Structural and Functional Differences in Two Cyclic Bacteriocins with the Same Sequences Produced by Lactobacilli. *Appl Environ Microbiol* **2004**, *70*, 2906–2911, doi:10.1128/AEM.70.5.2906-2911.2004.
271. Behsaz, B.; Bode, E.; Gurevich, A.; Shi, Y.-N.; Grundmann, F.; Acharya, D.; Caraballo-Rodríguez, A.M.; Bouslimani, A.; Panitchpakdi, M.; Linck, A.; et al. Integrating Genomics and Metabolomics for Scalable Non-Ribosomal Peptide Discovery. *Nat Commun* **2021**, *12*, 3225, doi:10.1038/s41467-021-23502-4.
272. Yooseph, S.; Sutton, G.; Rusch, D.B.; Halpern, A.L.; Williamson, S.J.; Remington, K.; Eisen, J.A.; Heidelberg, K.B.; Manning, G.; Li, W.; et al. The Sorcerer II Global Ocean Sampling Expedition: Expanding the Universe of Protein Families. *PLoS Biol* **2007**, *5*, e16, doi:10.1371/journal.pbio.0050016.
273. Tietz, J.I.; Schwalen, C.J.; Patel, P.S.; Maxson, T.; Blair, P.M.; Tai, H.-C.; Zakai, U.I.; Mitchell, D.A. A New Genome-Mining Tool Redefines the Lasso Peptide Biosynthetic Landscape. *Nat Chem Biol* **2017**, *13*, 470–478, doi:10.1038/nchembio.2319.
274. Della Sala, G.; Mangoni, A.; Costantino, V.; Teta, R. Identification of the Biosynthetic Gene Cluster of Thermoactinoamides and Discovery of New Congeners by Integrated Genome Mining and MS-Based Molecular Networking. *Front. Chem.* **2020**, *8*, doi:10.3389/fchem.2020.00397.
275. Atanasov, A.G.; Zotchev, S.B.; Dirsch, V.M.; Supuran, C.T. Natural Products in Drug Discovery: Advances and Opportunities. *Nat Rev Drug Discov* **2021**, *20*, 200–216, doi:10.1038/s41573-020-00114-z.
276. Weber, T.; Blin, K.; Duddela, S.; Krug, D.; Kim, H.U.; Bruccoleri, R.; Lee, S.Y.; Fischbach, M.A.; Müller, R.; Wohlleben, W.; et al. antiSMASH 3.0—a Comprehensive Resource for the Genome

Mining of Biosynthetic Gene Clusters. *Nucleic Acids Res* **2015**, *43*, W237–W243, doi:10.1093/nar/gkv437.
277. Blin, K.; Shaw, S.; Augustijn, H.E.; Reitz, Z.L.; Biermann, F.; Alanjary, M.; Fetter, A.; Terlouw, B.R.; Metcalf, W.W.; Helfrich, E.J.N.; et al. antiSMASH 7.0: New and Improved Predictions for Detection, Regulation, Chemical Structures and Visualisation. *Nucleic Acids Res* **2023**, *51*, W46–W50, doi:10.1093/nar/gkad344.
278. Carroll, L.M.; Larralde, M.; Fleck, J.S.; Ponnudurai, R.; Milanese, A.; Cappio, E.; Zeller, G. Accurate de Novo Identification of Biosynthetic Gene Clusters with GECCO 2021, 2021.05.03.442509.
279. Hannigan, G.D.; Prihoda, D.; Palicka, A.; Soukup, J.; Klempir, O.; Rampula, L.; Durcak, J.; Wurst, M.; Kotowski, J.; Chang, D.; et al. A Deep Learning Genome-Mining Strategy for Biosynthetic Gene Cluster Prediction. *Nucleic Acids Res* **2019**, *47*, e110, doi:10.1093/nar/gkz654.
280. Hoskisson, P.A.; Seipke, R.F. Cryptic or Silent? The Known Unknowns, Unknown Knowns, and Unknown Unknowns of Secondary Metabolism. *mBio* **2020**, *11*, e02642-20, doi:10.1128/mBio.02642-20.
281. Skinnider, M.A.; Johnston, C.W.; Gunabalasingam, M.; Merwin, N.J.; Kieliszek, A.M.; MacLellan, R.J.; Li, H.; Ranieri, M.R.M.; Webster, A.L.H.; Cao, M.P.T.; et al. Comprehensive Prediction of Secondary Metabolite Structure and Biological Activity from Microbial Genome Sequences. *Nat Commun* **2020**, *11*, 6058, doi:10.1038/s41467-020-19986-1.
282. Terlouw, B.R.; Blin, K.; Navarro-Muñoz, J.C.; Avalon, N.E.; Chevrette, M.G.; Egbert, S.; Lee, S.; Meijer, D.; Recchia, M.J.J.; Reitz, Z.L.; et al. MIBiG 3.0: A Community-Driven Effort to Annotate Experimentally Validated Biosynthetic Gene Clusters. *Nucleic Acids Res* **2023**, *51*, D603–D610, doi:10.1093/nar/gkac1049.
283. Li, X.; Guo, J.; Dai, S.; Ouyang, Y.; Wu, H.; Sun, W.; Wang, G. Exploring and Exploiting Microbial Diversity through Metagenomics for Natural Product Drug Discovery. *Current Topics in Medicinal Chemistry* **2009**, *9*, 1525–1535, doi:10.2174/156802609789909849.
284. Simon, D.P.; Anila, N.; Gayathri, K.; Sarada, R. Heterologous Expression of β-Carotene Hydroxylase in *Dunaliella Salina* by *Agrobacterium*-Mediated Genetic Transformation. *Algal Research* **2016**, *18*, 257–265, doi:10.1016/j.algal.2016.06.017.
285. Mao, X.; Liu, Z.; Sun, J.; Lee, S.Y. Metabolic Engineering for the Microbial Production of Marine Bioactive Compounds. *Biotechnology Advances* **2017**, *35*, 1004–1021, doi:10.1016/j.biotechadv.2017.03.001.
286. Pan, R.; Bai, X.; Chen, J.; Zhang, H.; Wang, H. Exploring Structural Diversity of Microbe Secondary Metabolites Using OSMAC Strategy: A Literature Review. *Front. Microbiol.* **2019**, *10*, doi:10.3389/fmicb.2019.00294.
287. Pinedo-Rivilla, C.; Aleu, J.; Durán-Patrón, R. Cryptic Metabolites from Marine-Derived Microorganisms Using OSMAC and Epigenetic Approaches. *Mar Drugs* **2022**, *20*, 84, doi:10.3390/md20020084.
288. Le Loarer, A.; Dufossé, L.; Bignon, J.; Frédérich, M.; Ledoux, A.; Fouillaud, M.; Gauvin-Bialecki, A. OSMAC Method to Assess Impact of Culture Parameters on Metabolomic Diversity and Biological Activity of Marine-Derived Actinobacteria. *Marine Drugs* **2024**, *22*, 23, doi:10.3390/md22010023.
289. Romano, S.; Jackson, S.A.; Patry, S.; Dobson, A.D.W. Extending the "One Strain Many Compounds" (OSMAC) Principle to Marine Microorganisms. *Marine Drugs* **2018**, *16*, 244, doi:10.3390/md16070244.
290. Williams, R.B.; Henrikson, J.C.; Hoover, A.R.; Lee, A.E.; Cichewicz, R.H. Epigenetic Remodeling of the Fungal Secondary Metabolome. *Org Biomol Chem* **2008**, *6*, 1895–1897, doi:10.1039/b804701d.
291. Lane, A.L.; Moore, B.S. A Sea of Biosynthesis: Marine Natural Products Meet the Molecular Age. *Nat. Prod. Rep.* **2011**, *28*, 411–428, doi:10.1039/C0NP90032J.
292. Cornelis, P.; Matthijs, S. Pseudomonas Siderophores and Their Biological Significance. In *Microbial Siderophores*; Varma, A., Chincholkar, S.B., Eds.; Springer: Berlin, Heidelberg, 2007; pp. 193–203 ISBN 978-3-540-71160-5.
293. Caudal, F.; Tapissier-Bontemps, N.; Edrada-Ebel, R.A. Impact of Co-Culture on the Metabolism of Marine Microorganisms. *Marine Drugs* **2022**, *20*, 153, doi:10.3390/md20020153.
294. Kitcha, S.; Cheirsilp, B. Enhanced Lipid Production by Co-Cultivation and Co-Encapsulation of Oleaginous Yeast Trichosporonoides Spathulata with Microalgae in Alginate Gel Beads. *Appl Biochem Biotechnol* **2014**, *173*, 522–534, doi:10.1007/s12010-014-0859-5.
295. Kapoore, R.V.; Padmaperuma, G.; Maneein, S.; Vaidyanathan, S. Co-Culturing Microbial Consortia: Approaches for Applications in Biomanufacturing and Bioprocessing. *Crit Rev Biotechnol* **2022**, *42*, 46–72, doi:10.1080/07388551.2021.1921691.

296. Mallmann, L.P.; O. Rios, A.; Rodrigues, E. MS-FINDER and SIRIUS for Phenolic Compound Identification from High-Resolution Mass Spectrometry Data. *Food Research International* **2023**, *163*, 112315, doi:10.1016/j.foodres.2022.112315.
297. Quinn, R.A.; Nothias, L.-F.; Vining, O.; Meehan, M.; Esquenazi, E.; Dorrestein, P.C. Molecular Networking As a Drug Discovery, Drug Metabolism, and Precision Medicine Strategy. *Trends Pharmacol Sci* **2017**, *38*, 143–154, doi:10.1016/j.tips.2016.10.011.
298. Scarpato, S.; Teta, R.; Della Sala, G.; Pawlik, J.R.; Costantino, V.; Mangoni, A. New Tricks with an Old Sponge: Feature-Based Molecular Networking Led to Fast Identification of New Stylissamide L from Stylissa Caribica. *Marine Drugs* **2020**, *18*, 443, doi:10.3390/md18090443.
299. Otasek, D.; Morris, J.H.; Bouças, J.; Pico, A.R.; Demchak, B. Cytoscape Automation: Empowering Workflow-Based Network Analysis. *Genome Biology* **2019**, *20*, 185, doi:10.1186/s13059-019-1758-4.
300. Mohimani, H.; Gurevich, A.; Shlemov, A.; Mikheenko, A.; Korobeynikov, A.; Cao, L.; Shcherbin, E.; Nothias, L.-F.; Dorrestein, P.C.; Pevzner, P.A. Dereplication of Microbial Metabolites through Database Search of Mass Spectra. *Nat Commun* **2018**, *9*, 4035, doi:10.1038/s41467-018-06082-8.
301. Dührkop, K.; Shen, H.; Meusel, M.; Rousu, J.; Böcker, S. Searching Molecular Structure Databases with Tandem Mass Spectra Using CSI:FingerID. *Proceedings of the National Academy of Sciences* **2015**, *112*, 12580–12585, doi:10.1073/pnas.1509788112.
302. Wang, P.; Shehu, A.I.; Ma, X. The Opportunities of Metabolomics in Drug Safety Evaluation. *Curr Pharmacol Rep* **2017**, *3*, 10–15, doi:10.1007/s40495-016-0079-5.
303. Bozza, D.; Barboni, D.; Spadafora, N.D.; Felletti, S.; De Luca, C.; Nosengo, C.; Compagnin, G.; Cavazzini, A.; Catani, M. Untargeted Metabolomics Approaches for the Characterization of Cereals and Their Derived Products by Means of Liquid Chromatography Coupled to High Resolution Mass Spectrometry. *Journal of Chromatography Open* **2024**, *6*, 100168, doi:10.1016/j.jcoa.2024.100168.
304. Alarcon-Barrera, J.C.; Kostidis, S.; Ondo-Mendez, A.; Giera, M. Recent Advances in Metabolomics Analysis for Early Drug Development. *Drug Discovery Today* **2022**, *27*, 1763–1773, doi:10.1016/j.drudis.2022.02.018.
305. Smith, C.A.; Maille, G.O.; Want, E.J.; Qin, C.; Trauger, S.A.; Brandon, T.R.; Custodio, D.E.; Abagyan, R.; Siuzdak, G. METLIN: A Metabolite Mass Spectral Database. *Therapeutic Drug Monitoring* **2005**, *27*, 747, doi:10.1097/01.ftd.0000179845.53213.39.
306. Marriott, P.J.; Chin, S.-T.; Nolvachai, Y. Techniques and Application in Comprehensive Multidimensional Gas Chromatography – Mass Spectrometry. *Journal of Chromatography A* **2021**, *1636*, 461788, doi:10.1016/j.chroma.2020.461788.

Overview of this PhD PROJECT

The aim of this doctoral research is to discover and characterise novel bioactive compounds produced by extremophilic marine bacteria and to identify their biosynthetic pathways, for future biotechnological applications.

In order to achieve this goal, an interdisciplinary approach was applied involving:

(a) fast functional screening, including colorimetric assays (CTAB, CAS), oil displacement assays, and liquid inhibition assays to detect the presence of relevant compounds such as biosurfactants, siderophores and antimicrobials.

(b) metabolomics, utilising high resolution mass spectrometry combined with feature-based molecular networking (FBMN), for a fast dereplication and identification of novel metabolites.

(c) genomics elucidating new biosynthetic clusters that encode for novel bioactive compounds, including antimicrobials, biosurfactants and siderophores and to evaluate the biotechnological potential of selected strains.

In particular, this PhD thesis is divided in three main chapters. The first two chapters are focused on the exploration of two marine extremophilic strains: a deep-sea *Bacillus* sp. BCP32, isolated from the Canyon Dohrn in the Gulf of Naples, and *Halomonas* sp. P26, isolated from the Bay of Piran in the Adriatic Sea. Both strains were selected through high-throughput screening for antimicrobial, biosurfactant and siderophore activity among approximately 300 marine strains (belonging to the SZN library). The third chapter is focused on the bioprospecting of novel Maldivian coral-associated microorganisms (CAMs) displaying antimicrobial, antioxidant and UV protectant properties.

In the first study, based on the screening results, *Bacillus* sp. BCP32 was selected for its ability to produce biosurfactants and antimicrobials. Using an integrated approach combining metabolomics, feature-based molecular networking

(FBMN), and functional bioassays, 71 new depsipeptide analogues were identified, belonging to TL-119/nobilamide molecules, along with known surfactins. Four compounds were isolated, including the well-known TL-119 and Nobilamide I, and two new analogues, T1 and S1. Among them, TL-119 and the novel compound S1 showed excellent antimicrobial activity against *Listeria monocytogenes* and multidrug-resistant *S. aureus* strains suggesting highlighting their therapeutic potential. Additionally, the surfactin fractions demonstrated significant surfactant activity and potent inhibitory effects against the fish pathogen *P. piscicida*. In addition, de novo genome sequencing of BCP32 led to the identification of the previously unknown biosynthetic gene cluster (BGC) encoding for the NRPS responsible for the production of nobilamides, providing valuable insights into their biosynthesis.

The second study investigated the halophilic strain *Halomonas* sp. P26 selected for its promising siderophore activity. Cultivating P26 under iron limited conditions followed by a bioactivity-guided fractionation approach and chemical analysis, 9 novel aquachelins (E-F-G-K-H-L-M-N-O), were identified and structurally characterized. The enriched fraction containing these amphiphilic siderophores exhibited strong antimicrobial activity against Gram-positive and Gram-negative pathogens, as well as significant antioxidant and biosurfactant properties. The biosynthetic pathway for aquachelins was elucidated, consisting of five NRPS-encoding genes, named *aql*.

In the third study, an investigation of the microbial community associated with the Maldivian corals *Porites lobata* and *Acropora gemmifera*, along with the identification of novel bioactive CAMs was carried out. In particular, approximately 50 bacterial strains were isolated from the two coral species, and 10 strains were selected for functional screening, focusing on antimicrobial, antioxidant and UV protection activities. The results demonstrated that, *Streptomyces* sp. 79, *Pseudoalteromonas* sp. 39, *Salinispora* sp. 93 and *Microbacterium*

sp. 92 exhibited potent antimicrobial activity against human and fish pathogens, as well as significant antioxidant and UV protectant properties. Three out four most promising strains were subjected to whole genome sequencing and annotation. Genome-based identity allowed to assign *Pseudoalteromonas* sp. 39 and *Microbacterium* sp. 92 to two novel species. The bioinformatic analysis also revealed a high number of genes involved in stress response and encoding for novel BGCs suggesting the high potential of the selected CAMs for coral restoration purposes and biotechnological applications.

This work highlights the immense potential of marine environment as a source of novel natural products. Using an integrated approach combining advanced omics techniques with functional assays, this research highlights the potential to unlock the unique capabilities of marine extremophilic bacteria paving the way for new strategies for drug discovery to combat antimicrobial resistance while contributing to generate further sustainable biotechnological solutions.

This work is part of the European funded project SECRETED (H2020-FNR-11-2020: SECRETED; Grant agreement: 101000794).

It is also co-founded by Programma Operativo Nazionale Ricerca e Innovazione 2014-2020, risorse FSE REACT-EU Azione IV.4 “Dottorati e contratti di ricerca su tematiche dell’innovazione” e Azione IV.5 ”Dottorati su Tematiche Green”

CHAPTER 1

Novel Insights into the Nobilamide Family from a Deep-Sea *Bacillus*: Chemical Diversity, Biosynthesis and Antimicrobial Activity towards MDR Bacteria

Abstract: With rising concerns about antimicrobial resistance (AMR), identifying new lead compounds targeting multidrug-resistant strains is mandatory. This study employed high-throughput screening to cultivate and probe for biosurfactant and antibacterial activities about 300 marine strains simultaneously, leading to the selection of the deep-sea *Bacillus halotolerans* BCP32. The integration of tandem mass spectrometry molecular networking and bioassay-guided fractionation unveiled this strain as a prolific factory of surfactins and nobilamides. Particularly, 84 nobilamide congeners were identified in the bacterial exometabolome, 71 of them being novel metabolites. Among these, four major compounds were isolated, including the known TL-119 and Nobilamide I as well as the two new nobilamides T1 and S1. Antimicrobial assays demonstrated that TL-119 and nobilamide S1 exhibited potent antibiotic activity against various multidrug-resistant *Staphylococcus* strains and other Gram-positive pathogens, including the foodborne pathogen *Listeria monocytogenes*. Moreover, *in silico* analysis of *Bacillus halotolerants* BCP32 genome revealed nobilamide biosynthesis to be directed by a previously unknown heptamodular nonribosomal peptide synthetase.

---

1. Introduction

During the last decades, the selective pressure caused by the overuse of antibiotics led to the development of a new class of bacteria, defined Multidrug Resistant (MDR) bacteria. Most of them are resistant to at least three classes of antibiotics and represent a serious threat to human health [1] with the real risk to recreate the pre-antibiotic era. Recently, World Health Organization (WHO) highlighted the issue represented by antimicrobial resistance showing a scaring

future scenario (https://www.who.int/publications/i/item/9789240093461) [2]. After COVID-19, this phenomenon was defined the "Silent Pandemic" [3]. To counteract this phenomenon, different strategies are needed. The bioprospecting of unexplored environments like (extreme) marine habitat could lead to the discovery of new Natural Products (NPs) especially produced by microorganisms. Marine microbial species have developed several adaptation strategies in order to survive to extreme environmental conditions, often through the production of relevant molecules with biotechnological interest [4,5] such as antibiotics with innovative mechanisms of action [6–10] able to overcome the resistance issue. As a fact, microbial NPs represent the largest source of new antibiotic molecules, covering about two-thirds of antibacterial therapies approved between 1980 and 2010 for human medicine [11,12]

Among relevant compounds, cell membrane–targeting molecules displaying a "detergent-like" activity represent one of the most promising NPs to prevent or reduce resistance mechanisms [13–15]. For example, daptomycin, a cyclic lipodepsipeptide produced by *Streptomyces roseosporus*, is among the last resort antibiotic for treatment of Gram-positive pathogens [16,17]. Depsipeptides are chemical compounds with both ester and amide bonds in their structures [18,19]. On a broader perspective, biosurfactants (BSs), including lipodepsipeptides, are bacterial membrane-disrupting biomolecules [20].

Today, there is a growing interest for microbial-derived biosurfactants, secreted molecules with the ability to reduce interfacial liquids tension showing eco-compatibility, cost-effectiveness, low toxicity and better selectivity compared to synthetic surfactants [21,22]. They also exhibit antimicrobial, antiviral, and antitumor properties [23–25].

Among (marine) microorganisms, the members of *Bacillus* genus are well-known to produce a variety of novel peptides and lipopeptides, which have high potential as antimicrobials and biosurfactants [26–28]. These molecules are

synthesized by biosynthetic gene clusters (BGCs), i.e. operonic genes, and can be easily predicted or elucidated by the support of genomic data. In fact, they are usually produced by large multimodular enzymes, known as non-ribosomal peptide synthetases (NRPSs), which work as assembly lines to build peptides by sequential amino acid condensation [29,30]. Nonribosomal peptides are non-essential compounds, classified as secondary metabolites, that confer advantages by inhibiting competitors and modulating symbiont interactions in challenging environments [37]. Typically, an NRPS module includes adenylation (A), peptidyl carrier protein (PCP), and condensation (C) domains, while the termination module has a thioesterase (TE) domain for releasing and/or cyclizing the peptide. Some modules also feature an epimerization (E) domain to convert amino acids from the L- to the D-form during synthesis, thereby introducing a mixture of L- and D-amino acids to give peptides a specific stereochemistry for selective interaction with the cellular target [32]. The identification of novel BGCs encoding new active molecules is of crucial importance in drug discovery, as providing the tools to create sustainable sources of NPs.

The present work describes the screening of around 300 marine bacteria leading to the identification of a deep-sea *Bacillus* sp. BCP32 with both antimicrobial and biosurfactant activity. Tandem mass spectrometry-based molecular networking analysis of bacterial exometabolome, demonstrated the production of the depsipeptides antibiotic TL-119/A-3302-B [33–36] and other known congeners reported as nobilamides [37], along with almost 70 new analogues, showing potent antimicrobial activity against drug resistant Gram-positive pathogens. On the other hand, the high biosurfactant effect has been attributed to the secretion of a rich mixture of surfactins [27,38], well-known lipopeptides from *Bacillus* spp., which were shown to exert significant antibacterial activity against *S. aureus* and the fish pathogen, *Photobacterium damselae* subsp. *piscicida.* Finally, *in silico* genome analysis enabled for the identification of the previously unknown BGC

encoding the biosynthesis of TL-119/ A-3302-B and the nobilamide family. This work emphasizes the importance of the exploration of marine microbial biodiversity for the discovery and production of novel clinically relevant molecules.

2. Results and Discussion

2.1. Microbial Collection Screening and Selection of Bacillus sp. *BCP32*

Aiming to discover new biosurfactants and antimicrobials, about 300 marine bacteria belonging to the Stazione Zoologica Anton Dohrn (SZN) library were screened. A miniaturized system was employed, setting-up a micro-cultivation system for metabolite production in four steps, including 1) starting cultures, 2) metabolites production, 3) cells separation, 4) bioassay detection (as described in Materials and Methods and shown in Figure 1). This method relies on the use of deep well microplates, thereby allowing to test a relatively high number of strains, cultivated in different growth media to enhance biosynthesis of a wide range of metabolites. The CTAB agar assay (followed by the oil-spreading assay for positive strains) and the agar well diffusion method [39] were employed to detect the presence of biosurfactants and antimicrobials, respectively, in bacterial supernatants. Among the 300 strains, around 10% of samples showed bioactivity. Particular attention was given to the strain *Bacillus* sp. BCP32 due to its significant potential as a biosurfactant in both the CTAB and oil spreading assay, and its notable inhibition halo against *S. aureus* 6538p. *Bacillus* sp. BCP32 is an extremophilic strain isolated from deep-sea sediments collected from Canyon Dohrn in the Gulf of Naples (Italy) [40].

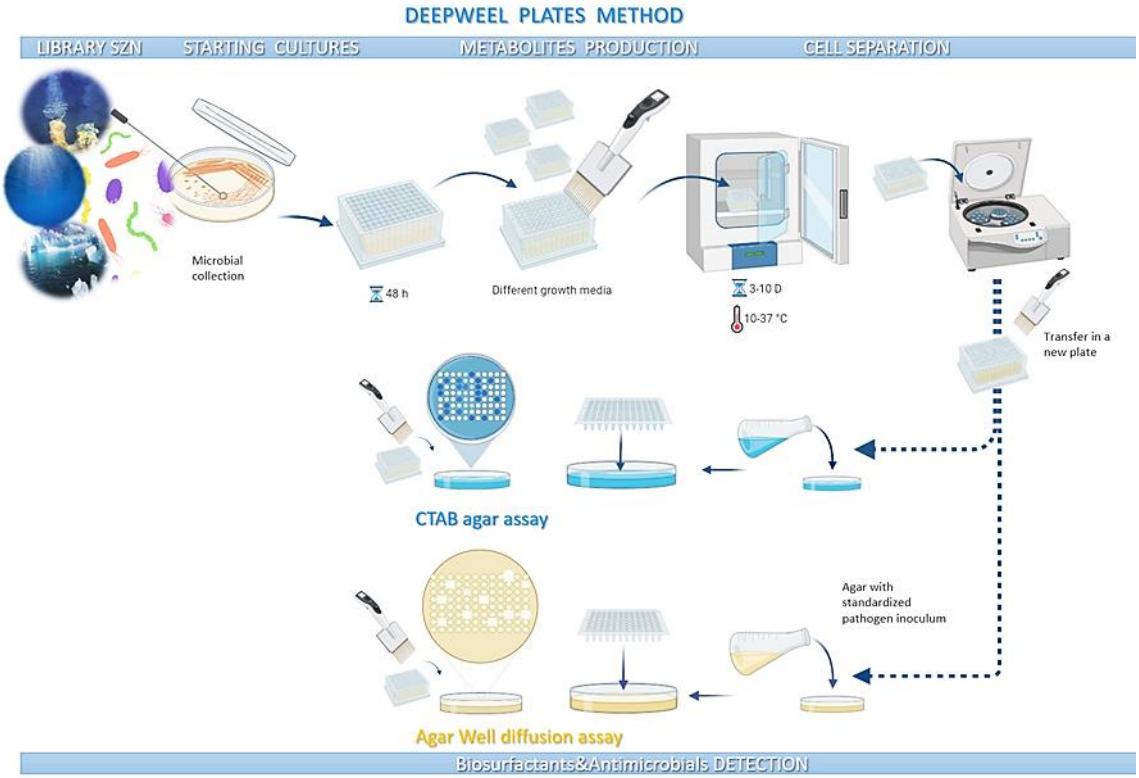

Figure 1. Graphical overview of the primary screening method applied to 300 marine bacteria from the Stazione Zoologica Anton Dohrn library. Bacterial cultures were grown in deep-well plates under various conditions, including different growth media, incubation periods, and temperatures. To evaluate their bioactivities, the CTAB agar assay was used to screen for biosurfactant production, while the agar diffusion well method was employed to assess antimicrobial activity.

2.2 Biological Activity Evaluation, Extraction and Fractionation of Bacillus sp. *BCP32 exhausted broth*

The selected bacterium was cultivated on a small scale (50 mL in a 250 mL flask) using liquid TYP medium at 28 °C for 2 days allowing the production of relevant metabolites to validate results from the primary screening. The exhausted broth was then extracted by ethyl acetate (EtOAc) obtaining 17 mg of crude extract and dissolved in DMSO (50 mg/mL) for biological assays. The oil spreading test was carried out confirming the biosurfactant activity of *Bacillus* sp. BCP32 extract. Furthermore, liquid inhibition assays were conducted against *Staphylococcus aureus* 6538p and *Escherichia coli* ATCC 10536 showing antibacterial activity with a MIC value of 15 ug/ml and 125 ug/ml, respectively.

Both pathogens have been selected because they are the primary causes of nosocomial infections and are increasingly developing resistance to conventional antibiotics [41,42]. Based on these results, BCP32 was scaled-up (1L) and culture broth was extracted by EtOAc obtaining 430 mg of organic extract, which was fractionated by solid-phase extraction (SPE) obtaining five fractions (F), as described in Materials and Methods. Each fraction was subjected to oil-spreading test and liquid inhibition assay and analysed through liquid chromatography-high resolution tandem mass spectrometry (LC-HRMS^2). Fraction eluted with 90% MeOH (F-90% MeOH) displayed the best bioactivity in both biosurfactant and antimicrobial assays (Tables 1 and S1, Figures 2 and S1). Concerning the antibacterial activity, the pathogens panel was expanded, including several *S. aureus* MDR strains, *S. epidermidis, S. xylosus,* and *Listeria monocytogenes*. The F-90% MeOH showed a MIC value ranging from 0,9 ug/ml to 3,9 ug/ml (Table 1) towards all the pathogens, with the only exception of vancomycin-resistant *S. aureus* (VRSA).

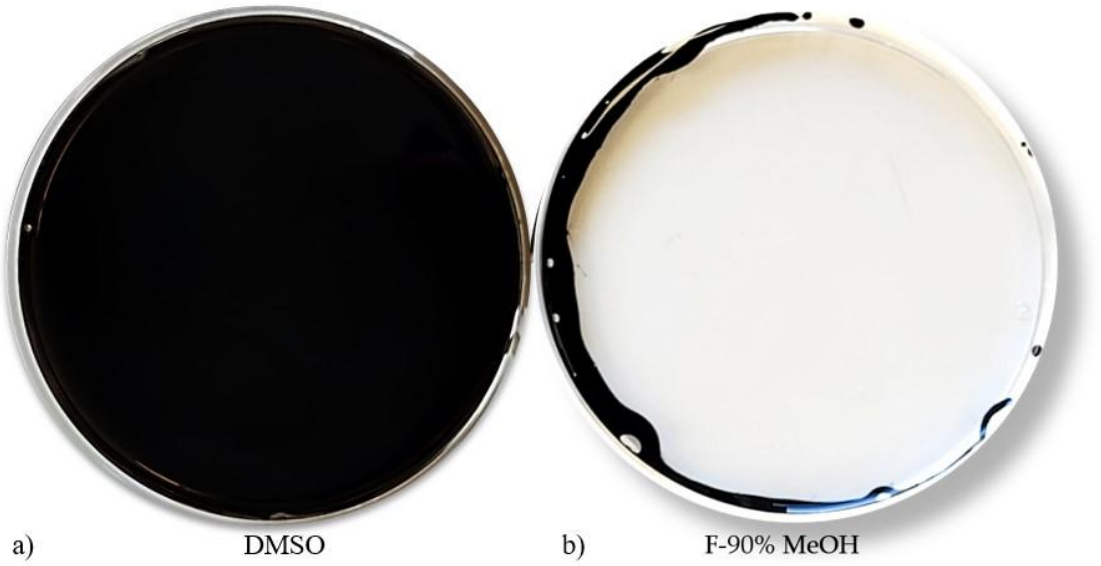

Figure 2. Surfactant activity of the F-90% MeOH from *Bacillus* sp. BCP32 in the oil spreading test. a) DMSO vehicle (4 μL) was used as negative control. b) The clear zone on the oil surface indicates the presence of biosurfactants.

Table 1. Antibacterial activity of the F-90% MeOH towards a panel of Gram-positive pathogens. MIC values are expressed in μg/mL.

Strain	F-90% MeOH
S. aureus 6538p	0.9
S. aureus 6538	0.9
S. aureus Methicillin Resistant	3.9
S. aureus Macrolide Resistant	3.9
S. aureus Quinolone Resistant	3.9
S. aureus Vancomycin Resistant	--
S. epidermidis RP206	1.9
S. xilosus MB5209	1.9
Listeria monocytogenes 677	0.9

2.3.Molecular Networking Analysis and Purification of Nobilamides

Since the F-90% MeOH showed both biosurfactant and antimicrobial activities, the chemical space present in this fraction was mapped by feature-based molecular networking (FBMN) analysis of untargeted MS^2 data, as previously reported [43,44]. The FBMN workflow is available at the GNPS2 platform (https://gnps2.org, accessed on 02/10/2024) and generates an MS^2 spectral similarity map, highlighting structurally related molecules. The molecular network of the F-90% MeOH (Figure 3) unveiled the presence of two dominant molecular clusters, including nobilamides (blue nodes) and surfactins (orange nodes).

While almost 70 nodes within the orange cluster could be promptly annotated as surfactins or surfactin analogues through the GNPS spectral library search, an in-depth manual dereplication of MS^2 data was required for the identification of nobilamides. The careful examination of product ion spectra of individual compounds within the blue cluster, allowed us for elucidation of 84 nobilamide congeners, 71 of them being novel molecules.

The nobilamide family mainly comprises cyclic N-acyldepsiheptapeptides, where the D-*allo*-Thr^4 side-chain OH group forms an ester bond with the C-terminal (*Z*)-2,3-dehydrobutyrine (Figure 4). Nevertheless, nobilamides may

occur also as linear heptapeptides (nobilamides A-C and S-W) [45,46]. Minor congeners including the cyclic N-acyldepsihexapeptide nobilamide D, the linear hexapeptides nobilamide C, and the linear pentapeptide nobilamide W, have been observed in *Streptomyces* and *Bacillus* spp. [45,46]. Besides the presence of cyclic N-acyldepsiheptapeptides (32) and linear heptapeptides (26), the nobilamide cluster from *Bacillus* sp. BCP32 was shown to be composed of cyclic N-acyldepsihexapeptides (11), cyclic N-acyldepsioctapeptides (2), cyclic N-acyldepsinonapeptide (1) as well as linear hexapeptides (4) and octapeptides (8), thus unveiling that the nobilamide biosynthesis may take divergent paths to create an outstanding chemical diversity (Figure 4).

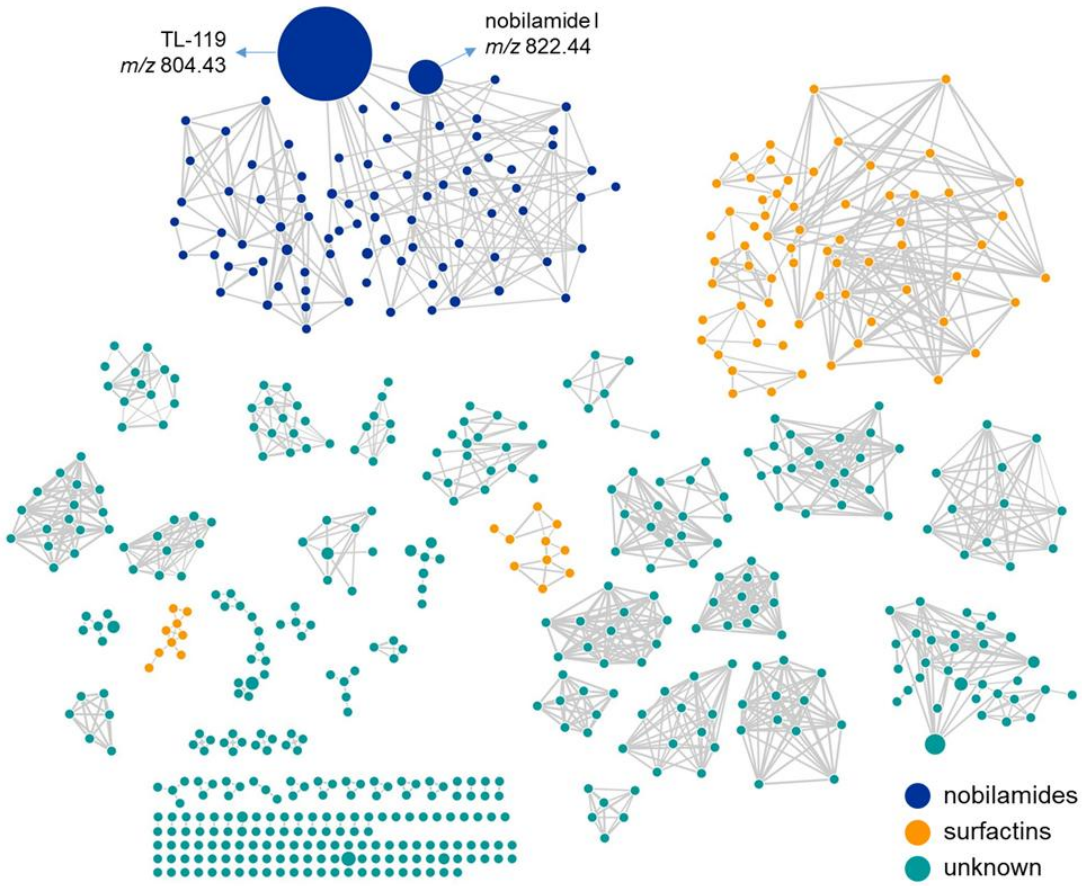

Figure 3. LC-HRMS² based molecular network (MN) of the F-90% MeOH from *Bacillus* sp. BCP32. The MN is dominated by two large clusters, i.e. nobilamides (blue nodes) and surfactins (orange nodes). Compounds are visualized as nodes and node size reflects compound peak area. Edge thickness is related to MS² spectra similarity.

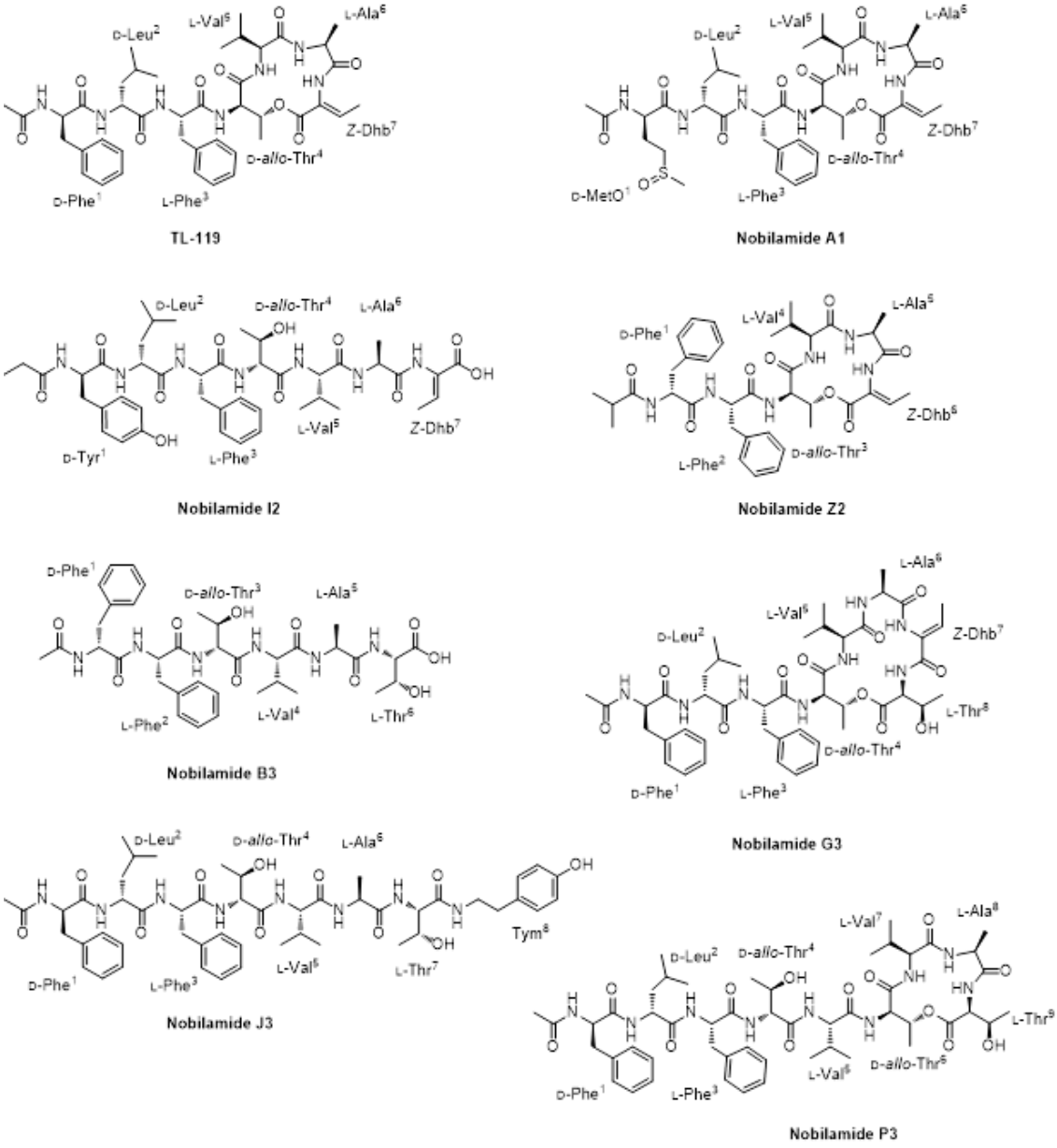

Figure 4. Chemical structures of representative nobilamides from *Bacillus* sp. BCP32.

2.4 Structural Characterization of Nobilamide Depsiheptapeptides and Linear Heptapeptides by Mass Spectrometry

The structural characterization of the 84 nobilamide congeners was performed by LC-HRMS^2 on a Q Exactive Focus Orbitrap mass spectrometer. The high resolution masses of the pseudomolecular ions $[M+H]^+$ included in the nobilamide network (blue nodes, Figure 3), designated the molecular formulas

reported in Tables 1-7 (mass accuracy ≤ 3.0 ppm). Nobilamide precursor ions were selected to be fragmented in the higher-energy collision dissociation cell (HCD) and acquire MS^2 data of individual compounds.

During mass fragmentation, cyclic nobilamides first underwent ring opening at the ester bond, thus yielding the linear fragment α, where the Thr residue forming the lactone ring is converted into a dehydrobutyrine residue (Figures 5A and S2). Sequential N- and C-terminal cleavages of the linear fragment generated a complete *y*- and *b*-type ion series which enabled the assignment of the amino acid sequence of nobilamides. In agreement with Iloabuchi and Spiteller [46], nobilamide lactones can be fairly distinguished from the linear counterparts as featuring a diagnostic neutral loss of the dehydrobutyrine residue (C_4H_5NO, 83.0371 amu) from the corresponding *b* fragment ion (e.g. b_4 ion in *N*-acyldepsiheptapeptides) (Figure 5). In addition, while linear nobilamides underwent in most cases a rearrangement reaction leading to loss of the C-terminal residue and formation of a b_{n-1}+H_2O ion [47], nobilamide lactones gave only the b_{n-1} fragment ion, losing an intact C-terminal amino acid after the ester bond cleavage. The b_2 fragment ions of *N*-acylated nobilamides displayed neutral loss of the fatty acyl chain as ketene, which was useful to infer the acyl group linked to the N-terminal amino acid (Figure 5A).

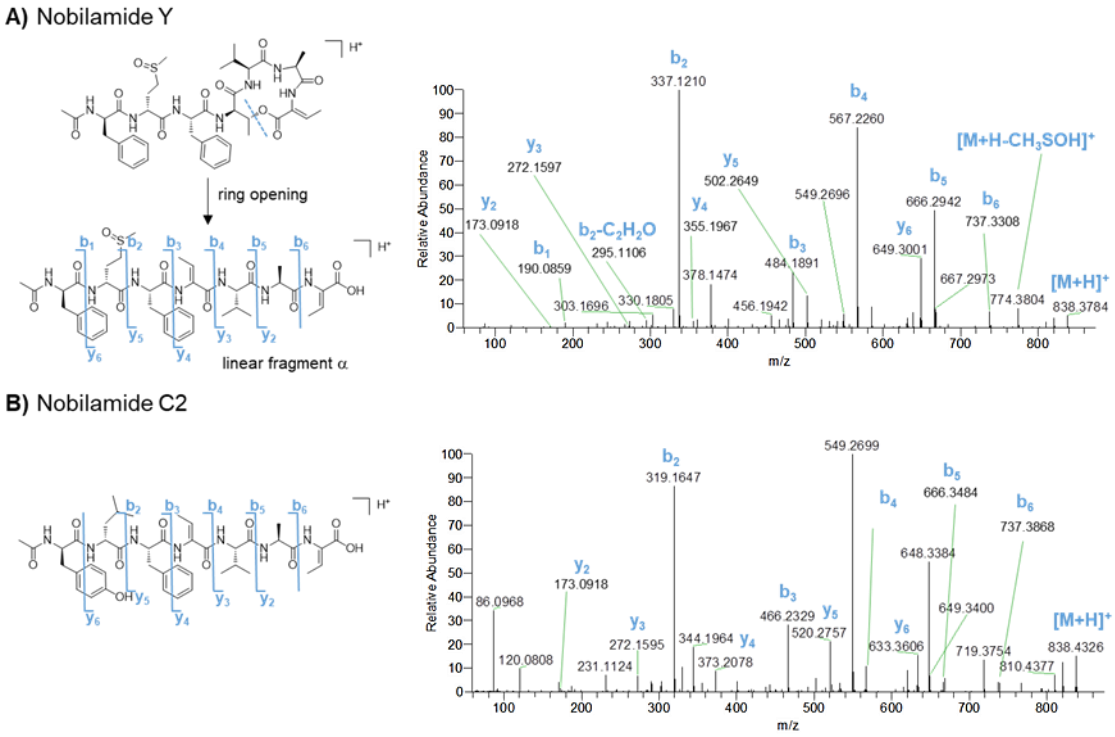

Figure 5. LC-HRMS^2 spectra of the $[M+H]^+$ pseudomolecular ions of representive cyclic (A) and linear (B) nobilamides from *Bacillus* sp. BCP32.

The consensus sequences of cyclic *N*-acyldepsiheptapeptides and linear heptapeptides from *Bacillus* sp. BCP32 is D-Phe^1-D-Leu^2-L-Phe^3-D-*allo*-Thr^4-L-Val^5-L-Ala^6-(*Z*)-2,3-dehydrobutyrine^7 (Tables 2 and 3) and nicely matches the specificity prediction of A domains in the nobilamide (*nbl*) synthetase (see section 2.7).

Phe^1 is replaced by either Leu, Met, MetO, or Tyr in a few congeners. When MetO is incorporated, product ion spectra of nobilamides display fragment ions arising from the neutral loss of methanesulfenic acid (CH_3SOH, 63.9983 Da), which is indicative of the sulfoxide group in-side chain of MetO. Leu^2 is conserved across all depsiheptapeptides and linear heptapeptides, except nobilamide X and Y, which feature MetO at position 2. Met, MetO, and Leu are also found in place of Phe^3 in some congeners; notably, nobilamide F2 bears an unprecedented putative kynurenine (Kyn) residue at position 3, as shown by the neutral loss of 190.0742 Da ($C_{10}H_{10}N_2O_2$) from the y_5 and b_3 ions (Figure S6). In general, by analogy with

the nobilamide structures described so far, we tentatively discriminated between the isobaric Ile and Leu residues, thus assigning Leu at positions 1, 2, and 3 where present. Interestingly, this assignment was corroborated by the A domain substrate selectivity predicted *in silico* (see section 2.7). Nobilamide depsiheptapeptides and linear heptapeptides from *Bacillus* sp. BCP32 share Thr^4, with only two congeners, i.e. nobilamide L1 and L2, including Ser^4. The most frequent amino acid at position 5 is Val, even if either Ile/Leu, Phe, Ala, or *homo*-Ala are incorporated in minor isoforms. We tentatively distinguished between the isomeric *homo*-Ala and *N*-Me-Ala in nobilamide B2 as *homo*-Ala was already reported in the structural analogue nobilamide M [46]. Ala^6 is replaced by either Gly, Ser, or Thr, while the last amino acid is most cases represented by (*Z*)-2,3-dehydrobutyrine, which can be substituted by Thr. Notably, the presence of diaminobutyric acid (Dab) in nobilamide B1, phenethylamine (Pea) in nobilamide Q2, and tyramine (Tym) in nobilamide J2 was observed at position 7, thus unveiling unique structural variations in the nobilamide family from *Bacillus* sp. BCP32.

Most nobilamide depsiheptapeptides and linear heptapeptides undergo N-terminal acetylation. Neverthless, isoforms having propanoyl, isobutanoyl, and C_5H_9O acyl groups have been identified together with deacylated derivatives.

The stereochemistry of the seven amino acids was assigned through bioinformatic prediction and by analogy with the stereochemistry of nobilamides determined by Marfey's method and NMR spectroscopy [35,46]. As the nobilamide synthetase includes three epimerization domains within modules 1, 2, and 4 (Figure 6), respectively, the presence of D-Phe^1, D-Leu^2 and D-*allo*-Thr^4 was inferred, while the remaining amino acids were assumed to possess the L configuration. The genomics-driven absolute configuration assignment turned out to be in agreement with the reported stereochemistry for nobilamides.

The F-90% MeOH was separated by reversed phase HPLC chromatography, thus yielding the pure cyclic depsiheptapeptides TL-119, nobilamide I, and the novel congeners T1 and S1 that were assessed for antimicrobial activity (see section 2.6).

Table 2. Cyclic depsiheptapeptides from *Bacillus* sp. BCP32. [a] The D-*allo*-Thr/Ser[4] side-chain OH group forms an ester bond with the C-terminal residue. [*] Nobilamides in bold have been already reported elsewhere. Abbreviations: Ac, acetyl; Pr, propanoyl; D-*a*-Thr, D-*allo*-threonine; Dhb, 2,3-dehydrobutyrine; Dab, diaminobutyric acid.

Nobilamide[*]	[M+H]$^+$	*m/z*	R_t (min)	R_1	aa-1	aa-2	aa-3	aa-4 [a]	aa-5	aa-6	aa-7
X	$C_{41}H_{58}N_7O_{11}S$	856.3907	14.8	Ac	D-Phe	D-MetO	L-Phe	D-*a*-Thr	L-Val	L-Ala	L-Thr
Y	$C_{41}H_{56}N_7O_{10}S$	838.3792	16.4	Ac	D-Phe	D-MetO	L-Phe	D-*a*-Thr	L-Val	L-Ala	Z-Dhb
Z	$C_{38}H_{58}N_7O_{10}S$	804.3950	16.8	Ac	D-Phe	D-Leu	L-MetO	D-*a*-Thr	L-Val	L-Ala	Z-Dhb
A1	$C_{38}H_{58}N_7O_{10}S$	804.3950	17.2	Ac	D-MetO	D-Leu	L-Phe	D-*a*-Thr	L-Val	L-Ala	Z-Dhb
B1	$C_{42}H_{63}N_8O_{10}$	839.4654	17.7	Ac	D-Phe	D-Leu	L-Phe	D-*a*-Thr	L-Val	L-Ala	L-Dab
I	**$C_{42}H_{60}N_7O_{10}$**	**822.4387**	**19.1**	**Ac**	**D-Phe**	**D-Leu**	**L-Phe**	**D-*a*Thr**	**L-Val**	**L-Ala**	**L-Thr**
C1	$C_{41}H_{60}N_7O_9$	794.4443	19.2	-	D-Phe	D-Leu	L-Phe	D-*a*-Thr	L-Leu/ Ile	L-Ala	L-Thr
N	**$C_{42}H_{58}N_7O_{10}$**	**820.4237**	**19.5**	**Ac**	**D-Phe**	**D-Leu**	**L-Phe**	**D-*a*Thr**	**L-Val**	**L-Ser**	***Z*-Dhb**
D1	$C_{38}H_{58}N_7O_9S$	788.4004	20.2	Ac	D-Met	D-Leu	L-Phe	D-*a*-Thr	L-Val	L-Ala	Z-Dhb
E1	$C_{41}H_{58}N_7O_{10}$	808.4234	20.2	Ac	D-Phe	D-Leu	L-Phe	D-*a*-Thr	L-Val	L-Gly	L-Thr
F1	$C_{41}H_{56}N_7O_{10}$	806.4087	20.3	Ac	D-Phe	D-Leu	L-Phe	D-*a*-Thr	L-Thr	L-Ala	Z-Dhb
G1	$C_{38}H_{58}N_7O_9S$	788.4009	20.5	Ac	D-Phe	D-Leu	L-Met	D-*a*-Thr	L-Val	L-Ala	Z-Dhb
L	**$C_{41}H_{56}N_7O_9$**	**790.4128**	**20.6**	**Ac**	**D-Phe**	**D-Leu**	**L-Phe**	**D-*a*Thr**	**L-Val**	**L-Gly**	***Z*-Dhb**
H1	$C_{42}H_{58}N_7O_{10}$	820.4236	20.7	Ac	D-Tyr	D-Leu	L-Phe	D-*a*-Thr	L-Val	L-Ala	Z-Dhb
Q	**$C_{39}H_{60}N_7O_9$**	**770.4446**	**21.2**	**Ac**	**D-Leu**	**D-Leu**	**L-Phe**	**D-*a*Thr**	**L-Val**	**L-Ala**	***Z*-Dhb**
I1	$C_{40}H_{54}N_7O_9$	776.3969	21.2	Ac	D-Phe	D-Leu	L-Phe	D-*a*-Thr	L-Ala	L-Ala	Z-Dhb
J1	$C_{43}H_{60}N_7O_{10}$	834.4380	21.3	Ac	D-Phe	D-Leu	L-Phe	D-*a*-Thr	L-Val	L-Thr	Z-Dhb
O	**$C_{39}H_{60}N_7O_9$**	**770.4446**	**21.4**	**Ac**	**D-Phe**	**D-Leu**	**L-Leu**	**D-*a*Thr**	**L-Val**	**L-Ala**	***Z*-Dhb**
K1	$C_{43}H_{60}N_7O_{10}$	834.4392	21.4	Pr	D-Tyr	D-Leu	L-Phe	D-*a*-Thr	L-Val	L-Ala	Z-Dhb
L1	$C_{41}H_{56}N_7O_9$	790.4133	21.7	Ac	D-Phe	D-Leu	L-Phe	D-Ser	L-Val	L-Ala	Z-Dhb
TL-119 (A-3302-B)	**$C_{42}H_{58}N_7O_9$**	**804.4289**	**22.0**	**Ac**	**D-Phe**	**D-Leu**	**L-Phe**	**D-*a*Thr**	**L-Val**	**L-Ala**	***Z*-Dhb**
M1	$C_{40}H_{62}N_7O_9$	784.4608	22.6	Pr	D-Leu	D-Leu	L-Phe	D-*a*-Thr	L-Val	L-Ala	Z-Dhb
N1	$C_{40}H_{62}N_7O_9$	784.4608	22.6	Pr	D-Phe	D-Leu	L-Leu	D-*a*-Thr	L-Val	L-Ala	Z-Dhb
O1	$C_{40}H_{62}N_7O_9$	784.4608	22.6	Ac	D-Leu	D-Leu	L-Phe	D-*a*-Thr	L-Leu/ Ile	L-Ala	Z-Dhb
A-3302-A	**$C_{43}H_{60}N_7O_9$**	**818.4446**	**23.5**	**Pr**	**D-Phe**	**D-Leu**	**L-Phe**	**D-*a*Thr**	**L-Val**	**L-Ala**	***Z*-Dhb**
P1	$C_{39}H_{54}N_7O_8$	748.4023	24.5	-	D-Phe	D-Leu	L-Phe	D-*a*-Thr	L-Val	L-Gly	Z-Dhb
J	$C_{44}H_{62}N_7O_9$	832.4604	24.5	C_4H_7O	D-Phe	D-Leu	L-Phe	D-*a*-Thr	L-Val	L-Ala	Z-Dhb
Q1	$C_{37}H_{58}N_7O_8$	728.4339	24.6	-	D-Leu	D-Leu	L-Phe	D-*a*-Thr	L-Val	L-Ala	Z-Dhb
R1	$C_{46}H_{58}N_7O_9$	852.4289	24.8	Ac	D-Phe	D-Leu	L-Phe	D-*a*-Thr	L-Phe	L-Ala	Z-Dhb
S1	$C_{43}H_{60}N_7O_9$	818.4447	24.8	Ac	D-Phe	D-Leu	L-Phe	D-*a*-Thr	L-Leu/ Ile	L-Ala	Z-Dhb
K	**$C_{45}H_{64}N_7O_9$**	**846.4763**	**25.5**	**C_5H_9O**	**D-Phe**	**D-Leu**	**L-Phe**	**D-*a*Thr**	**L-Val**	**L-Ala**	***Z*-Dhb**
T1	$C_{40}H_{56}N_7O_8$	762.4182	28.3	-	D-Phe	D-Leu	L-Phe	D-*a*-Thr	L-Val	L-Ala	Z-Dhb

Table 3. Linear heptapeptides from *Bacillus* sp. BCP32. * Nobilamides in bold have been already reported elsewhere. Abbreviations: Ac, acetyl; Pr, propanoyl; D-*a*-Thr, D-*allo*-threonine; Dhb, 2,3-dehydrobutyrine; *h*-Ala, *homo*-alanine; Kyn, kynurenine; Pea, phenethylamine; Tym, tyramine; OMe, methyl ester.

Nobilamide*	[M+H]+	*m/z*	*R*t (min)	R1	aa-1	aa-2	aa-3	aa-4	aa-5	aa-6	aa-7
U1	$C_{38}H_{60}N_7O_{11}S$	822.4068	15.1	Ac	D-MetO	D-Leu	L-Phe	D-*a*-Thr	L-Val	L-Ala	Z-Dhb
V1	$C_{38}H_{60}N_7O_{11}S$	822.4068	15.4	Ac	D-Phe	D-Leu	L-MetO	D-*a*-Thr	L-Val	L-Ala	Z-Dhb
W1	$C_{42}H_{62}N_7O_{12}$	856.4438	16.9	Ac	D-Phe	D-Leu	L-Tyr	D-*a*-Thr	L-Val	L-Ala	L-Thr
X1	$C_{41}H_{60}N_7O_{11}$	826.4336	17.3	Ac	D-Phe	D-Leu	L-Phe	D-*a*-Thr	L-Val	L-Gly	L-Thr
S	**$C_{42}H_{62}N_7O_{11}$**	**840.4491**	**17.4**	**Ac**	**D-Phe**	**D-Leu**	**L-Phe**	**D-*a*-Thr**	**L-Val**	**L-Ala**	**L-Thr**
Y1	$C_{40}H_{56}N_7O_{10}$	794.4071	17.7	Ac	D-Phe	D-Leu	L-Phe	D-*a*-Thr	L-Ala	L-Ala	Z-Dhb
Z1	$C_{38}H_{60}N_7O_{10}S$	806.4104	17.7	Ac	D-Met	D-Leu	L-Phe	D-*a*-Thr	L-Val	L-Ala	Z-Dhb
A2	$C_{42}H_{60}N_7O_{11}$	838.4339	18.1	Ac	D-Phe	D-Leu	L-Phe	D-*a*-Thr	L-Val	L-Ser	Z-Dhb
B2	$C_{41}H_{58}N_7O_{10}$	808.4232	18.3	Ac	D-Phe	D-Leu	L-Phe	D-*a*-Thr	L-*h*-Ala	L-Ala	Z-Dhb
A	**$C_{42}H_{60}N_7O_{10}$**	**822.4388**	**18.3**	**Ac**	**D-Phe**	**D-Leu**	**L-Phe**	**D-*a*-Thr**	**L-Val**	**L-Ala**	***Z*-Dhb**
C2	$C_{42}H_{60}N_7O_{11}$	838.4336	18.4	Ac	D-Tyr	D-Leu	L-Phe	D-*a*-Thr	L-Val	L-Ala	Z-Dhb
D2	$C_{43}H_{64}N_7O_{11}$	854.4650	18.4	Ac	D-Phe	D-Leu	L-Phe	D-*a*-Thr	L-Val	L-Ala	L-Thr-OMe
E2	$C_{39}H_{62}N_7O_{10}$	788.4544	18.6	Ac	D-Phe	D-Leu	L-Leu	D-*a*-Thr	L-Val	L-Ala	Z-Dhb
F2	$C_{43}H_{61}N_8O_{11}$	865.4446	18.7	Ac	D-Phe	D-Leu	L-Kyn	D-*a*-Thr	L-Val	L-Ala	Z-Dhb
G2	$C_{39}H_{62}N_7O_{10}$	788.4538	18.8	Ac	D-Leu	D-Leu	L-Phe	D-*a*-Thr	L-Val	L-Ala	Z-Dhb
H2	$C_{41}H_{58}N_7O_{10}$	808.4232	18.8	Ac	D-Phe	D-Leu	L-Phe	D-*a*-Thr	L-Val	L-Gly	Z-Dhb
I2	$C_{43}H_{62}N_7O_{11}$	852.4490	18.8	Pr	D-Tyr	D-Leu	L-Phe	D-*a*-Thr	L-Val	L-Ala	Z-Dhb
J2	$C_{46}H_{64}N_7O_9$	858.4751	19.4	Ac	D-Phe	D-Leu	L-Phe	D-*a*-Thr	L-Val	L-Ala	Tym
K2	$C_{43}H_{62}N_7O_{10}$	836.4543	19.5	Ac	D-Phe	D-Leu	L-Phe	D-*a*-Thr	L-Val	L-Ala	Z-Dhb-OMe
B	**$C_{43}H_{62}N_7O_{10}$**	**836.4544**	**20.0**	**Pr**	**D-Phe**	**D-Leu**	**L-Phe**	**D-*a*-Thr**	**L-Val**	**L-Ala**	***Z*-Dhb**
L2	$C_{43}H_{62}N_7O_{10}$	836.4544	20.0	Pr	D-Phe	D-Leu	L-Phe	D-Ser	L-Leu/Ile	L-Ala	Z-Dhb
M2	$C_{40}H_{58}N_7O_9$	780.4287	20.4	-	D-Phe	D-Leu	L-Phe	D-*a*-Thr	L-Val	L-Ala	Z-Dhb
N2	$C_{44}H_{64}N_7O_{10}$	850.4705	20.8	C_4H_7O	D-Phe	D-Leu	L-Phe	D-*a*-Thr	L-Val	L-Ala	Z-Dhb
O2	$C_{45}H_{66}N_7O_{10}$	864.4863	21.6	C_5H_9O	D-Phe	D-Leu	L-Phe	D-*a*-Thr	L-Val	L-Ala	Z-Dhb
P2	$C_{45}H_{66}N_7O_{10}$	864.4863	21.6	C_4H_7O	D-Phe	D-Leu	L-Phe	D-*a*-Thr	L-Leu/Ile	L-Ala	Z-Dhb
Q2	$C_{46}H_{64}N_7O_8$	842.4785	21.7	Ac	D-Phe	D-Leu	L-Phe	D-*a*-Thr	L-Val	L-Ala	Pea

2.5 Structural Characterization of Cyclic and Linear Hexa-, Octa-, and Nonapeptides by Mass Spectrometry

Manual inspection of the nobilamide cluster within the molecular network led to the identification of cyclic N-acyldepsihexapeptides and linear hexapeptides (Tables 4 and 5). These congeners bear the same structural features as cyclic depsiheptapeptides and linear heptapeptides, except for nobilamide A3 having an unusual $C_6H_9O_2$ acyl group, tentatively identified as a 4-methyl-2-oxovaleryl moiety, which may either be recruited by the first NRPS module of the Nbl synthetase [48] or derive from oxidative deamination of a leucine starter unit. Cyclic nobilamides R2-U2, V2, and W2 and linear nobilamides C3 and E3 are truncated isoforms at the N- or C-terminus of the cognate heptapeptide analogues, while nobilamides X2-B3 and D3 are closely related to the already known nobilamide D, where the second amino acid, i.e. D-Leu, is missing. These findings suggest that modules 1, 2 and 7 of the Nbl synthetase might be skipped for the generation of the truncated congeners, likely as a result of an aberrant event leading to production of minor metabolites [49]. While module skipping processes occurred in several PKSs and hybrid PKS/NRPS systems, this event has been described only once for multimodular NRPS so far, that is the case of myxochromide S biosynthesis [50].

Table 4. Cyclic depsihexapeptides from *Bacillus* sp. BCP32. * Nobilamides in bold have been already reported elsewhere. [a] The D-*allo*-Thr[4] side-chain OH group forms an ester bond with the C-terminal residue. [b] $[M+H+NH_3]^+$. Abbreviations: Ac, acetyl; Pr, propanoyl; D-*a*-Thr, D-*allo*-threonine; Dhb, 2,3-dehydrobutyrine.

Nobilamide*	$[M+H]^+$	*m/z*	R_t (min)	R_1	aa-1	aa-2	aa-3	aa-4	aa-5	aa-6
R2	$C_{37}H_{54}N_7O_8$[b]	724.4009	17.4	Ac	D-Phe	D-Leu	L-Phe	D-*a*-Thr[a]	L-Val	L-Gly
S2	$C_{38}H_{53}N_6O_8$	721.3908	18.2	Ac	D-Phe	D-Leu	L-Phe	D-*a*-Thr[a]	L-Val	L-Ala
T2	$C_{39}H_{58}N_7O_8$[b]	752.4331	18.5	Pr	D-Phe	D-Leu	L-Phe	D-*a*-Thr[a]	L-Val	L-Ala
U2	$C_{39}H_{58}N_7O_8$[b]	752.4331	18.5	Ac	D-Phe	D-Leu	L-Phe	D-*a*-Thr[a]	L-Leu/Ile	L-Ala
D	**$C_{36}H_{47}N_6O_8$**	**691.3438**	**18.9**	**Ac**	**D-Phe**	**L-Phe**	**D-*a*-Thr[a]**	**L-Val**	**L-Ala**	***Z*-Dhb**
V2	$C_{33}H_{49}N_6O_8$	657.3594	19.3	Ac	D-Leu	L-Phe	D-*a*-Thr[a]	L-Val	L-Ala	Z-Dhb
W2	$C_{33}H_{49}N_6O_8$	657.3599	19.7	Ac	D-Phe	L-Leu	D-*a*-Thr[a]	L-Val	L-Ala	Z-Dhb
X2	$C_{37}H_{49}N_6O_8$	705.3600	19.7	Pr	D-Phe	L-Phe	D-*a*-Thr[a]	L-Val	L-Ala	Z-Dhb

Y2	$C_{37}H_{49}N_6O_8$	705.3597	19.9	Ac	D-Phe	L-Phe	D-*a*-Thr[a]	L-Leu/Ile	L-Ala	Z-Dhb
Z2	$C_{38}H_{51}N_6O_8$	719.3756	20.8	C_4H_7O	D-Phe	L-Phe	D-*a*-Thr[a]	L-Val	L-Ala	Z-Dhb
A3	$C_{40}H_{53}N_6O_9$	761.3869	23.9	$C_6H_9O_2$	D-Phe	L-Phe	D-*a*-Thr[a]	L-Val	L-Ala	Z-Dhb

Table 5. Linear hexapeptides from *Bacillus* sp. BCP32. Abbreviations: Ac, acetyl; D-*a*-Thr, D-*allo*-threonine; Dhb, 2,3-dehydrobutyrine.

Nobilamide	$[M+H]^+$	*m/z*	R_t (min)	R_1	aa-1	aa-2	aa-3	aa-4	aa-5	aa-6
B3	$C_{36}H_{51}N_6O_{10}$	727.3658	15.7	Ac	D-Phe	L-Phe	D-*a*Thr	L-Val	L-Ala	L-Thr
C3	$C_{33}H_{51}N_6O_9$	675.3702	16.8	Ac	D-Leu	L-Phe	D-*a*Thr	L-Val	L-Ala	*Z*-Dhb
D3	$C_{36}H_{49}N_6O_9$	709.3544	16.9	Ac	D-Phe	L-Phe	D-*a*Thr	L-Val	L-Ala	*Z*-Dhb
E3	$C_{38}H_{53}N_6O_8$	721.3905	17.7	Ac	D-Phe	D-Leu	L-Phe	*Z*-Dhb	L-Val	L-Ala

Differently from the other nobilamide-producing strains, *Bacillus* sp. BCP32 showed the biosynthetic ability to assemble cyclic octa- and nona- depsipeptides and linear octapeptides (Tables 6-8). Nobilamides F3 and G3 are cyclic octadepsipeptides, which differ from TL-119 as having at the C-terminus an additional amino acid, i.e. L-dehydro-Asn and L-Thr, respectively, involved in the formation of the lactone ring with the side-chain OH group of D-*allo*-Thr^4 (Figures S6). Linear octapeptides H3-O3 have the hexapeptide motif Phe^1-D-Leu^2-L-Phe^3-D-*allo*-Thr^4-L-Val^5-L-Ala^6, while structural diversification results from amino acid substitutions in positions 7 and 8 (Figures S6). Indeed, either L-Thr, L-Thr-O-methyl ether, or (*Z*)-2,3-dehydrobutyrine is incorporated at position 7, whereas Pea, Tyr, Leu/Ile, Phe, or Ala may occupy position 8. Considering that Nbl synthetase includes only 7 modules, it can be argued that cyclic octadepsipeptides may derive from the iterative use of module 7, which is expected to allow for the accommodation of L-dehydro-Asn and L-Thr - structurally similar amino acids - and catalyse cyclization for the assemblage of nobilamides F3 and G3. On the other hand, linear octapeptides H3-O3 apparently derive from linear/cyclic heptapeptides which could undergo spontaneous nucleophilic acyl substitution at the C-terminus with aromatic amines (Pea, Tym) or amino acids. It has been demonstrated that aromatic amine accumulation due to amino acid decarboxylation, may provide building blocks for spontaneous

condensation reactions leading to biosynthesis of imidazolium alkaloids, i.e. discolins, from *Tenacibaculum discolor* sv11 [51]. However, it cannot be excluded that a TE domain, as reported for bacillothiazols [52], or even a C-type domain present elsewhere in the chromosome, as speculated for crochelins [53], may be involved in the addition of the additional C-terminus moietes beyond the prediction of the heptamodular assembly line [54].

The peptide backbone of nobilamide P3 was determined as Phe[1]-D-Leu[2]-L-Phe[3]-D-*allo*-Thr[4]-L-Val[5]- D-*allo*-Thr[6]-L-Val[7]-L-Ala[8]- L-Thr[9], where the D-*allo*-Thr[6] side-chain OH group was predicted to form an ester bond with the C-terminal L-Thr[9] (Figures S6). Biosynthetically, nobilamide P3 may be the result of an aberrant process where modules 4 and 5 are used twice to generate this nonapeptide lactone, which is unusual among its congeners.

Table 6. Cyclic depsioctapeptides from *Bacillus* sp. BCP32 [a] The D-*allo*-Thr[4] side-chain OH group forms an ester bond with the C-terminal residue. [b][M+H+NH_3]$^+$. Abbreviations: Ac, acetyl; D-*a*-Thr, D-*allo*-threonine; Dhb, 2,3-dehydrobutyrine.

Nobilamide	[M+H]$^+$	*m/z*	R_t (min)	R_1	aa-1	aa-2	aa-3	aa-4 [a]	aa-5	aa-6	aa-7	aa-8
F3	$C_{46}H_{62}N_9O_{11}$	916.4557	18.6	Ac	D-Phe	D-Leu	L-Phe	D-*a*Thr	L-Val	L-Ala	*Z*-Dhb	L-dehydro-Asn
G3	$C_{46}H_{65}N_8O_{11}$	905.4762	20.8	Ac	D-Phe	D-Leu	L-Phe	D-*a*Thr	L-Val	L-Ala	*Z*-Dhb	L-Thr

Table 7. Linear octapeptides from *Bacillus* sp. BCP32. Abbreviations: Nob, nobilamide; Ac, acetyl; D-*a*-Thr, D-*allo*-threonine; Dhb, 2,3-dehydrobutyrine; Pea, phenethylamine; Tym, tyramine; OMe-L-Thr, L-threonine methyl ether.

Nob	[M+H]$^+$	*m/z*	R_t (min)	R_1	aa-1	aa-2	aa-3	aa-4	aa-5	aa-6	aa-7	aa-8
H3	$C_{48}H_{73}N_8O_{12}$	953.5333	18.1	Ac	D-Phe	D-Leu	L-Phe	D-*a*-Thr	L-Val	L-Ala	L-Thr	L-Leu/ Ile
I3	$C_{51}H_{71}N_8O_{12}$	987.5175	18.3	Ac	D-Phe	D-Leu	L-Phe	D-*a*-Thr	L-Val	L-Ala	L-Thr	L-Phe
J3	$C_{50}H_{71}N_8O_{11}$	959.5222	19.0	Ac	D-Phe	D-Leu	L-Phe	D-*a*-Thr	L-Val	L-Ala	L-Thr	Tym
K3	$C_{45}H_{65}N_8O_{11}$	893.4757	19.6	Ac	D-Phe	D-Leu	L-Phe	D-*a*-Thr	L-Val	L-Ala	*Z*-Dhb	L-Ala
L3	$C_{49}H_{75}N_8O_{12}$	967.5503	21.1	Ac	D-Phe	D-Leu	L-Phe	D-*a*-Thr	L-Val	L-Ala	OMe-L-Thr	L-Leu/ Ile
M3	$C_{50}H_{71}N_8O_{10}$	943.5279	22.6	Ac	D-Phe	D-Leu	L-Phe	D-*a*-Thr	L-Val	L-Ala	L-Thr	Pea
N3	$C_{51}H_{73}N_8O_{11}$	973.5398	26.4	Ac	D-Phe	D-Leu	L-Phe	D-*a*-Thr	L-Val	L-Ala	OMe-L-Thr	Tym
O3	$C_{50}H_{69}N_8O_{10}$	941.5132	28.0	Ac	D-Phe	D-Leu	L-Phe	*Z*-Dhb	L-Val	L-Ala	L-Thr	Tym

Table 8. Cyclic depsinonapeptide from *Bacillus* sp. BCP32 [a] The D-*allo*-Thr[6] side-chain OH group forms an ester bond with the C-terminal residue. Abbreviations: Nob, nobilamide; Ac, acetyl; D-*a*-Thr, D-*allo*-threonine.

Nob	[M+H]$^+$	*m/z*	R_t (min)	R_1	aa-1	aa-2	aa-3	aa-4	aa-5	aa-6 [a]	aa-7	aa-8	aa-9
P3	$C_{51}H_{76}N_9O_{13}$	1022.5545	18.8	Ac	D-Phe	D-Leu	L-Phe	D-*a*-Thr	L-Val	D-*a*-Thr	L-Val	L-Ala	L-Thr

2.6. Surfactant and Antibacterial Activity of Nobilamides and Surfactins

F-90% MeOH was subjected to HPLC to obtain pure nobilamides T1, I, TL-119, and S1 as well as surfactin C and a mixture of two isomers of surfactin B - featuring identical MS^2 spectra , which could not be resolved (major isomer 56%, minor isomer 44%) (Figure S5).

Surfactins demonstrated high biosurfactant activity in the oil spreading test (Figure S3) and antimicrobial activity against a) the human pathogens *S. aureus* 6538 and 6538p (MIC values ranging from 15,6 to 64,5 μg/mL), and b) the fish pathogen *Photobacterium damselae* subsp. *piscicida*, at a MIC value of 3 μg/mL for surfactin C and 7 μg/mL for surfactin B (Table S2). No activity was observed against antibiotic resistant *S. aureus* strains, *S. epidermidis*, *S. xylosus*, and *L. monocytogenes*.

As lacking antibacterial activity against gram-negative bacteria, such as *E. coli* ATCC 10536 and *Acinetobacter baumannii* Ab13, nobilamides T1, I, TL-119, and S1 were assessed against a panel of Gram-positive pathogens. TL-119 was the most potent antibacterial agent, with MIC values ranging from 0,24 μg/mL to 7,8 ug/mL towards all tested pathogens, while no nobilamides showed activity against VRSA (Table 9). This could suggest nobilamides may have a mechanism of action similar to that of vancomycin, which targets bacterial membranes, by inhibiting cell wall synthesis [55,56].

Interestingly, even if less active as compared to TL-119, the novel nobilamide S1 mantained potent growth inhibition towards *S. aureus* 6538, *S. aureus* 6538p and *L. monocytogenes 677* and mild effects against *S. xilosus* MB5209 (Table 9). To the best of our knowledge, TL-119 and one of its congeners, i.e. nobilamde S1, were demonstrated for the first time to possess antibiotic activity towards *Listeria* and antibiotic-resistant *Staphylococcus* strains.

Table 9. Antibacterial activity of nobilamides from *Bacillus* sp. BCP32 towards a panel of Gram-positive pathogens. MIC values are expressed in μg/mL.

Strain	Nobilamide T1	Nobilamide I	Tl-119	Nobilamide S1
S. aureus 6538p	-	-	0.24	15.6
S. aureus 6538	-	-	0.24	7.8
S. aureus Methicillin Resistant	-	-	3.9	-
S. aureus Macrolide Resistant	-	-	1.9	-
S. aureus Quinolone Resistant	-	-	0.9	-
S. aureus Vancomycin Resistant	-	-	-	-
S. epidermidis RP206	-	-	7.8	-
S. xilosus MB5209	-	-	7.8	31.5
Listeria monocytogenes 677	-	-	0.24	3.9

These findings unveiled structural features essential for maintaining growth inhibitory effects against the panel of human pathogens reported in Table 9. The absence of the N-acetyl group on Phe^{1} led to loss of bioactivity of nobilamide T1, although having the same peptide backbone as the N-acetyl encapped TL-119. In addition, Dhb^{7} is crucial to keep antibiotic activity of TL-119, as the molecule became inactive, when replaced by Thr as in nobilamide I. The Val^{5}→Leu/Ile^{5} substitution observed in nobilamide S1 weakened markedly growth inhibitory properties of TL-119. Finally, previous results revealed the lactone ring - and the C-terminal Dhb - as a key structural motif for the antimicrobial effects of nobilamides against *S. aureus* and *L. sphaericus* [46].

Nobilamides did not show any activity in the oil spreading test, thereby indicating that only surfactins are responsible for the surfactant effects of F-90% MeOH (Figure S3).

2.7 Whole Genome Sequencing and Identification of Nobilamide Biosynthetic Gene Cluster

Bacillus sp. BCP32 was subjected to whole genome sequencing for the correct taxonomical assignment of the species and to search for biosynthetic gene clusters (BGCs), encoding the discovered compounds. DNA sequencing was performed using both Illumina short-read sequencing and Oxford Nanopore

technology's long-read sequencing, thus yielding the complete closed genome sequence. BCP32 genome has a total length of 4.186.340 bp with a G+C content of 43.76%. The analysis of its 16S rRNA gene, through EzBioCloud [57,58] revealed high similarity with *Bacillus halotolerans* ATCC 25096 (99.93%), *Bacillus mojavensis* RO-H-1 (99.86%) and *Bacillus cabrialesii* TE3 (99,80%). The BCP32 assembled genome was compared with the genomes of the above-mentioned strains by using the OrthoANI Genomic Similarity tool. *Bacillus* sp. BCP32 shared the highest ANI value with *B. halotolerans* ATCC 25096 (98%), thus allowing for species assignment. The presence of *Bacillus halotolerans* was already reported from deep-sea and salty environments, demonstrating its capability to adapt to extreme conditions [59,40,60].

Although the first member of the nobilamide family, i.e. TL-119, was discovered in 1975 [33], there is no evidence about the nobilamide biosynthesis so far. Aiming to detect the biosynthetic pathway for nobilamides, the *Bacillus* sp. BCP32 genome was mined by antiSMASH for NRPS and RiPP BGCs, that are known to assemble peptide secondary metabolites. AntiSMASH enabled the detection of 6 NRPS and RiPP pathways, including the surfactin, bacillaene, bacillabactin, fengycin, subtilosin A, and a putative novel multimodular NRPS BGCs. Nobilamide biosynthesis was inferred to be directed by this orphan multimodular NRPS, designated as Nbl, based on the collinearity between the adenylation (A) domain specificity within each NRPS module and the chemical structure of TL-119 (see Table S3). The putative *nbl* operon is 27723 bp long and is made up of seven NRPS modules. *In silico* prediction of the A domain substrate selectivity nicely correlates with the consensus sequence D-Phe^{1}-D-Leu^{2}-L-Phe^{3}-D-*allo*-Thr^{4}-L-Val^{5}-L-Ala^{6}-(*Z*)-Dhb^{7}, inferred by MS-based structural characterization of cyclic depsiheptapeptides and linear heptapeptides (section 2.4), except for Dhb^{7} (Figure 6, Table S3). Indeed, antiSMASH analysis predicted Nbl_A7 to recruit Thr and this is likely true considering that Dhb^{7} may derive

from Thr dehydration. The incorporation of dehydroamino acids - such as Dhb and Dha (α,β-dehydroalanine)- in nonribosomal peptides has been reported to involve a threonine/serine dehydration step, which can be catalysed either by the so-called "modified AA" condensation domains (C_{modAA}), such as AlbB_ C_{modAA} in albopeptide biosynthesis, or by a distinct class of $^{D}C_{L}$ domains, such as NocB_C5 in nocardicin biosynthesis [61]. The *nbl* gene cluster apparently lacks a C domain in the last module which can presumably participate in Thr dehydration, as Nbl_C7 did not cluster with any of these unique C domains in a phylogenetic analysis performed with NaPDoS [62]. Therefore, it remains unclear whether Nbl_C7 or an auxiliary tailoring enzyme is responsible for dehydration of Thr^{7} and how this mechanism is regulated to generate Dhb^{7} or Thr^{7} –containing nobilamide isoforms. Three typical epimerization domains are present in modules 1, 2, and 4, thereby suggesting the D configuration for aa^{1}, aa^{2}, and aa^{4} of cyclic depsiheptapeptides and linear heptapeptides of the nobilamide family, which is consistent with the reported stereochemistry for nobilamides. The last module terminates with a canonical thioesterase (TE) domain, which is expected to catalyse the peptide release through hydrolysis or cyclization to give linear or cyclic nobilamides, respectively. Most nobilamide variants bear an acyl group at the N-terminus, which is in most cases represented by an acetyl unit. N-acetylated cyclic peptides are extremely rare in nature. Beyond nobilamides, chaiyaphumines from *Xenorhabdus* sp. PB61.4, heptarhizin from the endosymbiotic bacterium *Burkholderia rhizoxinica*, and griselimycins from *Streptomyces* DSM 40835 are among the few N-acetyl encapped peptides reported so far [63–65]. Following a typical lipoinitiation strategy, starter C domains (Cs) catalyze N-acetylation of the nonribosomal peptides griselimycins and heptarhizin. However, Nbl synthetase lacks a canonical Cs domain, although featuring a C domain in the first module, which obviously does not share significant similarity with Cs domains deposited in the NaPDoS database.

Therefore, the acetylation mechanism remains elusive, raising the question of whether Nbl_C1 may acylate nobilamides at the N-terminus. In addition, acyltransferases or acyl-CoA ligases, presumably located in a different locus of the bacterial genome, could participate in nobilamide acetylation.

Interestingly, the detection of nobilamide variants containing more/less than seven amino acids clearly indicates that the Nbl synthetase may deviate from the canonical "collinearity" rule. Generation of these "odd", minor isoforms can be traced back to aberrant biochemical processes, such as module skipping or iterative use of specific modules, rather than programmed biosynthetic events. In addition, following amine/amino acids accumulation, spontaneous nucleophile-mediated ring opening reactions could trigger formation of unexpected linear octapeptide congeners from cyclic heptadepsipeptides.

These processes together with the relaxed substrate selectivity of the Nbl adenylation domains have contributed to expand the chemical diversity of the nobilamide family.

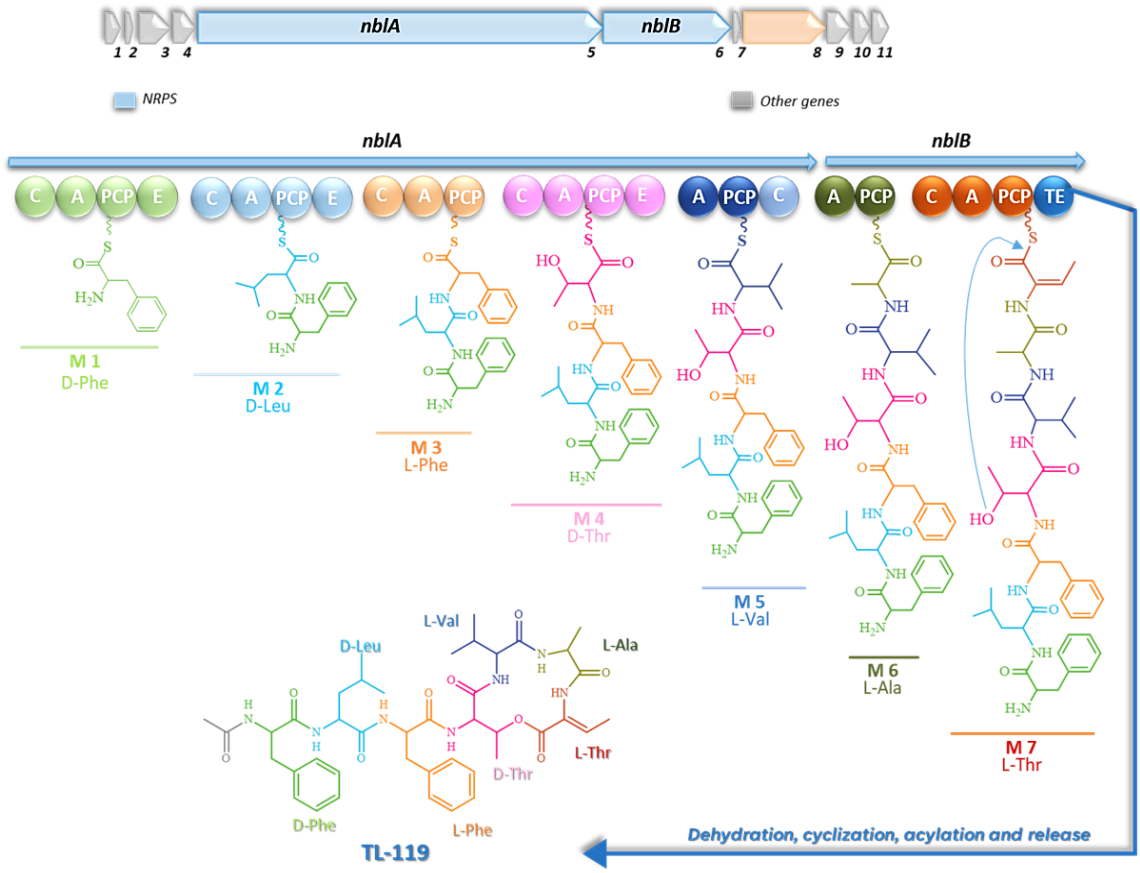

Figure 6. Putative biosynthesis of TL-119. Abbreviations: C, condensation domain; A, adenylation domain; PCP, peptidyl-carrier protein; E, epimerase; TE, thioesterase.

3. Materials and Methods

3.1. Strain Isolation and Identification

The strain *Bacillus* sp. BCP32 was isolated, along with other 300 bacteria, from a 450 m deep-sea sediment sample collected from the Canyon Dohrn at 19 km off the coast of the Gulf of Naples (Italy). The isolation was conducted using MB agar plates with 5 dilution of water sample. The strain was identified as belonging to the genus *Bacillus* via 16S rRNA gene amplification and subsequent phylogenetic analysis. PCR was carried out in a total volume of 40 µL containing 25 µL of PCR Master Mix 2× ExtraWhiteTaq (a ready-to-use solution containing TaqPol, buffer, $MgCl_2$ and dNTPs), 0.2 µM of both primers 27F (Forward, seq: 5′-AGAGTTTGATCCTGGCTCAG-3′) and 1492R (Reverse, seq 5′-GGTTACCTTGTTACGACTT-3′) [66]. PCR was carried out under the following

conditions: initial denaturation at 95 °C for 5 min, followed by 33 cycles of 95 °C for 30 s, 58 °C for 30 s and 72 °C for 1.30 min, with a final extension at 72 °C for 7 min.

Afterwards PCR products were evaluated on 1% agarose gel and then purified with the GeneAll kit and sequenced by Eurofins Genomics. Finally, the phylogenetical affiliation was assigned by using the EzBioCloud (http://ezbiocloud.net).

3.2. Primary Screening

The collected marine psychrophilic bacteria were subjected to a primary screening, in order to select promising strains for the production of the molecules of interest. Micro-cultivation was carried out in 96 multiwell plates. After 2 days of incubation in the most suitable medium at 20 °C under shaking condition, 20 µL of microcultures were transferred in a new 96-deepwell (Thermo Scientific™ 278743) with different growth media. Secondary metabolite production was evaluated in a range of 3-10 days of cultivation at temperatures between 10-37 °C. Afterwards the cultures were centrifuged to separate the cells from the supernatant, which was then transferred into a new deep well plate. Particularly, 10 µL of the supernatant were used for biosurfactant assays (CTAB agar assay and oil displacement test) and 100 µL for the agar well diffusion assay to assess antibacterial activity.

3.3. Bacterial Cultivation, Chemical Extraction and Compounds Isolation

After selection of *Bacillus* sp. BCP32 as one of the most active strains in the SZN library, a single colony of the bacterial isolate was used to inoculate 3 mL of liquid TYP medium (16 g/L bacto-tryptone, 16 g/L yeast extract, 10 g/L NaCl) in sterile bacteriological tubes. After 48 h of incubation at 20 °C at 200 rpm, the preinoculum was used to inoculate 4x250 mL flasks, each containing 50 mL of TYP medium, at a concentration of 0.01 OD_{600}/mL. Bacterial cultures were

incubated at 28 °C under shaking (150 rpm) for 48h. Then cultures were centrifuged at 7500 rpm at 4 °C for 30 min to collect supernatants, and extracted with two volumes of EtOAc. Successively, organic phases were combined and evaporated with a rotary evaporator (Buchi R-100, Büchi Labortechnik AG, Postfach, Switzerland) to afford crude extract. Finally, the obtained extract was dissolved in DMSO at 50 mg/mL and stored at 4 °C to be tested for bioactivities. For large scale fermentation of *Bacillus* sp. BCP32 and subsequent compounds isolation, 4x500ml flask, each containing 250mL of TYP medium, were inoculated at an initial concentration of 0.01 OD_{600}/mL and incubated at 28 °C under shaking (150 rpm). After two days, the aforementioned extraction protocol was performed to obtain the crude extract from exhausted culture broth. The EtOAc extract (430 mg) was fractionated into five fractions by solid-phase fractionation (SPE) using reverse-phase Chromabond C-18 column Cartridge (Macherey-Nagel GmbH & Co. KG, Duren, Germany). Briefly, the extract was resuspended in the minimum volume of MeOH and uploaded on the pre-activated SPE column. The elution was performed with two column volumes of different mixtures of MeOH and H_2O, as follows: 1) 100% H_2O, 2) 50% MeOH/H_2O (v/v), 3) 90% MeOH/H_2O (v/v), 4) 100% MeOH, and 5) MeOH+0.1%TFA. Aliquots of the obtained fractions were dissolved in DMSO at 50 and 25 mg/mL to perform antibiotic and biosurfactant assays. The 90% MeOH fraction (238.2 mg) was subjected to reverse-phase HPLC separation on a semi-preparative Jupiter Proteo column (4 μm, 250 x 10 mm), thus affording nobilamide T1 (R_t = 6.8 min, 1.5 mg), nobilamide I (R_t = 8.6 min, 5.2 mg), TL-119 (R_t = 11.1 min, 6.4 mg), nobilamide S1 (R_t = 12.7 min, 1.9 mg), surfactin A (R_t = 21.9 min, 4.4 mg), surfactin B (mixture of two isomers, R_t = 22.7 min, 7.6 mg), and surfactin C (R_t = 23.6 min, 26 mg). The column was eluted at room temperature at a flow rate of 5 mL/min with H_2O and CH_3CN (both eluents supplemented with 0.1% TFA), following the gradient elution program: 0-60% CH_3CN 0-1min, 60−75% CH_3CN 1-14 min, 75−85%

CH_3CN 14-15 min, 85%-100% CH_3CN 15-35 min. Detection was achieved through at 210 nm wavelength.

3.4. LC-HRMS² analysis of the 90% MeOH Fraction

The F-90% MeOH fraction from *Bacillus* sp. BCP32 crude extract was dissolved in MeOH at a concentration of 1 mg/mL for LC-HRMS² analysis, as previously described [67]. Chemical profiling was conducted using a Thermo Scientific Q Exactive Focus Orbitrap mass spectrometer coupled to a Thermo Ultimate 3000 HPLC system equipped with an Hypersil C18 column (100 x 4.6 mm, 3 μm). The column was eluted at room temperature at a flow rate of 400 μL/min with H_2O (containing 0.1% HCOOH) and CH_3CN, following the gradient elution program: 25% CH_3CN for 3 minutes, 25–80% CH_3CN over 60 minutes, and 95% CH_3CN for 7 minutes. Mass spectra were recorded in positive ion mode with a mass accuracy of ≤ 3 ppm. MS parameters were: spray voltage of 4.8 kV, capillary temperature of 285 °C, sheath gas flow rate of 32 units N_2 (~150 mL/min), and auxiliary gas flow rate of 15 units N_2. MS² data were collected in data-dependent acquisition mode to fragment the three most intense ions from a full-scan mass spectrum, with an m/z range of 50 to 2000 Daltons. HRMS² scans were performed HCD fragmentation, using an isolation width of 2.0 m/z, a normalized collision energy of 15 units, and an automated injection time.

3.5. Feature-Based Molecular Networking

Raw files from LC-HRMS² analysis of the 90% MeOH fraction were processed by MZmine 2.53, using parameters reported in Table S4 to obtain a .mgf file. This file was employed as input on the GNPS2 Analysis Hub (https://gnps2.org, accessed on 2/10/2024) [68] to build a molecular network with the feature-based molecular networking (FBMN) workflow [69]. For FBMN analysis, the precursor ion mass tolerance was set to 0.02 Da, and the MS² fragment ion tolerance was set to 0.05 Da. Subsequently, a molecular network was constructed, setting to 100 the

maximum number of nodes in one cluster, with edges filtered to have a cosine score above 0.7 with a minimum of four matching peaks. Analogues were also searched, not exceeding the difference of 300 Da between the query and the hit; the analogues had to follow the same clustering rules as mentioned above. Finally, the network was visualized by the Cytoscape software v. 3.8.2 and can be publicly accessed at https://gnps2.org/status?task=1b1c1180d47d47debeeea7f688d989fb.

3.6. Biosurfactant and Antimicrobial assays

Biosurfactant and antimicrobial assays were performed to assess bioactivity of crude extracts, SPE fractions, and purified compounds.

3.6.1. Biosurfactants Assays

Biosurfactant-producing bacteria were screened using cetyltrimethylammonium bromide (CTAB) agar assay [70] and oil displacement test [71].

CTAB Agar Assay

The CTAB agar plates method is a semi-quantitative test for the detection of anionic surfactants, devised by Wagner and Siegmund [70].The test is positive if the extracts contain anionic surfactants due to the formation of an insoluble ion pair between the anionic biosurfactant, CTAB and methylene blue. Therefore, positivity is revealed by the dark blue halos around the extracts. For this assay 1 µL of the extracts at 50 µg/mL, dissolved in DMSO were spotted on the blue agar plates. As a negative control, 4 µL of pure DMSO were used, while 4 µL of 0.1% and 0.01% sodium dodecyl sulphate (SDS) were used as positive controls. After 2 days at 4 °C, the extracts containing biosurfactants were selected by the presence of a dark blue halo around.

Oil Displacement Test

The oil spreading assay, also called oil displacement test [71], was performed in a Petri dish of polystyrene containing 40 µl of crude oil added to the surface of 40 ml of distilled water to form a thin oil layer. Then, 10 µl of culture supernatant and 1 µl of extracts at 50 µg/mL were gently placed on the centre of the oil layer. The diameter of the clear zone on the oil surface is related to surfactant activity, due to the presence of the biosurfactant that displaces the oil.

3.6.2. Antimicrobial Assays-Minimal Inhibitory Concentration Assay (MIC)

To assess the antibacterial activity of the 300 bacteria screened, the agar well-diffusion method (ADM), was performed against *Escherichia coli* ATCC 10536, *S. aureus* ATCC® 6538™. This method involves inoculating an agar plate with a standardized microbial inoculum and placing 100 ul of culture supernatants into the agar through wells, previously obtained as shown in Figure 1. The sample diffuses into the medium for 24h at 37°C , and if the sample has activity, a zone of inhibition forms around the applied area, which is measured to assess the level of effectiveness [72] . While, to evaluate the antimicrobial potential of all extracts, the MICs for *E. coli* ATCC 10536 , *S. aureus* ATCC® 6538™, *S. aureus* ATCC® 6538p™, methicillin-resistant *S. aureus* (MRSA), macrolide-resistant *S. aureus* (MRSA), quinolone-resistant *S. aureus* (QRSA), vancomycin-resistant *S. aureus* (VRSA) [73] *Staphylococcus epidermidis* RP206 [7], *Staphylococcus xylosus* MB 5209 [74] were determined by the broth microdilution method [75]. The surfactins fractions B and C were also tested against two fish-pathogens strains, like *Photobacterium damselae* subsp. *piscicida* ATCC® 51736™ and *Vibrio anguillarum* ATCC® 19264™. Briefly, the bacterial strain was inoculated in 3 mL of liquid Mueller-Hinton broth (MHB) (HiMedia, Einhausen, Germany) in sterile bacteriological tube, and incubated in agitation at 37 °C until they reached the turbidity of 0.5 McFarland. Differently from the remaining pathogens, *Listeria*

monocytogenes MB 677 [76] was diluted in Trypticasein Soy Broth (TSB) medium with an additional 0.6% yeast extract, while for the fish pathogen strains was used Marine Broth (MB) (Condalab, Spain) as medium. Finally, serial dilutions of the inoculum were performed to obtain a final bacterial concentration of about 5×10^5 CFU/mL. Then, 4 μL of each sample was added into a 96-well microtiter plate containing 200 μL of MH medium. After serially diluted using MH medium, 100 μL of bacterial suspension was inoculated into the broth (~5×10^4 CFU/well) and incubated statically for 18h at 37°C. DMSO was used as control to determine the effect of solvent on cell growth. The MIC was identified as the lowest concentration that completely inhibited growth of the pathogens, which was measured the absorbance at 600 nm by using a ELX800 Absorbance Microplate Reader (Biotek, Winoosky,VT, USA) by monitoring the absorbance.

3.7. Whole-genome Sequencing and Bioinformatics

1 μg of genomic DNA was used for whole genome sequencing of *Bacillus* sp. BCP32, performed by Eurofins Genomics (Ebersberg,Germany) using the Illumina NovaSeq 6000 platform. All sequenced paired-ends reads were clipped and trimmed with Trimmomatic tool [77] to remove adaptor and low quality sequences, and a quality check was obtained with FastQC [78]. Bacterial genome was assembled with MEGAhit algorithm [79], employing the genome of Bacillus halotolerans ZB201702 (NZ_CP029364.1) as a reference to direct the arrangement and alignment of contigs. In addition, the whole genome was re-sequenced using the Oxford-Nanopore technology (ONT) [80], to obtain longer reads, sending 30 μL of genomic DNA at 20 ng/ml to Eurofins Genomics. Then, to obtain a closed genome, a hybrid assembly was performed by various k-mer analyses using the bioinformatic tool "create assemblies with Unicycler" [81] on the Galaxy Europe 0.5.0 server (https://usegalaxy.eu/), by inputting the raw data of both sequencing processes [82]. The assembled genome identification was carried out using ANI

Calculator by EzBioCloud [57] and the digital DNA:DNA hybridization (dDDH) analysis by Type (strain) Genome Server (https://tygs.dsmz.de). Subsequently the assembly was analyzed using the genome mining tool anti-SMASH 7.0 web server (http://antismash.secondarymetabolites.org, leading to the identification of biosynthetic gene clusters (BGCs).

4. Conclusions

In this study, the exploration of marine microbial biodiversity by a rapid and effective screening allowed for the identification of a deep-sea *Bacillus* of biotechnological interest. The strain showed both potent antimicrobial and biosurfactant activities in the same growth condition. Feature based molecular networking analysis of bacterial exometabolome shed light on the presence of two molecular families, namely surfactins and nobilamides, thereby explaining the observed bioactivities. Manual inspection of MS^2 spectra of the nobilamide cluster enabled for the structural characterization of 84 nobilamide congeners - 71 of them being novel molecules -, thus expanding the outstanding chemical diversity of these nonribosomal peptides. The well-known TL-119 and the novel congener nobilamide S1 were isolated as pure compounds and shown to be promising antibiotics against a range of Gram-positive bacteria, including several *S. aureus* MDR strains, *S. epidermidis*, *S. xylosus*, and *Listeria monocytogenes*. A significant finding of this study was the potent activity of TL-119 against the foodborne pathogen *Listeria*, which has been demonstrated for the first time, suggesting it could be an alternative to β-lactams in the treatment of listeriosis. In addition, the novelty of this work lies in elucidating the previously unknown BGC of nobilamides. Future studies will foresee the scale-up of *Bacillus* sp. BCP32 culture in order to purify and assess for antibiotic activity most of the novel nobilamides identified so far.

Supplementary

Figure S1. Surfactant activity evaluation of SPE fractions from *Bacillus* sp. BCP32 by oil spreading test. DMSO (4 μL) was used as negative control. The clear zone on the oil surface indicates the presence of biosurfactants. F-90% MeOH showed the best surfactant effect.

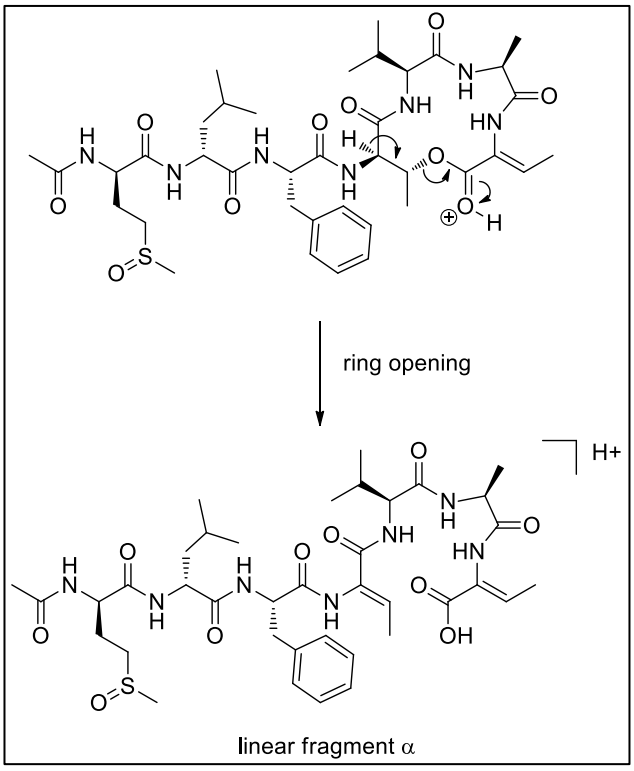

Figure S2. Ring opening of cyclic nobilamides during mass fragmentation. The cleavage of the ester bond generates the linear fragment α, where the Thr residue forming the lactone ring is converted into a dehydrobutyrine residue.

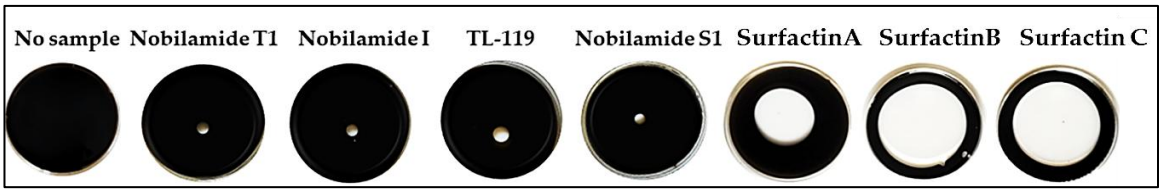

Figure S3. Surfactant activity evaluation of nobilamides T1, I, TL-119, and S1 and surfactins A, B, and C. DMSO (4 µL) was used as negative control. Surfactins displaced oil and formed a clear zone in the oil layer, thus indicating potent surfactant activity.

Table S1. Antibacterial activity of SPE fractions from Bacillus sp. BCP32 crude extract towards a panel of Gram-positive pathogens. MIC values are expressed in µg/mL.

Strain	F-H_2O	F-50%MeOH	F-90%MeOH	F-100%MeOH	F-100%MeOH
S. aureus 6538p	-	31.2	0.9	62.5	125
S. aureus 6538	-	15.6	0.9	62.5	125
S. aureus Methicillin Resistant	-	-	3,9	-	-
S. aureus Macrolide Resistant	-	125	3.9	62.5	62.5
S. aureus Quinolone Resistant	-	125	3.9	62.5	-
S. aureus Vancomycin Resistant	-	-	-	-	-
S. epidermidis RP206	-	62.5	1.9	125	250
S. xilosus MB5209	-	62.5	1.9	125	250
Listeria monocytogenes 677	125	15.6	0.9	31.2	62.5

Table S2. Antibacterial activity of surfactins B (mixture of two isomers) and C. MIC values are expressed in µg/mL.

Strain	surfactin B	surfactin C
S. aureus 6538p	62,5	15,6
S. aureus 6538	31,2	15,6
Photobacterium damselae subsp. *piscicida* 5173	7	3
Vibrio anguillarum 19264	-	-

Table S3. Binding pocket signatures of adenylation domains from the Nbl synthetase.

antiSMASH Prediction		Binding pocket signatures (position)[a]									
		235	236	239	278	299	301	322	330	331	517
Nbl_A1	**Phe**	D	A	W	T	I	A	A	I	C	K
Nbl_A2	**Leu**	D	A	W	L	I	G	A	I	I	K
Nbl_A3	**Phe**	D	A	W	T	I	A	A	I	C	K
Nbl_A4	**Thr**	D	F	W	N	I	G	M	V	H	K
Nbl_A5	**Val**	D	A	F	W	I	G	G	T	F	K
Nbl_A6	**Ala**	D	V	T	N	F	A	I	I	Y	K
Nbl_A7	**Thr**	D	F	W	N	I	G	M	V	H	K
Nbl_A1	**Phe**	D	A	W	T	I	A	A	I	C	K

[a] as reported by Della Sala et al. [43].

Table S4. MZmine2 parameters for MS raw data processing.

Feature detection	
MS level 1	1.0e5
MS level 2	1.0e3
ADAP chromatogram builder	• group intensity threshold: 1.0e5 • minimum highest intensity: 1.0e5 • *m*/*z* tolerance: 0.01 *m*/*z* or 10 ppm
Chromatogram deconvolution	
local minimum search	• chromatographic threshold: 10% • search minimum in RT range: 0.50 min • minimum relative height: 30% • minimum absolute height: 1.0e5 • minimum ratio of peak top/edge: 1.2 • peak duration: 0-10 min • m/z range for MS2 scan pairing: 0.01 Da • RT range for MS2 scan pairing: 0.2 min
Alignment	
Join aligner	• *m*/*z* tolerance: 0.002 *m*/*z* or 5 ppm • retention time tolerance: 0.2 min
Identification	
Adduct search ([M+Na–H], [M+K–H], [M+Mg–2H], [M+NH_3], [M-Na+NH_4], [M+1, ^{13}C])	• retention time tolerance: 0.1 min • *m*/*z* tolerance: 0.002 *m*/*z* or 5 ppm • max relative adduct peak height: 100%

Table S5. Putative genes flanking the *nbl* gene cluster.

protein	amino acids	closest homolog (protein, origin)	identities/ positives (%)	accession #
ORF1	197	DUF881 domain-containing protein [Bacillus halotolerans]	100/100	WP_202852504.1
ORF2	121	small basic family protein [Bacillus]	100/100	WP_010334164.1
ORF3	440	cell division protein FtsA [Bacillus]	100/100	WP_024121323.1
ORF4	382	cell division protein FtsZ [Bacillus]	98/98	WP_095843675.1
*nbl*A	7068	non-ribosomal peptide synthase [Bacillus subtilis]	98/99	WP_160243239.1
*nbl*B	2116	non-ribosomal peptide synthase [Bacillus subtilis]	99/99	WP_240304268.1
ORF7	91	cell division protein FtsZ [Bacillus spizizenii]	99/98	MCY8131166.1
ORF8	1434	S8 family peptidase [Bacillus halotolerans]	97/99	WP_227599196.1
ORF9	317	Sporulation sigma-E factor processing peptidase (SpoIIGA) [Bacillus mojavensis]	99/99	QJC96072.1
ORF10	239	RNA polymerase sporulation sigma factor SigE [Bacillus]	100/100	WP_024121327.1

ORF11	260	RNA polymerase sporulation sigma factor SigG [Bacillus]	100/100	WP_010334169.1

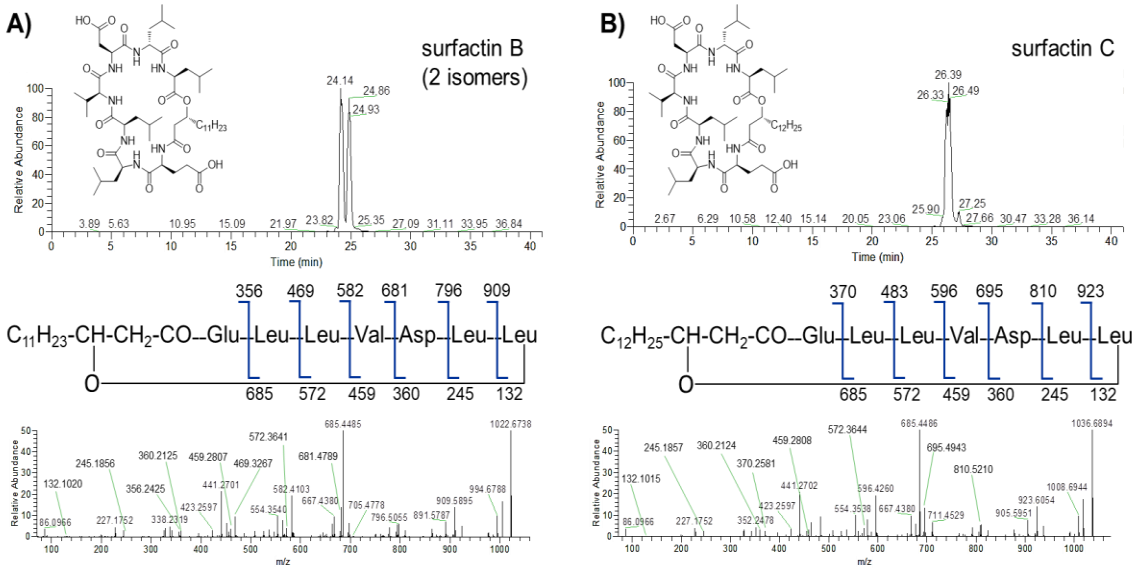

Figure S5. LC-MS chromatograms (upper panel) and HRMS² spectra (lower panel) of surfactin B isomers (A) and surfactin C (B).

Figures S6. LC-HRMS² spectra for nobilamides from the strain *Bacillus* sp. BCP32. Vertical lines across the structure show the mass-to-charge ratio values for the y and b fragments obtained via HRMS².

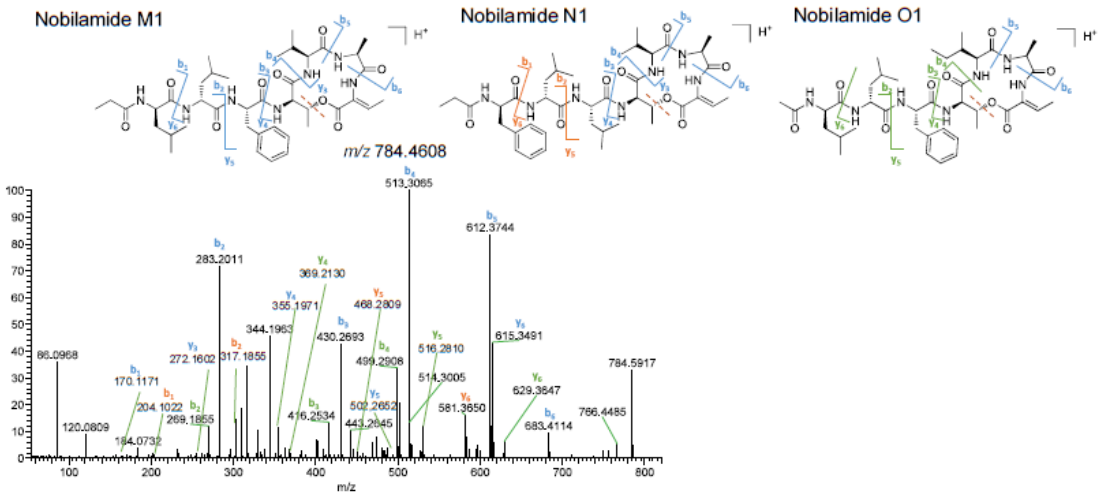

Nobilamide C3

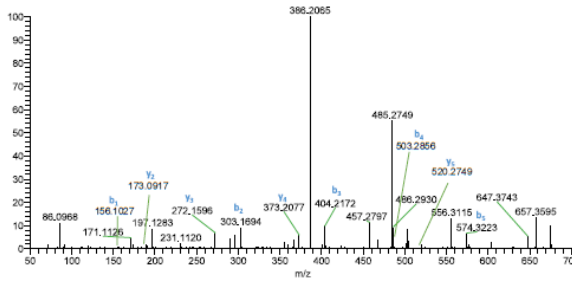

Nobilamide V2

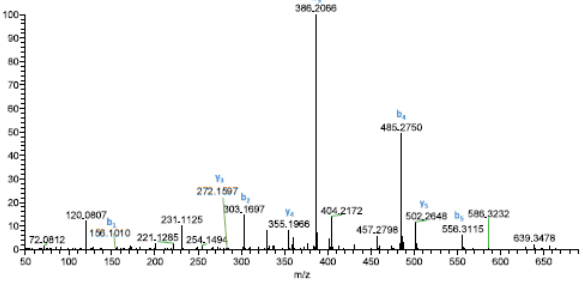

Nobilamide X2

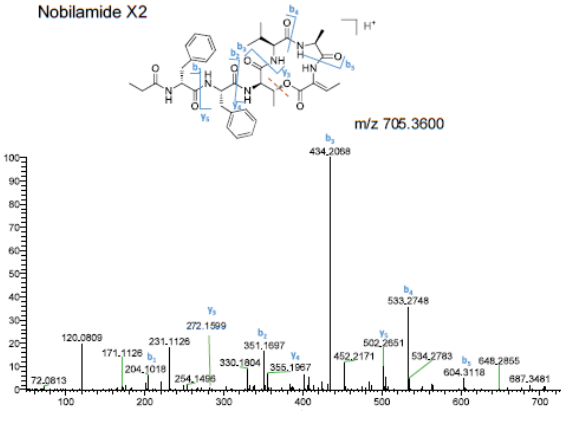

Nobilamide W2

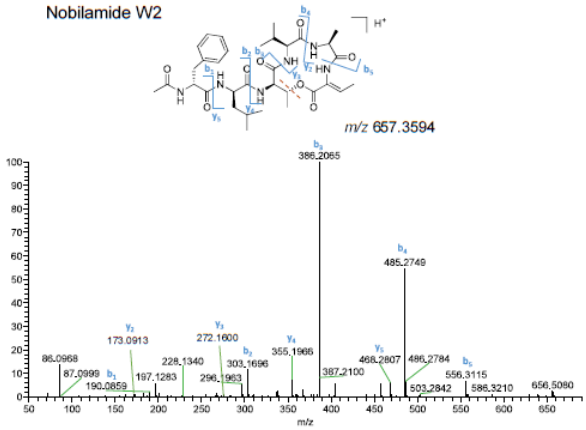

Nobilamide Q1

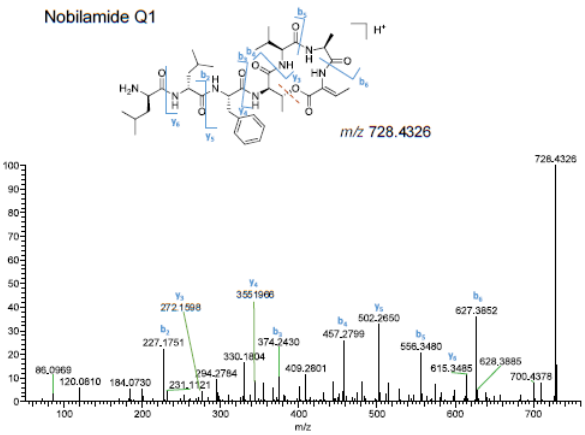

Nobilamide P1

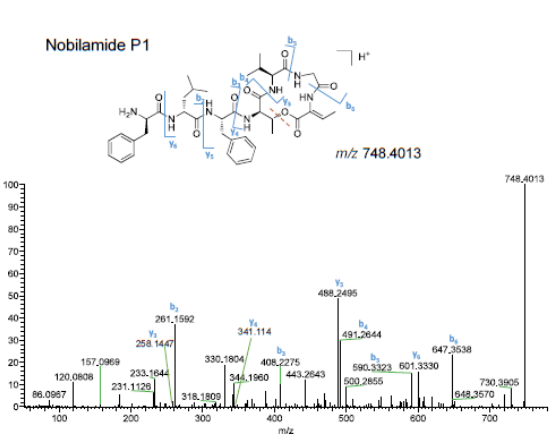

Nobilamide T1

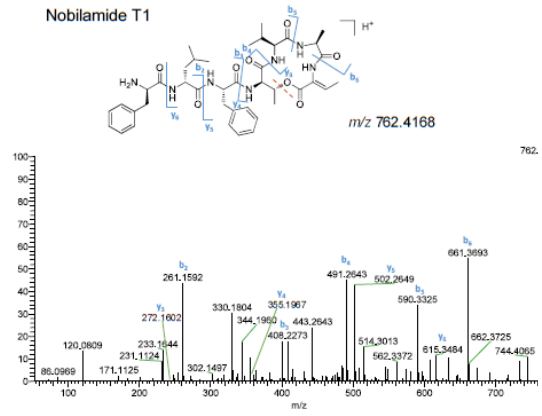

Nobilamide O

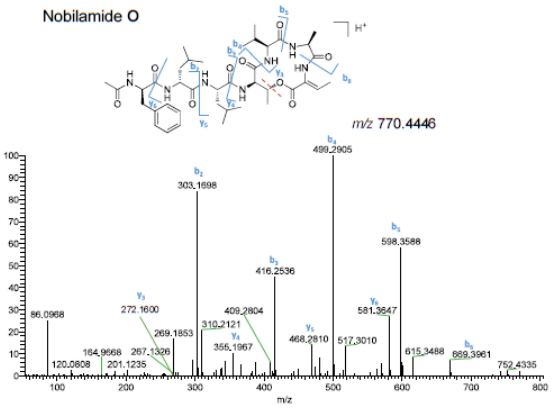

Nobilamide M2

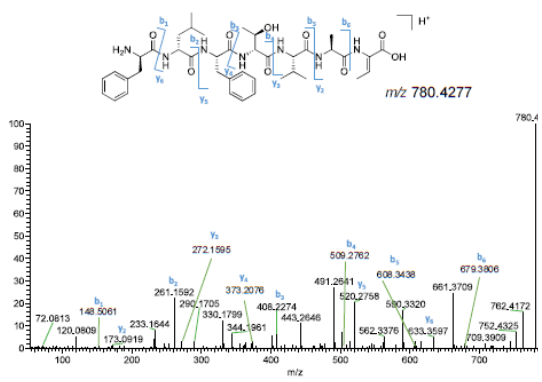

Nobilamide Q

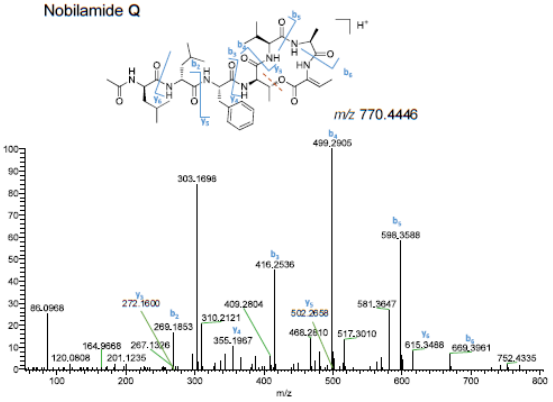

Nobilamide I1

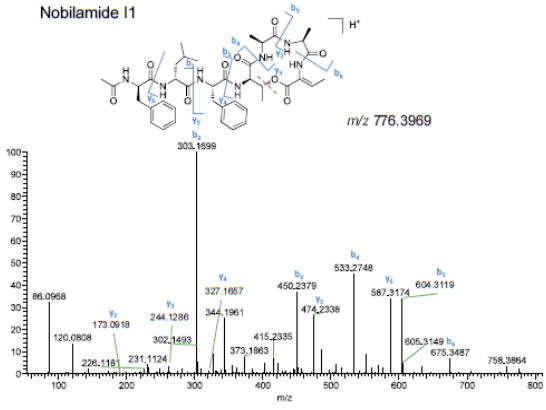

Nobilamide X

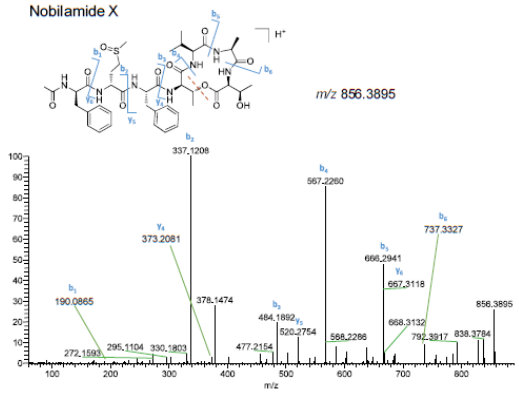

Nobilamide D1

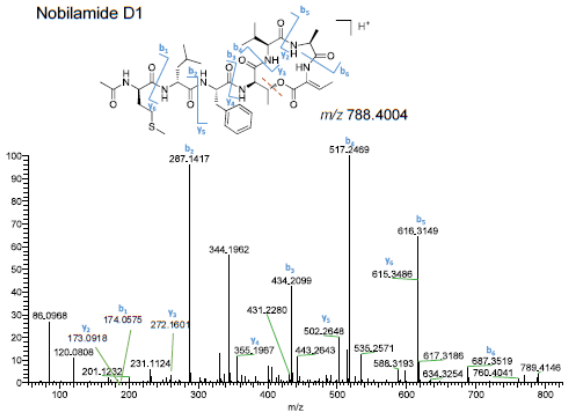

Nobilamide E2

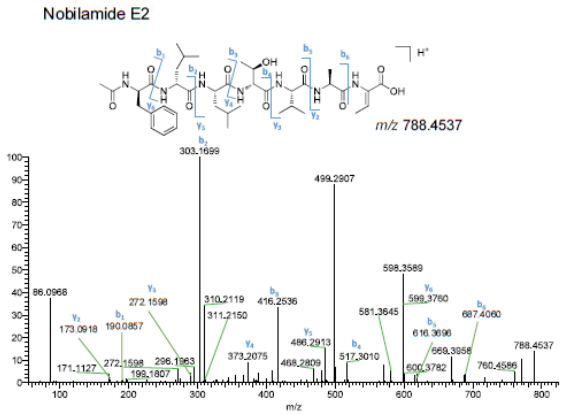

Nobilamide G1

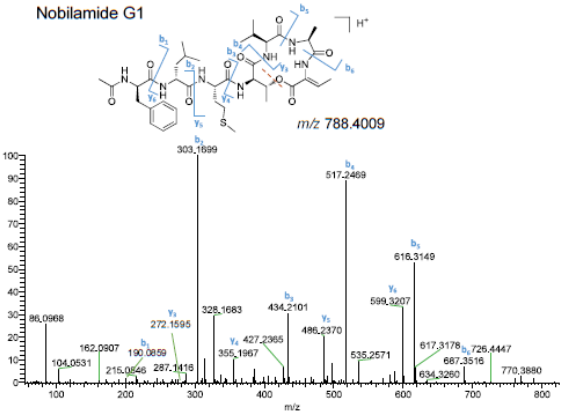

Nobilamide G2

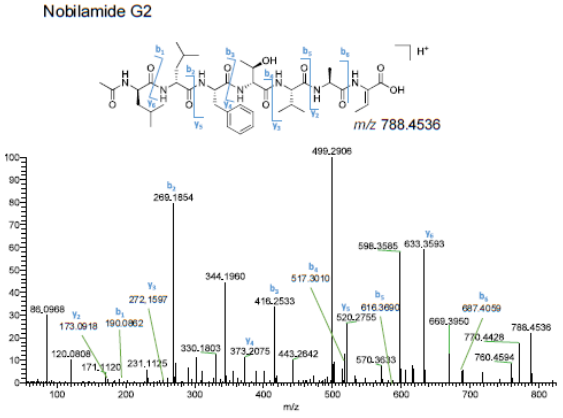

Nobilamide L

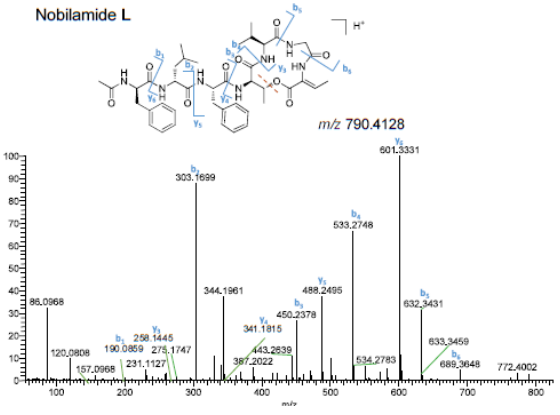

Nobilamide L1

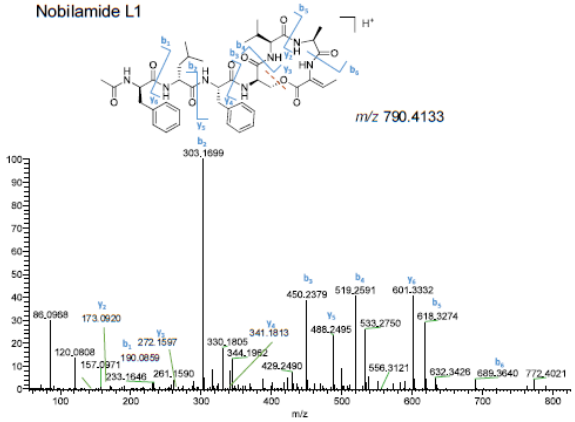

Nobilamide Y1

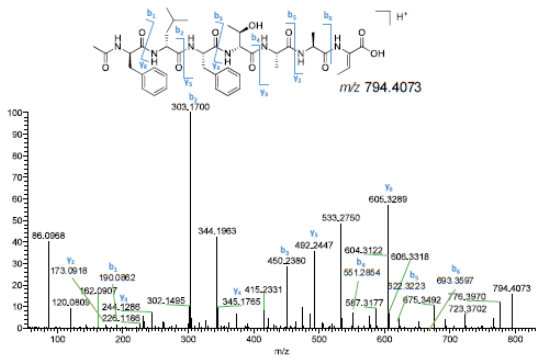

Nobilamide A1

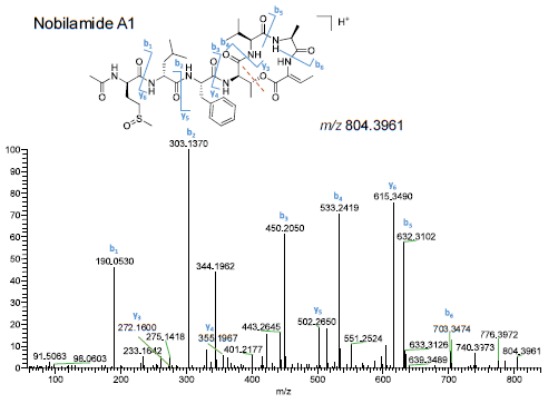

Nobilamide Z

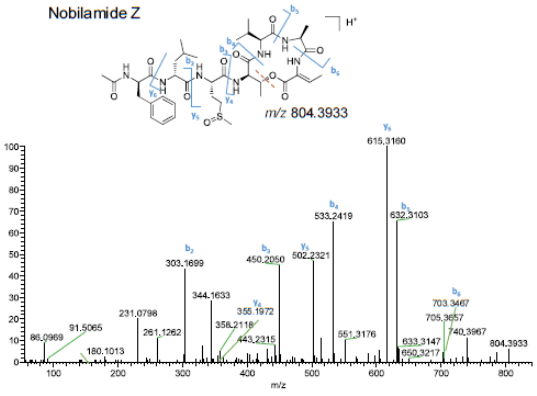

TL-119 (A-3302-B)

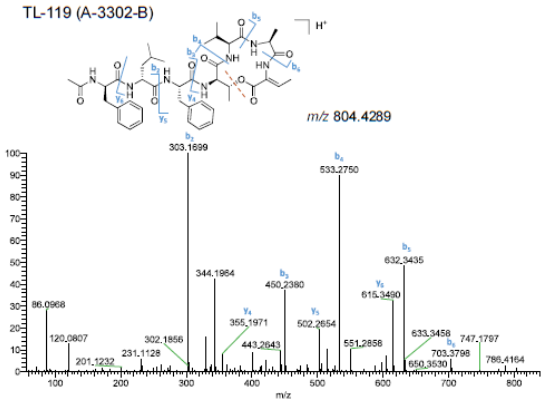

Nobilamide U1

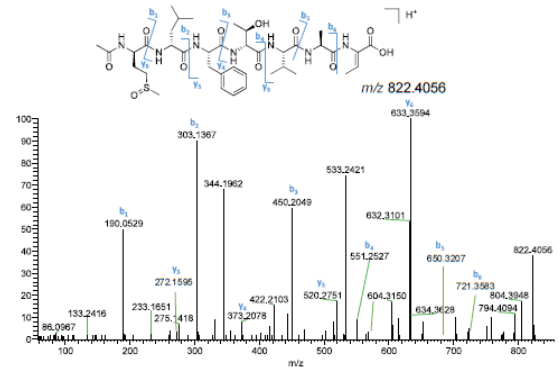

Nobilamide U1

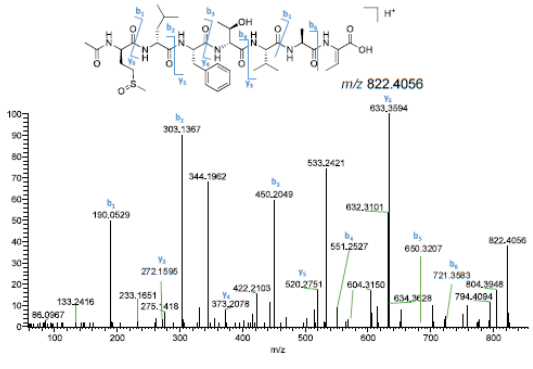

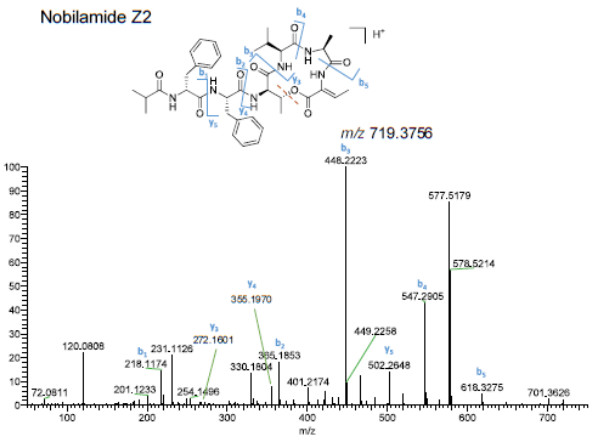
Nobilamide Z2
m/z 719.3756

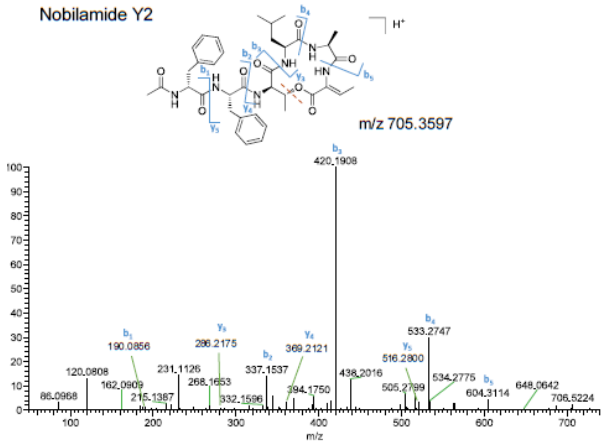
Nobilamide Y2
m/z 705.3597

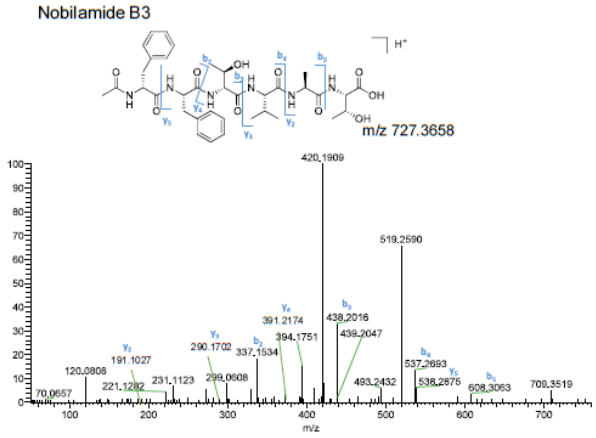
Nobilamide B3
m/z 727.3658

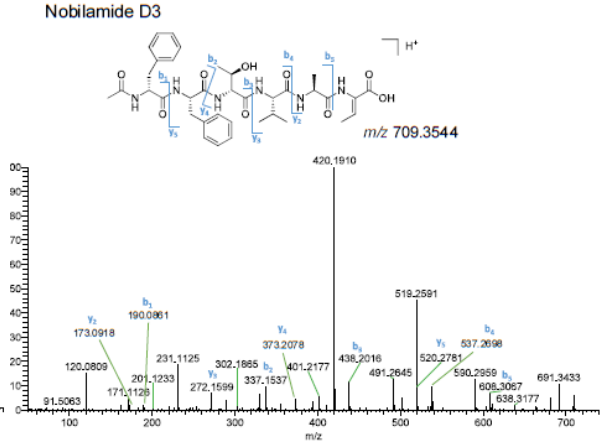
Nobilamide D3
m/z 709.3544

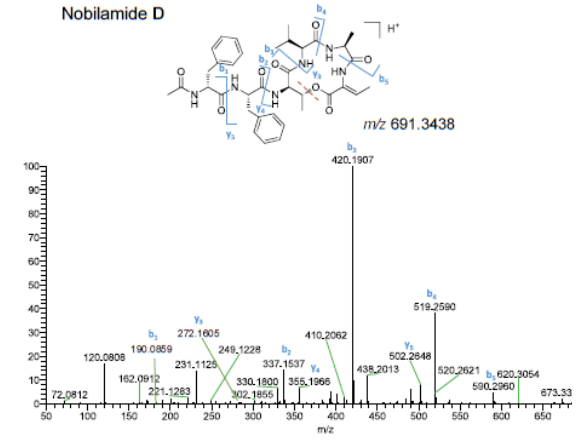
Nobilamide D
m/z 691.3438

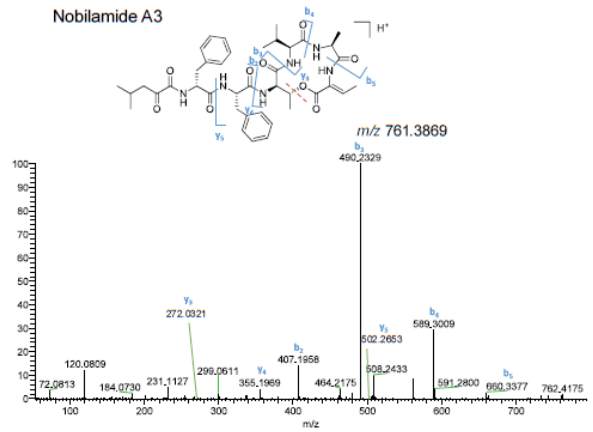
Nobilamide A3
m/z 761.3869

Nobilamide F1

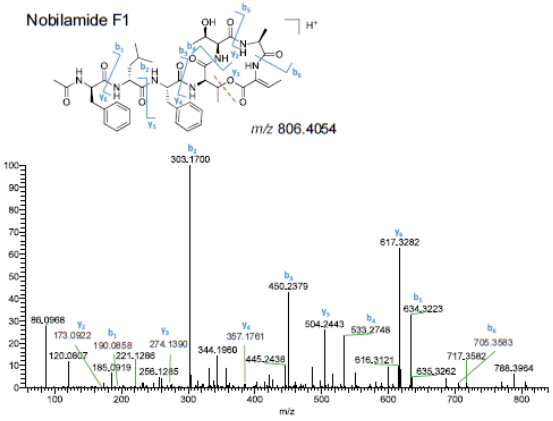

Nobilamide E1

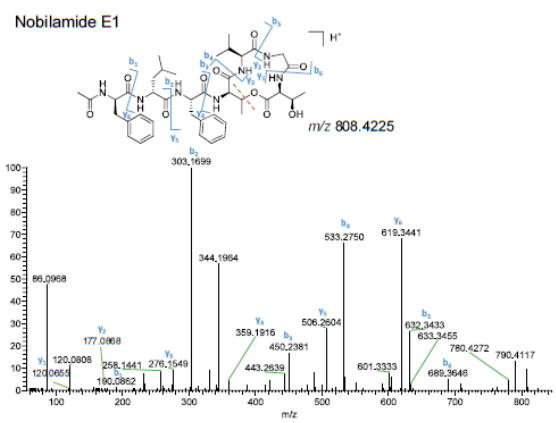

Nobilamide Z1

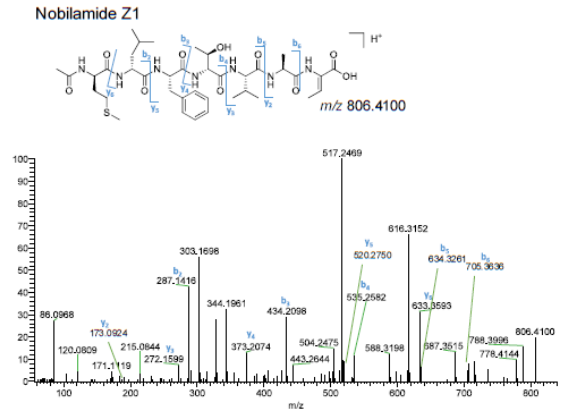

Nobilamide B2

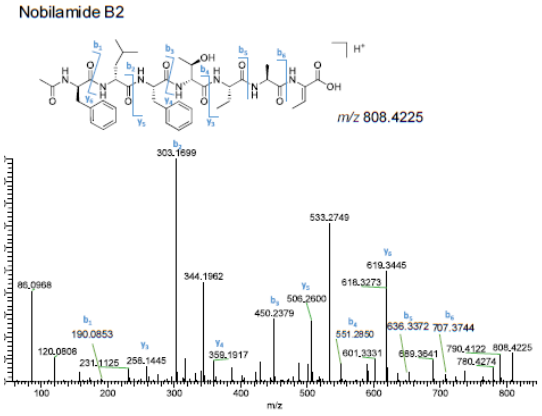

Nobilamide H2

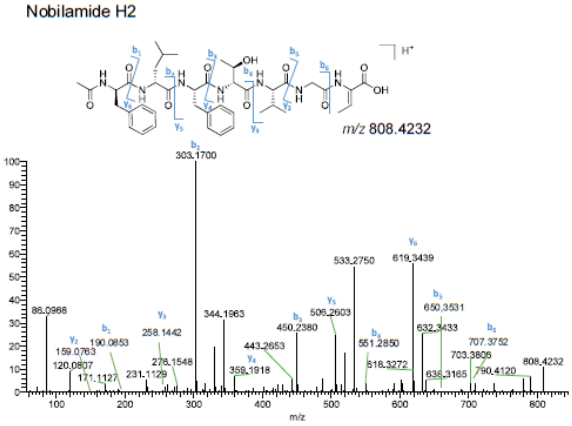

Nobilamide N

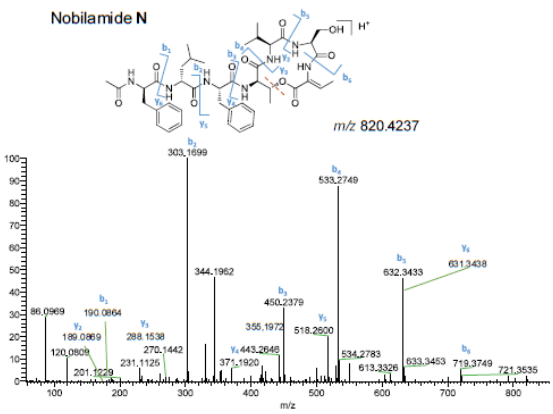

Nobilamide V1

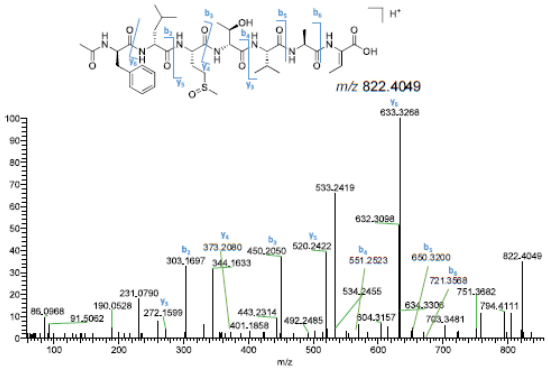

Nobilamide I

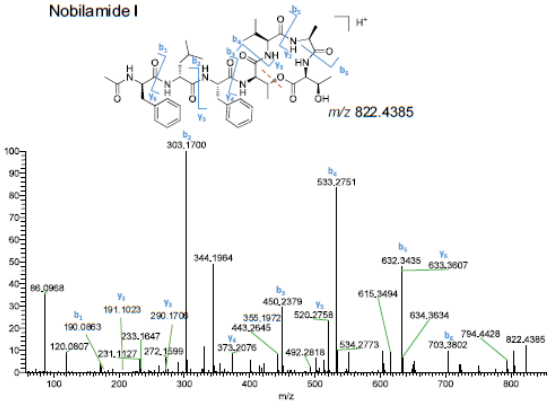

Nobilamide A

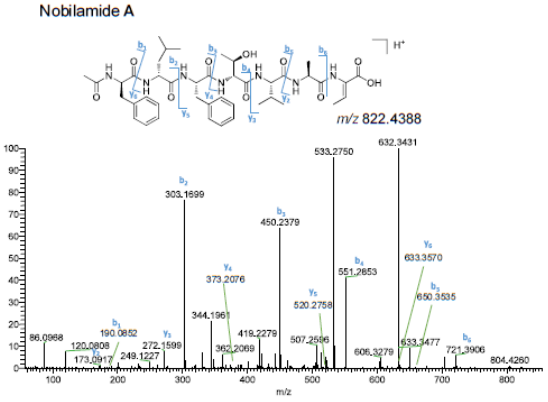

Nobilamide J

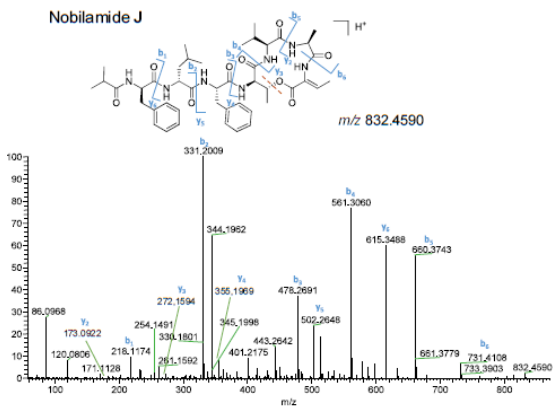

Nobilamide N2

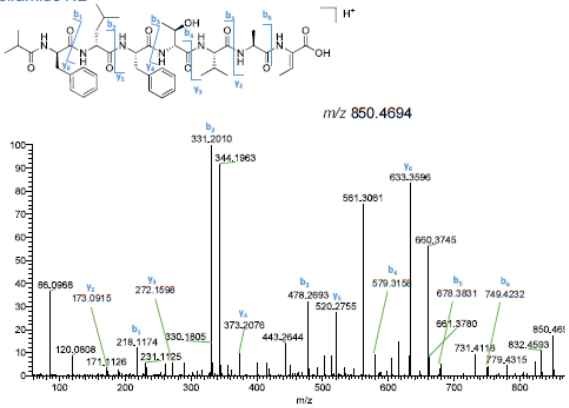

Nobilamide I2

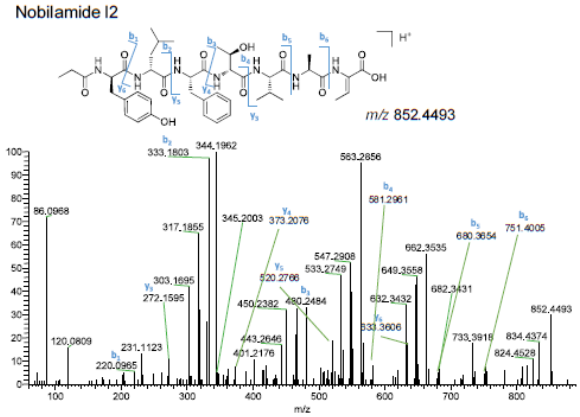

Nobilamide K1

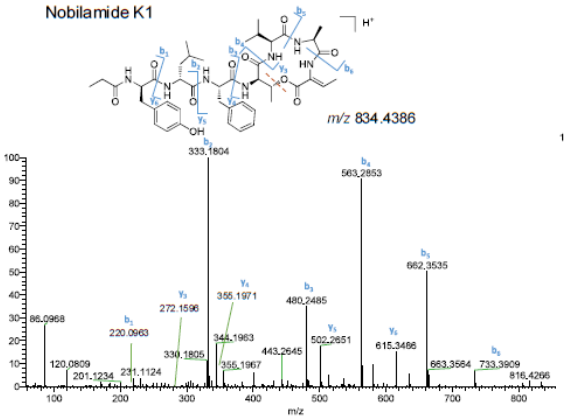

Nobilamide A2

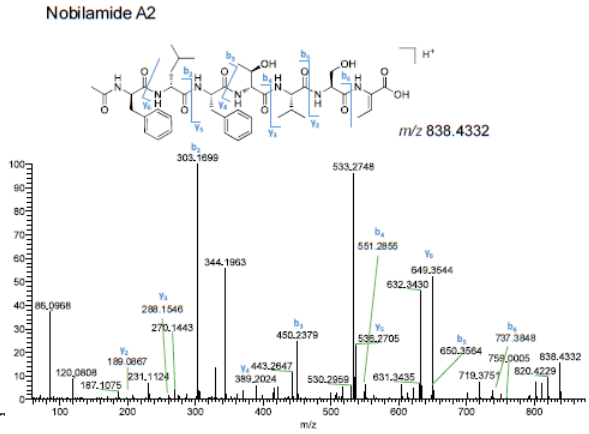

Nobilamide J1

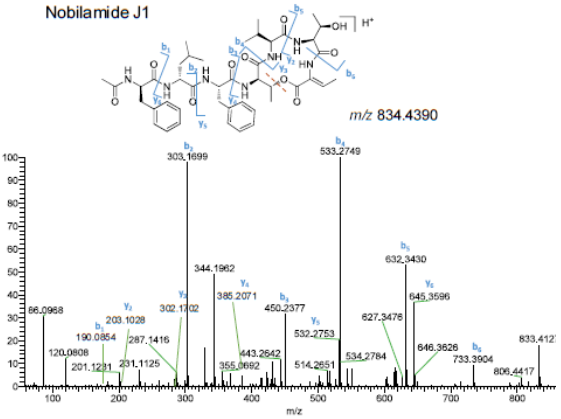

Nobilamide C2

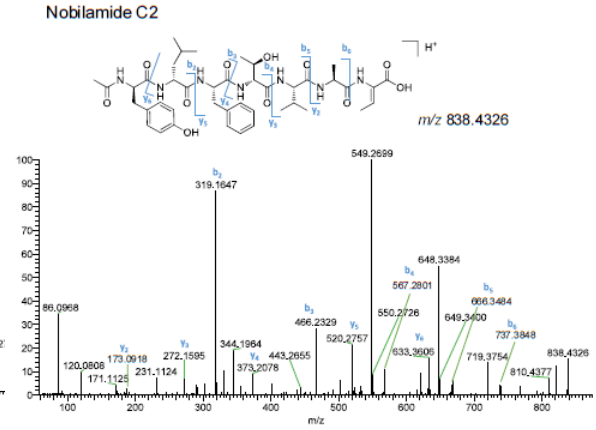

Nobilamide K

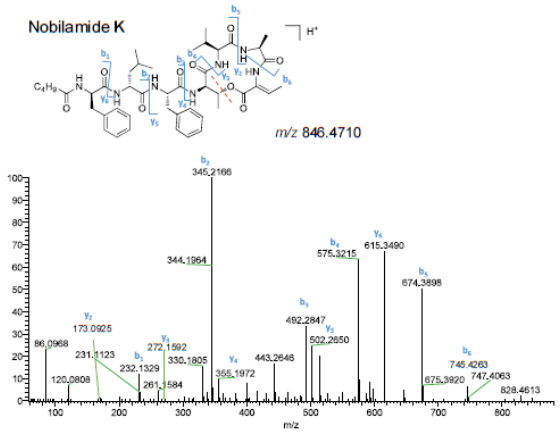

Nobilamide R1

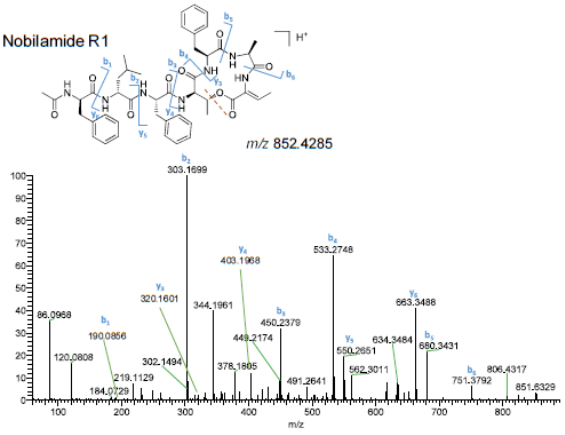

Nobilamide Y

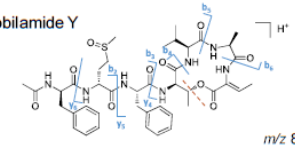

m/z 838.3785

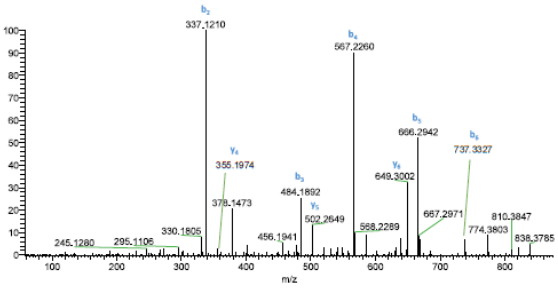

A-3302-A

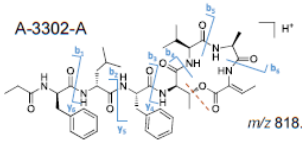

m/z 818.4446

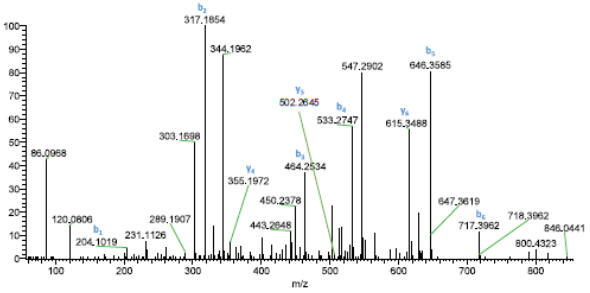

Nobilamide G3

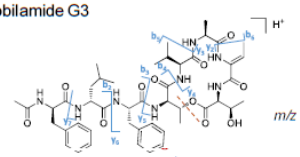

m/z 905.4759

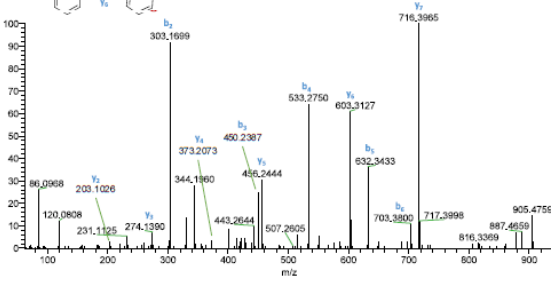

Nobilamide S1

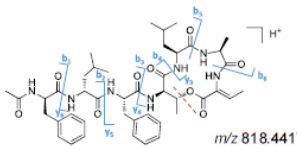

m/z 818.4417

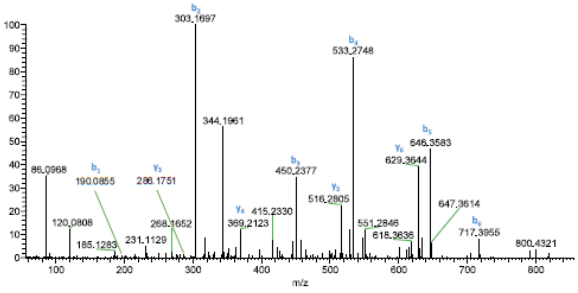

Nobilamide F2

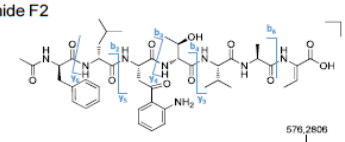

m/z 865.4442

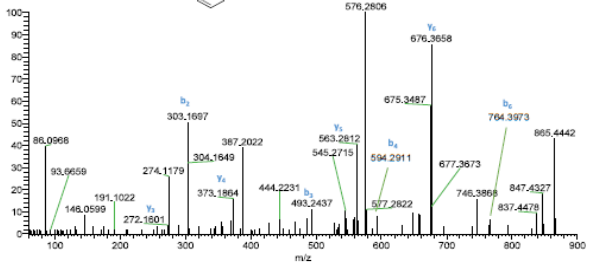

Nobilamide K2

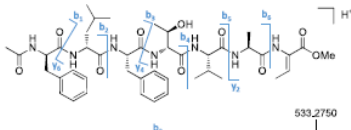

m/z 836.4543

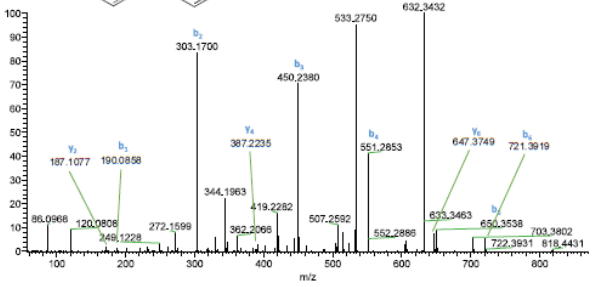

Nobilamide C1

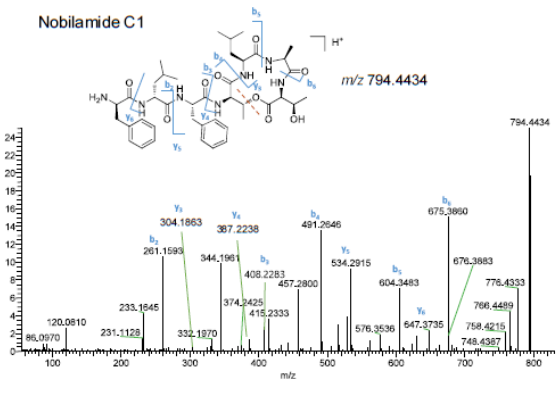

Nobilamide S

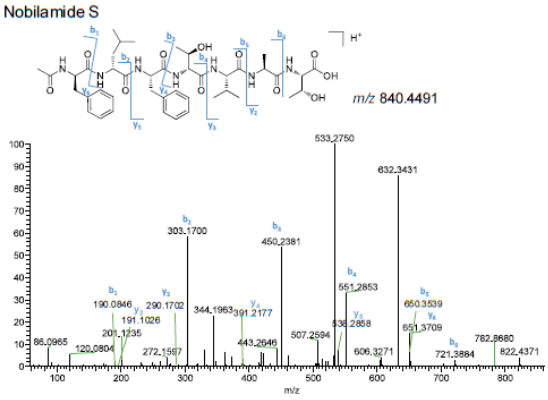

Nobilamide X1

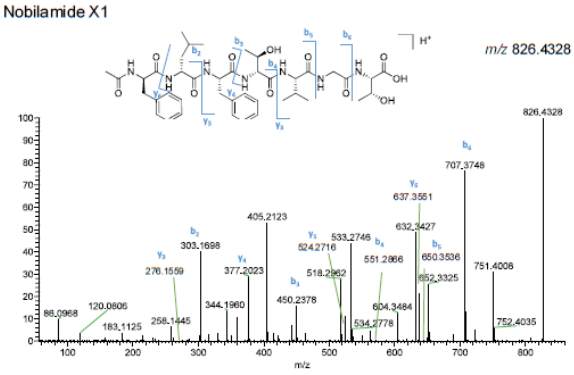

Nobilamide B1

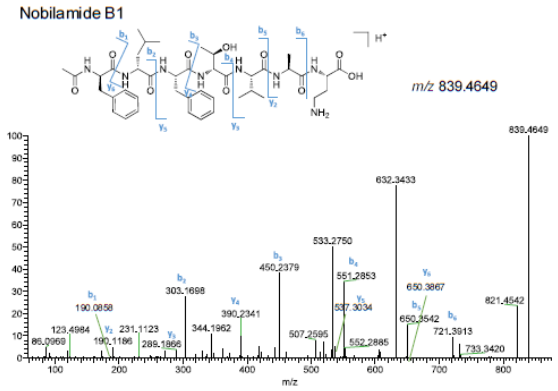

Nobilamide B

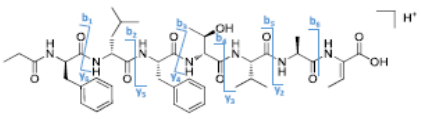

Nobilamide L2

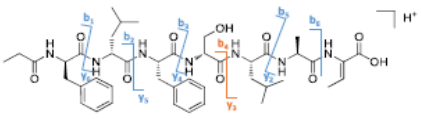

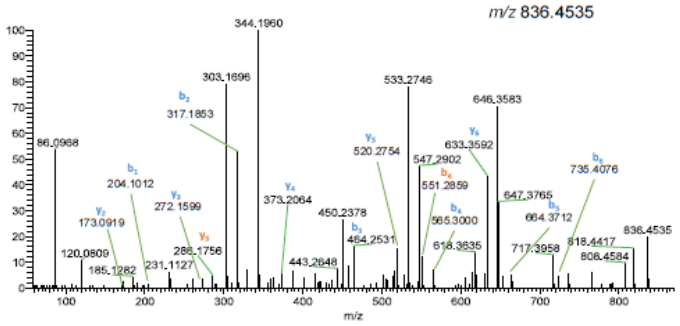

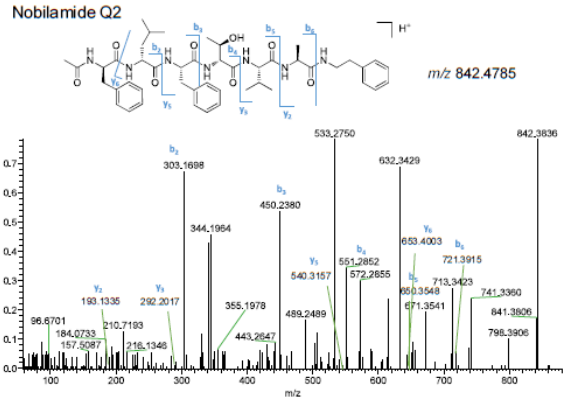
Nobilamide Q2
H+
m/z 842.4785
533.2750
842.3836
303.1698
632.3429
450.2380
344.1964
653.4003
551.2852
721.3915
540.3157
572.2655
713.3423
650.3548
741.3360
671.3541
841.3806
355.1978
489.2489
443.2647
798.3906
96.6701
210.7193
184.0733
157.5087
216.1346
m/z

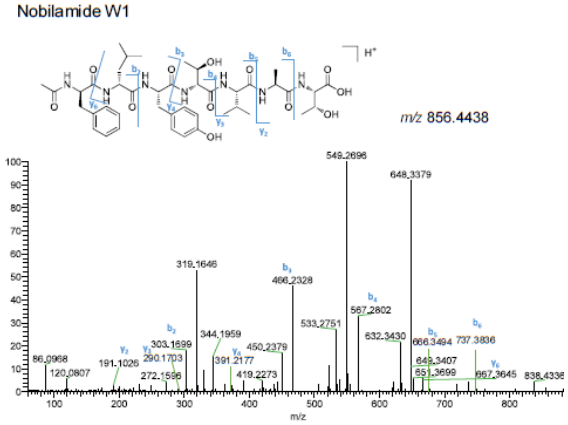
Nobilamide W1
H+
m/z 856.4438
548.2696
648.3379
319.1646
466.2328
567.2802
533.2751
632.3430
344.1959
303.1699
450.2379
666.3494
737.3836
649.3407
191.1026
290.1703
391.2177
419.2273
272.1596
667.3645
838.4336
86.0968
120.0807
m/z

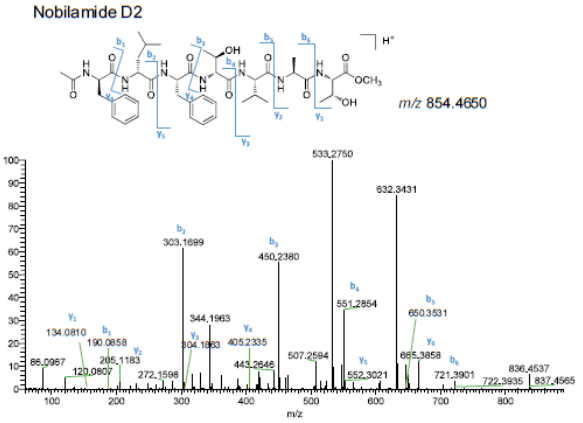
Nobilamide D2
H+
m/z 854.4650
533.2750
632.3431
303.1699
450.2380
551.2854
344.1963
650.3531
134.0810
190.0858
304.1893
405.2335
507.2594
665.3858
86.0957
205.1183
443.2646
552.3021
721.3901
836.4537
120.0807
272.1598
722.3935
837.4565
m/z

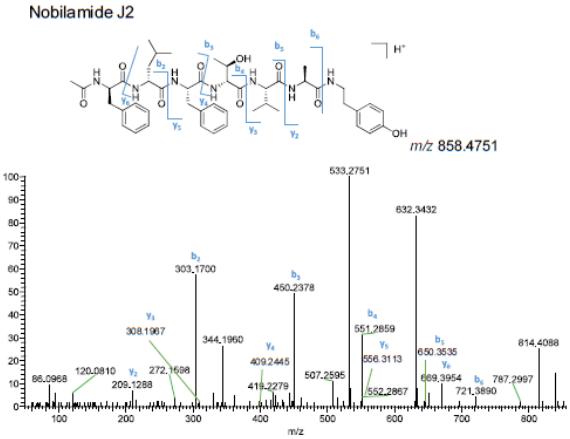
Nobilamide J2
H+
m/z 858.4751
533.2751
632.3432
303.1700
450.2378
308.1967
551.2859
344.1960
650.3535
814.4088
409.2445
556.3113
507.2595
689.3954
787.2997
86.0968
120.0810
272.1598
209.1288
419.2279
552.2867
721.3890
m/z

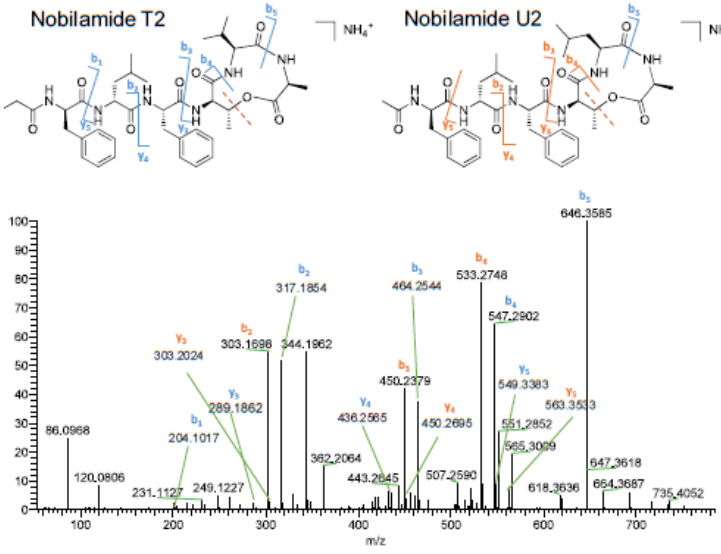
Nobilamide T2
NH4+
Nobilamide U2
NH4+
m/z 752.4331
646.3585
317.1854
464.2544
533.2748
547.2902
303.2024
303.1698
344.1962
549.3383
563.3533
289.1862
450.2379
436.2565
450.2695
551.2852
86.0968
204.1017
565.3009
382.2064
647.3618
120.0806
443.2645
507.2590
664.3687
231.1127
249.1227
618.3636
735.4052
m/z

Nobilamide F3

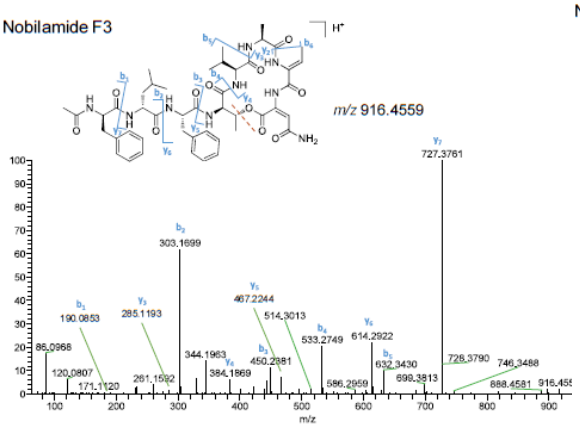

Nobilamide S2

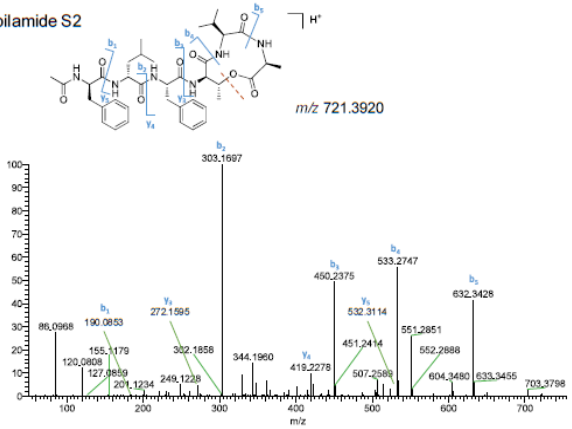

Nobilamide E3

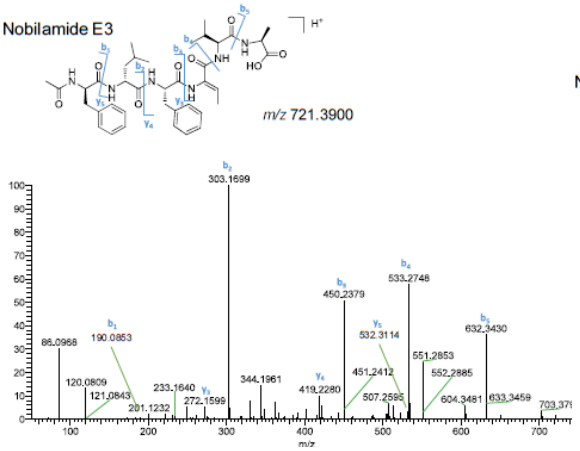

Nobilamide R2

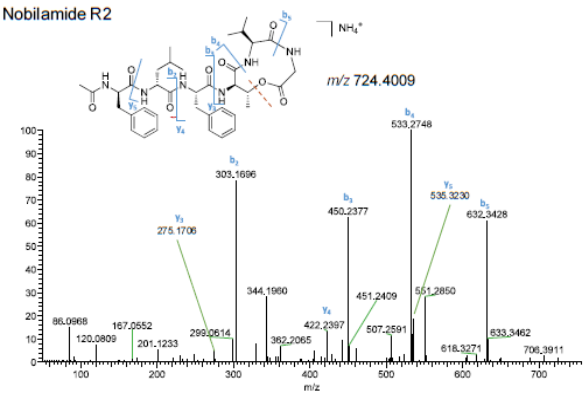

Nobilamide O2

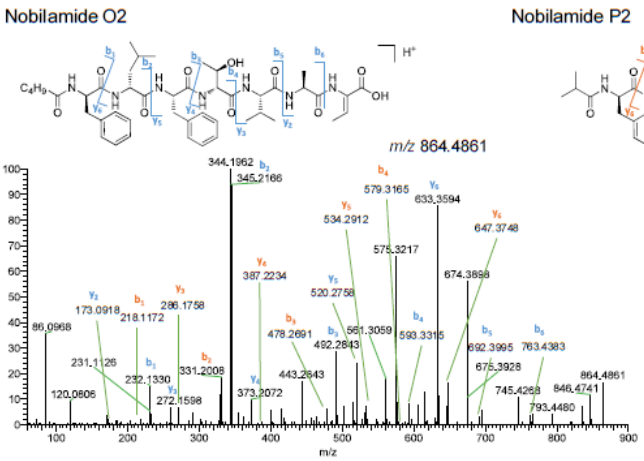

Nobilamide P2

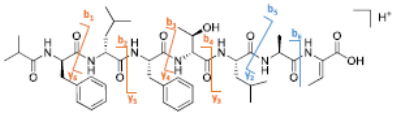

Nobilamide P3

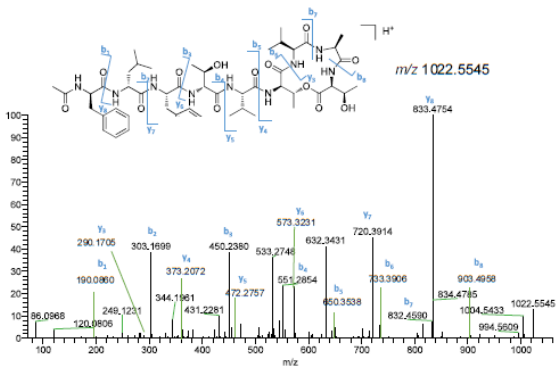

Nobilamide H3

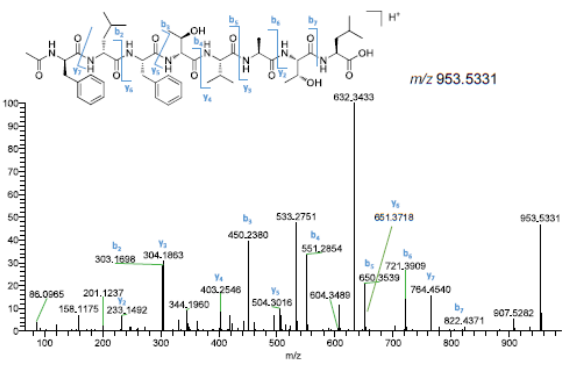

Nobilamide M3

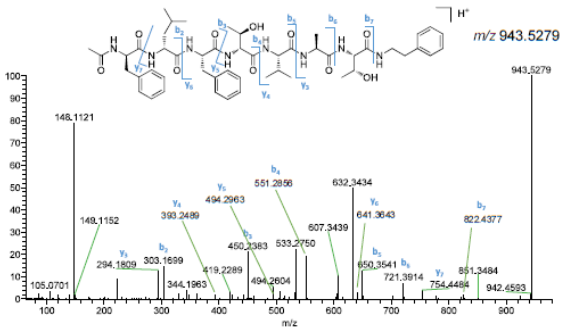

Nobilamide J3

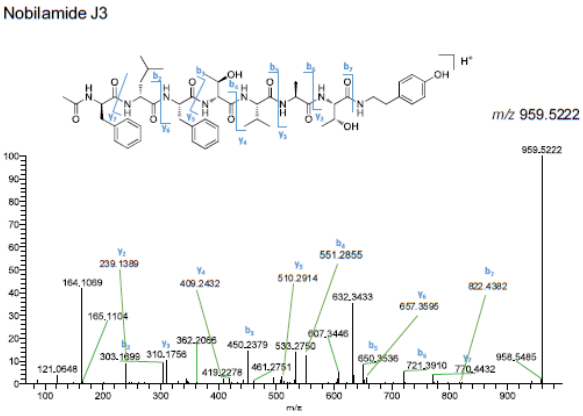

Nobilamide K3

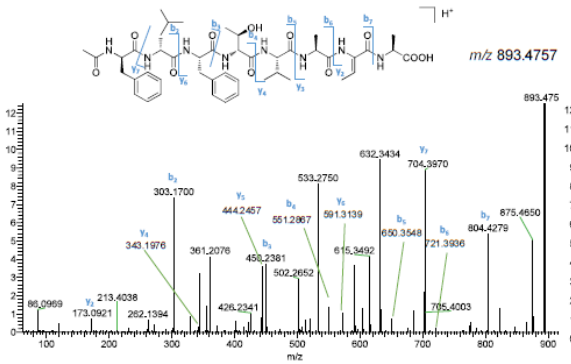

Nobilamide O3

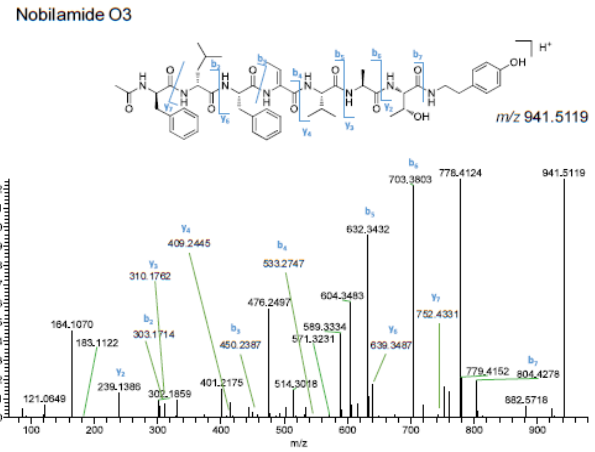

Nobilamide L3

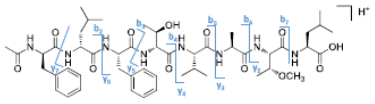

m/z 967.5498

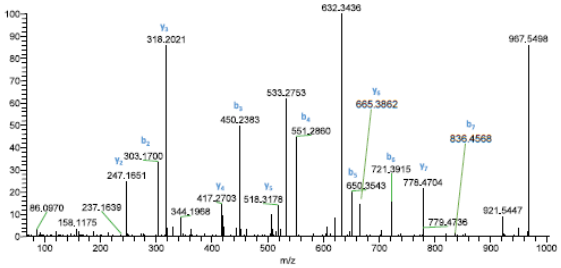

Nobilamide I3

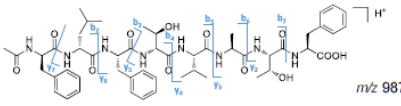

m/z 987.5173

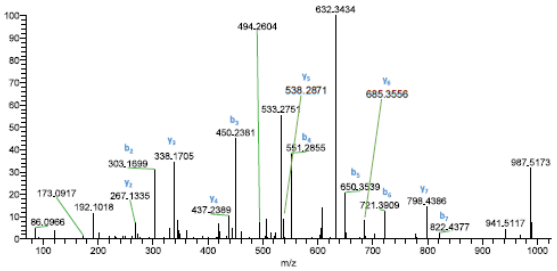

Nobilamide N3

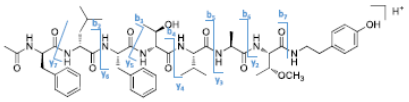

m/z 973.5382

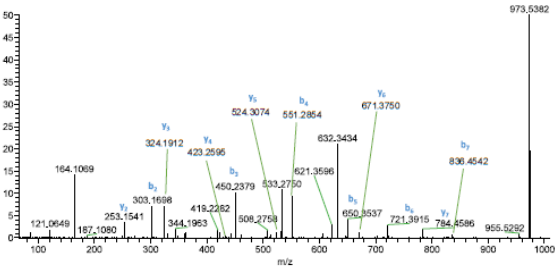

*Refe*rences

1. Zhao, X.-Q. Genome-Based Studies of Marine Microorganisms to Maximize the Diversity of Natural Products Discovery for Medical Treatments. Evid Based Complement Alternat Med 2011, 2011, 384572, doi:10.1155/2011/384572.
2. GBD 2021 Antimicrobial Resistance Collaborators Global Burden of Bacterial Antimicrobial Resistance 1990-2021: A Systematic Analysis with Forecasts to 2050. Lancet 2024, 404, 1199–1226, doi:10.1016/S0140-6736(24)01867-1.
3. Antimicrobial Resistance: A Silent Pandemic. Nat Commun 2024, 15, 6198, doi:10.1038/s41467-024-50457-z.
4. Xie, C.-L.; Xia, J.-M.; Wang, J.-S.; Lin, D.-H.; Yang, X.-W. Metabolomic Investigations on Nesterenkonia Flava Revealed Significant Differences between Marine and Terrestrial Actinomycetes. Marine Drugs 2018, 16, 356, doi:10.3390/md16100356.
5. Ajar Nath, Y. Microbial Biotechnology for Bio-Prospecting of Microbial Bioactive Compounds and Secondary Metabolites. J App Biol Biotech. 2021, doi:10.7324/JABB.2021.92ed.
6. Magiorakos, A.-P.; Srinivasan, A.; Carey, R.B.; Carmeli, Y.; Falagas, M.E.; Giske, C.G.; Harbarth, S.; Hindler, J.F.; Kahlmeter, G.; Olsson-Liljequist, B.; et al. Multidrug-Resistant, Extensively Drug-Resistant and Pandrug-Resistant Bacteria: An International Expert Proposal for Interim Standard Definitions for Acquired Resistance. Clinical Microbiology and Infection 2012, 18, 268–281, doi:10.1111/j.1469-0691.2011.03570.x.
7. Kannappan, A.; Sivaranjani, M.; Srinivasan, R.; Rathna, J.; Pandian, S.K.; Ravi, A.V. Inhibitory Efficacy of Geraniol on Biofilm Formation and Development of Adaptive Resistance in Staphylococcus Epidermidis RP62A. Journal of Medical Microbiology 2017, 66, 1506–1515, doi:10.1099/jmm.0.000570.
8. Chianese, G.; Esposito, F.P.; Parrot, D.; Ingham, C.; De Pascale, D.; Tasdemir, D. Linear Aminolipids with Moderate Antimicrobial Activity from the Antarctic Gram-Negative Bacterium Aequorivita Sp. Marine Drugs 2018, 16, 187, doi:10.3390/md16060187.
9. Palma Esposito, F.; Ingham, C.J.; Hurtado-Ortiz, R.; Bizet, C.; Tasdemir, D.; de Pascale, D. Isolation by Miniaturized Culture Chip of an Antarctic Bacterium Aequorivita Sp. with Antimicrobial and Anthelmintic Activity. Biotechnology Reports 2018, 20, e00281, doi:10.1016/j.btre.2018.e00281.
10. De Oliveira, D.M.P.; Forde, B.M.; Kidd, T.J.; Harris, P.N.A.; Schembri, M.A.; Beatson, S.A.; Paterson, D.L.; Walker, M.J. Antimicrobial Resistance in ESKAPE Pathogens. Clinical Microbiology Reviews 2020, 33, 10.1128/cmr.00181-19, doi:10.1128/cmr.00181-19.
11. Newman, D.J.; Cragg, G.M. Natural Products as Sources of New Drugs over the 30 Years from 1981 to 2010. J Nat Prod 2012, 75, 311–335, doi:10.1021/np200906s.
12. Bologa, C.G.; Ursu, O.; Oprea, T.I.; Melançon, C.E.; Tegos, G.P. Emerging Trends in the Discovery of Natural Product Antibacterials. Curr Opin Pharmacol 2013, 13, 678–687, doi:10.1016/j.coph.2013.07.002.
13. Kaur, P.; Li, Y.; Cai, J.; Song, L. Selective Membrane Disruption Mechanism of an Antibacterial γ-AApeptide Defined by EPR Spectroscopy. Biophys J 2016, 110, 1789–1799, doi:10.1016/j.bpj.2016.02.038.
14. Bechinger, B.; Gorr, S.-U. Antimicrobial Peptides: Mechanisms of Action and Resistance. J Dent Res 2017, 96, 254–260, doi:10.1177/0022034516679973.
15. Giugliano, R.; Della Sala, G.; Buonocore, C.; Zannella, C.; Tedesco, P.; Palma Esposito, F.; Ragozzino, C.; Chianese, A.; Morone, M.V.; Mazzella, V.; et al. New Imidazolium Alkaloids with Broad Spectrum of Action from the Marine Bacterium Shewanella Aquimarina. Pharmaceutics 2023, 15, 2139, doi:10.3390/pharmaceutics15082139.
16. Ng, I.-S.; Ye, C.; Zhang, Z.; Lu, Y.; Jing, K. Daptomycin Antibiotic Production Processes in Fed-Batch Fermentation by Streptomyces Roseosporus NRRL11379 with Precursor Effect and Medium Optimization. Bioprocess Biosyst Eng 2014, 37, 415–423, doi:10.1007/s00449-013-1007-2.
17. Rimal, B.; Chang, J.; Liu, C.; Rashid, R.; Singh, M.; Kim, S.J. The Effects of Daptomycin on Cell Wall Biosynthesis in Enterococcal Faecalis. Sci Rep 2023, 13, 12227, doi:10.1038/s41598-023-39486-8.
18. Alonzo, D.A.; Schmeing, T.M. Biosynthesis of Depsipeptides, or Depsi: The Peptides with Varied Generations. Protein Science 2020, 29, 2316–2347, doi:10.1002/pro.3979.
19. Zeng, M.; Tao, J.; Xu, S.; Bai, X.; Zhang, H. Marine Organisms as a Prolific Source of Bioactive Depsipeptides. Marine Drugs 2023, 21, 120, doi:10.3390/md21020120.

20. Sayyed, R.Z.; El-Enshasy, H.A.; Hameeda, B. Microbial Surfactants: Volume I: Production and Applications; CRC Press, 2021; ISBN 978-1-00-041565-0.
21. Haque, E.; Kayalvizhi, K.; Hassan, S. Biocompatibility, Antioxidant and Anti-Infective Effect of Biosurfactant Produced by Marinobacter Litoralis MB15. International Journal of Pharmaceutical Investigation 2020, 10, 173–178, doi:10.5530/ijpi.2020.2.32.
22. Kumar, A.; Singh, S.K.; Kant, C.; Verma, H.; Kumar, D.; Singh, P.P.; Modi, A.; Droby, S.; Kesawat, M.S.; Alavilli, H.; et al. Microbial Biosurfactant: A New Frontier for Sustainable Agriculture and Pharmaceutical Industries. Antioxidants 2021, 10, 1472, doi:10.3390/antiox10091472.
23. Rofeal, M.; El-Malek, F.A. Valorization of Lipopeptides Biosurfactants as Anticancer Agents. Int J Pept Res Ther 2021, 27, 447–455, doi:10.1007/s10989-020-10105-8.
24. Giugliano, R.; Buonocore, C.; Zannella, C.; Chianese, A.; Palma Esposito, F.; Tedesco, P.; De Filippis, A.; Galdiero, M.; Franci, G.; de Pascale, D. Antiviral Activity of the Rhamnolipids Mixture from the Antarctic Bacterium Pseudomonas Gessardii M15 against Herpes Simplex Viruses and Coronaviruses. Pharmaceutics 2021, 13, 2121, doi:10.3390/pharmaceutics13122121.
25. Buonocore, C.; Giugliano, R.; Della Sala, G.; Palma Esposito, F.; Tedesco, P.; Folliero, V.; Galdiero, M.; Franci, G.; de Pascale, D. Evaluation of Antimicrobial Properties and Potential Applications of Pseudomonas Gessardii M15 Rhamnolipids towards Multiresistant Staphylococcus Aureus. Pharmaceutics 2023, 15, 700, doi:10.3390/pharmaceutics15020700.
26. Xiao, S.; Chen, N.; Chai, Z.; Zhou, M.; Xiao, C.; Zhao, S.; Yang, X. Secondary Metabolites from Marine-Derived Bacillus: A Comprehensive Review of Origins, Structures, and Bioactivities. Marine Drugs 2022, 20, 567, doi:10.3390/md20090567.
27. Ali, N.; Pang, Z.; Wang, F.; Xu, B.; El-Seedi, H.R. Lipopeptide Biosurfactants from Bacillus Spp.: Types, Production, Biological Activities, and Applications in Food. Journal of Food Quality 2022, 2022, 3930112, doi:10.1155/2022/3930112.
28. Huang, L.; Ling, X.; Peng, S.; Tan, M.; Yan, L.; Liang, Y.; Li, G.; Li, K. A Marine Lipopeptides-Producing Bacillus Amyloliquefaciens HY2-1 with a Broad-Spectrum Antifungal and Antibacterial Activity and Its Fermentation Kinetics Study. World J Microbiol Biotechnol 2023, 39, 196, doi:10.1007/s11274-023-03643-y.
29. Süssmuth, R.D.; Mainz, A. Nonribosomal Peptide Synthesis-Principles and Prospects. Angew Chem Int Ed Engl 2017, 56, 3770–3821, doi:10.1002/anie.201609079.
30. Agrawal, S.; Acharya, D.; Adholeya, A.; Barrow, C.J.; Deshmukh, S.K. Nonribosomal Peptides from Marine Microbes and Their Antimicrobial and Anticancer Potential. Front. Pharmacol. 2017, 8, doi:10.3389/fphar.2017.00828.
31. Fouillaud, M.; Dufossé, L. Microbial Secondary Metabolism and Biotechnology. Microorganisms 2022, 10, 123, doi:10.3390/microorganisms10010123.
32. Strieker, M.; Tanović, A.; Marahiel, M.A. Nonribosomal Peptide Synthetases: Structures and Dynamics. Current Opinion in Structural Biology 2010, 20, 234–240, doi:10.1016/j.sbi.2010.01.009.
33. Shoji, J.; Hinoo, H.; Wakisaka, Y.; Koizumi, K.; Mayama, M. Isolation of a New Peptide Antibiotic TL-119. Studies on Antibiotics from the Genus Bacillus. IV. J Antibiot (Tokyo) 1975, 28, 126–128, doi:10.7164/antibiotics.28.126.
34. Nakagawa, Y.; Nakazawa, T.; Shoji, J. On the Structure of a New Antibiotic TL-119 (Studies on Antibiotics from the Genus Bacillus. VI). J Antibiot (Tokyo) 1975, 28, 1004–1005, doi:10.7164/antibiotics.28.1004.
35. Kitajima, Y.; Waki, M.; Shoji, J.; Ueno, T.; Izumiya, N. Revised Structure of the Peptide Lactone Antibiotic, TL-119 and/or A-3302-B. FEBS Letters 1990, 270, 139–142, doi:10.1016/0014-5793(90)81253-K.
36. Sureram, S.; Arduino, I.; Ueoka, R.; Rittà, M.; Francese, R.; Srivibool, R.; Darshana, D.; Piel, J.; Ruchirawat, S.; Muratori, L.; et al. The Peptide A-3302-B Isolated from a Marine Bacterium Micromonospora Sp. Inhibits HSV-2 Infection by Preventing the Viral Egress from Host Cells. International Journal of Molecular Sciences 2022, 23, 947, doi:10.3390/ijms23020947.
37. Nobilamides A–H, Long-Acting Transient Receptor Potential Vanilloid-1 (TRPV1) Antagonists from Mollusk-Associated Bacteria | Journal of Medicinal Chemistry Available online: https://pubs.acs.org/doi/abs/10.1021/jm101621u (accessed on 11 July 2024).
38. Chen, X.; Lu, Y.; Shan, M.; Zhao, H.; Lu, Z.; Lu, Y. A Mini-Review: Mechanism of Antimicrobial Action and Application of Surfactin. World J Microbiol Biotechnol 2022, 38, 143, doi:10.1007/s11274-022-03323-3.

39. Holder, I.A.; Boyce, S.T. Agar Well Diffusion Assay Testing of Bacterial Susceptibility to Various Antimicrobials in Concentrations Non-Toxic for Human Cells in Culture. Burns 1994, 20, 426–429, doi:10.1016/0305-4179(94)90035-3.
40. O'Connor, E.; Hynes, S.; Chen, W. Estimating the Non-Market Benefit Value of Deep-Sea Ecosystem Restoration: Evidence from a Contingent Valuation Study of the Dohrn Canyon in the Bay of Naples. Journal of Environmental Management 2020, 275, 111180, doi:10.1016/j.jenvman.2020.111180.
41. Khan, H.A.; Baig, F.K.; Mehboob, R. Nosocomial Infections: Epidemiology, Prevention, Control and Surveillance. Asian Pacific Journal of Tropical Biomedicine 2017, 7, 478–482, doi:10.1016/j.apjtb.2017.01.019.
42. Ashfaq, M.; Talreja, N.; Chauhan, D.; Viswanathan, M.R. Synthesis of Cu-Doped 2D-WS2 Nanosheet-Based Nano-Antibiotic Materials for Inhibiting E. Coli and S. Aureus Bacterial Strains. New J. Chem. 2022, 46, 5581–5587, doi:10.1039/D1NJ05931A.
43. Della Sala, G.; Mangoni, A.; Costantino, V.; Teta, R. Identification of the Biosynthetic Gene Cluster of Thermoactinoamides and Discovery of New Congeners by Integrated Genome Mining and MS-Based Molecular Networking. Front. Chem. 2020, 8, doi:10.3389/fchem.2020.00397.
44. Teta, R.; Sala, G.D.; Esposito, G.; Stornaiuolo, M.; Scarpato, S.; Casazza, M.; Anastasio, A.; Lega, M.; Costantino, V. Monitoring Cyanobacterial Blooms during the COVID-19 Pandemic in Campania, Italy: The Case of Lake Avernus. Toxins 2021, 13, 471, doi:10.3390/toxins13070471.
45. Lin, Z.; Reilly, C.A.; Antemano, R.; Hughen, R.W.; Marett, L.; Concepcion, G.P.; Haygood, M.G.; Olivera, B.M.; Light, A.; Schmidt, E.W. Nobilamides A–H, Long-Acting Transient Receptor Potential Vanilloid-1 (TRPV1) Antagonists from Mollusk-Associated Bacteria. J. Med. Chem. 2011, 54, 3746–3755, doi:10.1021/jm101621u.
46. Iloabuchi, K.; Spiteller, D. The Epiphyte Bacillus Sp. G2112 Produces a Large Diversity of Nobilamide Peptides That Promote Biofilm Formation in Pseudomonads and Mycobacterium Aurum. Biomolecules 2024, 14, 1244, doi:10.3390/biom14101244.
47. Medzihradszky, K.F.; Chalkley, R.J. Lessons in de Novo Peptide Sequencing by Tandem Mass Spectrometry. Mass Spectrometry Reviews 2015, 34, 43–63, doi:10.1002/mas.21406.
48. Magarvey, N.A.; Ehling-Schulz, M.; Walsh, C.T. Characterization of the Cereulide NRPS α-Hydroxy Acid Specifying Modules: Activation of α-Keto Acids and Chiral Reduction on the Assembly Line. J. Am. Chem. Soc. 2006, 128, 10698–10699, doi:10.1021/ja0640187.
49. Wenzel, S.C.; Müller, R. Formation of Novel Secondary Metabolites by Bacterial Multimodular Assembly Lines: Deviations from Textbook Biosynthetic Logic. Current Opinion in Chemical Biology 2005, 9, 447–458, doi:10.1016/j.cbpa.2005.08.001.
50. Wenzel, S.C.; Meiser, P.; Binz, T.M.; Mahmud, T.; Müller, R. Nonribosomal Peptide Biosynthesis: Point Mutations and Module Skipping Lead to Chemical Diversity. Angewandte Chemie International Edition 2006, 45, 2296–2301, doi:10.1002/anie.200503737.
51. Wang, L.; Linares-Otoya, V.; Liu, Y.; Mettal, U.; Marner, M.; Armas-Mantilla, L.; Willbold, S.; Kurtán, T.; Linares-Otoya, L.; Schäberle, T.F. Discovery and Biosynthesis of Antimicrobial Phenethylamine Alkaloids from the Marine Flavobacterium Tenacibaculum Discolor Sv11. J. Nat. Prod. 2022, 85, 1039–1051, doi:10.1021/acs.jnatprod.1c01173.
52. Shen, Q.; Zhou, H.; Dai, G.; Zhong, G.; Huo, L.; Li, A.; Liu, Y.; Yang, M.; Ravichandran, V.; Zheng, Z.; et al. Characterization of a Cryptic NRPS Gene Cluster in Bacillus Velezensis FZB42 Reveals a Discrete Oxidase Involved in Multithiazole Biosynthesis. ACS Catal. 2022, 12, 3371–3381, doi:10.1021/acscatal.1c05131.
53. Baars, O.; Zhang, X.; Gibson, M.I.; Stone, A.T.; Morel, F.M.M.; Seyedsayamdost, M.R. Crochelins: Siderophores with an Unprecedented Iron-Chelating Moiety from the Nitrogen-Fixing Bacterium Azotobacter Chroococcum. Angewandte Chemie International Edition 2018, 57, 536–541, doi:10.1002/anie.201709720.
54. Chen, H.; Zhong, L.; Zhou, H.; Bai, X.; Sun, T.; Wang, X.; Zhao, Y.; Ji, X.; Tu, Q.; Zhang, Y.; et al. Biosynthesis and Engineering of the Nonribosomal Peptides with a C-Terminal Putrescine. Nat Commun 2023, 14, 6619, doi:10.1038/s41467-023-42387-z.
55. Gardete, S.; Tomasz, A. Mechanisms of Vancomycin Resistance in Staphylococcus Aureus. J Clin Invest 2014, 124, 2836–2840, doi:10.1172/JCI68834.
56. Kapoor, G.; Saigal, S.; Elongavan, A. Action and Resistance Mechanisms of Antibiotics: A Guide for Clinicians. J Anaesthesiol Clin Pharmacol 2017, 33, 300–305, doi:10.4103/joacp.JOACP_349_15.

57. Yoon, S.-H.; Ha, S.-M.; Kwon, S.; Lim, J.; Kim, Y.; Seo, H.; Chun, J. Introducing EzBioCloud: A Taxonomically United Database of 16S rRNA Gene Sequences and Whole-Genome Assemblies. Int J Syst Evol Microbiol 2017, 67, 1613–1617, doi:10.1099/ijsem.0.001755.
58. Chalita, M.; Kim, Y.O.; Park, S.; Oh, H.-S.; Cho, J.H.; Moon, J.; Baek, N.; Moon, C.; Lee, K.; Yang, J.; et al. EzBioCloud: A Genome-Driven Database and Platform for Microbiome Identification and Discovery. International Journal of Systematic and Evolutionary Microbiology 2024, 74, 006421, doi:10.1099/ijsem.0.006421.
59. Zhang, Z.; Yin, L.; Li, X.; Zhang, C.; Liu, C.; Wu, Z. The Complete Genome Sequence of Bacillus Halotolerans ZB201702 Isolated from a Drought- and Salt-Stressed Rhizosphere Soil. Microb Pathog 2018, 123, 246–249, doi:10.1016/j.micpath.2018.07.019.
60. Wu, X.; Wu, H.; Wang, R.; Wang, Z.; Zhang, Y.; Gu, Q.; Farzand, A.; Yang, X.; Semenov, M.; Borriss, R.; et al. Genomic Features and Molecular Function of a Novel Stress-Tolerant Bacillus Halotolerans Strain Isolated from an Extreme Environment. Biology 2021, 10, 1030, doi:10.3390/biology10101030.
61. Patteson, J.B.; Fortinez, C.M.; Putz, A.T.; Rodriguez-Rivas, J.; Bryant, L.H.I.; Adhikari, K.; Weigt, M.; Schmeing, T.M.; Li, B. Structure and Function of a Dehydrating Condensation Domain in Nonribosomal Peptide Biosynthesis. J. Am. Chem. Soc. 2022, 144, 14057–14070, doi:10.1021/jacs.1c13404.
62. Ziemert, N.; Podell, S.; Penn, K.; Badger, J.H.; Allen, E.; Jensen, P.R. The Natural Product Domain Seeker NaPDoS: A Phylogeny Based Bioinformatic Tool to Classify Secondary Metabolite Gene Diversity. PLoS One 2012, 7, e34064, doi:10.1371/journal.pone.0034064.
63. Grundmann, F.; Kaiser, M.; Schiell, M.; Batzer, A.; Kurz, M.; Thanwisai, A.; Chantratita, N.; Bode, H.B. Antiparasitic Chaiyaphumines from Entomopathogenic Xenorhabdus Sp. PB61.4. J. Nat. Prod. 2014, 77, 779–783, doi:10.1021/np4007525.
64. Lukat, P.; Katsuyama, Y.; Wenzel, S.; Binz, T.; König, C.; Blankenfeldt, W.; Brönstrup, M.; Müller, R. Biosynthesis of Methyl-Proline Containing Griselimycins, Natural Products with Anti-Tuberculosis Activity. Chem. Sci. 2017, 8, 7521–7527, doi:10.1039/C7SC02622F.
65. Niehs, S.P.; Dose, B.; Scherlach, K.; Roth, M.; Hertweck, C. Genomics-Driven Discovery of a Symbiont-Specific Cyclopeptide from Bacteria Residing in the Rice Seedling Blight Fungus. ChemBioChem 2018, 19, 2167–2172, doi:10.1002/cbic.201800400.
66. Weisburg, W.G.; Barns, S.M.; Pelletier, D.A.; Lane, D.J. 16S Ribosomal DNA Amplification for Phylogenetic Study. J Bacteriol 1991, 173, 697–703.
67. Palma Esposito, F.; Giugliano, R.; Della Sala, G.; Vitale, G.A.; Buonocore, C.; Ausuri, J.; Galasso, C.; Coppola, D.; Franci, G.; Galdiero, M.; et al. Combining OSMAC Approach and Untargeted Metabolomics for the Identification of New Glycolipids with Potent Antiviral Activity Produced by a Marine Rhodococcus. Int J Mol Sci 2021, 22, 9055, doi:10.3390/ijms22169055.
68. Wang, M.; Carver, J.J.; Phelan, V.V.; Sanchez, L.M.; Garg, N.; Peng, Y.; Nguyen, D.D.; Watrous, J.; Kapono, C.A.; Luzzatto-Knaan, T.; et al. Sharing and Community Curation of Mass Spectrometry Data with Global Natural Products Social Molecular Networking. Nat Biotechnol 2016, 34, 828–837, doi:10.1038/nbt.3597.
69. Nothias, L.-F.; Petras, D.; Schmid, R.; Dührkop, K.; Rainer, J.; Sarvepalli, A.; Protsyuk, I.; Ernst, M.; Tsugawa, H.; Fleischauer, M.; et al. Feature-Based Molecular Networking in the GNPS Analysis Environment. Nat Methods 2020, 17, 905–908, doi:10.1038/s41592-020-0933-6.
70. Siegmund, I.; Wagner, F. New Method for Detecting Rhamnolipids Excreted byPseudomonas Species during Growth on Mineral Agar. Biotechnol Tech 1991, 5, 265–268, doi:10.1007/BF02438660.
71. Morikawa, M.; Hirata, Y.; Imanaka, T. A Study on the Structure–Function Relationship of Lipopeptide Biosurfactants. Biochimica et Biophysica Acta (BBA) - Molecular and Cell Biology of Lipids 2000, 1488, 211–218, doi:10.1016/S1388-1981(00)00124-4.
72. Balouiri, M.; Sadiki, M.; Ibnsouda, S.K. Methods for in Vitro Evaluating Antimicrobial Activity: A Review. Journal of Pharmaceutical Analysis 2016, 6, 71–79, doi:10.1016/j.jpha.2015.11.005.
73. Franci, G.; Folliero, V.; Cammarota, M.; Zannella, C.; Sarno, F.; Schiraldi, C.; de Lera, A.R.; Altucci, L.; Galdiero, M. Epigenetic Modulator UVI5008 Inhibits MRSA by Interfering with Bacterial Gyrase. Sci Rep 2018, 8, 13117, doi:10.1038/s41598-018-31135-9.
74. Dordet-Frisoni, E.; Dorchies, G.; De Araujo, C.; Talon, R.; Leroy, S. Genomic Diversity in Staphylococcus Xylosus. Appl Environ Microbiol 2007, 73, 7199–7209, doi:10.1128/AEM.01629-07.
75. Weinstein, M.P.; Patel, J.B. Methods for Dilution Antimicrobial Susceptibility Tests for Bacteria That Grow Aerobically: M07-A11; Documents / Clinical and Laboratory Standards Institute; 11. edition.; Committee for Clinical Laboratory Standards: Wayne, PA, 2018; ISBN 978-1-56238-836-2.

76. Osek, J.; Lachtara, B.; Wieczorek, K. Listeria Monocytogenes – How This Pathogen Survives in Food-Production Environments? Front. Microbiol. 2022, 13, doi:10.3389/fmicb.2022.866462.
77. Bolger, A.M.; Lohse, M.; Usadel, B. Trimmomatic: A Flexible Trimmer for Illumina Sequence Data. Bioinformatics 2014, 30, 2114–2120, doi:10.1093/bioinformatics/btu170.
78. Babraham Bioinformatics - FastQC A Quality Control Tool for High Throughput Sequence Data Available online: https://www.bioinformatics.babraham.ac.uk/projects/fastqc/ (accessed on 11 July 2024).
79. Li, D.; Liu, C.-M.; Luo, R.; Sadakane, K.; Lam, T.-W. MEGAHIT: An Ultra-Fast Single-Node Solution for Large and Complex Metagenomics Assembly via Succinct de Bruijn Graph. Bioinformatics 2015, 31, 1674–1676, doi:10.1093/bioinformatics/btv033.
80. Wang, Y.; Zhao, Y.; Bollas, A.; Wang, Y.; Au, K.F. Nanopore Sequencing Technology, Bioinformatics and Applications. Nat Biotechnol 2021, 39, 1348–1365, doi:10.1038/s41587-021-01108-x.
81. Wick, R.R.; Judd, L.M.; Gorrie, C.L.; Holt, K.E. Unicycler: Resolving Bacterial Genome Assemblies from Short and Long Sequencing Reads. PLoS Comput Biol 2017, 13, e1005595, doi:10.1371/journal.pcbi.1005595.
82. Bankevich, A.; Nurk, S.; Antipov, D.; Gurevich, A.A.; Dvorkin, M.; Kulikov, A.S.; Lesin, V.M.; Nikolenko, S.I.; Pham, S.; Prjibelski, A.D.; et al. SPAdes: A New Genome Assembly Algorithm and Its Applications to Single-Cell Sequencing. J Comput Biol 2012, 19, 455–477, doi:10.1089/cmb.2012.0021.

CHAPTER 2

Characterization of Novel Aquachelin Siderophores from *Halomonas* sp. P26: Bioactivity evaluation and Biosynthetic Gene Cluster identification

Abstract: The *Halomonas* genus is known for producing amphiphilic siderophores, which play a crucial role in the iron cycle in marine environments. This study focused on exploring the natural products of *Halomonas* sp. P26, isolated from the Bay of Piran in the Adriatic Sea. The analysis led to the identification of nine new aquachelin (siderophores) analogues through bioassay-guided fractionation combined with feature-based molecular networking (FBMN). Structural characterization via in-depth LC-HRMS^2 analysis revealed that these compounds share a common core structure consisting of a linear hexapeptide with β-hydroxyaspartate and two hydroxamate functional groups that coordinate iron binding. The new aquachelin variants were characterized by different amino acid substitutions at positions 1, 5, and 7, as well as variations in the length and saturation of the fatty acid chains. Further genome sequencing and bioinformatics analysis identified the biosynthetic gene cluster (BGC), confirming the production of these siderophores via a multimodular non-ribosomal peptide synthetase (NRPS) pathway. The fraction containing the novel compounds exhibited strong antimicrobial activity against Gram-negative bacteria, including *E. coli* and *S. enterica*, as well as significant antioxidant and biosurfactant activity. These findings suggest that *Halomonas* sp. P26 is a promising resource for discovering new bioactive compounds with biotechnological applications.

---

1. Introduction

Iron (Fe) is essential for marine microorganisms, as it serves as a cofactor for enzymes involved in vital processes such as photosynthesis, respiration and nitrogen fixation [1]. However, iron availability in marine environments is

extremely limited [2]. Under aerobic conditions and physiological pH, the highly insoluble oxidised form Fe (III) prevails, forming solid compounds such as oxides and hydroxides. Consequently, the concentration of bioavailable iron in the oceans reaches extremely low values, on the order of (10^{-18} M), imposing a significant challenge for microorganisms that depend on it for survival and growth [3,4]. Bacteria overcome this challenge by producing iron-chelators called siderophores, low molecular weight compounds (500–1500 Da) with a high affinity for Fe(III) [5,6]. These siderophores scavenge insoluble iron present in the environment, forming soluble complexes that can be transported into the bacterial cell via specific transport systems [7,8]. Once inside, the iron is released and integrated into essential structures, such as [Fe-S]-containing ferredoxins and heme-containing cytochromes, to support vital metabolic functions [9]. Due to their high affinity for iron, siderophores regulate its availability in seawater, binding around 99% of the iron present [10]. They have the ability to capture and sequester iron from a variety of sources, including the solubilisation of particulate forms of iron, effectively making it more accessible for microbial uptake even in challenging environments [11–15]. Traditionally, the functional groups responsible for iron binding have been classified into three main categories: hydroxamates, catecholates and hydroxycarboxylates [16]. However, additional siderophore structures have been discovered, such as oxazolin, α-keto acid components, thiazoline, and α- and β-hydroxy acids. Unlike terrestrial siderophores, some marine siderophores, which are still poorly studied, display a peculiar amphiphilic nature, combining a polar peptide group with a hydrophobic fatty acid chain attached to the N-terminus [17–19]. This property allows marine siderophores to self-assemble into supramolecular structures, such as micelles and vesicles, which enhance their ability to capture and transport iron in the marine environment [20]. The structural diversity of siderophores is surprising and reflects the need for microorganisms to adapt to a wide range of

environments. Furthermore, marine siderophores, such as aquachelins, loihichelins, variochelins, imaqobactin and amphibactins, show a peculiar photochemical reactivity due to the presence of functional groups such as β-hydroxyaspartic acid [21–25]. These groups allow the photo-reduction of Fe(III) to Fe(II) and photo-oxidation of the ligand, a process that not only facilitates iron uptake by microorganisms, but also contributes to the overall nutrient dynamics in the oceans by providing a source of iron accessible to other marine organisms, such as phytoplankton [26,27]. An emblematic example of photoreactive siderophores is represented by aquachelins, isolated for the first time by *Halomonas aquamarina* DS40M3, and later by *Halomonas meridiana* HC4321C1 [20]. They are characterised by a unique structure comprising a heptapeptide core attached to N-terminal fatty acid chains ranging from C10 to C14. These molecules have a remarkable ability to bind iron through the coordinated activity of two hydroxamate groups and a β-hydroxy-aspartic acid residue. The fatty acid chains present in aquachelins include both saturated and cis-configured unsaturated variants, highlighting their strong amphiphilicity, facilitating its interaction with biological membranes and aquatic environments [28]. Thanks to their distinctive characteristics and properties, marine siderophores possess considerable potential for biotechnological applications, particularly in their capacity to effectively solubilise iron and interact specifically with marine environments[6]. *Halomonas* species are Gram-negative, non-spore-forming rods widely distributed in saline environments such as salt lakes, marine habitats, and hydrothermal vents [29]. Known for their metabolic and physiological versatility, they thrive in mesophilic temperatures (25–37°C), neutral pH (6.8–7.8), and moderate salinity (2.5–10% NaCl) [30] . This adaptability allows *Halomonas* to exploit diverse resources, making them one of the most abundant genus in marine ecosystems [31,32] . Although many siderophores have been identified in marine bacteria, the number of siderophores that have been fully characterized

is still much smaller compared to those isolated from terrestrial bacteria [18]. This gap is largely due to the complexity of marine ecosystems and the technical challenges associated with isolating and analyzing these compounds. Advances in genomics and bioinformatics have recently unlocked new opportunities for exploring the biosynthetic potential of these compounds, leading to the discovery of novel pathways and mechanisms [22]. Marine siderophores are often synthesised by large multi-modular enzymes known as non-ribosomal peptide synthases (NRPS) [33]. The modular structure of NRPS allows for the production of a wide range of molecules, introducing variations such as epimerisation, methylation or addition of specific functional groups [33] and the introduction of genome mining could guide the discovery of new NRPS, expanding the siderophores potential applications [34,35]. The current study describes the identification and structural characterization of nine novel amphiphilic aquachelin siderophores produced by *Halomonas* sp. P26. The biosynthetic pathway for aquachelins has also been elucidated, shedding light on the molecular mechanisms behind their synthesis. In addition, the antibacterial, biosurfactant and antioxidant properties of the fraction containing the siderophores were evaluated, displaying significant bioactivity. These findings contribute to the growing knowledge of *Halomonas* as a promising source of novel bioactive compounds with potential biotechnological applications.

2. Results and Discussion

2.1. Selection of Halomonas sp. *P26, Cultivation and Fractionation*

As part of efforts to explore marine biotechnology and identify novel bioactive siderophores, about 300 marine bacterial strains from the Stazione Zoologica Anton Dohrn (SZN) collection were screened. A micro-cultivation approach was used to optimise the screening procedure (as described in Chapter 1, section 3.6). Siderophore activity was assessed using the CAS liquid assay in multiwell plates,

targeting compounds present in the bacterial supernatants. Approximately 5% of the strains tested showed a positive result in the CAS assay. Among these, strain *Halomonas* sp. P26 was selected for its strong siderophore activity, indicated by an intense red color in the CAS assay. Halomonas species rive in hypersaline environments, often contaminated with heavy metals, hydrocarbons, and other toxic substances. The selected bacterium was previously isolated from a *Mytilus galloprovincialis* collected in the Bay of Piran (Northern Adriatic sea), that is a highly urbanised and polluted maritime area affected by heavy port traffic, including large quantities of oil, petroleum products and other pollutants [36].

To enhance siderophore production, the strain *Halomonas* sp. P26 was cultivated in 500mL ASG medium containing casamino acids and glucose as nitrogen and carbon sources, respectively, and under iron starvation conditions by supplementing only 1 μM $FeCl_3$ [35,37–39]. After six days of incubation at 28 °C the exhausted broth was extracted by EtOAc. The crude EtOAc extract yielded 216 mg and 16 mg were resuspended in DMSO (50 mg/mL) for bioactivity assay. The CAS liquid assay confirmed the siderophore activity, as indicated by a color change from blue to red/pink.

Furthermore, the crude EtOAc extract was fractionated by solid phase extraction (SPE) using C-18 cartridges, obtaining six fractions (F) as described in Materials and Methods. Each fraction was solubilised in MeOH and DMSO to perform metabolomic analysis and to evaluate the biological activity, respectively.

2.2. Siderophores Detection and Chemical Dereplication by Molecular Networking

To further investigate the bioactive metabolites, functional screening was performed to identify the most active fraction. Siderophore activity was assessed using both liquid and agar CAS assays, which revealed that the F-75% MeOH (F-75) fraction exhibited the highest activity (strongest red/orange color), while the

F-50% MeOH (F-50) and F-100% MeOH (F-100) fractions showed only a weak effect (Figure 1).

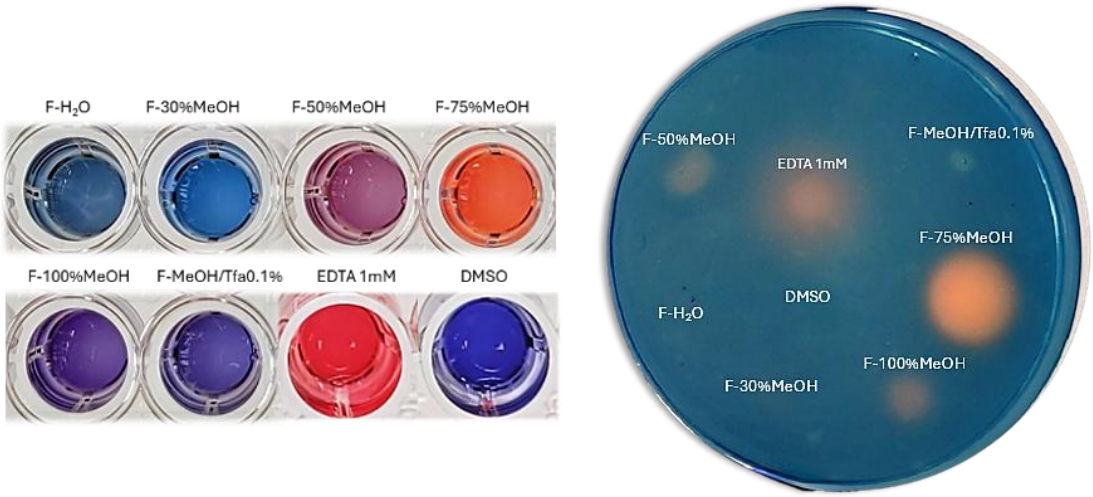

Figure 1. Siderophores activity evaluation of all fractions of *Halomonas* sp. P26 by CAS liquid and agar assay. 4 μL of EDTA 1 mM and DMSO are used as positive and negative controls, respectively.

Based on functional screening results, the F-75 was selected to assess its chemical composition and was analysed by liquid chromatography coupled with untargeted high-resolution tandem mass spectrometry (LC-HRMS^2). Raw LC-HRMS^2 data acquired in positive ion mode were processed by MZmine [40]. The output files were submitted to the Global Natural Products Social Molecular Networking (GNPS2) platform to build a molecular network using the Feature Based Molecular Networking (FBMN) workflow [41], which allows clustering molecules based on MS^2 fragmentation similarity. The metabolites are then visualised using Cytoscape 3.8.2 as nodes connected by edges [42]. The thickness of each edge is related to the similarity of the MS^2 spectra of connected nodes. The molecular networking (MN) unveiled a dominant molecular cluster including the amphiphilic siderophores aquachelins.

The mass fragmentation analysis of aquachelins from *Halomonas* sp. P26 provided insights into their structural diversity revealing the presence of novel analogues (E- F-G-K-L-M-N-O) (Figure 6), along with other known aquachelins (A-J). In detail, MN via GNPS2 identified matches for aquachelins A-J, grouped in a single molecular cluster, connected with a number of unidentified related

compounds (Figure 2). Specifically, aquachelins B, C, and D were found as protonated ions ($[M+H]^+$), while aquachelins A, I, and J appeared as iron adducts ($[M-2H+Fe]^+$). Titanium adducts ($[M-3H+Ti]^+$) of aquachelins A, B, C, and D were also identified in the same molecular cluster, further corroborating the presence of these siderophores.

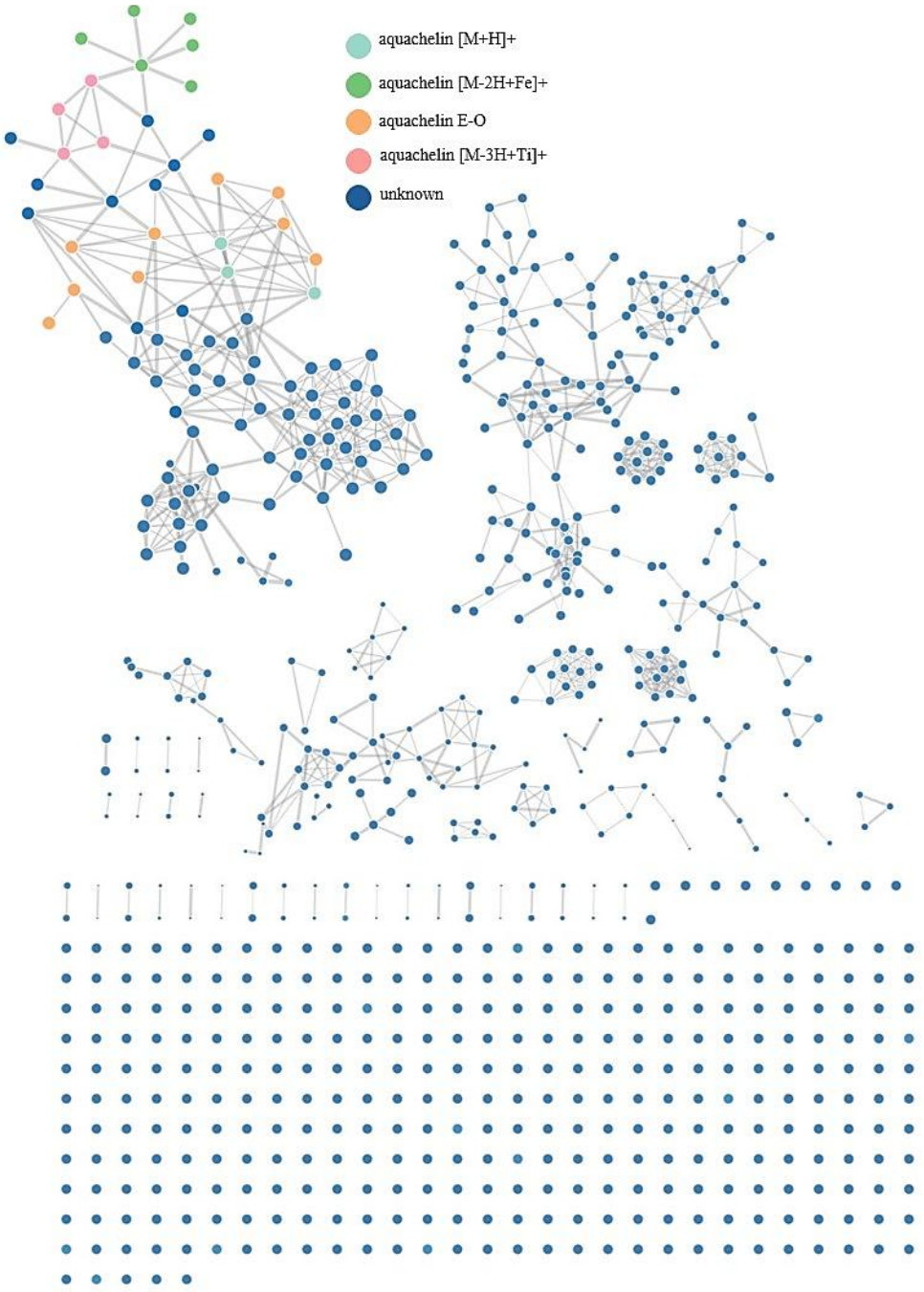

Figure 2. LC-HRMS^2 based molecular networking (MN) of the F-75% MeOH from *Halomonas* sp. P26. Compounds are visualized as nodes and node size reflects compound peak area. Edge thickness is related to MS^2 spectra similarity.

Fragmentation patterns in the MS^2 spectra of known aquachelins A-J showed conserved "y" ions at m/z 191, m/z 278, m/z 450, m/z 578, m/z 665, and m/z 752, supporting the heptapeptide structure (Figure 3) [20]. As reported by Martinez et al., these peptides feature a conserved backbone consisting of N-acetyl-N-hydroxy-D-ornithine, L-serine, D-serine, D-glutamine, and L-*threo*-β-hydroxy-aspartate, with fatty acid chains varying in length (C10-C14) and saturation [20]. The consensus sequence L-*threo*-β-OH-Asp[1]-D-Ser[2]-L-Ser[3]-D-Gln[4]-D-N-Ac-N-OH-Orn[5]-D-ser[6]-L-N-Ac-N-OH-Orn[7] matches the specificity predictions for the aquachelin biosynthetic gene cluster (*aql*) from the genome of strain P26 (see section 2.4.).

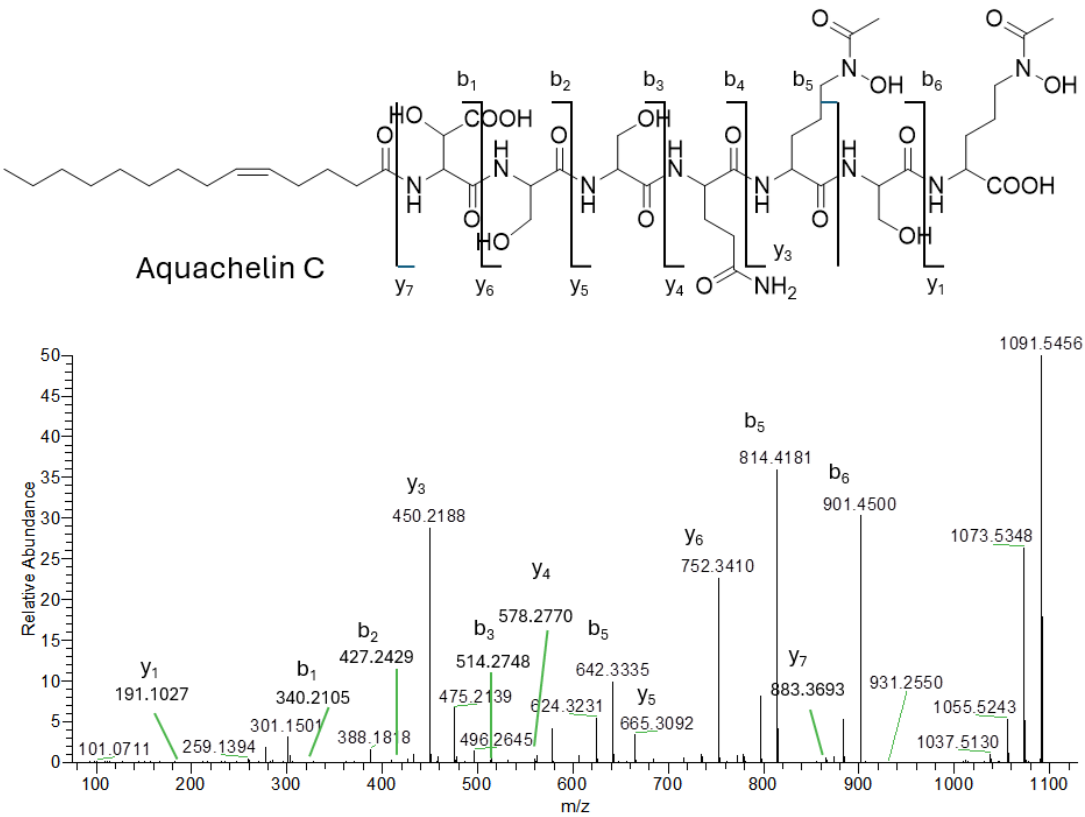

Figure 3. LC-$HRMS^2$ spectrum for aquachelin C from the strain *Halomonas* sp. P26. Vertical lines across the structure show the mass-to-charge ratio values for the y and b fragments obtained via $HRMS^2$. The nomenclature "y" and "b" refer to the charge when retained by the COOH-terminal fragment or the NH_2-terminal fragment of the peptide, respectively [43].

Structural characterization of not-annotated nodes revealed nine novel aquachelin analogues through an in-depth analysis of the fragmentation pattern of the relevant pseudomolecular ions $[M+H]^+$. These congeners exhibited

structural differences due to substitutions in positions 1, 5, and 7 of the peptide backbone and variations in the length and saturation of the fatty acid chain. Sequential N- and C-terminal fragmentation provided three diagnostic ions, enabling unambiguous amino acid sequence assignment (Figure 4, Table1).

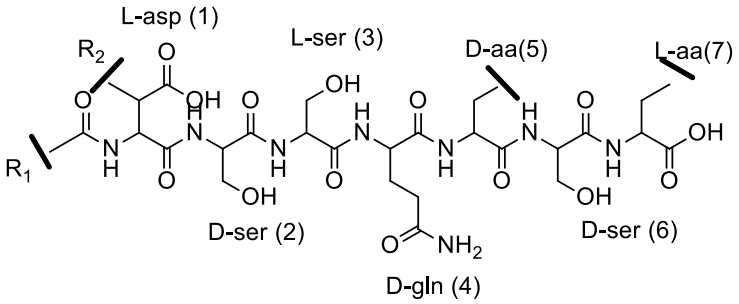

Figure 4. General structure of aquachelins.

Table 1. Structures of aquachelins E-O (1-9) from *Halomonas* sp. P26. Abbreviations: Rt, retention time; FA, fatty acid; aa, amino acid;

Aquachelin	$[M+H]^+$	*m/z*	R_t (min)	R_1 (FA)[a]	R_2	d-aa-5	l-aa-7
aquachelin E (**1**)	$C_{44}H_{75}N_{10}O_{19}$	1047.5210	18.36	$C_{13}H_{22}$ (C14:1)	-OH	N-Ac-N-OH-orn*	Gln
aquachelin F (**2**)	$C_{44}H_{77}N_{10}O_{19}$	1049.5341	17.30	$C_{11}H_{23}$ (C12:0)	-OH	N-Ac-N-orn*	N-OH-N-OAc-orn
aquachelin G (**3**)	$C_{44}H_{77}N_{10}O_{19}$	1049.5341	18.10	$C_{11}H_{23}$ (C12:0)	-H	N-Ac-N-OH-orn	N-OH-N-OAc-orn
aquachelin H (**4**)	$C_{44}H_{77}N_{10}O_{19}$	1049.5341	19.30	$C_{13}H_{27}$ (C14:0)	-OH	N-Ac-N-OH-orn*	Gln
aquachelin K (**5**)	$C_{46}H_{79}N_{10}O_{19}$	1075.5493	18.56	$C_{13}H_{22}$ (C14:1)	-OH	N-Ac-N--orn*	N-OH-N-OAc-orn
aquachelin L (**6**)	$C_{46}H_{79}N_{10}O_{19}$	1075.5493	19.30	$C_{13}H_{22}$ (C14:1)	-H	N-Ac-N-OH-orn*	N-OH-N-OAc-orn
aquachelin M (**7**)	$C_{46}H_{81}N_{10}O_{19}$	1077.5642	19.56	$C_{13}H_{27}$ (C14:0)	-OH	N-Ac-N-orn*	N-OH-N-OAc-orn
aquachelin N (**8**)	$C_{46}H_{81}N_{10}O_{19}$	1077.5642	20.45	$C_{13}H_{27}$ (C14:0)	-H	N-Ac-N-OH-orn*	N-OH-N-OAc-orn
aquachelin O (**9**)	$C_{48}H_{76}N_9O_{19}$	1082.5257	19.30	$C_{13}H_{22}$ (C14:1)	-OH	Tyr	N-OH-N-OAc-orn

*Abbreviations: δ-N-Acetyl-δ-N-hydroxyornithine.

In detail, aquachelins G, L, and N feature a L-aspartate in position 3 rather than the typical L-*threo*-β-hydroxy-aspartate of known aquachelins, identified by the neutral loss of 115.0269 Da. Sharing a conserved peptide backbone which gives a fragment ion at m/z 867.3695, these congeners differ only in the fatty acid chain. Aquachelins F, K, and M lack the OH group on the side chain of N-acetyl-D-

ornithine in position 5, as indicated by the neutral loss of 156.0889 Da (instead of 172.0848) from the b_5 fragment ion. As for aquachelins G, L, and N, the peptide core of aquachelins F, K, and M gives the y_7 fragment ion at m/z 867.3695, with the variability among the latter being located in fatty acid appendages.

The analogues aquachelins E and H replace the terminal L-N-OH-N-Ac-ornithine in position 7 with L-glutamine, as shown by the loss of 146.0691 Da from the relevant pseudomolecular ions, corresponding to glutamine ($C_5H_{10}N_2O_3$). Aquachelin H differs from aquachelins E as bearing a fully saturated C14 fatty acyl chain.

Aquachelin O shows a pseudomolecular ion $[M+H]^+$ at m/z 1082.5229 and features a D-tyrosine in position 5 instead of D-N-OH-N-Ac-ornithine. This substitution was confirmed by the b_5 ion fragmentation, showing the neutral loss of a tyrosine residue (Figure 5). The exact molecular formulas of $[M+H]^+$ ions and retention times of these analogues are detailed in Table 1.

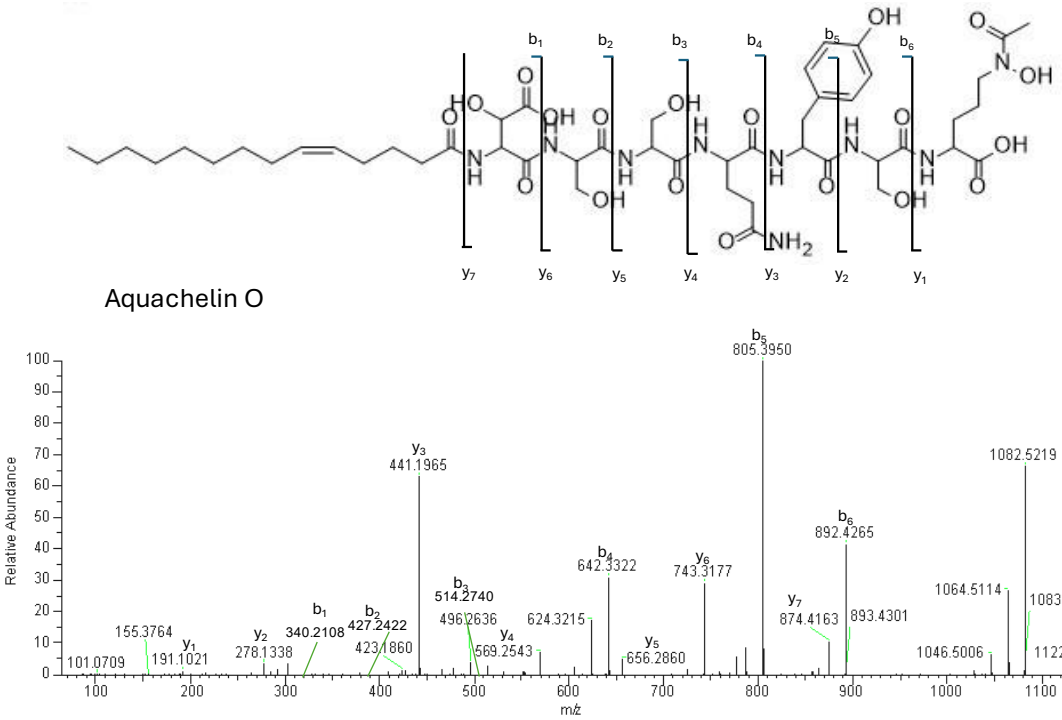

Figure 5. LC-HRMS² spectrum for aquachelin O from the strain *Halomonas* sp. P26. Vertical lines across the structure show the mass-to-charge ratio values for the y and b fragments obtained via HRMS². The nomenclature "y" and "b" refers to the charge when retained by the COOH-terminal fragment or the NH_2-terminal fragment of the peptide, respectively [43].

The aquachelins exhibit a mixture of D- and L-amino acids, with absolute configurations assigned through bioinformatics predictions (Figure 6) These findings highlight the structural diversity of aquachelins, emphasizing their potential for therapeutic applications.

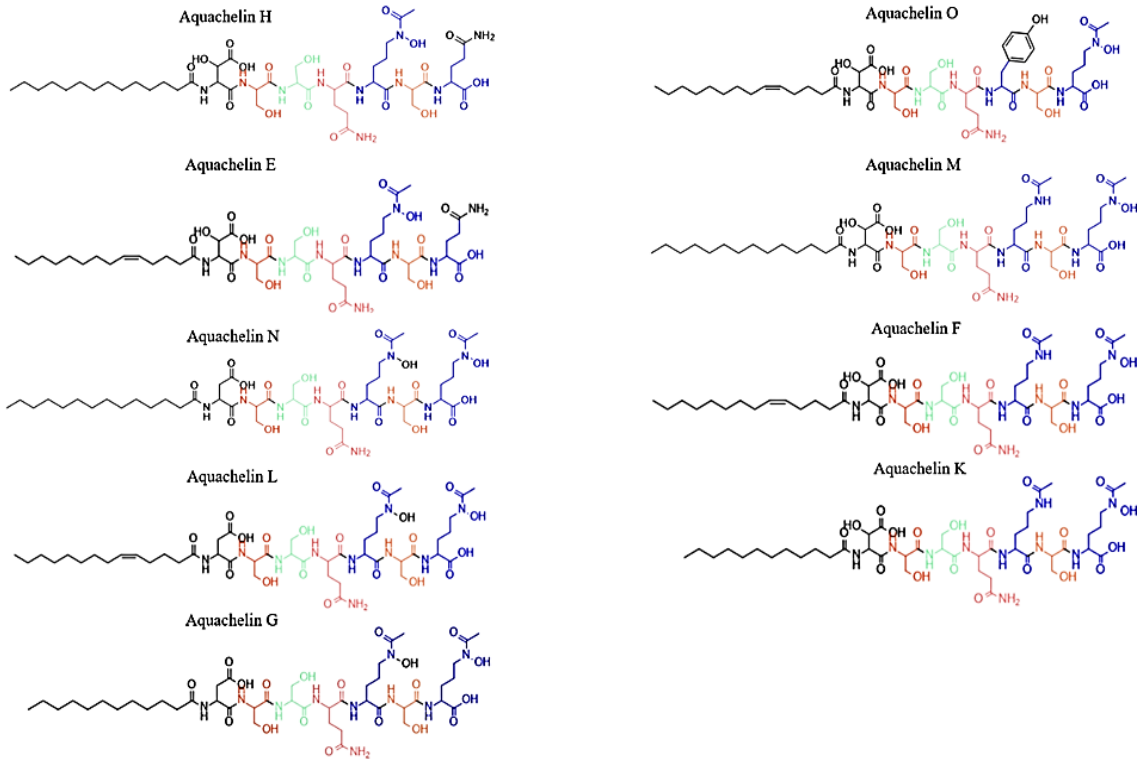

Figure 6. Chemical structures of novel aquachelins E-O from *Halomonas* sp. P26.

2.3. Expanding the Biological Activity of Halomonas sp. *P26*

Based on the F-75% MeOH chemical characterisation and due to the identification of aquachelins, additional assays have been performed to evaluate the biological potential of *Halomonas* sp. P26, including antimicrobial, antioxidant and biosurfactant activity.

2.3.1. Evaluation of the Antimicrobial Activity

The antimicrobial activity of the active fraction (F-75% MeOH), in addition to all the P26 fractions, was evaluated using the microdilution method, determining MIC values for each pathogen. DMSO at an initial concentration of 2% (v/v) was used as a negative control. The results, detailed in Table 2, show

that F-75 exhibits the strongest antibacterial activity demonstrated. This fraction was active against both Gram-negative and Gram-positive pathogens, with the lowest MIC value of 31 μg/mL against *E. coli* and *S. enterica*.

Table 2. Antibacterial activity of all fractions of *Halomonas* sp. P26 towards a panel of Gram-positive and Gram-negative pathogens.

Strain	F-30%MeOH (ug/mL)	F-50%MeOH (ug/mL)	F-75%MeOH (ug/mL)	F-100%MeOH (ug/mL)
S. aureus 6538p	-	-	500	500
E. coli ATCC 10536	-	500	31	500
P. damselae subsp. *Piscicida* ATCC 51736	-	-	500	500
Vibrio anguillarum ATCC 19264	-	-	250	250
Listeria monocytogenes MB 677	-	50	125	-
S. enterica	-	125	31	-

The antimicrobial properties of F-75 could be attributed to aquachelins as, being amphiphilic siderophores, they are known for their dual role in iron chelation and interaction with bacterial membranes. Their structure, characterized by long fatty acid chains, could enables them to disrupt membrane integrity, similar to the action of biosurfactants [44–49]. This mechanism could impair the structural stability of bacterial membranes, leading to cell lysis or disruption of nutrient acquisition pathways. This dual functionality is not unique to aquachelins. Other amphiphilic siderophores, such as loihichelins and marinobactins, have demonstrated antimicrobial properties through similar membrane-targeting mechanisms [20]. Additionally, these compounds may act as competitive tools in marine ecosystems, limiting iron availability to other microbes and indirectly inhibiting their growth [19].

In addition, the use of siderophores as carriers for antimicrobials, known as "sideromycins", highlights their potential to combat bacterial resistance. These 'Trojan Horse' strategies involve conjugating a bactericidal head to a siderophore, using the bacterial iron uptake system to facilitate the targeted delivery and uptake of the antibiotic [28,50,51]. This approach has been applied to synthetic

constructs, improving therapeutic efficiency against multi-drug-resistant Gram-negative pathogens. Examples of siderophore-antibiotic conjugates, such as those involving catecholate or hydroxamate groups, have shown promising results in preclinical studies [52].

Natural sideromycins, such as grisein from *Streptomyces griseus*, serve as foundational examples for this strategy [53]. Among the five known families of natural sideromycins, three (albomycins, ferrimycins, and salmycins) use hydroxamate-based iron-chelating fractions [54]. Albomycins, the most studied, are particularly effective against organisms expressing the FhuA receptor in their outer membranes, showcasing their ability to bypass microbial cell wall permeability barriers [19]. Similarly, aquachelins, could serve as effective hydroxamate-based sideromycins, offering targeted antimicrobial effects against resistant bacteria.

2.3.2. Evaluation of the Biosurfactant Activity

In addition, all the fractions were also tested for biosurfactant activity. Once again, the F-75 fraction displayed the best activity, as shown in Figure 7, which can therefore be attributed to the aquachelines.

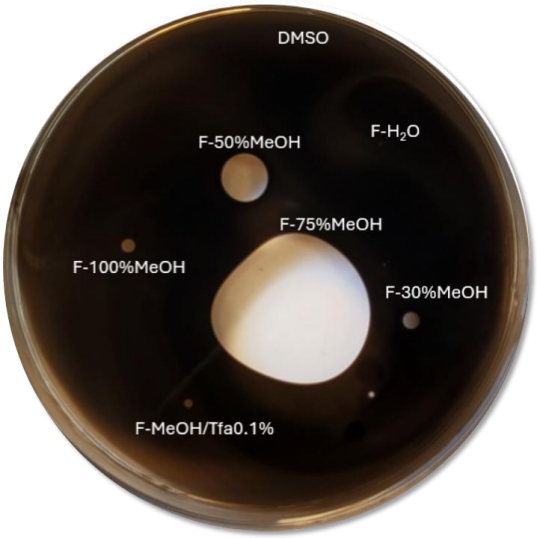

Figure 7. Biosurfactants activity evaluation of all fractions of *Halomonas* sp. P26 using oil spreading test. 4 µL of DMSO are used as negative controls.

The strong biosurfactant activity observed can be attributed to the amphiphilic nature of aquachelines. These compounds, with a hydrophilic head and a shorter hydrophobic tail compared to other marine siderophores like amphibactins, exhibit surfactant-like behavior, reducing surface tension and facilitating the solubilization of hydrocarbons [20]. Similar to amphibactins found in oil spill regions such as the Deepwater Horizon disaster, aquachelins leverage their amphiphilic properties to help bacteria thrive in challenging environments by enhancing both iron acquisition and hydrocarbon degradation [55]. The dual function of these siderophores, acting as both iron chelators and surfactants, likely offers significant adaptive advantages, especially in oil-rich environments where they can increase the solubility of nutrients and provide protection against environmental stresses. Unlike other siderophores that associate with bacterial membranes, aquachelins are secreted into the extracellular environment, making them particularly effective in oil-contaminated sites [56]. This characteristic could enhance their role in bioremediation facilitating the degradation of hydrocarbons.

2.3.3. Evaluation of the Antioxidant Activity

The antioxidant activity of P26 fractions was evaluated using the DPPH assay, one of the most rapid and reliable methods for determining the radical-scavenging capacity of bioactive compounds. Results showed that among the six fractions analyzed, F-30 and F-75 displayed significant antioxidant effect, exceeding 50% of activity, with fraction F-75 reaching 68% activity at a concentration of 0,31 mg/mL (Figure 8). While all fractions demonstrated some level of antioxidant activity, further chemical analyses are required to identify the compounds responsible for this effect.

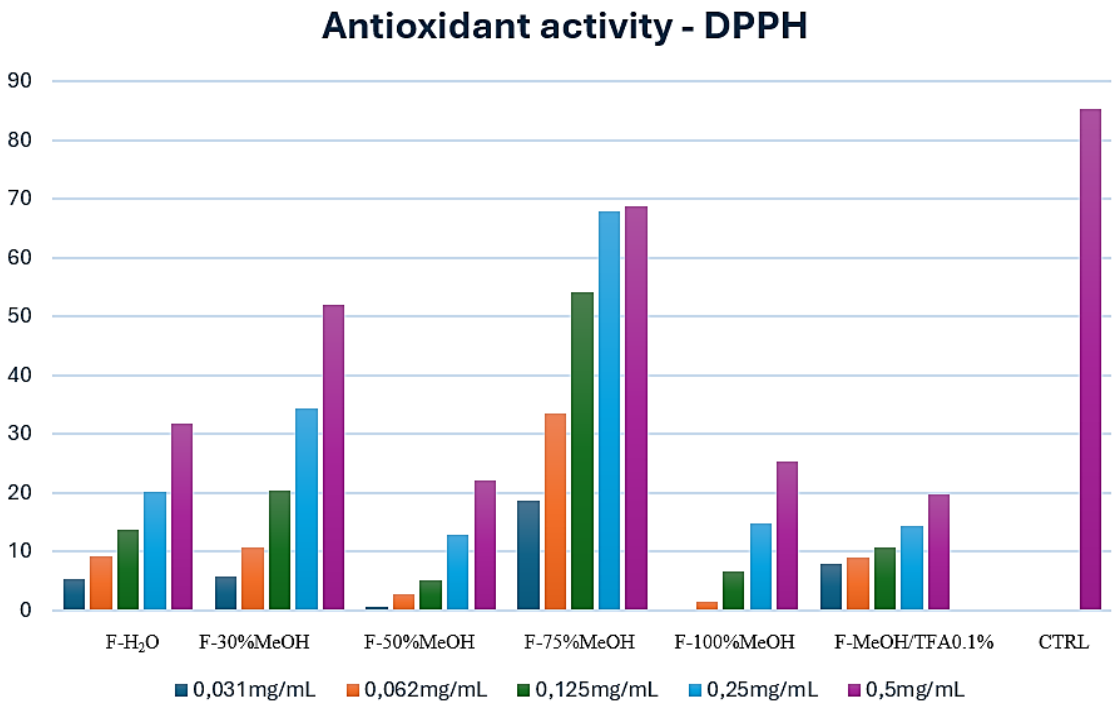

Figure 8. Antioxidant activity evaluation of all fractions of *Halomonas* sp. P26 using DPPH assay. 8 µL of ascorbic acid (at 25 mg/mL) is used as positive control.

Species of *Halomonas*, known for their metabolic versatility and adaptability to extreme environmental conditions, represent a promising source of bioactive compounds, including molecules with antioxidant properties. Some species, characterized by the production of orange pigments, have been shown to have a high polyphenol content and significant antioxidant activity, as demonstrated by numerous biological and chemical analyses [40–42]. A plausible hypothesis is that the high antioxidant activity observed in the F-75% MeOH fraction may be influenced by the presence of aquachelins, which are known for their potential in reducing reactive oxygen species (ROS) [43]. Previous studies suggest that siderophores not only facilitate iron acquisition but also perform "non-classical" functions, such as ROS detoxification [44]. For example, catechol-type siderophores produced by bacteria such as *Pseudomonas aeruginosa*, *Salmonella*, and *Escherichia coli* have demonstrated ROS scavenging capabilities, protecting bacteria from oxidative stress and promoting bacterial cooperation in adverse environmental conditions [45,46]. These findings suggest that siderophores

produced by *Halomonas* may contribute to the observed antioxidant activity of the fractions, particularly in extreme environments such as endolithic or saline soils.

2.4. Genome Mining and Elucidation of Aquachelin BGC

To explore the biosynthetic potential of the halophilic strain and identify the biosynthetic gene cluster (BGC) responsible for producing the identified siderophores, the P26 whole-genome was sequenced. Genomic DNA was extracted from a single colony grown on a Marine Agar plate. The de novo whole genome assembly was further refined and optimized with the Medusa scaffolding software obtaining 64 contigs, with a total length of 3,418,53 bp and a G+C content of 56,81%. This value falls within the G+C content range reported for species of this genus, which varies from 52% to 74.3 mol% [47]. In addition, annotation of the genome using PATRIC [48] identified 3277 coding sequences and an N50 value of 152.201 bp., The phylogenetic identity and species affiliation of the strain *Halomonas* sp. P26 was established by using a genome-based identity approach. This included orthologous average nucleotide identity (OrthoANI) using the EZBioCloud algorithm [49] and digital DNA-DNA hybridization (dDDH) analysis via the Type (Strain) Genome Server [50]. The results demonstrated that *Halomonas* sp. P26 clustered closely with other *Halomonas* species such as *Halomonas axialensis* DSM 15723, *Halomonas meridiana* ACAM 246, *Halomonas aquamarina* 558, exceeding the species affiliation cut-off values of 96.1, 70.0, 73.6, respectively. In agreement with this analysis, the highest ANI value (97,7%) corresponds to *Halomonas axialensis (Vreelandella aquamarine* DS40M3, GenBank GCA_028580285.1), a halophilic bacterial species found in deep-sea environments [51]. Subsequently the genome analysis was performed using the software antiSMASH 7.1.0, to predict and annotate the BGCs that encode for secondary metabolites. As a result, a total 4 putative BGCs have been identified,

including an NRP-Methallophore gene cluster, identified in the region 8.1, which showed 39% similarity with Potashchelin (BGC0002117 from *Halomonas* sp. MG34) a lipid siderophore [52]. The collinearity rule in the biosynthesis of modular NRPS made possible to infer *in silico* the functions of the catalytic domains, confirming the correspondence of this NRPS with the chemical structure of aquachelines [53] (Table 3).

Table 3. Binding pocket signatures of adenylation domains from the Aql synthetase.

antiSMASH Prediction		**Binding pocket signatures (position)[a]**									
		235	236	239	278	299	301	322	330	331	517
Aql_C1	Asp	D	L	T	K	I	G	H	V	G	K
Aql_D1	Ser	D	V	W	H	V	S	L	I	D	K
Aql_D2	Ser	D	V	W	H	V	S	L	I	D	K
Aql_E1	Unknown	D	A	E	Y	I	G	A	I	S	K
Aql_E2	Unknown	D	V	W	N	M	G	L	I	H	K
Aql_E3	Ser	D	V	W	H	V	S	L	I	D	K
Aql_E4	Unknown	D	V	W	N	M	G	L	I	H	K

[a] as reported by Della Sala et al. 2020 [70].

Although the first aquachelin molecule was identified in 2000 [20], its biosynthetic pathway has not yet been elucidated. The BGC responsible for aquachelin synthesis consists of five modular NRPS enzymes, designated *aql*A, *aql*B, *aql*C, *aql*D and *aql*E, which operate in an end-extension model. The specificity of the adenylation (A) domains in each module is directly aligned with the sequence of the heptapeptide backbone of the identified aquachelin compounds (see Table 3 for details). Each NRPS module consists of three main domains: the adenylation domain (A), the PCP (peptidyl transporter protein) domain and the condensation domain (C). These domains work together to ensure the precise synthesis of siderophores, as illustrated in (Figure 9). The predicted *aql* NRPS has a length of 50,353 bp, located on the contig 8, and organised into eight modules, one for process initiation and seven for peptide extension and termination. The consensus sequence L-*threo*-β-OH-Asp^{1}-D-Ser^{2}-L-Ser^{3}-D-Gln^{4}-D-N-Ac-N-OH-Orn^{5}-D-Ser^{6}-L-N-Ac-N-OH-Orn^{7}, obtained from

the structural characterisation of aquachelins A, B, C and D by MS analysis, is strongly associated with the *in silico* prediction of substrate selectivity of the A domain. The domain arrangement in the *aql* operon loading module was also found in the BGCs of other siderophores such as variochelin, taiwachelin and potashchelin, suggesting a common biosynthetic mechanism between these molecules [54,52,55]. A distinctive feature of this BCG is the presence of two core biosynthetic genes, *aqlA* and *aqlB*, which contain the TauD (hydroxylase) and CAL domain, respectively. The TauD domain is also involved in the removal of methyl groups, which contributes to modifying the final structure of the peptide and enhances its affinity for metals. This modification is crucial for the function of siderophores, which play a key role in metal binding and transport. Whereas the CAL (CoA-ligase) domain is crucial for the aquachelin acetylation, usually catalyzed by the initial condensation domain (Cs) [56]. To be included in biosynthesis, fatty acids must first be activated in the form of coenzyme A or transported by acyl-carrier proteins. In this context, the orf6 and orf7 protein, a 4'-phosphopanthenyl transferase [57] and a thioesterase, may be involved in the formation of the fatty acid moiety. In addition, orf8 (MbtH-like) appears to play a role in the activation and optimisation of the NRPS biosynthetic complex. MbtH-like proteins (MLPs) are essential for the proper functioning of the adenylation (A) domains of non-ribosomal peptide synthetases [58]. For example, in the biosynthesis of taxtomine A in *Streptomyces scabiei*, the TxtH protein, an MLP, acts as a chaperone, promoting the correct folding of the NRPS TxtA and TxtB. Although the mechanism of action of MLPs is not fully understood, they are critical for the soluble expression and optimal activity of many NRPS enzymes and may interact with several biosynthetic pathways [59]. In addition, the analysis of NCBI BlastP of orf9, situated downstream of the NRPS gene, revealed that the gene encodes for a transport-related protein identified as FhuD, a periplasmic binding protein for iron (III)-hydroxamate siderophore,

either linear and nonlinear. Furthermore, the protein encodes by the orf1 gene, belonging to the ABC (Multidrug Resistance ATP-binding Cassette) family of transporters, which translocate molecules by coupling the flow of drugs or lipids to the energy generated by ATP hydrolysis [60]. This suggests that this gene may be involved in the transport of the aquachelin-Fe complex within bacterial cells [61]. Once the Fe(III)-siderophore complex crosses the outer membrane, the ABC transporter transfers it into the cytoplasm, where the iron is reduced to Fe(II) and absorbed by the cell [62]. This NRPS cluster could also be exploited as a 'Trojan horse' to combat difficult-to-treat resistant pathogens [63]. In this case, the design of the linker is crucial to ensure full antibacterial efficacy [64]. However, the genes necessary for the synthesis of an acetyltransferase and an N-monooxygenase, enzymes involved in the biosynthesis of the amino acid precursor N(δ)-OH-orn, seem to be absent [65]. The index of the condensation C domain is crucial for the stereospecificity of amino acid binding to the peptide. This domain possesses Dual-function Epimerization/Condensation (E/C) domains possess both epimerization activity and DCL condensation functionality. These domains first convert the substrate amino acid to its D-configuration through epimerization, and subsequently catalyze the condensation reaction between the D-aminoacyl/peptidyl-PCP donor and an L-aminoacyl-PCP acceptor. There are four dual C domains, in modules 3, 5, 6, and 7. This suggests that the amino acids aa-2, aa-4, aa-5, and aa-6 in the N-acetyl-eptapeptides of the aquachelins family have a D configuration, in accordance with the structural elucidation by $HRMS^2$ spectra analysis. Finally, Module 7 presents a thioesterase (TE) domain, which plays a key role in cleaving the final product from the polypeptide chain, allowing the release of the synthesised siderophore.

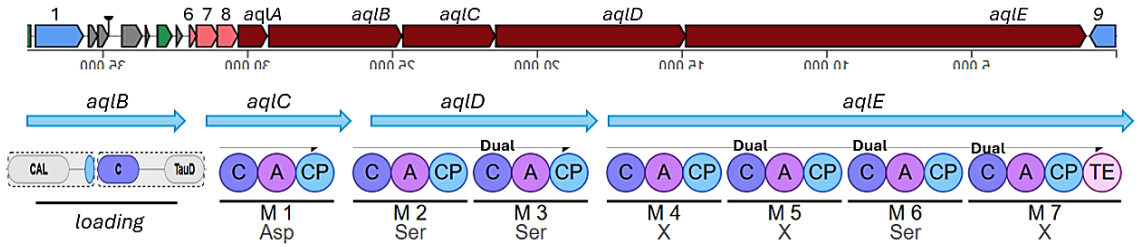

Figure 9. Putative biosynthesis of aquachelins. Abbreviations: C, condensation domain; A, adenylation domain; PCP, peptidyl-carrier protein; E, epimerase; Cs, starter condensation domain; TE, thioesterase.

3. Materials and Methods

3.1. Bacterial Isolation and Screening

The strain *Halomonas* sp. P26 was isolated, along with other 150 bacteria, from a mussel *Mytilus galloprovincialis* collected at 200 mt off the coast of the Bay of Piran, Slovenia, at the northern extremity of the Adriatic Sea [66]. The isolation was conducted by serial dilutions using LB agar plates. The strain was identified as the genus *Halomonas* via 16S rRNA genes amplification and subsequent phylogenetic analysis. PCR was carried out in a total volume of 40 µL containing 25 µL of PCR Master Mix 2× ExtraWhiteTaq (a ready-to-use solution containing TaqPol, buffer, MgCl2 and dNTPs), 0.2 µM of both primers 27F (Forward, seq: 5′-AGAGTTTGATCCTGGCTCAG-3′) and 1492R (Reverse, seq 5′-GGTTACCTTGTTACGACTT-3′) [67]. The reaction conditions used were: 1 cycle (95 °C for 5 min), 30 cycles (95 °C for 30 s, 58 °C for 30 s, and 72 °C for 1.30 min), with a final extension of 7 min at 72 °C. Afterwards PCR products were evaluated on 1% agarose gel and then purified with the GeneAll kit and sequenced by Eurofins Genomics. Finally, the phylogenetical affiliation was assigned by using the EzBioCloud (http://ezbiocloud.net) for the phylogenetic affiliation.

In order to identify the most promising strains for the production of bioactive molecules, the isolated halophilic bacteria were screened.

The cultivation was conducted in 96-deepwell plates (Thermo Scientific™ 278743), varying growth conditions (medium composition, incubation period between 3 and 10 days, temperature range of 10 to 37°C) to optimise production

and confirm the presence of the desired compounds (as described in Chapter 1, section 3.6). Subsequently, centrifugation was performed to recover the supernatant, which was then subjected to biological activity tests. In particular, 10 μL of supernatant was used for each siderophore detection assay, performed by the CAS method on agar and in liquid.

3.2. Bacterial Cultivation and Fractionation

For siderophore isolation, the strain *Halomonas* P26 was inoculated into 3 mL ASG (medium composition (ASG-Fe) containing 1L of doubly deionized water (Barnstead Nanopure II), 1.0 g of NH_4Cl, 10 g of casamino-acids, 1.0 g of glycerophosphate, 12.4 g of $MgSO_4 \cdot 7H_2O$, 3 g of $CaCl_2 \cdot 2H_2O$, 17.5g of NaCl, 0.75 g of KCl, and 3 mL of glycerol. After autoclave sterilization, 10 mL of filter-sterilized 1.0 M HEPES buffer (pH 7.4), 2 mL of filter-sterilized 1.0 M $NaHCO_3$, and 10 mL of filter-sterilized BME vitamins 100x solution-Sigma-Aldrich) in sterile tubes. After 48 hours of incubation at 20°C with shaking at 200 rpm, the pre-inoculum was transferred into 4x500mL flask each containing 125 mL of ASG supplemented with 1 μM di $FeCl_3$, with an initial cell concentration of 0.01 OD600/mL, and incubated at 28 °C on a rotary shaker (180 rpm). The glassware was deferrated with Chelex (Sigma Aldrich) resin and also was washed with acid (HCl 6M), to remove all traces of iron, because iron-starved media promotes maximum siderophore production. Siderophore detection (CAS liquid assay) were done once a day, taking 100 μL of supernatant from the growths to check the production of the molecules of interest. Then after 6 days, the cultures were harvested by centrifugation at 7,500 rpm for 30 minutes at 4°C and the supernatant was extracted with two volumes of ethyl acetate (EtOAc). The organic phases were collected, concentrated using a rotary vacuum evaporation (Buchi R-100, Büchi Labortechnik AG, Switzerland) and united to provide a

single sample of crude extract. Finally, the extract was dissolved in DMSO at 50 mg/mL and stored at 4°C for future characterization and bioactivity tests.

The concentrated EtOAc extract (216 mg) was further fractionated using the solid phase extraction (SPE) through a reverse phase Chromabond C-18 column (45 μm, 45 mL/5000 mg -Macherey-Nagel GmbH & Co. KG, Düren, Germany), yielding 6 fractions. In practice, the extract was resuspended in the lowest volume of methanol (MeOH) and loaded onto the pre-activated SPE column. The elution was performed with three column volumes of increasing gradient elution of MeOH/H_2O, used in this order: 1) 100% H_2O (10 mg), 2) 30% MeOH/H_2O (v/v) (22 mg), 3) 50% MeOH/H_2O (v/v) (27 mg), 4) 75% MeOH (v/v) (101,5 mg), 5) 100% MeOH (v/v) (7.6 mg) and 6) MeOH+0,1%TFA (trifluoroacetic acid) (5 mg) respectively. Finally, all the obtained fractions were collected, dried, dissolved in DMSO at 50 mg/mL and stored at 4°C for bioactivity tests (CAS assay, antimicrobial and antioxidant activity) and for future characterization.

3.3. LC-HRMS² Analysis of the 75% MeOH Fraction

The most active fraction for siderophore effect (F-75% MeOH fraction), was solubilised in MeOH at a concentration of 1 mg/mL and analysed by LC-HRMS². Chemical profiling was carried out using a Thermo LTQ Orbitrap XL high-resolution electrospray ionisation mass spectrometer in conjunction with a Thermo U3000 high-performance liquid chromatography system and a Kinetex C18 column (5 μm, 50 × 2.10 mm). The column was maintained at 25 °C with a flow rate of 400 μL/min, eluting with a gradient of H_2O and ACN, with 0.1% HCOOH: initially 10% ACN for 1 minute, then 10 –100% ACN over 40 minutes, and finally 10 min reconditioning of the column with 100% CAN. Mass spectra were acquired in positive ion mode with an accuracy of ≤ 3 ppm. The MS settings included a spray voltage of 4.8 kV, a capillary temperature of 285 °C, a sheath gas flow rate of 32 units of N_2 (~150 mL/min), and an auxiliary gas flow rate of 15

units of N_2 (~50 mL/min). MS^2 data were obtained through data-dependent acquisition, with the five most intense ions in each full-scan mass spectrum within an m/z range of 50–2000 Dalton selected for analysis. The $HRMS^2$ analysis was conducted using CID fragmentation with an isolation width of 2 m/z, a normalized collision energy of 35, an activation Q of 0.250, and an activation time of 30 ms. The relative areas of in-source fragments were quantified using the Thermo Xcalibur Software (version 2.2, Thermo Fisher Scientific, Waltham, MA, USA).

3.4. Feature-Based Molecular Networking

The metabolome was studied by analyzing the raw files from LC-$HRMS^2$ analysis of the F-75% MeOH fraction were converted to mzXML format, processed by MZmine 2.53 [40] to remove noise, filter isotopes and align the data. Then, the output files were uploaded to Global Natural Products Social Molecular Networking (GNPS2) (https://gnps2.org accessed on 27/11/2024) and used to build a feature-based molecular network (FBMN) [41]. For FBMN analysis, the precursor ion mass tolerance was set to 0.02 Da, and the MS2 fragment ion tolerance was set to 0.05 Da. After, a MN was constructed, setting to 100 the maximum number of nodes in one cluster, with edges filtered to have a cosine score above 0.7 with a minimum of four matching peaks. The search of analogues was not exceeding the difference of 300 Da between the query and the hit; the analogues had to follow the same clustering rules as mentioned above. Finally, the data was exported, and the network was visualized by the Cytoscape software v. 3.8.2 and can be publy accessed at https://cytoscape.gnps2.org/process?override_path=nf_output%2Fnetworking%2Fnetwork_singletons.graphml&task=68fcb3d0f4e94389a17dd2ada8c228fb [42].

3.5. Bioactivity Evaluation of All Fraction from Halomonas sp. *P26*

A series of functional assays were conducted to evaluate the bioactivity of the crude and fractionated extracts.

3.5.1. Siderophores Assays - CAS Liquid and Agar Assays

The chrome azurol S (CAS) universal assay is a colorimetric method, created by Schwyn and Neilands[68]. The CAS/HDTMA solution was prepared by dissolving chrome azurol sulfonate (60 mg) in 50 mL of H_2O, followed by the addition of 10 mL of 2,7 mg $FeCl_3$ in 10 mM HCl to form Solution I. In parallel, HDTMA (73 mg) was dissolved in 40 mL of H_2O to create Solution II. Solution I was gradually mixed into Solution II with gentle stirring to prevent foam formation. Solution I was then gradually mixed with Solution II while stirring to prevent foam formation. The resulting mixture was sterilized by autoclaving at 121 °C for 20 minutes and subsequently cooled in a water bath. The CAS liquid assay was conducted in 96 multi-well plates, using a CAS solution diluted 1:4 with distilled water. Each well is filled with 100 μL of CAS solution and 100 μL of supernatant, or alternatively, 192 μL of CAS and 8 μL of extract. EDTA 1mM was used as positive control. For the CAS agar assay, an agar solution (500 mL, 17 g/L) was prepared, autoclaved and then cooled in a water bath at 60 °C. The previously prepared CAS/HDTMA solution was combined with the agar solution, and the plates were poured under a laminar flow hood and allowed to solidify. The agar plates were double-checked for siderophore production. A drop of 4 μL of extract, dissolved in DMSO at 50 mg/mL were spotted on the CAS agar plates. As a negative control, 8 μL of pure DMSO were used, while 4 μL of EDTA 1mM were used as positive control. After 2 days at 4 °C, the extracts containing siderophores were detected by the presence of a clear zone around the sample.

3.5.2. Minimal Inhibitory Concentration Assay (MIC)

To evaluate the antimicrobial potential of all extracts, the MICs for *ATCC® 6538™*, *S. aureus* ATCC® 6538p™, *E. coli* ATCC 10536, *Pseudomonas aeruginosa PA01*, *Photobacterium damselae* subsp. *piscicida* ATCC® 51736™, *Vibrio anguillarum* ATCC® 19264™ , *Salmonella enterica* subsp. *enterica Serovar Sloterdijk (ATCC 15791)* and *Listeria monocytogenes* MB677 were determined by the broth microdilution method [69]. Briefly, the bacterial strain was inoculated in 3 mL of liquid Mueller-Hinton broth (MHB) (HiMedia, Einhausen, Germany) and TSB medium, for *Lysteria*, in sterile bacteriological tube, and incubated in agitation at 37 °C until they reached the turbidity of 0.5 McFarland. Differently, for the fish pathogen strains was used Marine Broth (MB) (Condalab, Spain) as medium. Finally, serial dilutions of the inoculum were performed to obtain a final bacterial concentration of about 5 × 105 CFU/mL. Then, 4 μL of each sample was added into a 96-well microtiter plate containing 200 μL of MH medium. After serially diluted using MH medium, 100 μL of bacterial suspension was inoculated into the broth (~5 × 104 CFU/well) and each plate was incubated statically for 18h at 37 °C to allow optimal bacterial growth. DMSO was used as negative. The MIC was identified as the lowest concentration that completely inhibited growth of the pathogens, and was measured with a by ELX800 Absorbance Microplate Reader (Biotek, Winoosky, VT, USA) by monitoring the absorbance at 600 nm.

3.5.3. Biosurfactants assay - Oil spreading test

The oil spreading assay, also known as the oil displacement test, was conducted using polystyrene Petri dishes (100 mm x 15 mm) [70]. In this method, 40 μl of crude oil was gently applied to the surface of 30 mL of distilled water to create a thin oil layer. Then, a drop of 10 μL of filtered supernatant and 1 μL of extracts were carefully pipetted on the centre of the oil layer. The size of the clear zone on the oil surface is directly related to the surfactant activity, due to the presence of the biosurfactant displacing the oil.

3.5.4. Antioxidant assays-DPPH Radical Scavenging Activity Assay

The antioxidant activity of the fractions obtained from *Halomonas* sp. P26 was evaluated using 2,2-diphenyl-1-picrylhydrazyl (DPPH) to assess free radical scavenging capacity [71]. Briefly, 4 μL of each sample (at a concentration of 50 mg/mL) was added into a 96-multiwell plate containing 196 μL of DPPH (0.002% in MeOH) solution. After serially diluted using MeOH (100%), 100 μL of DPPH solution was added. After 30 minutes of incubation in the dark at room temperature, the optical density (OD) was measured at 517 nm. The absorbance of the control (DPPH without the sample) was also measured, and all readings were performed in triplicate. Ascorbic acid at 25 mg/mL was used as positive control. The scavenging activity was expressed using Equation:
Scavenging activity (%) = [(Acontrol − Asample)/Acontrol] × 100; where A control is the absorbance of the DPPH solution; A sample is the absorbance of the sample mixed with DPPH.

3.5.5. Genomic DNA Sequencing, Assembly and Bioinformatics Analysis

A total of 1 μg of genomic DNA was used for the whole genome sequencing of Halomonas sp. P26 performed by Eurofins Genomics (Ebersberg, Germany) using the Illumina NovaSeq 6000 platform. All sequenced paired-ends reads were clipped and trimmed with Trimmomatic tool [7] to remove adaptor and low quality sequences, and a quality check was obtained with FastQC [8]. The de novo assembly was performed with PATRIC, which various k-mer analyses using the bioinformatic tool "Unicycler" and then and employing the genome *Vreelandella aquamarine* DS40M3 (GCA_028580285.1) as a reference to direct the scaffold and alignment of contigs through MEDUSA scaffolder algorithm [48,72]. The assembled genome identification was carried out using ANI Calculator by EzBioCloud [49] and the digital DNA:DNA hybridization (dDDH) analysis by Type (strain) Genome Server (https://tygs.dsmz.de) [50]. Subsequently the

assembly was analyzed using the genome mining tool anti-SMASH 7.0 [73] web server (http://antismash.secondarymetabolites.org, leading to the identification of BGCs.

4. Conclusions

The findings of this study have unveiled the immense biotechnological potential of *Halomonas* sp. P26, as a source of novel amphiphilic aquachelin siderophores with broad applications. The identification and structural characterization of nine new aquachelin analogues emphasize their critical role in addressing pressing challenges such as antimicrobial resistance and oxidative stress. Acting as both iron chelators and bioactive agents, these compounds present significant opportunities for advancements in biotechnology and pharmacology.

Moreover, this study underscores the importance of integrating advanced metabolomic approaches, functional assays, and genomic analyses to uncover the biosynthetic capabilities of marine bacteria. The elucidation of the aquachelin biosynthetic pathway via genome mining offers valuable insights into the molecular mechanisms governing their synthesis and paves the way for further exploration of their therapeutic potential. These findings contribute substantially to the growing knowledge of marine-derived bioactive compounds, highlighting their potential in addressing global health and environmental challenges. By expanding our understanding of marine natural products, this research also sets the stage for their future application in sustainable biotechnological solutions.

References

1. Raven, J.A.; Evans, M.C.W.; Korb, R.E. The Role of Trace Metals in Photosynthetic Electron Transport in O2-Evolving Organisms. *Photosynthesis Research* **1999**, *60*, 111–150, doi:10.1023/A:1006282714942.
2. Liu, X.; Millero, F.J. The Solubility of Iron in Seawater. *Marine Chemistry* **2002**, *77*, 43–54, doi:10.1016/S0304-4203(01)00074-3.
3. Boyd, P.W.; Ellwood, M.J. The Biogeochemical Cycle of Iron in the Ocean. *Nature Geosci* **2010**, *3*, 675–682, doi:10.1038/ngeo964.
4. Gledhill, M.; Buck, K.N. The Organic Complexation of Iron in the Marine Environment: A Review. *Front. Microbiol.* **2012**, *3*, doi:10.3389/fmicb.2012.00069.
5. Ahmed, E.; Holmström, S.J.M. Siderophores in Environmental Research: Roles and Applications. *Microbial Biotechnology* **2014**, *7*, 196–208, doi:10.1111/1751-7915.12117.
6. Butler, A. Marine Microbial Siderophores: Reactivity and Structural Diversity. *The chemist* **2022**.
7. Amin, S.A.; Green, D.H.; Küpper, F.C.; Carrano, C.J. Vibrioferrin, an Unusual Marine Siderophore: Iron Binding, Photochemistry, and Biological Implications. *Inorg. Chem.* **2009**, *48*, 11451–11458, doi:10.1021/ic9016883.
8. Cornelis, P. Iron Uptake and Metabolism in Pseudomonads. *Appl Microbiol Biotechnol* **2010**, *86*, 1637–1645, doi:10.1007/s00253-010-2550-2.
9. Braun, V.; Killmann, H. Bacterial Solutions to the Iron-Supply Problem. *Trends in Biochemical Sciences* **1999**, *24*, 104–109, doi:10.1016/S0968-0004(99)01359-6.
10. Manck, L.E.; Park, J.; Tully, B.J.; Poire, A.M.; Bundy, R.M.; Dupont, C.L.; Barbeau, K.A. Petrobactin, a Siderophore Produced by Alteromonas, Mediates Community Iron Acquisition in the Global Ocean. *The ISME Journal* **2022**, *16*, 358–369, doi:10.1038/s41396-021-01065-y.
11. Neilands, J.B. Siderophores. *Archives of Biochemistry and Biophysics* **1993**, *302*, 1–3, doi:10.1006/abbi.1993.1172.
12. Yoshida, T.; Hayashi, K.; Ohmoto, H. Dissolution of Iron Hydroxides by Marine Bacterial Siderophore. *Chemical Geology* **2002**, *184*, 1–9, doi:10.1016/S0009-2541(01)00297-2.
13. Borer, P.M.; Sulzberger, B.; Reichard, P.; Kraemer, S.M. Effect of Siderophores on the Light-Induced Dissolution of Colloidal Iron(III) (Hydr)Oxides. *Marine Chemistry* **2005**, *93*, 179–193, doi:10.1016/j.marchem.2004.08.006.
14. Leventhal, G.E.; Ackermann, M.; Schiessl, K.T. Why Microbes Secrete Molecules to Modify Their Environment: The Case of Iron-Chelating Siderophores. *Journal of The Royal Society Interface* **2019**, *16*, 20180674, doi:10.1098/rsif.2018.0674.
15. Hofmann, M.; Heine, T.; Malik, L.; Hofmann, S.; Joffroy, K.; Senges, C.H.R.; Bandow, J.E.; Tischler, D. Screening for Microbial Metal-Chelating Siderophores for the Removal of Metal Ions from Solutions. *Microorganisms* **2021**, *9*, 111, doi:10.3390/microorganisms9010111.
16. Butler, A.; Theisen, R.M. Iron(III)–Siderophore Coordination Chemistry: Reactivity of Marine Siderophores. *Coordination Chemistry Reviews* **2010**, *254*, 288–296, doi:10.1016/j.ccr.2009.09.010.
17. Homann, V.V.; Sandy, M.; Tincu, J.A.; Templeton, A.S.; Tebo, B.M.; Butler, A. Loihichelins A−F, a Suite of Amphiphilic Siderophores Produced by the Marine Bacterium Halomonas LOB-5. *J. Nat. Prod.* **2009**, *72*, 884–888, doi:10.1021/np800640h.
18. Vraspir, J.M.; Holt, P.D.; Butler, A. Identification of New Members within Suites of Amphiphilic Marine Siderophores. *Biometals* **2011**, *24*, 85–92, doi:10.1007/s10534-010-9378-1.
19. Schalk, I.J. Bacterial Siderophores: Diversity, Uptake Pathways and Applications. *Nat Rev Microbiol* **2025**, *23*, 24–40, doi:10.1038/s41579-024-01090-6.
20. Martinez, J.S.; Zhang, G.P.; Holt, P.D.; Jung, H.-T.; Carrano, C.J.; Haygood, M.G.; Butler, A. Self-Assembling Amphiphilic Siderophores from Marine Bacteria. *Science* **2000**, *287*, 1245–1247, doi:10.1126/science.287.5456.1245.
21. Sandy, M.; Butler, A. Microbial Iron Acquisition: Marine and Terrestrial Siderophores. *Chem. Rev.* **2009**, *109*, 4580–4595, doi:10.1021/cr9002787.
22. Homann, V.V.; Edwards, K.J.; Webb, E.A.; Butler, A. Siderophores of Marinobacter Aquaeolei: Petrobactin and Its Sulfonated Derivatives. *Biometals* **2009**, *22*, 565–571, doi:10.1007/s10534-009-9237-0.
23. Sandy, M.; Han, A.; Blunt, J.; Munro, M.; Haygood, M.; Butler, A. Vanchrobactin and Anguibactin Siderophores Produced by Vibrio Sp. DS40M4. *J. Nat. Prod.* **2010**, *73*, 1038–1043, doi:10.1021/np900750g.

24. Gauglitz, J.M.; Zhou, H.; Butler, A. A Suite of Citrate-Derived Siderophores from a Marine *Vibrio* Species Isolated Following the Deepwater Horizon Oil Spill. *Journal of Inorganic Biochemistry* **2012**, *107*, 90–95, doi:10.1016/j.jinorgbio.2011.10.013.
25. Kurth, C.; Schieferdecker, S.; Athanasopoulou, K.; Seccareccia, I.; Nett, M. Variochelins, Lipopeptide Siderophores from Variovorax Boronicumulans Discovered by Genome Mining. *J. Nat. Prod.* **2016**, *79*, 865–872, doi:10.1021/acs.jnatprod.5b00932.
26. Barbeau, K.; Rue, E.L.; Bruland, K.W.; Butler, A. Photochemical Cycling of Iron in the Surface Ocean Mediated by Microbial Iron(Iii)-Binding Ligands. *Nature* **2001**, *413*, 409–413, doi:10.1038/35096545.
27. Butler, A.; Harder, T.; Ostrowski, A.D.; Carrano, C.J. Photoactive Siderophores: Structure, Function and Biology. *Journal of Inorganic Biochemistry* **2021**, *221*, 111457, doi:10.1016/j.jinorgbio.2021.111457.
28. Al Shaer, D.; Al Musaimi, O.; de la Torre, B.G.; Albericio, F. Hydroxamate Siderophores: Natural Occurrence, Chemical Synthesis, Iron Binding Affinity and Use as Trojan Horses against Pathogens. *European Journal of Medicinal Chemistry* **2020**, *208*, 112791, doi:10.1016/j.ejmech.2020.112791.
29. Luque, R.; Béjar, V.; Quesada, E.; Martínez-Checa, F.; Llamas, I. Halomonas Ramblicola Sp. Nov., a Moderately Halophilic Bacterium from Rambla Salada, a Mediterranean Hypersaline Rambla. *International Journal of Systematic and Evolutionary Microbiology* **2012**, *62*, 2903–2909, doi:10.1099/ijs.0.039453-0.
30. Gunde-Cimerman, N.; Plemenitaš, A.; Oren, A. Strategies of Adaptation of Microorganisms of the Three Domains of Life to High Salt Concentrations. *FEMS Microbiology Reviews* **2018**, *42*, 353–375, doi:10.1093/femsre/fuy009.
31. Poli, A.; Finore, I.; Romano, I.; Gioiello, A.; Lama, L.; Nicolaus, B. Microbial Diversity in Extreme Marine Habitats and Their Biomolecules. *Microorganisms* **2017**, *5*, 25, doi:10.3390/microorganisms5020025.
32. Qiu, X.; Cao, X.; Xu, G.; Wu, H.; Tang, X. Halomonas Maris Sp. Nov., a Moderately Halophilic Bacterium Isolated from Sediment in the Southwest Indian Ocean. *Arch Microbiol* **2021**, *203*, 3279–3285, doi:10.1007/s00203-021-02317-3.
33. Agrawal, S.; Acharya, D.; Adholeya, A.; Barrow, C.J.; Deshmukh, S.K. Nonribosomal Peptides from Marine Microbes and Their Antimicrobial and Anticancer Potential. *Front. Pharmacol.* **2017**, *8*, doi:10.3389/fphar.2017.00828.
34. Saha, M.; Sarkar, S.; Sarkar, B.; Sharma, B.K.; Bhattacharjee, S.; Tribedi, P. Microbial Siderophores and Their Potential Applications: A Review. *Environ Sci Pollut Res* **2016**, *23*, 3984–3999, doi:10.1007/s11356-015-4294-0.
35. Khasheii, B.; Mahmoodi, P.; Mohammadzadeh, A. Siderophores: Importance in Bacterial Pathogenesis and Applications in Medicine and Industry. *Microbiological Research* **2021**, *250*, 126790, doi:10.1016/j.micres.2021.126790.
36. Bajt, O. Aliphatic Hydrocarbons in Surface Sediments of the Gulf of Trieste (Northern Adriatic)—Sources and Spatial and Temporal Distributions. *J Soils Sediments* **2017**, *17*, 1948–1960, doi:10.1007/s11368-016-1642-8.
37. Raymond, K.N.; Dertz, E.A.; Kim, S.S. Enterobactin: An Archetype for Microbial Iron Transport. *Proceedings of the National Academy of Sciences* **2003**, *100*, 3584–3588, doi:10.1073/pnas.0630018100.
38. Andrews, S.C.; Robinson, A.K.; Rodríguez-Quiñones, F. Bacterial Iron Homeostasis. *FEMS Microbiology Reviews* **2003**, *27*, 215–237, doi:10.1016/S0168-6445(03)00055-X.
39. Dauros-Singorenko, P.; Swift, S. The Transition from Iron Starvation to Iron Sufficiency as an Important Step in the Progression of Infection. *Science Progress* **2014**, *97*, 371–382, doi:10.3184/003685014X14151846374739.
40. Patkar, S.; Shinde, Y.; Chindarkar, P.; Chakraborty, P. Evaluation of Antioxidant Potential of Pigments Extracted from Bacillus Spp. and Halomonas Spp. Isolated from Mangrove Rhizosphere. *BioTechnologia* **2021**, *102*, 157–169, doi:10.5114/bta.2021.106522.
41. Orhan, F.; Ceyran, E. Valorisation of Cheese Whey for Ectoine Production by Halomonas Neptunia. *International Journal of Dairy Technology* **2024**, *77*, 146–155, doi:10.1111/1471-0307.13008.
42. Mansour, M.; Kara Ali, M.; Berkani, M.; Flahaut, S.; Chaoua, S.; Kamyab, H.; Vasseghian, Y.; Kacem Chaouche, N. Optimization of Physicochemical Parameters for Lipopeptides Surfactin Production by *Bacillus Halotolerans* under Oat Straw Medium Using Box-Behnken Design and Artificial Neural Networks. *Sustainable Chemistry and Pharmacy* **2024**, *37*, 101419, doi:10.1016/j.scp.2023.101419.
43. Khilyas, I.V.; Markelova, M.I.; Valeeva, L.R.; Ivoilova, T.M.; Shagimardanova, E.; Laikov, A.V.; Elistratova, A.A.; Berkutova, E.S.; Lochnit, G.; Sharipova, M.R. Genomic Insights and Anti-

Phytopathogenic Potential of Siderophore Metabolome of Endolithic Nocardia Mangyaensis NH1. *Sci Rep* **2024**, *14*, 5676, doi:10.1038/s41598-024-54095-9.
44. Johnstone, T.C.; Nolan, E.M. Beyond Iron: Non-Classical Biological Functions of Bacterial Siderophores. *Dalton Trans.* **2015**, *44*, 6320–6339, doi:10.1039/C4DT03559C.
45. Peralta, D.R.; Adler, C.; Corbalán, N.S.; García, E.C.P.; Pomares, M.F.; Vincent, P.A. Enterobactin as Part of the Oxidative Stress Response Repertoire. *PLOS ONE* **2016**, *11*, e0157799, doi:10.1371/journal.pone.0157799.
46. Bogomolnaya, L.M.; Tilvawala, R.; Elfenbein, J.R.; Cirillo, J.D.; Andrews-Polymenis, H.L. Linearized Siderophore Products Secreted via MacAB Efflux Pump Protect Salmonella Enterica Serovar Typhimurium from Oxidative Stress. *mBio* **2020**, *11*, 10.1128/mbio.00528-20, doi:10.1128/mbio.00528-20.
47. Arahal, D.R.; Ventosa, A. The Family Halomonadaceae. In *The Prokaryotes: A Handbook on the Biology of Bacteria Volume 6: Proteobacteria: Gamma Subclass*; Dworkin, M., Falkow, S., Rosenberg, E., Schleifer, K.-H., Stackebrandt, E., Eds.; Springer: New York, NY, 2006; pp. 811–835 ISBN 978-0-387-30746-6.
48. Gillespie, J.J.; Wattam, A.R.; Cammer, S.A.; Gabbard, J.L.; Shukla, M.P.; Dalay, O.; Driscoll, T.; Hix, D.; Mane, S.P.; Mao, C.; et al. PATRIC: The Comprehensive Bacterial Bioinformatics Resource with a Focus on Human Pathogenic Species ▿. *Infect Immun* **2011**, *79*, 4286–4298, doi:10.1128/IAI.00207-11.
49. Chalita, M.; Kim, Y.O.; Park, S.; Oh, H.-S.; Cho, J.H.; Moon, J.; Baek, N.; Moon, C.; Lee, K.; Yang, J.; et al. EzBioCloud: A Genome-Driven Database and Platform for Microbiome Identification and Discovery. *International Journal of Systematic and Evolutionary Microbiology* **2024**, *74*, 006421, doi:10.1099/ijsem.0.006421.
50. Meier-Kolthoff, J.P.; Göker, M. TYGS Is an Automated High-Throughput Platform for State-of-the-Art Genome-Based Taxonomy. *Nat Commun* **2019**, *10*, 2182, doi:10.1038/s41467-019-10210-3.
51. Tsurumaki, M.; Deno, S.; Galipon, J.; Arakawa, K. Complete Genome Sequence of Halophilic Deep-Sea Bacterium Halomonas Axialensis Strain Althf1. *Microbiology Resource Announcements* **2019**, *8*, 10.1128/mra.00839-19, doi:10.1128/mra.00839-19.
52. Li, Y.; Liu, L.; Zhang, G.; He, N.; Guo, W.; Hong, B.; Xie, Y. Potashchelins, a Suite of Lipid Siderophores Bearing Both L-Threo and L-Erythro Beta-Hydroxyaspartic Acids, Acquired From the Potash-Salt-Ore-Derived Extremophile Halomonas Sp. MG34. *Front. Chem.* **2020**, *8*, doi:10.3389/fchem.2020.00197.
53. Della Sala, G.; Mangoni, A.; Costantino, V.; Teta, R. Identification of the Biosynthetic Gene Cluster of Thermoactinoamides and Discovery of New Congeners by Integrated Genome Mining and MS-Based Molecular Networking. *Front. Chem.* **2020**, *8*, doi:10.3389/fchem.2020.00397.
54. Niehs, S.P.; Dose, B.; Scherlach, K.; Roth, M.; Hertweck, C. Genomics-Driven Discovery of a Symbiont-Specific Cyclopeptide from Bacteria Residing in the Rice Seedling Blight Fungus. *ChemBioChem* **2018**, *19*, 2167–2172, doi:10.1002/cbic.201800400.
55. Haedar, J.R.; Yoshimura, A.; Wakimoto, T. New Variochelins from Soil-Isolated Variovorax Sp. H002. *Beilstein J. Org. Chem.* **2024**, *20*, 692–700, doi:10.3762/bjoc.20.63.
56. Hur, G.H.; Vickery, C.R.; Burkart, M.D. Explorations of Catalytic Domains in Non-Ribosomal Peptide Synthetase Enzymology. *Nat. Prod. Rep.* **2012**, *29*, 1074–1098, doi:10.1039/C2NP20025B.
57. Flugel, R.S.; Hwangbo, Y.; Lambalot, R.H.; Cronan, J.E.; Walsh, C.T. Holo-(Acyl Carrier Protein) Synthase and Phosphopantetheinyl Transfer in Escherichia Coli *. *Journal of Biological Chemistry* **2000**, *275*, 959–968, doi:10.1074/jbc.275.2.959.
58. Herbst, D.A.; Boll, B.; Zocher, G.; Stehle, T.; Heide, L. Structural Basis of the Interaction of MbtH-like Proteins, Putative Regulators of Nonribosomal Peptide Biosynthesis, with Adenylating Enzymes *. *Journal of Biological Chemistry* **2013**, *288*, 1991–2003, doi:10.1074/jbc.M112.420182.
59. Li, Y.; Tahlan, K.; Bignell, D.R.D. Functional Cross-Talk of MbtH-Like Proteins During Thaxtomin Biosynthesis in the Potato Common Scab Pathogen Streptomyces Scabiei. *Front. Microbiol.* **2020**, *11*, doi:10.3389/fmicb.2020.585456.
60. Clarke, T.E.; Braun, V.; Winkelmann, G.; Tari, L.W.; Vogel, H.J. X-Ray Crystallographic Structures of the Escherichia Coli Periplasmic Protein FhuD Bound to Hydroxamate-Type Siderophores and the Antibiotic Albomycin *. *Journal of Biological Chemistry* **2002**, *277*, 13966–13972, doi:10.1074/jbc.M109385200.
61. Noinaj, N.; Guillier, M.; Travis J. Barnard; Buchanan, S.K. TonB-Dependent Transporters: Regulation, Structure, and Function. *Annual Review of Microbiology* **2010**, *64*, 43–60, doi:10.1146/annurev.micro.112408.134247.

62. Luo, V.C.; Peczuh, M.W. Location, Location, Location: Establishing Design Principles for New Antibacterials from Ferric Siderophore Transport Systems. *Molecules* **2024**, *29*, 3889, doi:10.3390/molecules29163889.
63. Johnston, C.W.; Wyatt, M.A.; Li, X.; Ibrahim, A.; Shuster, J.; Southam, G.; Magarvey, N.A. Gold Biomineralization by a Metallophore from a Gold-Associated Microbe. *Nat Chem Biol* **2013**, *9*, 241–243, doi:10.1038/nchembio.1179.
64. Ferguson, A.D.; Coulton, J.W.; Diederichs, K.; Welte, W.; Braun, V.; Fiedler, H.-P. Crystal Structure of the Antibiotic Albomycin in Complex with the Outer Membrane Transporter FhuA. *Protein Science* **2000**, *9*, 956–963, doi:10.1110/ps.9.5.956.
65. Kreutzer, M.F.; Kage, H.; Nett, M. Structure and Biosynthetic Assembly of Cupriachelin, a Photoreactive Siderophore from the Bioplastic Producer Cupriavidus Necator H16. *J. Am. Chem. Soc.* **2012**, *134*, 5415–5422, doi:10.1021/ja300620z.
66. Nemanič, T.M.; Leskovšek, H.; Horvat, M.; Vrišer, B.; Bolje, A. Organotin Compounds in the Marine Environment of the Bay of Piran, Northern Adriatic Sea. *J. Environ. Monit.* **2002**, *4*, 426–430, doi:10.1039/B111582K.
67. Weisburg, W.G.; Barns, S.M.; Pelletier, D.A.; Lane, D.J. 16S Ribosomal DNA Amplification for Phylogenetic Study. *J Bacteriol* **1991**, *173*, 697–703.
68. Schwyn, B.; Neilands, J.B. Universal Chemical Assay for the Detection and Determination of Siderophores. *Anal Biochem* **1987**, *160*, 47–56, doi:10.1016/0003-2697(87)90612-9.
69. Kowalska-Krochmal, B.; Dudek-Wicher, R. The Minimum Inhibitory Concentration of Antibiotics: Methods, Interpretation, Clinical Relevance. *Pathogens* **2021**, *10*, 165, doi:10.3390/pathogens10020165.
70. Nayarisseri, A.; Singh, P.; Singh, S.K. Screening, Isolation and Characterization of Biosurfactant Producing Bacillus Subtilis Strain ANSKLAB03. *Bioinformation* **2018**, *14*, 304–314, doi:10.6026/97320630014304.
71. Ahn, M.-R.; Kumazawa, S.; Hamasaka, T.; Bang, K.-S.; Nakayama, T. Antioxidant Activity and Constituents of Propolis Collected in Various Areas of Korea. *J. Agric. Food Chem.* **2004**, *52*, 7286–7292, doi:10.1021/jf048726s.
72. Wick, R.R.; Judd, L.M.; Gorrie, C.L.; Holt, K.E. Unicycler: Resolving Bacterial Genome Assemblies from Short and Long Sequencing Reads. *PLoS Comput Biol* **2017**, *13*, e1005595, doi:10.1371/journal.pcbi.1005595.
73. Blin, K.; Shaw, S.; Augustijn, H.E.; Reitz, Z.L.; Biermann, F.; Alanjary, M.; Fetter, A.; Terlouw, B.R.; Metcalf, W.W.; Helfrich, E.J.N.; et al. antiSMASH 7.0: New and Improved Predictions for Detection, Regulation, Chemical Structures and Visualisation. *Nucleic Acids Res* **2023**, *51*, W46–W50, doi:10.1093/nar/gkad344.

Paper in preparation

CHAPTER 3

Discovery of Novel Maldivian Coral-Associated Microorganisms displaying Antimicrobial, Antioxidant, and UV-Protectant Activities

Abstract: Coral survival is crucial for socio-ecological interest of many countries, particularly for the Republic of Maldives, an atoll nation in the Indian Ocean built by coral reefs, whose health and integrity strongly affect the country's livelihoods and economy. Maldivian reefs cover approximately 4,500 km^2, representing the 7^{th} largest coral reef system in the world. However, these reefs are increasingly impacted by multiple stressors, leading to significant declines in biodiversity and abundance. This alarming trend has spurred interest in coral restoration efforts, where enhancing coral resilience is a primary objective. In the last decades, researchers focused on the study of coral associated microorganisms (CAMs) to better understand their symbiotic roles in coral health and resilience. Emerging evidence suggests that certain CAMs confer critical benefits and protection to corals by the production of microbial natural products, such as UV protectants, antimicrobials, antioxidants, among others. Intriguingly, these microbial-derived molecules hold significant potential for a broad range of biotechnological and pharmaceutical applications. While metabarcoding analysis has been widely utilized to study CAMs diversity under various conditions, it is limited in its ability to elucidate their functional roles. To address this limitation, the cultivation of bacterial strains remains indispensable for validating ecological and biotechnological hypotheses derived from multi-omics data. In this study, we isolated approximately 50 CAMs, identifying two novel microbial species, and evaluated the promising antimicrobial, antioxidant and UV protectant properties of selected strains. Remarkably, the crude extracts of the selected CAMs exhibited strong antibiotic activity against a panel of ten different human and fish pathogenic strains, alongside other bioactive effects. Furthermore, genome annotation revealed their significant potential to contribute to both coral restoration and drug discovery strategies. These findings highlight the dual ecological and biotechnological relevance of CAMs, representing an

important step toward the identification of novel bacterial species with the potential to benefit both coral reef ecosystems and human health.

---

1. Introduction

Coral reefs are considered among the largest hot spot of marine biodiversity including chemical and genetic diversity [1] and one of the most productive ecosystems globally, offering vital ecological, economic, and social benefits. Unfortunately, these ecosystems face escalating threats from human activities, including climate change, overfishing, and pollution [2–4]. To counteract the alarming degradation of coral reefs, restoration efforts have become a critical strategy. Techniques such as coral transplantation and assisted evolution supported by microorganisms show considerable promise; however, their long-term effectiveness depends on a deeper understanding of the intricate relationships between corals and their associated microorganisms. At microscopic scale, coral reefs are composed by millions of polyps that live in symbiosis with dinoflagellates of the Symbiodiniaceae (photosynthetic microalgae) family. In addition to corals-microalgae relation, the whole coral holobiont is also composed by archaea, bacteria, fungi and viruses forming a small ecosystem and primarily cooperating for mutual nutrient exploitation [5]. This associated microbial community rapidly respond to environmental stimuli and signals, changing its composition and metabolic activities as consequence of heat waves, acidification, light intensity, pollutions [6]. As an effect, recent studies have been focused on coral-associated microorganisms (CAMs) for a better understanding of their role within symbiosis. For example, certain bacterial symbionts may offer benefits to corals playing a crucial ecological role in numerous processes being involved for example in food supply, participating in the carbon, nitrogen and sulphur cycles, thermal stress mitigation, in defence strategies against pathogens and predators. The term Beneficial Microorganisms

for Corals (BMC) has been proposed to identify symbionts that promote coral health and which could be exploited for coral restoration purposes [7]. This concept is analogue to the known term "Plant Growth Promoting Rhizosphere" used to identify microorganisms, especially localised within the rizosphere, which promote plant growth. These beneficial processes are mediated through secretion of bioactive compounds (e.g., antimicrobial, antioxidant and photoprotective molecules) making corals more resilient to environmental changes and stressors [7–10]. Hundreds of marine natural products (MNPs) have been discovered form CAMs, displaying relevant biotechnological and pharmaceutical applications [11].

Harnessing and manipulating these microbial interactions can potentially enhance coral resilience and improve restoration outcomes. More specifically, CAMs could be utilised to protect corals form bleaching, phenomenon driven by environmental stressors such as elevated temperatures and high solar irradiance, and closely linked to the overproduction of reactive oxygen species (ROS) and reactive nitrogen species (RNS) [12,13]. Molecules provided by CAMs such as scavenging enzymes including catalase, superoxide dismutase (SOD), and non-enzymatic antioxidants (mannitol, glutathione and carotenoids) could provide additional ROS scavenging capacity that can mitigate ROS damage [14]. In terms of RNS detoxification, genes encoding nitric oxide reductase may help reduce harmful interactions between ROS and RNS, alleviating oxidative damage during stress [15]. Approaches such as probiotics, microbial transplantation, and the development of stress-tolerant microbial strains are being actively explored to strengthen coral health under challenging conditions [7]. These interventions align with the emerging concept of "assisted microbiome engineering," which involves tailoring microbial communities to deliver specific benefits to the coral host. For instance, applying probiotics has been shown to improve coral survival during heat stress, presenting a promising strategy to mitigate the effects of

climate change [16,17]. However, the relevance of the CAMs should be further investigated to better expand the concept of BMC, through i) elucidation of coral microbiome compositions and distribution ii) isolating cultivable (and "uncultivable") associated microbes iii) exploring the biotech potential through the discovery of novel microbial natural products produced by the isolated strains. As a matter of fact, while most of the knowledge about CAMs has been generated through metabarcoding or metagenomic analysis, still scares are the studies involving the isolation of microorganisms and even less, the evaluation of their biotechnological activities. Moreover, the microbial cultivability still represents a barrier which hampers the access to the real chemical diversity. This study aims to use a holistic approach to examine microbial community compositions associated to the Maldivian *Porites lobata* and *Acropora gemmifera* corals at different growth stages and depths, isolate associated bacteria with relevant biological activities in terms of antimicrobial, antioxidant and photoprotective effects and investigate their genome looking for relevant genes which could be involved in the coral-microbes beneficial relation. This work lays the basis for future coral restoration strategies, together with the identification of potential new marine sources for human health applications.

2. Results

2.1. Comparative Analysis of Coral Associated Microbiomes

Samples from *Acropora gemmifera* colonies consistently showed the lowest ASV richness, ranging from 44 to 119 Amplicon Sequence Variants (ASVs) (Figure S1). Higher richness values were reached in *Porites* samples, which ranged from 176 to 587 ASVs. However, the highest values were found for seawater samples (up to 1449 ASVs).

Beta-diversity analyses showed that seawater and sediment samples clustered together, both deep and shallow samples. Different results were obtained for the

two coral species, which showed very different microbial communities. *Porites lobata* microbiome collected in depth cluster close to microbiome found in shallow colonies. *Acropora gemmifera* exhibited higher grade of diversity if microbiome from shallow colonies was compared to microbial composition of deep coral (Figure S2).

Taxonomic analyses carried out on the samples showed that, indeed, prokaryotic assemblaged associated with coral samples were different from those of either seawater or sediment samples. Environmental microbiome was mainly composed of by Cyclobacteriaceae, Rhodobacteriaceae, Kiloniellaceae and Woeseiaceae families, with relative abundances among 5 and 10%. Endozoicomonadaceae was recorded as main bacterial family of *Acropora gemmifera* microbiome. It was recorded with higher percentage in shallow colonies, (90% and 60% for small and large colonies, respectively). In deep environment, Endozoicomonadaceae remained the most abundant identified falimy, but it was recorded at lower percentages (less than 10% for small and large colonies). *Porites lobata* showed a diversified family predominance in the four samples analysed. In shallow water, big colonies were found associated with Cyclobacteriaceae and Desulfovibrionaceae (30% of each family), whereas microbiome of small colonies showed predominance of Endozoicomonadaceae (30%). Different microbiome profiling was recorded for *Porites lobata* collected on deep reef. In this ecosystem, big colonies were mainly characterized by Rhizobiaceae (40%), and microbiome of small colonies was composed for 20% of Microtrichaceae (Figure S3).

2.2. Bacterial CAMs Isolation

Around 50 strains were islated from the different coral samples, 37 strains from *Acropora gemmifera* and 18 from *Porites lobata*. Morphologically different strains were selected and identified based on 16 rRNA gene. The isolates ranged from 10different genera such as, the most abundant *Bacillus* and *Vibrio,* followed

by *Exiguobacterium, Priestia, Metabacillus, Pseudoalteromonas, Saccharopolyspora, Streptomyces, Salinispora and Microbacterium* (Figure 1).

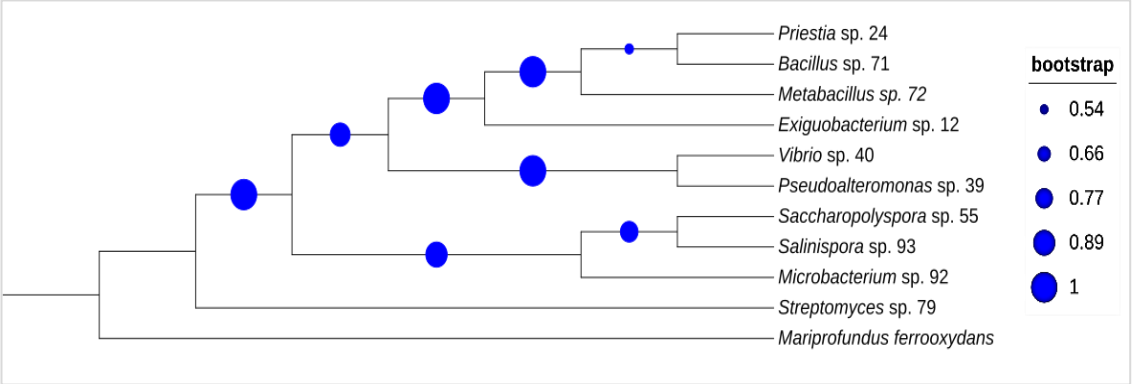

Figure 1. Phylogenetic relationships among members of the different genera isolated from *Acropora* and *Porites*. Sequences were aligned using the MUSCLE algorithm and evolutionary distances were calculated using maximum likelihood method in MEGA11. Blue circles represent bootstrap values based on 100 replicates. The 16S rRNA gene sequence from *Mariprofundus ferrooxydans* was chosen as an outgroup to define the root of the tree.

No significant trend was observed among the different conditions/samples which instead emerges by the metabarcoding data, meaning that the isolation procedure limits and strongly impact on the selection of relevant genera. Moreover, among the isolates some industrially relevant actinobacteria were retrieved, which emerged after long incubation period (>45 days), *Streptomyces* and *Salinispora,* reflecting, especially for the latter, their slow growth rate. In order to explore the biotechnological potential of coral-associated bacteria bioactivities were evaluated.

2.3. Bioactivity Evaluation of CAMs

The 10 selected strains were cultivated in MB-modified medium (250 mL), extracted by organic solvents (EtAOc for the exhausted broth and MeOH for the bacterial biomass) and the extracts evaluated for different bioactivities including i) antimicrobial activity to identify strains able to defend corals from pathogens, ii) antioxidant activity relevant in response to oxidative stress due to climate change and iii) UV protection to identify bacteria able to cope with high solar irradiation potentially bringing benefits to corals. As above-mentioned, in future

molecules responsible for those bioactivities could be adopted both in coral restoration strategies and applied in the pharmaceutical sector.

2.3.1 Evaluation of the Antimicrobial Activity

A panel of 11 different pathogens have been implied as target strains, including fish and multidrug resistant human pathogens. Among the 10 selected CAMs, the extracellular extracts generated from *Pseudoalteromonas* sp. 39, *Streptomyces* sp. 79, *Microbacterium* sp. 92 and *Salinispora* sp. 93 displayed the highest bioactivity (Table 1). In particular, *Streptomyces* sp. 79 was able to inhibit 8 out of the 11 tested strains, showing the strongest effect towards *P. damselae* subsp. *piscicida* (a fish pathogen) with a MIC value of 0.0098 μg/mL. Similarly, *Microbacterium* sp. 92 and *Salinispora* 93 inhibited 7 out of 11 pathogens ranging from 125 to 0.3 μg/mL. *Pseudoalteromonas* sp. 39 instead showed potent antimicrobial activity (MIC 0.031 μg/mL) against *V. anguillarum* (a fish and coral pathogen) and *P. damselae* (MIC 30 μg/mL). Notably, no extracts were reported to have effect towards *S. aureus* vancomycin resistant and *P. aeuroginosa,* while only a weak inhibition was displayed by *Streptomyces* sp. 79 against *E. coli*. It is also important to note that these are crude complex extracts, for this reason, further fractionation and purification processes could concentrate the active molecules and enhance the antimicrobial properties.

Table 1: Antimicrobial activity reporting the MIC of the most active extracts towards the pathogens panel.

Pathogen Strains	Active Strain	[ ] μg/mL
E. coli ATCC 10536	79	500
L. monocytogenes MB 677	79	1
	92	1
	93	0.5
P. damselae subps. *Piscicida* ATCC 51736	39	30
	79	0.0098
	92	125
	93	125
S. aureus methicillin resistant	39	500
	79	1
	92	125
	93	31
S. aureus - chinolone resistant	79	500
	92	2
	93	1
S. aureus - macrolide resistant	79	0.5
	92	2
	93	20
S. aureus 6538p	39	125
	79	0.3
	92	0.313
	93	1.25
V. anguillarium ATCC 19264	39	0.031
	92	20
	93	60
C. albicans ATCC 76485	79	0.25
S. aureus - vancomycin resistant	-	-
P. aeruginosa	-	-

2.3.2. Evaluation of the Antioxidant Activity

Antioxidant assays highlighted the high level of bioactivity of strain 39, which reached the ascorbic acid antioxidant potential at 125 μg/mL and Trolox level at 250 μg/mL (Figure 2). In addition, this extract had a dose-response effect, with decrease of antioxidant activity at 10% for the lowest concentration (15,62 μg/mL) in both assays. The second extract with interesting activity is strain 93, with comparable Trolox antioxidant effect at highest concentration tested 250 μg/mL. All the other extracts showed moderate or low antioxidant potential.

a)

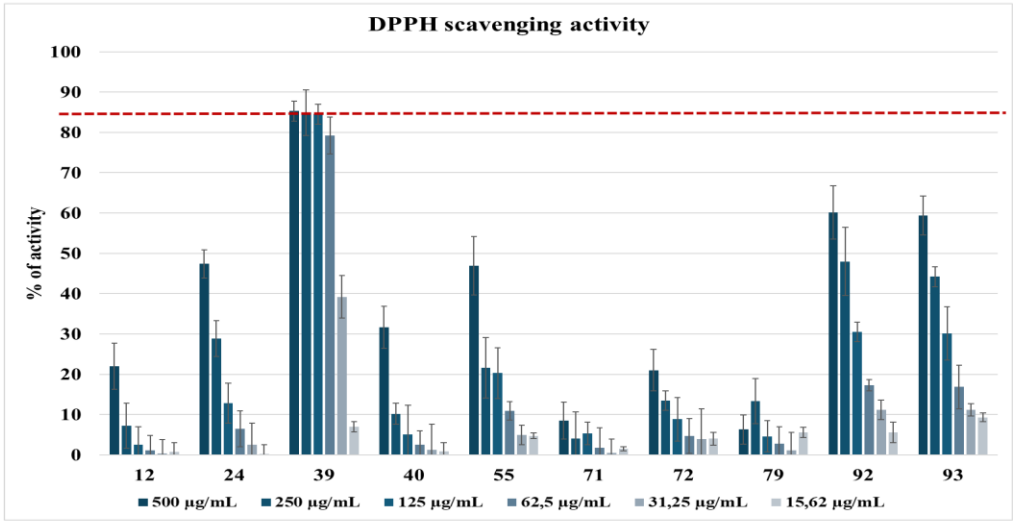

b)

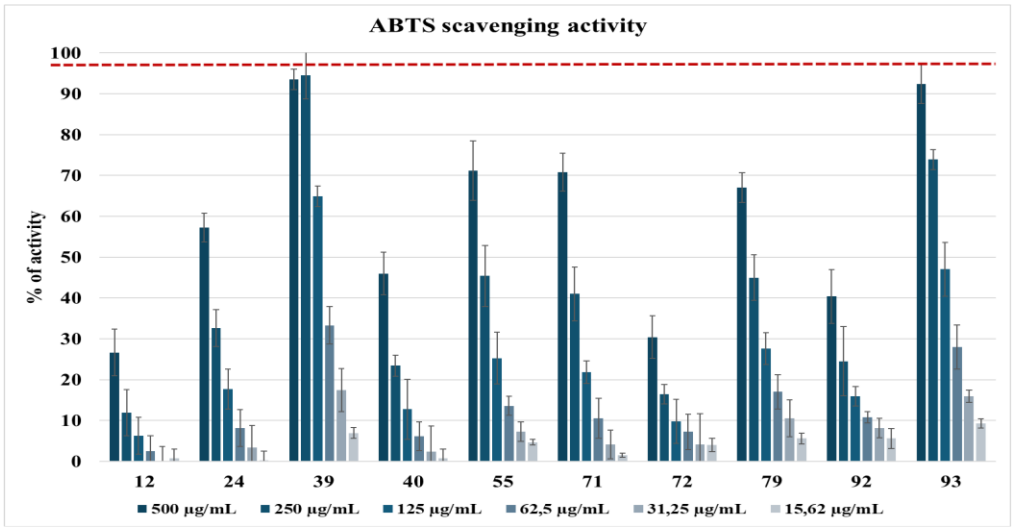

Figure 2. Mean % activity of DPPH. **a)** and ABTS **b)** assays. Bars represent the mean ± SD (n = 3) from triplicate measurements for total extracellular extracts of the 10 selected strains. In DPPH assay, ascorbic acid was used as positive control (red dotted line). In ABTS assay, trolox was used as positive control (red dotted line).

2.3.3. Evaluation of the UV Protection Effect

Untreated HaCat cells exposed for 30 seconds to UVC reduced cell viability at 55%. Cells pre-treated with Uvinul and Vanillin exhibited protection against cell death induced by UVC exposure, increasing cell viability at 80%. Intracellular extracts were tested for their potential protective effect on HaCat cells injured with UVC (Figure 3). No significant effect was detected by the extracellular extracts (Data not shown). Strain 39 exhibited the most significant effect, since extract at 200 µg/mL reached highest level of cell viability (74%), comparable to

the two positive controls. Lower concentration of strain 39 (100 µg/mL) was also able to increase cell viability (63%) with respect to untreated cells. Extracts from 12, 24 and 93 strains showed a moderate protective effect only at higher concentration (64, 70, 67% of viable cells, respectively).

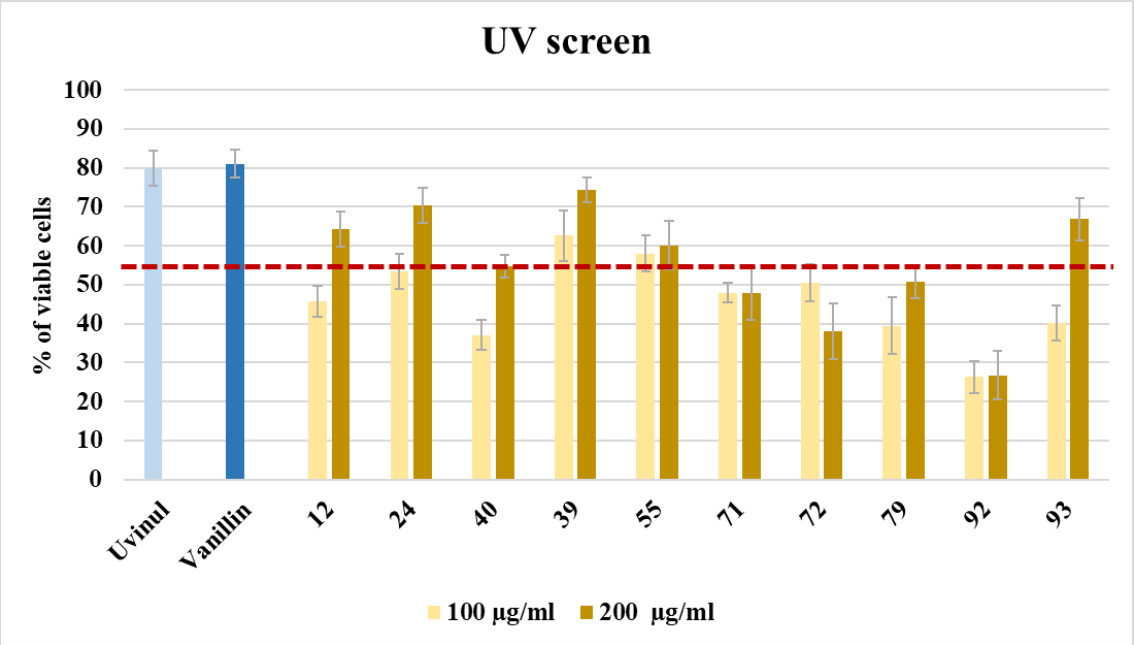

Figure 3. Protective effect of intracellular bacterial extracts on viability of HaCat cells injured with UVC. Control without UVC exposure represents 100% of viable cells. Red dotted line represents viability of UVC injured cells, without extract pre-treatments. Uvinul and Vanillin have been used at 100µM as positive control (well-known UV-absorbing properties).

2.4. Bacterial Genome-Based Identification

Due to the well-known metabolic potential of these genera and the strong demonstrated bioactivity, *Pseudoalteromonas* sp. 39, *Streptomyces* sp. 79 and *Microbacterium* sp. 92 were selected for whole genome sequencing. Summarised results are showed in the table below (Table 2).

Table 2. General features of the whole genome of the 3 selected strains

Attribute	*Pseudoalteromonas sp.* 39	*Streptomyces sp.* 79	*Microbacterium sp.* 92
Genome size (bp)	5,126,368	8,179,209	3,274,840
DNA G+C (%)	43.2	71.6	70.2
Number of contigs	33	19	2
N50 (bp)	225,663	239,681	1,441,367
Number of Coding Sequences	4,646	7,428	2
RNA genes (tRNA+rRNA)	70	74	48

The bacterial genomes of the three strains were subjected to average nucleotide identity (ANI) and digital DNA-DNA hybridization (dDDH, also known as d4). These analyses were performed in comparison to the closest phylogenetic relatives for each strain. *Pseudoalteromonas sp.* 39 showed a dDDH value of 25%, 24.9%, 24.7%, 24.5% and ANI values of 82.12%, 82.09%, 81.89%, 81.77%, when compared to *P. flavipulchra* (GenBank: GCA_000259115.1), *P. maricaloris* (GenBank: GCA_012641725.1), *P. piscicida* (GenBank: GCA_000382005.1) & *P. galatheae* (GenBank: GCA_005886105.2). Both values were below the standard cutoff (dDDH <70% and ANI <95%) and strongly supporting the classification of this strain as a novel species. Similarly, low dDDH (31.1%, 30.6%, 27.9% and 27.9%) and ANI (86.52%, 86.09%, 84.91%, 84.75%) values were detected for *Microbacterium* sp. 92 when compared to *Microbacterium plantarum (GenBank:* GCA_028737425.1*), M. arborescens* (GenBank: GCA_030369635.1) *M. imperiale* (GeneBank: GCA_017876655.1) and *M. thalli* (GenBank: GCA_028737415.2). These results confirmed its designation as a novel species. For *Streptomyces* sp. 79, the corresponding dDDH (89.3%) and ANI (98.72%) assigned this strain to *S. parvus* (GenBank: GCA_008632535.1). In summary, *Pseudoalteromonas* sp. 39 and *Microbacterium* sp. 92 represent novel species based on both ANI and dDDH analyses (Figure 4).

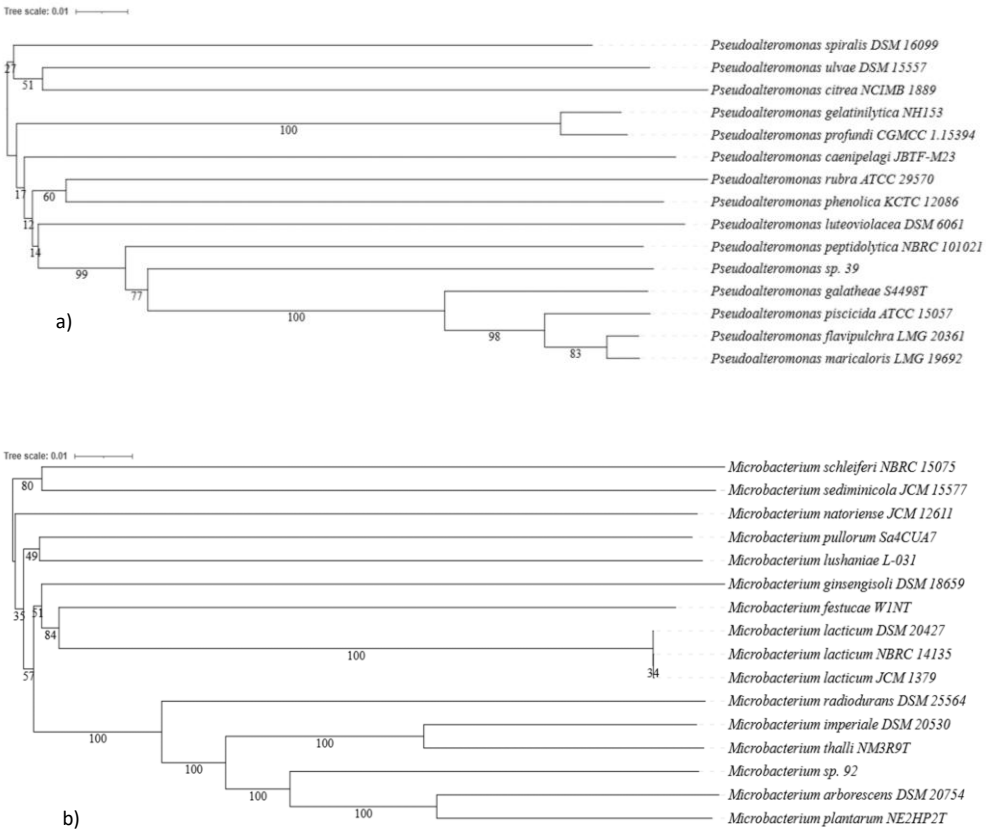

Figure 4: Phylogenetic tree of novel coral associated bacteria based on TYGS Whole Genome Newick file and processed in iToL. a) *Pseudolateromonas* sp. 39, b) *Microbacterium* sp. 92.

2.5. Genome Annotation and Biosynthetic Potential Analysis of selected strains

In order to assess the potential of the selected strains as future coral probiotics and to validate the presence of relevant BGCs, the genomes of strain 39, 79 and 92 were interrogated by genome annotation using RAST (Figure S4 and Table 3) and antiSMASH (Figure S5). As target, we selected specific genes involved in oxidative and nitrogen stress response (ROS and RNS), ability to produce pigments and antimicrobial compounds. The analysis summarised in Table 3 (Figure S5 and Table S1) reveals significant features linked to stress response and secondary metabolite biosynthesis in accordance with the detected bioactivities.

Pseudoalteromonas sp. 39 revealed high potential for antioxidant activity. Its genome annotation revealed the presence of 92 genes involved in stress response from which 38 are related to oxidative stress, in particular genes which neutralise or reduce ROS (glutathione, SOD, peroxidases, catalase). Regarding RNS, this strain shows genes necessary to cope with nitrosative stress (*nnrS* and *norR*). Moreover, *Pseudoalteromonas* has lipoate regulatory protein YbeD and arylpolyene compounds, both involved in the antioxidant activity and holds more than 8 NRPS clusters putatively encoding for novel bioactive peptides. Concerning *Streptomyces parvus* 79, a total of 12 genes corresponding to ROS and RNS response and presence of pigments similarly to *Pseudoalteromonas* sp. 39, were detected. Furthermore, it shows terpene genes related to the production of carotenoids and numerous BGCs encoding for potentially novel antimicrobial compounds. Finally, *Microbacterium* sp. 92 shows low number of genes involved in the oxidative stress response and no genes related to RNS response. According to the antiSMASH analysis it also encodes for terpenes carotenoids and for a limited number of antibiotic molecules.

Table 3: Summary table of RAST results on genes involved in the response to oxidative and nitrogen stress present in strains sp. 39, sp. 79, sp. 92. For each strain, 1 indicates the presence of the gene, 0 its absence.

	***Pseudoalteromonas* sp. 39**	***Streptomyces* sp. 79**	***Microbacterium* sp. 92**
Glutathione biosynthesis	1	1	1
ß-Carotene	0	1	0
Mannitol synthesis	0	0	1
DMS	0	0	0
DMSP	0	0	0
Peroxinitrite reduction (ahpC)	1	0	0
Nitric oxide reductase	1	0	0
Lipoic Acid Metabolism	1	1	1

Catalase-peroxidase (KatG)	1	1	1
Catalase (KatE)	1	1	1
SOD (One of the following: Mn, Fe, Cu-Zn, Nickel-dependant, Mn/Fe, Fe-Zn)	1	1	1
Nitrosative Stress (Present one of the following: NnrS, NorR, flavorubredoxin, NsrR)	1	1	0

3. Discussion

This paper analysed coral microbiomes of two among the most abundant species of coral in Maldives, *Porites lobata* and *Acropora gemmifera*. No data are present in literature on the microbial characterization of these two coral species in Maldivians reefs and this is the first study that describes their associated microbial communities both at molecular and microbiological level. The study also considers two distinct growth phases (small and big colonies) in two different environments (shallow and deep reefs) for the understanding of main bacteria groups that characterise their microbiomes in these ecologically related ecosystems. Microbial composition recorded for the two coral microbiomes showed different response to environment of origin in terms of bacteria family composition. *Acropora gemmifera* microbial composition is similar in terms of family taxonomic groups among the four conditions. In this coral species, microbiome is mainly characterised by the presence, at family level, of Endozoicomonadaceae, that in the swallow water contributed for more than 50% of whole microbiome composition for both small and big colonies in shallow reef. Same microbial family is present in the deep reef, but at lower percentages. Opposite results were obtained from comparative analysis of *Porites lobata* samples. In this case, microbial compositions changed along size colony and reef depth. This coral species showed, in shallow water, predominance of

Cyclobacteriaceae and Desulfovibrionaceae on big colonies and of Endozoicomonadaceae on small colonies. Other two families were found in deep environment, where Rhizobiaceae characterize microbiome of large colonies and Microtrichaceae was abundant in small colonies. Endozoicomonadaceae was found among the most common families of coral associated bacteria. Recent studies recorded this family in *Acropora* species corals in 99 reefs across the Pacific Ocean [36]. The high percentage of Rhizobiaceae in *Porites lobata* microbiome was also confirmed in other studies, as corals sampled in carrabian reefs [37].

In order to elucidate the nature of those complex interactions, the isolation of microorganisms in pure cultures is crucial. However, one of the main issue is represented by the microbial (un)cultivability [38]. Less than 1% of microorganisms present in an environmental sample is cultivable in standard laboratory conditions and this is also true for CAMs. In response to this limitation, different strategies have been successfully developed and applied to increase the microbial cultivable fractions [39,40]. Recent evidence report that, when CAMs have been cultivated their relevance and ecological role have been demonstrated. For example, in a recent review, Mohamed *et al*., listed the bacteria which potentially have a beneficial or antagonistic relationship with corals. The authors showed that most bacteria that confer benefit to the holobiont belong mostly to the α- and γ -proteobacteria and to a lesser extent the, *Actinomycetia, Cytophagia, Flavobacteriia, Bacilli, and Oligoflexia* classes [10]. In our work, ten different bacterial genera were identified and screened for several bioactivities. Among them, the most active have been identified as *Pseudoalteromonas* sp. 39, *Microbacterium* sp. 92, *Streptomyces* sp. 79 and *Salinispora* sp. 93. With only exception of 93, the whole genome of the other selected strains has been sequenced, allowing to establish *Pseudoalteromonas* sp. 39 and *Microbacterium* sp. 92 as novel species. The genus *Pseudoalteromonas* includes 47 described species (https://lpsn.dsmz.de/genus/pseudoalteromonas) and is known for its diverse

ecological roles, including both pathogenicity and beneficial activity. For example, some species, like *Pseudoalteromonas piratica*, are implicated in coral diseases like white syndrome [41,42], whereas others produce bioactive compounds with antimicrobial, antioxidant, and antifouling properties [43,42]. In the work by Shnit-Orland et al., five out six *Pseudoalteromonas* spp. isolated from different coral species showed antimicrobial activity against Gram positive strains, especially *Bacillus cereus*, *Staphylococcus aureus* [41]. More recently Ushijima et al., developed a potential probiotic treatment for infectious coral diseases in aquarium studies using *Pseudoalteromonas* sp. McH1-7. This bacterium produces at least two broad-spectrum antibacterials, korormicin and tetrabromopyrrole, along with other molecules (pseudoalterins), potentially active against many coral pathogens [44]. *P. shioyasakiensis* isolated from *Mussismilia braziliensis* showed to detoxify radicals and ROS mainly by producing ROS-reactive pigments, working as antioxidant [45]. Similarly, three different *Pseudoalteromonas* symbionts of soft-coral showed antioxidant effect by producing carotenoid pigments [46]. Pigmented *Pseudoalteromonas* strains are particularly prolific in producing secondary metabolites, with their pigmentation often linked to antifouling and antibacterial activities [43]. In our study, the novel *Pseudoalteromonas* sp. 39 exhibited moderate antibacterial activity against *Vibrio anguillarum*, *Photobacterium damselae*, and *Staphylococcus aureus*. It also demonstrated antioxidant activity, and an orange pigmentation observed after one day of growth at 28 °C. Accordingly with these results, the genome annotation of strain 39 shows high number of genes potentially involved in stress response, especially towards ROS and RNS and pigments production. AntiSMASH analysis of this strain revealed a diverse biosynthetic repertoire, including phosphonate, RiPP-like clusters, hybrid NRPS-like, arylpolyene and T3PKS-NRPS hybrids BGCs. The limited similarity of these BGCs to known clusters suggests a strong potential for the discovery of novel

antimicrobial/bioactive compounds. Regarding the other selected strains object of this study, *Salinispora*, *Streptomyces*, and the novel identified *Microbacterium*, they belong to actinobacteria and are among the most prolific in terms of secondary metabolites production. As a matter of fact, most of the current drugs currently on the market derive or are inspired by *Streptomyces*, so it is not surprisingly that the current isolate shows strong antimicrobial activity against most of target strains [47–49]. A wide range of new molecules endowed with antimicrobial activity have already been discovered from *Streptomyces*-associated corals confirming the enormous potential of these filamentous bacteria in the biotech industry [50]. In coral ecosystems, these bacteria contribute significantly to the health and resilience of their hosts. They are involved in processes such as nutrient cycling, protection against pathogens, and chemical signalling. Specifically, *Streptomyces* strains produce bioactive compounds that act as antimicrobials, deterring opportunistic infections and maintaining the stability of the coral microbiome. Their production of antioxidants and UV-protectant molecules further underscores their importance in mitigating environmental stressors, such as oxidative damage and solar radiation [51]. Moreover, the unique adaptations of these bacteria to the coral environment suggest that they may harbour unexplored pathways for the biosynthesis of compounds with unique structures and functions [52]. Despite their ecological and biotechnological significance, our understanding of Streptomyces strains in coral ecosystems remains limited. Future research should focus on isolating and characterizing these bacteria, elucidating their metabolic capabilities, and evaluating their potential for both coral restoration and the development of innovative biotechnological solutions.

The novel *Microbacterium* sp. 92 isolated in this study exhibited antimicrobial activity towards 7 out of the 10 pathogens tested and demonstrated a diverse biosynthetic potential as revealed by antiSMASH analysis. Currently there are

155 species included in this genus (https://lpsn.dsmz.de/ genus/microbacterium) having around 20% isolated from marine habitats [53]. From the antiSMASH results it appears to have cryptic BGCs showing low similarity with known compounds. These bacteria are integral members of the coral microbiome. Recent studies indicate that *Microbacterium* strains produce a range of bioactive compounds, including enzymes, antimicrobial agents, and antioxidants, which aid in mitigating environmental stressors and maintaining coral homeostasis [54].

Lastly, although relatively understudied in coral ecosystems, and with only 9 species described (https://lpsn.dsmz.de/genus/salinispora) the strictly marine genus *Salinispora* is widely recognized for its prolific production of secondary metabolites exhibiting potent antimicrobial, anticancer, and anti-inflammatory properties, with potential applications in pharmaceuticals [55]. Notable examples include salinosporamide A, a potent proteasome inhibitor currently in clinical trials for cancer therapy. The unique chemical structures of *Salinispora*-derived compounds make them attractive candidates for drug development and other industrial applications [56,51]. In the coral environment, *Salinispora* strains contribute to the protection of their host by producing natural products that inhibit the growth of pathogenic microorganisms, thereby enhancing coral health and resilience [56,57]. The ability of *Salinispora* to thrive in nutrient-limited marine environments underscores their metabolic versatility and their importance in sustaining coral ecosystems [58]. These bacteria hold promise for coral restoration efforts, as their bioactive compounds can be leveraged to mitigate disease outbreaks and promote coral resilience.

Despite their recognized significance, much remains to be uncovered about the role of *Salinispora* in coral ecosystems. Future research should aim to explore their functional diversity, isolate novel strains, and evaluate their contributions to both coral health and biotechnological innovation.

4. Materials and Methods

4.1 Sampling Site and Coral Collection

All sampling activities were conducted at the MaRHE Center (University of Milano Bicocca), on Magoodhoo island, Faafu Atoll, Republic of Maldives. The "*wall street barrier*" was chosen as sampling site within Faafu Atoll (3°6'52.08"N; 72°59'4.48"E, see Figure S6A). The sampling site is characterized by patch reefs interspersed with small sand pockets, with high coral diversity. Coral colonies were identified and sampled following the scheme illustrated in figure S6B. Two sampling areas were identified at 5 and 17 m depth. In these areas small ($\leq$ 10 cm) and large colonies ($\geq$ 30 cm) of *Porites lobata* and *Acropora gemmifera* were collected in biological triplicate. Water and sediments were collected closely to coral colonies. Pieces of coral colonies were collected by scuba divers and stored in sterile bags in seawater. Sediments were collected in triplicate using 50 ml tubes from sand pockets closest to each sampling area. Seawater (3L per replicate) was collected from the colonies surrounding using sterile bags. Samples were quickly stored in a refrigerated box until reached the laboratory. Coral fragments were washed with filtered seawater, reduced into smaller pieces with sterile hammer and scalpel, placed into 50 mL tubes containing RNA later and stored at 4°C. Seawater was removed from tubeswith sediments and then filled with RNA later and stored at 4°C. Seawater samples were vacuum filtered using sterile nitrocellulose filters (0.2 μm porosity; 47mm diameter), stored in 2mL tubes filled with RNA later and stored at 4°C.

4.2 DNA Extraction and Sequencing

Sediments and corals were extracted using DNeasy PowerSoil Pro Kit (Qiagen, cat. n. 47014). Corals were fragmented using pestle and mortar prior to DNA extraction. Seawater filters were extracted using Dneasy PowerWater Kit (Qiagen, cat. n. 14900-100-NF). Seawater filters were reduced in smaller pieces using sterile scalpels prior to DNA extraction. DNA concentrations were assessed

with NanoDrop microvolume spectrophotometer (ThermoFisher Scientific) and with Qubit™ dsDNA Quantification Assay Kit (High Sensitivity, cat. N. Q32851). Size range and DNA integrity was evaluated on agarose gel electrophoresis (0.8%). The Next Generation Sequencing was performed by the external service Eurofins Genomics (https://eurofinsgenomics.eu/, Ebersberg, Germany).

4.3 Microbial Community Characterization

Raw sequences were analysed through the QIIME2 pipeline (version 2022.2; https://qiime2.org/; [18]). The cutadapt plugin [19] was used to trim sequences to the amplified region. Trimmed paired-end sequences were analysed through the DADA2 procedure [20] thus removing chimeric sequences, correcting sequencing errors, and generating Amplicon Sequence Variants (ASVs). Taxonomy was assigned using the reference databases SILVA (version 138 nr SSU) [21]. Taxonomic affiliation was performed through the VSEARCH plugin [22] after trimming the reference dataset to the region amplified by the chosen primers. For a proper comparison among samples for alpha- and beta-diversity analyses, as well as for taxonomic investigation of the assemblage composition, the ASV table was rarefied to a common sampling depth [23] of 23000 sequences. After rarefaction, data analysis was performed with R (v4.2; R Core Team, 2022), within the Rstudio program, using the Microeco package [24].

4.4 Bacterial Isolation and Preliminary Molecular Identification

Coral samples were resuspended in filtered sea water (FSW) for enrichment. Corals and FSW were shaked in 50 mL tube for 30 min, allowing the release of coral-associated bacteria in liquid solution. Then, 1 mL of enriched FSW was collected from the eight coral samples and serially diluted until 10^{-7}. Each dilution was spread on two different solid growth media and incubated at 28°C up to 3 months, allowing the development of slow-growing strains. Growth media used for the experiments were prepared using 1L of distilled water as follows:

Marine Broth modified (MBmod - 19.4 g NaCl, 8.8 g MgCl, 20 g Bacteriological Peptone, 3.24 g NaSO4, 1.8 g $CaCl_2$, 1 g Yeast Extract, 0.55 g KCl, 0.16 g $NaHCO_3$, 0.10 g Fe(III) Citrate, 0.08 g KBr, 0.034 g $SrCl_2$, 0.022 g H_3BO_3, 0.008 g Na_2HPO_4, 0.004 g Na-Silicate, 0.0024 g NaF, 0.0016 g NH_4NO_3, pH 7.6 at 25°C, in distilled water); M1 medium (10 g Starch, 4 g Yeast extract, 2 g Peptone, in filtered sea water).

Solid media were prepared adding 17 g of Agar. $CaCO_3$ (2 g) was used to supplement all media. Moreover, 50 mg/L of Nystatin and 25 μg/mL Nalidixic acid were added to M1 to inhibit the growth of fungi and reduce the presence of fast-growing strains, respectively. After the incubation period, selected single colonies were propagated in liquid and stored at -80°C in presence of 20% glycerol.

The phylogenetic affiliation of bacterial isolates was performed through the 16S rRNA genes amplification and analysis. The freeze and thaw method was used to obtain bacterial genomic DNA. Colonies from each isolate were picked, transferred in 0.5 mL tube, dissolved in 100 μL of sterile water, mixed and frozen at -20°C for 1 h. Thereafter, the frozen tubes were incubated for 15 min at 99°C in a thermocycler and centrifuged for 10 min at 8900 rpm; then, 50 μL of supernatant was transferred in a new 0.5 mL tube and used as template for the amplification via PCR of 16S rDNA genes. PCR was carried out in a total volume of 40 μL, containing 20 μL of Super White Master MIX 2X, 1.5 μL of each primer (Eub27 F - Forward, seq: 5′-AGAGTTTGATCCTGGCTCAG-3′; Univ1492R – Reverse, seq: 5′-GGTTACCTTGTTACGACTT-3′) and 12 μL of sterile water and 5 μL of each sample. Reaction conditions used were: 1 initial cycle (93°C for 2 min), 30 amplification cycles (92°C for 30 s, 55°C for 30 s, and 72°C for 1 min), and a final extension cycle of 5 min at 72°C. PCR products were then purified, sequenced and submitted to BLAST and EzBioCloud [25] for the phylogenetic affiliation.

4.5 Bacterial Cultivation and Extraction

Single colonies of selected bacteria were used to inoculate 3 mL of liquid MB mod medium in sterile bacteriological tubes. After 48 h of incubation at 28 °C at 180 rpm, the preinoculum was used to inoculate 250 mL of MBmod medium in a 1 L flasks, at cell concentration of 0.05 OD_{600}/mL. The flasks were incubated at 28 °C with 150 rpm constant shaking for 4 days and 9 days (for the slow-growing strains). Then the cultures were centrifuged at 7500 rpm at 4 °C for 20 min, and the obtained exhausted broth were extracted with two volumes of EtOAc, while the intracellular material extracted by incubating the pellet with 3 volumes of MeOH for 3 hours in agitation. Successively, both organic phases were collected and evaporated with a rotary evaporator (Buchi R-100, Büchi Labortechnik AG, Postfach, Switzerland) to obtain crude extracts. Finally, all the extracts were weighted and dissolved in DMSO to achieve 50 mg/mL and stored at - 20°C to be tested for bioactivities.

4.6 Functional Screening of All Extracts from the Isolated Strains

To assess the bioactivity of all the extracts obtained from the isolated strains, antimicrobial, antioxidant and anti-UV assays were performed.

4.6.1 Antimicrobial Assay

The antimicrobial activities were assessed on a panel of both human and fish/coral pathogens including *Staphylococcus aureus* ATCC 6538p™, methicillin-resistant *S. aureus* (MRSA), quinolone-resistant *S. aureus* (QRSA), vancomycin-resistant *S. aureus* (VRSA), *Vibrio anguillarum* ATCC 19264™, *Photobacterium damselae* subsp. *Piscicida* ATCC 51736™, *Escherichia coli* ATCC 10536™, macrolide-resistant *S. aureus* (MRSA), *Listeria monocytogenes* MB 677, *Pseudomonas aeruginosa* PAO1 and *Candida albicans* ATCC 76485™. Each strain was plated on MB or LB agar plates and incubated overnight, at 28°C or 37 °C, depending on cultivation requirements. Then, 2-3 fresh colonies were transferred in 3 mL of

medium (MB, LB, TSB or YPD) and incubated in agitation overnight, at 28 °C or 37 °C. Finally, a bacterial concentration of about 5×10^5 CFU/mL was used for the liquid inhibition assay [26]. To evaluate the antimicrobial potential of the coral extracts, samples were placed into each well of a 96-well microtiter plate at an initial concentration of 0.5 mg/mL and serially diluted using the respective medium. Wells containing no compound represented the negative control. DMSO was used as positive control to determine the effect of solvent on cell growth. Briefly, 8 μL of each sample was dispensed into 200 μL of appropriate medium in a microtiter plate, and twofold serially diluted. Then 100 μL of bacterial suspension were inoculated into the broth (~5×10^4 CFU/well) and incubated statically for 18h-24h, at 28°C or 37 °C and growth was measured with a Cytation3 Plate Reader (Biotek, Winoosky, VT, USA) by monitoring the absorbance at 600 nm.

4.6.2. Antioxidant Assay

DPPH Assay

The capacity to scavenge the stable radical DPPH (Diphenyl-1-picrydrazyl) of all the extracts produced was assessed [27]. The extracts were dissolved in MeOH at an initial concentration of 50 mg/mL, and 4 μL of each extract were put in the first well, while the other wells were filled with 100 μL of the same solvent. Then, a 2-fold serial dilution starting from the first well was performed for all the extracts. Finally, the final volume of 200 μL was reached by adding 100 μL of a 0.2 mM methanolic solution of DPPH to all the wells. Ascorbic acid (AA) and MeOH were used respectively as positive and negative controls.

ABTS Assay

The scavenging activity of the ABTS radical was determined according the method provided by Ahn [28]. Briefly, an ABTS stock solution (7 mM ABTS, in water) was mixed with 2.45 mM $K_2S_2O_8$ (final concentration) and incubate in a dark room for 16–18 h at room temperature, allowing ABTS radical cation

generation. Then, the ABTS was mixed with ddH_2O to create the working solution with an absorbance about 0.7 ± 0.05 at 734 nm. 4 μL (25 mg/ml) of each sample were added in 196 μL of ABTS working solution, mixed and hold in the dark at 25–27 ◦C for 7 min; the absorbance was read at 734 nm. 96-well microplates were used for test.

The scavenging activity was expressed using Equation:

Scavenging activity (%) = [(Ab control − Ab sample)/Ab control] × 100

where Ab control is the absorbance of the ABTS solution; Ab sample is the absorbance of the sample mixed with ABTS. Trolox was used as positive control.

4.6.3. UV Screen in Vitro Assay

The immortalized human epidermal keratinocyte cell line (HaCaT, cat. n° SCCE020, Sigma-Aldrich) were cultured at 37 °C in a humidified atmosphere of 95% air, and 5% CO_2 in DMEM high glucose medium (ATCC, 30-2002 ™) supplemented with 10% Fetal Bovine Serum (FBS, ATCC, 30-2020 ™) and 1% penicillin/streptomycin (ATCC, 30-2300 ™). Cells were seeded at a density of 2x10^4 cells/well in 96-well plates and grown in completed DMEM medium for 24h. For each 96 wells plate, a maximum of 60 inner wells were seeded, to ensure each well to be fully irradiated [29]. Prior to UVC irradiation, cells were pre-treated with or without intracellular bacterial extracts (100 and 200 μg/mL), in PBS (Corning, cat. n° 21-040-CM) for 1h. Uvinul® MC 80 and Vanillin (100 μM) were used as positive control, due to their UV shielding proprieties. After the pre-treatment, the HaCaT cells were exposed to UVC radiation for 30 seconds. The UVC exposure was performed locating the 96-well plates, without the lid, inside the laminar flow hood, directly underneath and 55 cm of distance from the UVC lamp (germicidal lamp TUV T8 GL15, PHILIPS) [29]. After UVC exposure, the intracellular bacterial extracts in PBS were removed and replaced with fresh DMEM supplemented with the same extracts. After 24h from the UVC exposure, the cell viability (MTT assay, cat. n° 475989, Sigma-Aldrich) was assessed to

define the shielding and/or repairing effects of intracellular extracts on the UVC-irradiated HaCaT cells. More in detail, 10μL of MTT (5 mg/ml) was added to each well. After 3h of incubation at 37 °C, the well's content was removed, and the isopropanol was added to dissolve formazan crystals. Absorbance was measured by a microplate reader (Biotek Synergy HT Multi-Mode Microplate Reader) at 570 nm. Cell viability was expressed as a percentage of cell viability calculated as the ratio between the mean absorbance of each sample and the mean absorbance of the control.

4.7. Whole Genome Sequencing and Annotation

Genomic DNA (1 μg) from the strains *Pseudoalteromonas sp. 39*, *Streptomyces sp. 79*, and *Microbacterium sp. 92* was sequenced using the Illumina NovaSeq 6000 platform by Eurofins Genomics (Ebersberg, Germany), to obtain the whole genome sequence. Sequenced paired-end reads were processed with Trimmomatic tool [30] for adapter removal and quality trimming, followed by validation with FastQC [31]. The de novo genome assemblies and scaffolding were conducted with MEGAhit algorithm [32] and SPAdes [33], guided by closely related reference genomes (*P. flavipulchra* (GenBank: GCA_000259115.1), *S. parvus* (GenBank: GCA_008632535.1), *Microbacterium plantarum (GenBank:* GCA_028737425.1*),* to direct the arrangement and alignment of contigs. The whole genome sequencing of *Salinispora* sp. 93 is still ongoing. The tool ANI Calculator by EzBioCloud was used for the assembled genome identification [34] while the Type (strain) Genome Server (https://tygs.dsmz.de) was employed for the digital DNA:DNA hybridization (dDDH) . The obtained genome was automatically annotated using both RASTtk (v1.073) [35] through the KBase platform [32]. Subsequently the genome mining tool anti-SMASH 7.0 web server (http://antismash.secondarymetabolites.org) was applied to identify and annotate the biosynthetic gene clusters (BGCs) of the whole genome.

5. Conclusion

This study shows the taxonomic, genomic, and functional diversity of coral-associated microorganisms and their critical roles in coral health and resilience. In the context of assisted evolution, leveraging beneficial CAMs for coral restoration involves enhancing these bacterial functions through targeted microbiome manipulation. By promoting microbial communities that confer stress tolerance, it is possible to improve coral's overall resilience to climate change. Genetic selection and microbial inoculation may offer promising strategies to accelerate coral adaptation, ensuring their survival and continued ecological function in increasingly hostile ocean environments. The identification of novel species such as *Pseudoalteromonas* sp. 39 and *Microbacterium* sp. 92, and other relevant strains such as *Streptomyces* sp. 79 and *Salinispora* sp. 93, alongside the characterization of their biotechnological potential, provide a strong foundation to continue working on these strains to uncover their full potential. By addressing oxidative stress, nutrient imbalances, and pathogen defence, these bacteria represent promising tools for microbiome-based coral restoration strategies. Further exploration of coral microbiomes across diverse environmental conditions and experimental validation of these bacterial functions will enhance our understanding of host-microbe interactions under climate change scenarios. Future challenges include the identification and the application of the right stimuli to CAMs to support coral restoration along with the valorisation of microbial-derived natural products for pharmaceutical applications.

Supplementary

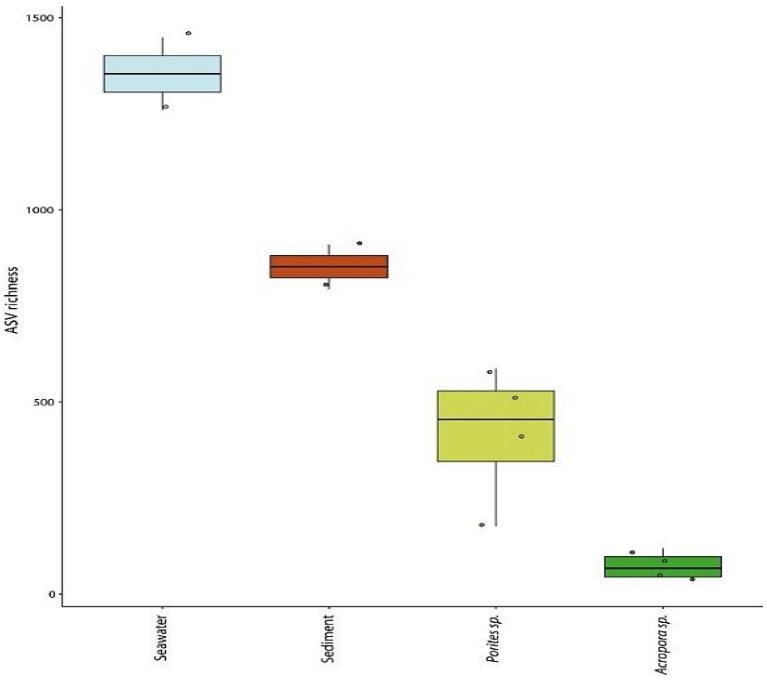

Figure S1. Boxplots showing the number of ASVs identified per sample type.

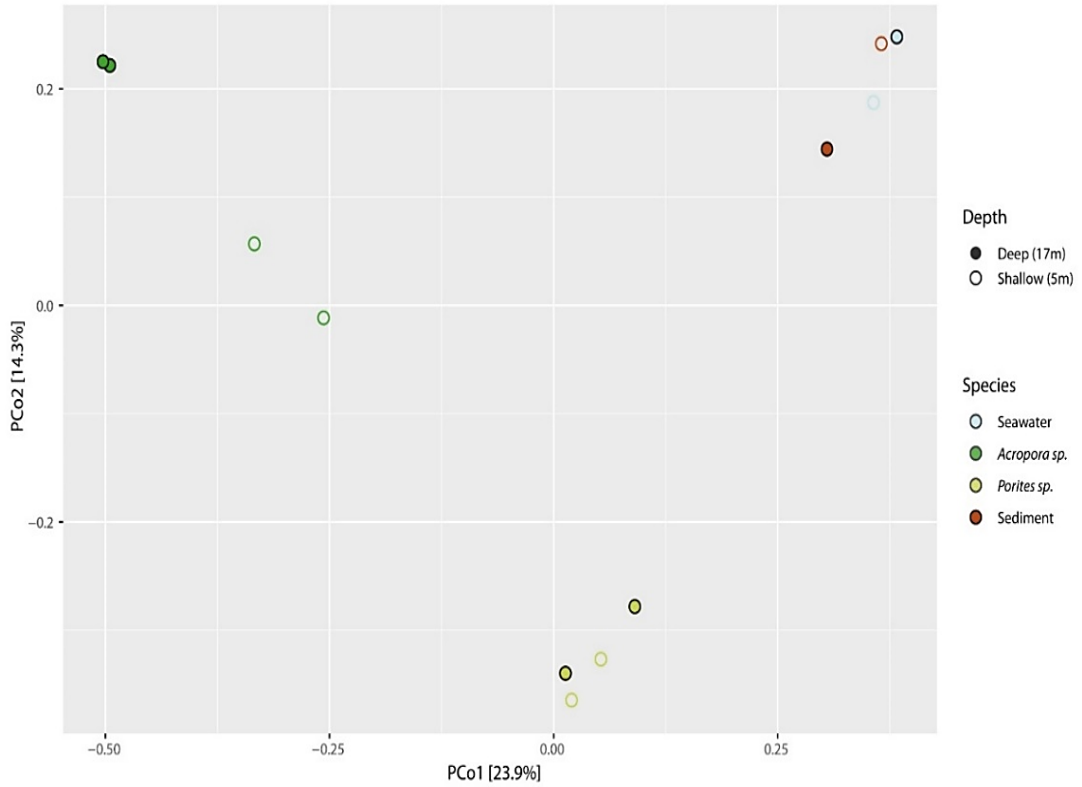

Figure S2. Full dots represent deep samples, while empty ones the shallow samples (Depth legend). The four matrices were represented with different colour (species legend).

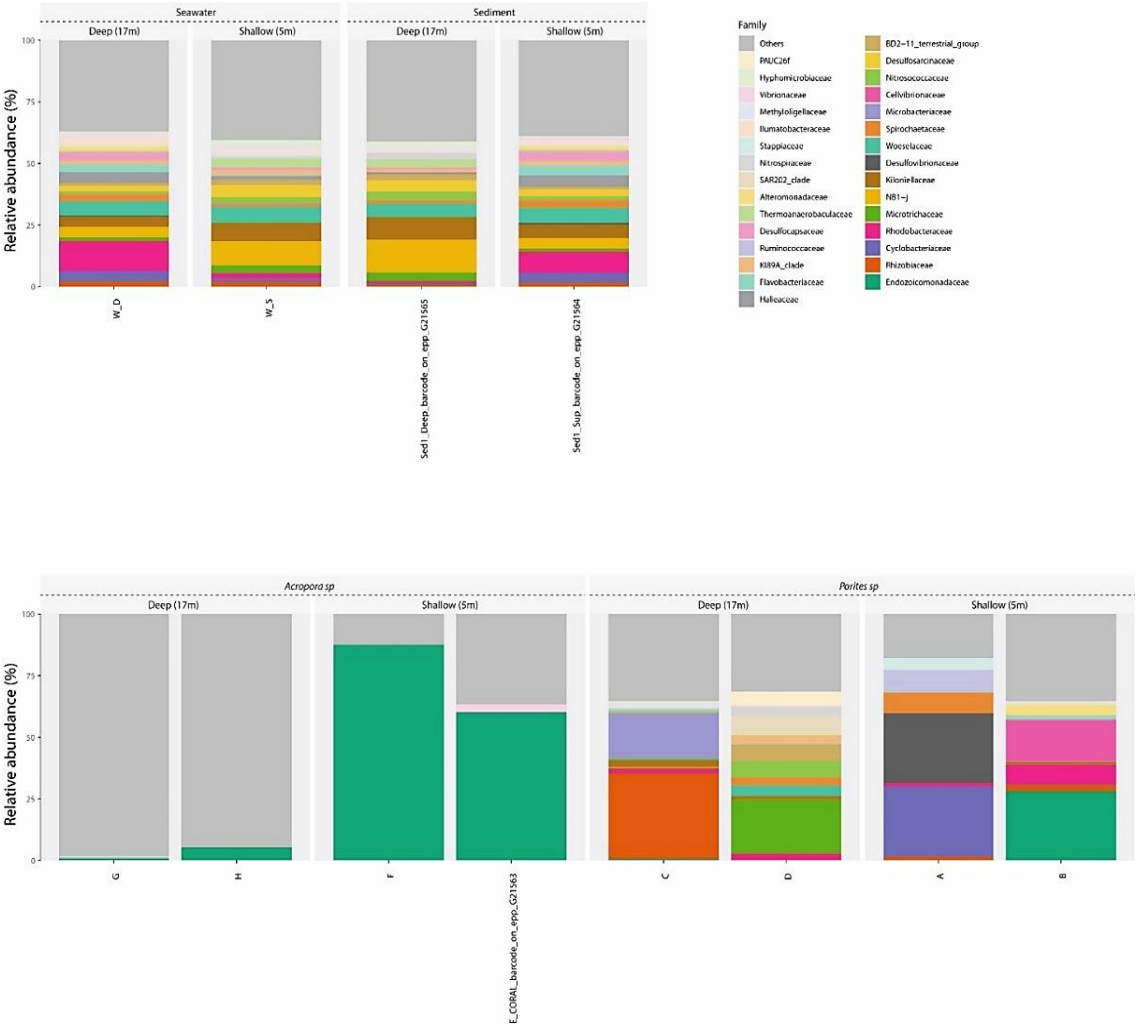

Figure S3. Barplot showing the composition of prokaryotic assemblages associated with each sample. For the two coral species, the barplots (A-C-E-G) refer to large size, while the barplots (B-D-F-H) refer to small size.

	Strain	contig_id	feature_id	start	stop	strand	function
Glutathione:_biosynthesis	39	Scaffold_10	fig|666666.13	296315	296758	+	Hypothetical flavoprotein YqcA (clustered with tRNA pseudouridine synthase C)
	39	Scaffold_10	fig|666666.13	334440	336017	+	Glutamate--cysteine ligase (EC 6.3.2.2)
	39	Scaffold_14	fig|666666.13	495623	493881	-	Gamma-glutamyltranspeptidase (EC 2.3.2.2) @ Glutathione hydrolase (EC 3.4.19.13)
	39	Scaffold_4	fig|666666.13	22891	21131	-	Gamma-glutamyltranspeptidase (EC 2.3.2.2) @ Glutathione hydrolase (EC 3.4.19.13)
	39	Scaffold_8	fig|666666.13	286662	287621	+	Glutathione synthetase (EC 6.3.2.3)
	39	Scaffold_8	fig|666666.13	608774	607080	-	Gamma-glutamyltranspeptidase (EC 2.3.2.2) @ Glutathione hydrolase (EC 3.4.19.13)
	79	Scaffold_11	fig|1883.4678.	52288	50792	-	hypothetical protein
	79	Scaffold_14	fig|1883.4678.	1566	817	-	Regulatory protein RecX
	79	Scaffold_7	fig|1883.4678.	163792	162476	-	Glutamate--cysteine ligase (EC 6.3.2.2)
	79	Scaffold_8	fig|1883.4678.	521170	519353	-	Gamma-glutamyltranspeptidase (EC 2.3.2.2) @ Glutathione hydrolase (EC 3.4.19.13)
	92	Scaffold_1	fig|3882.357.	730143	731132	+	Integral membrane protein
	92	Scaffold_1	fig|3882.357.	1237732	1239519	+	Gamma-glutamyltranspeptidase (EC 2.3.2.2) @ Glutathione hydrolase (EC 3.4.19.13)
	92	Scaffold_2	fig|3882.357.	757206	758054	+	Oxidoreductase
glutamate--cysteine (gshA)	39	Scaffold_10	fig|666666.13	334440	336017	+	Glutamate--cysteine ligase (EC 6.3.2.2)
	79	Scaffold_7	fig|1883.4678.	163792	162476	-	Glutamate--cysteine ligase (EC 6.3.2.2)
gamma-glutamyl_cycle	39	Scaffold_10	fig|666666.13	296315	296758	+	Hypothetical flavoprotein YqcA (clustered with tRNA pseudouridine synthase C)
	39	Scaffold_10	i666.1395253.1	336134	336742	+	putative lipoprotein
	39	Scaffold_14	fig|666666.13	495623	493881	-	Gamma-glutamyltranspeptidase (EC 2.3.2.2) @ Glutathione hydrolase (EC 3.4.19.13)
	39	Scaffold_4	fig|666666.13	22891	21131	-	Gamma-glutamyltranspeptidase (EC 2.3.2.2) @ Glutathione hydrolase (EC 3.4.19.13)
	39	Scaffold_8	fig|666666.13	286662	287621	+	Glutathione synthetase (EC 6.3.2.3)
	39	Scaffold_8	fig|666666.13	608774	607080	-	Gamma-glutamyltranspeptidase (EC 2.3.2.2) @ Glutathione hydrolase (EC 3.4.19.13)
	79	Scaffold_11	fig|1883.4678.	52288	50792	-	hypothetical protein
	79	Scaffold_14	fig|1883.4678.	1566	817	-	Regulatory protein RecX
	79	Scaffold_7	fig|1883.4678.	163792	162476	-	Glutamate--cysteine ligase (EC 6.3.2.2)
	79	Scaffold_8	fig|1883.4678.	521170	519353	-	Gamma-glutamyltranspeptidase (EC 2.3.2.2) @ Glutathione hydrolase (EC 3.4.19.13)
	92	Scaffold_1	fig|3882.357.	730143	731132	+	Integral membrane protein
	92	Scaffold_1	fig|3882.357.	1237732	1239519	+	Gamma-glutamyltranspeptidase (EC 2.3.2.2) @ Glutathione hydrolase (EC 3.4.19.13)
	92	Scaffold_2	fig|3882.357.	757206	758054	+	Oxidoreductase
Carotene	39	Scaffold_10	fig|666666.13	189321	188473	-	Fatty acid hydroxylase family (carotene hydroxylase/sterol desaturase)
	79	Scaffold_11	fig|1883.4678.	262245	263762	+	Beta-carotene ketolase
	79	Scaffold_17	fig|1883.4678.	1367166	1368101	+	Fatty acid hydroxylase family (carotene hydroxylase/sterol desaturase)
	79	Scaffold_8	fig|1883.4678.	58259	57318	-	Fatty acid hydroxylase family (carotene hydroxylase/sterol desaturase)
b-carotene	79	Scaffold_11	fig|1883.4678.	262245	263762	+	Beta-carotene ketolase
	92	Scaffold_2	fig|3882.357.	550100	551683	+	PTS system, mannitol-specific IIC component / PTS system, mannitol-specific IIB component (EC 2.7.1.197)
	92	Scaffold_2	fig|3882.357.	551770	552207	+	PTS system, mannitol-specific IIA component (EC 2.7.1.197)
	92	Scaffold_2	fig|3882.357.	552204	553370	+	Mannitol-1-phosphate 5-dehydrogenase (EC 1.1.1.17)
Peroxynitrite Reduction (ahpC)	39	Scaffold_7	fig|666666.13	107589	108047	+	AhpC/TSA family protein
	40	Scaffold_7	fig|662.1993.p	696772	696299	-	Antioxidant, AhpC/Tsa family
Nitric oxide reductase	39	Scaffold_11	fig|666666.13	170944	170798	-	Anaerobic nitric oxide reductase transcription regulator NorR
	39	Scaffold_12	fig|666666.13	83656	82094	-	Anaerobic nitric oxide reductase transcription regulator NorR
	79	Scaffold_12	fig|1883.4678.	29818	30666	+	Anaerobic nitric oxide reductase transcription regulator NorR
	92	Scaffold_1	fig|3882.357.	1047151	1046801	-	Anaerobic nitric oxide reductase transcription regulator NorR
Lipoic_acid_metabolism	39	Scaffold_8	fig|666666.13	108169	108447	+	Proposed lipoate regulatory protein YbeD
	79	Scaffold_8	fig|1883.4678.	492352	493416	+	Lipoate-protein ligase A
	92	Scaffold_2	fig|3882.357.	727368	726319	-	Lipoate-protein ligase A
catalase-peroxidase (KatG)	39	Scaffold_12	fig|666666.13	164185	166374	+	Catalase-peroxidase KatG (EC 1.11.1.21)
	39	Scaffold_5	fig|666666.13	102621	104843	+	Catalase-peroxidase KatG (EC 1.11.1.21)
	79	Scaffold_5	fig|1883.4678.	59143	56888	-	Catalase-peroxidase KatG (EC 1.11.1.21)
	92	Scaffold_2	fig|3882.357.	489199	486857	-	Catalase-peroxidase KatG (EC 1.11.1.21)
Catalase (KatE)	39	Scaffold_10	fig|666666.13	157531	158538	+	Catalase KatE (EC 1.11.1.6)
	39	Scaffold_9	fig|666666.13	65808	67250	+	Catalase KatE (EC 1.11.1.6)
	79	Scaffold_13	fig|1883.4678.	39539	40996	+	Catalase KatE (EC 1.11.1.6)
	79	Scaffold_14	fig|1883.4678.	249089	247566	-	Catalase KatE (EC 1.11.1.6)
	79	Scaffold_14	fig|1883.4678.	729420	727969	-	Catalase KatE (EC 1.11.1.6)
	92	Scaffold_2	fig|3882.357.	243700	245355	+	Catalase KatE (EC 1.11.1.6)
Superoxide Dismutase (SOD)	39	Scaffold_12	fig|666666.13	101291	100680	-	Superoxide dismutase [Mn] (EC 1.15.1.1)
	39	Scaffold_14	fig|666666.13	141962	142543	+	Superoxide dismutase [Fe] (EC 1.15.1.1)
	79	Scaffold_14	fig|1883.4678.	644563	644958	+	Nickel-dependent superoxide dismutase (EC 1.15.1.1)
	79	Scaffold_17	fig|1883.4678.	432530	431889	-	Superoxide dismutase [Fe-Zn] (EC 1.15.1.1)
	92	Scaffold_1	fig|3882.357.	683570	684190	+	Superoxide dismutase [Mn/Fe] (EC 1.15.1.1)
Denitrification	39	Scaffold_12	fig|666666.13	84042	85259	+	NnrS protein involved in response to NO
Nitrosative_stress	39	Scaffold_12	fig|666666.13	83656	82094	-	Anaerobic nitric oxide reductase transcription regulator NorR
	39	Scaffold_12	fig|666666.13	84042	85259	+	NnrS protein involved in response to NO
	79	Scaffold_14	fig|1883.4678.	669721	670167	+	Nitrite-sensitive transcriptional repressor NsrR

Table S1. Description of the function of oxidative and nitrogen stress-related genes (ROS and RNS) present in the sp. 39, sp. 79 and sp. 92 genomes by RAST annotation.

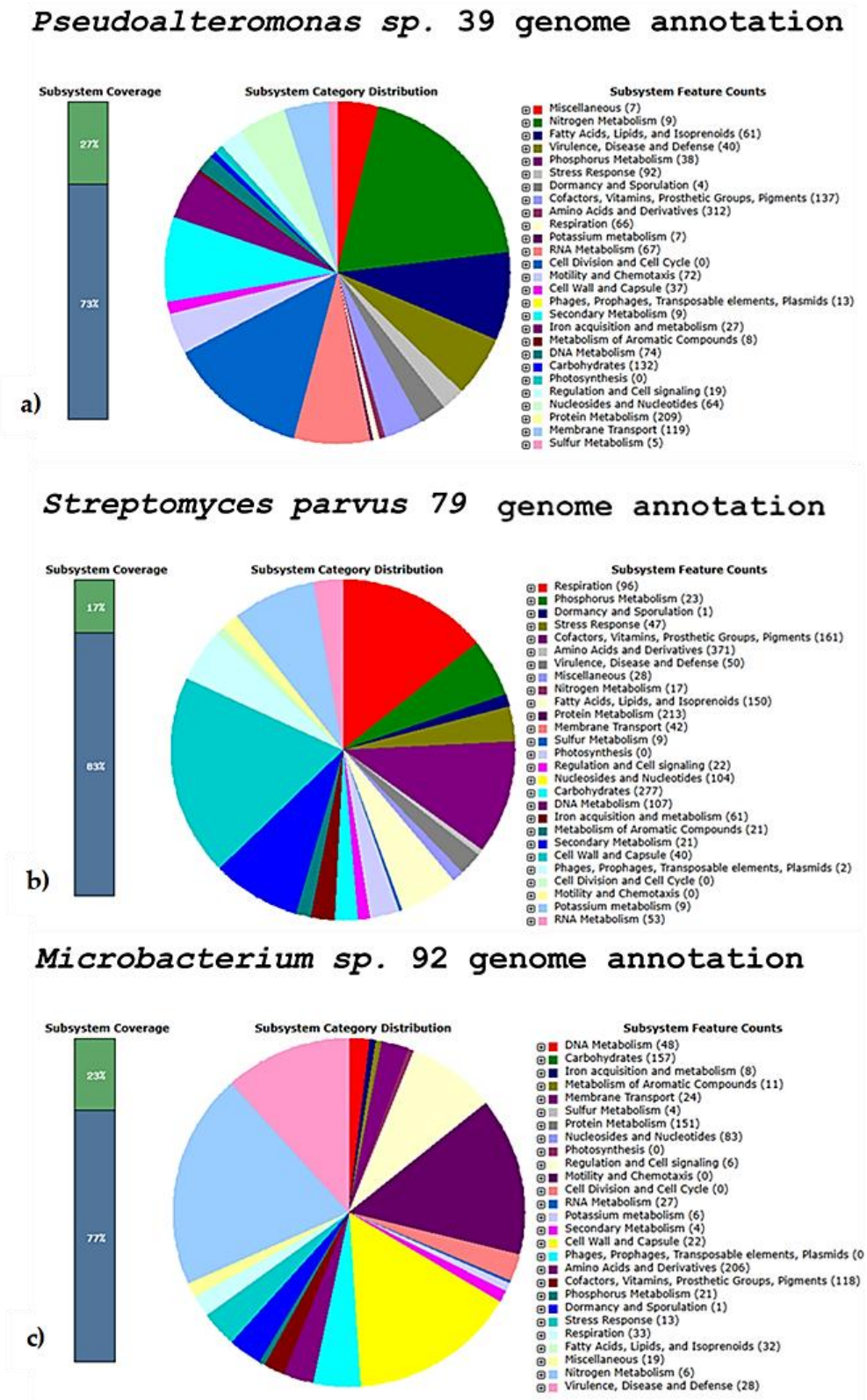

Figure S4. Overview of functional categories assigned to predicted genes from sp. 39, sp. 79, sp. 92 genomes, annotated using RAST. The number of genes assigned to each category is indicated.

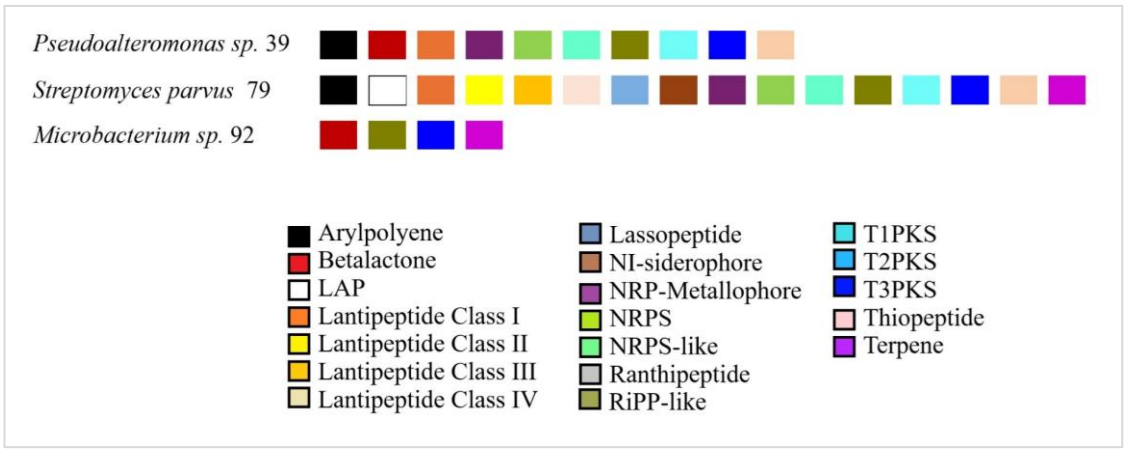

Figure S5. Graphical visualisation of the BCGs present in the strains sp.39, sp.79, sp.92 obtained from antiSMASH analysis.

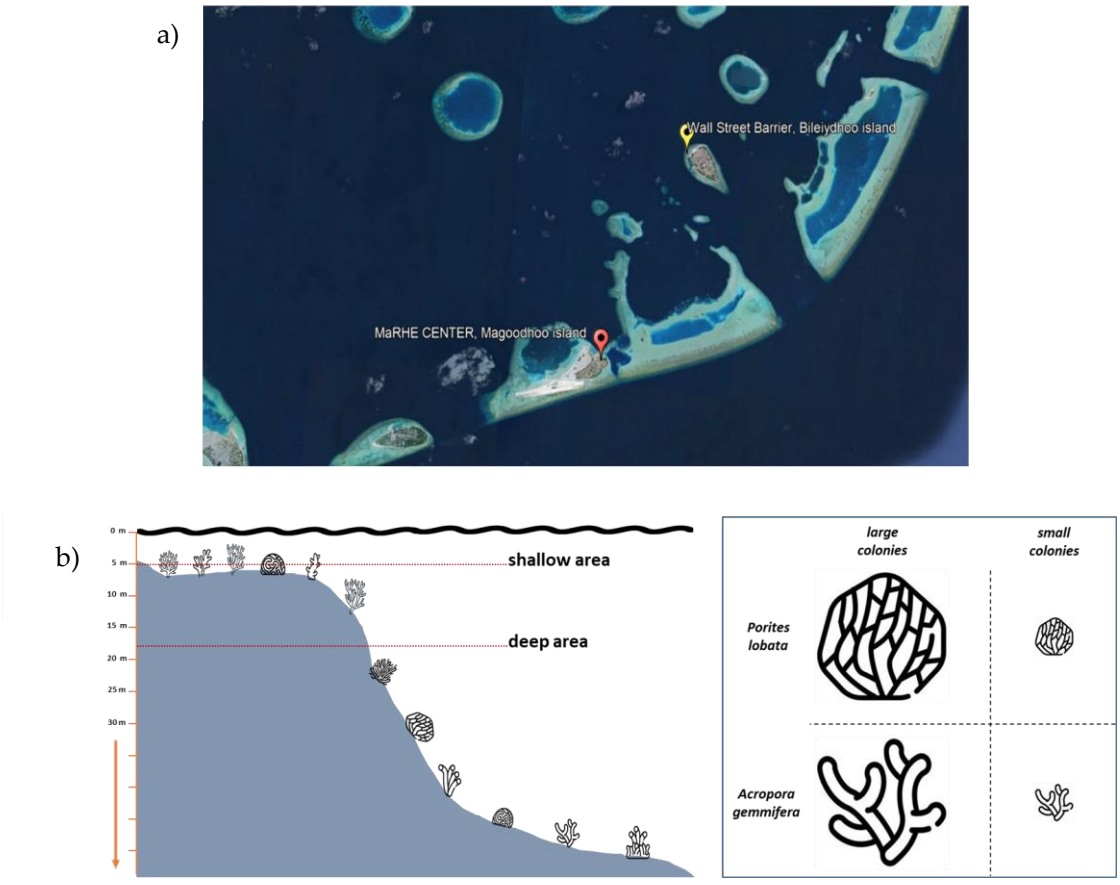

Figure S6. A) Southeast side of Faafu Atoll; Red marker indicates MaRHE center, while yellow marker is on wall street barrier (the sampling site). B) sampling design. Two sampling areas were identified at 5 and 17 m depth. In these areas small (< 10 cm) and large colonies (> 30 cm) of Porites lobata and Acropora gemmifera were collected in biological triplicate.

References

1. Sobha, T.R.; Vibija, C.P.; Fahima, P. Coral Reef: A Hot Spot of Marine Biodiversity. In Conservation and Sustainable Utilization of Bioresources; Sukumaran, S.T., T R, K., Eds.; Springer Nature: Singapore, 2023; pp. 171–194 ISBN 978-981-19584-1-0.
2. Hoegh-Guldberg, O.; Poloczanska, E.S.; Skirving, W.; Dove, S. Coral Reef Ecosystems under Climate Change and Ocean Acidification. Front. Mar. Sci. 2017, 4, doi:10.3389/fmars.2017.00158.
3. Hodapp, D.; Roca, I.T.; Fiorentino, D.; Garilao, C.; Kaschner, K.; Kesner-Reyes, K.; Schneider, B.; Segschneider, J.; Kocsis, Á.T.; Kiessling, W.; et al. Climate Change Disrupts Core Habitats of Marine Species. Glob. Change Biol. 2023, 29, 3304–3317, doi:10.1111/gcb.16612.
4. Trégarot, E.; D'Olivo, J.P.; Botelho, A.Z.; Cabrito, A.; Cardoso, G.O.; Casal, G.; Cornet, C.C.; Cragg, S.M.; Degia, A.K.; Fredriksen, S.; et al. Effects of Climate Change on Marine Coastal Ecosystems – A Review to Guide Research and Management. Biol. Conserv. 2024, 289, 110394, doi:10.1016/j.biocon.2023.110394.
5. Vanwonterghem, I.; Webster, N.S. Coral Reef Microorganisms in a Changing Climate. iScience 2020, 23, 100972, doi:10.1016/j.isci.2020.100972.
6. Webster, N.S.; Reusch, T.B.H. Microbial Contributions to the Persistence of Coral Reefs. ISME J. 2017, 11, 2167–2174, doi:10.1038/ismej.2017.66.
7. Peixoto, R.S.; Rosado, P.M.; Leite, D.C. de A.; Rosado, A.S.; Bourne, D.G. Beneficial Microorganisms for Corals (BMC): Proposed Mechanisms for Coral Health and Resilience. Front. Microbiol. 2017, 8, doi:10.3389/fmicb.2017.00341.
8. Silveira, C.B.; Cavalcanti, G.S.; Walter, J.M.; Silva-Lima, A.W.; Dinsdale, E.A.; Bourne, D.G.; Thompson, C.C.; Thompson, F.L. Microbial Processes Driving Coral Reef Organic Carbon Flow. FEMS Microbiol. Rev. 2017, 41, 575–595, doi:10.1093/femsre/fux018.
9. van de Water, J.A.; Tignat-Perrier, R.; Allemand, D.; Ferrier-Pagès, C. Coral Holobionts and Biotechnology: From Blue Economy to Coral Reef Conservation. Curr. Opin. Biotechnol. 2022, 74, 110–121, doi:10.1016/j.copbio.2021.10.013.
10. Mohamed, A.R.; Ochsenkühn, M.A.; Kazlak, A.M.; Moustafa, A.; Amin, S.A. The Coral Microbiome: Towards an Understanding of the Molecular Mechanisms of Coral–Microbiota Interactions. FEMS Microbiol. Rev. 2023, 47, fuad005, doi:10.1093/femsre/fuad005.
11. Hou, X.-M.; Hai, Y.; Gu, Y.-C.; Wang, C.-Y.; Shao, C.-L. Chemical and Bioactive Marine Natural Products of Coral-Derived Microorganisms (2015-2017). Curr. Med. Chem. 2019, 26, 6930–6941, doi:10.2174/0929867326666190626153819.
12. Weis, V.M. Cellular Mechanisms of Cnidarian Bleaching: Stress Causes the Collapse of Symbiosis. J. Exp. Biol. 2008, 211, 3059–3066, doi:10.1242/jeb.009597.
13. Szabó, M.; Larkum, A.W.D.; Vass, I. A Review: The Role of Reactive Oxygen Species in Mass Coral Bleaching. In Photosynthesis in Algae: Biochemical and Physiological Mechanisms; Larkum, A.W.D., Grossman, A.R., Raven, J.A., Eds.; Springer International Publishing: Cham, 2020; pp. 459–488 ISBN 978-3-030-33397-3.
14. Lesser, M.P. Oxidative Stress in Marine Environments: Biochemistry and Physiological Ecology. Annu. Rev. Physiol. 2006, 68, 253–278, doi:10.1146/annurev.physiol.68.040104.110001.
15. Perez, S.; Weis, V. Nitric Oxide and Cnidarian Bleaching: An Eviction Notice Mediates Breakdown of a Symbiosis. J. Exp. Biol. 2006, 209, 2804–2810, doi:10.1242/jeb.02309.
16. Rosado, P.M.; Leite, D.C.A.; Duarte, G.A.S.; Chaloub, R.M.; Jospin, G.; Nunes da Rocha, U.; P. Saraiva, J.; Dini-Andreote, F.; Eisen, J.A.; Bourne, D.G.; et al. Marine Probiotics: Increasing Coral Resistance to Bleaching through Microbiome Manipulation. ISME J. 2019, 13, 921–936, doi:10.1038/s41396-018-0323-6.
17. Santoro, E.P.; Borges, R.M.; Espinoza, J.L.; Freire, M.; Messias, C.S.M.A.; Villela, H.D.M.; Pereira, L.M.; Vilela, C.L.S.; Rosado, J.G.; Cardoso, P.M.; et al. Coral Microbiome Manipulation Elicits Metabolic and Genetic Restructuring to Mitigate Heat Stress and Evade Mortality. Sci. Adv. 2021, 7, eabg3088, doi:10.1126/sciadv.abg3088.
18. Hall, M.; Beiko, R.G. 16S rRNA Gene Analysis with QIIME2. Methods Mol. Biol. Clifton NJ 2018, 1849, 113–129, doi:10.1007/978-1-4939-8728-3_8.
19. Martin, M. Cutadapt Removes Adapter Sequences from High-Throughput Sequencing Reads. EMBnet.journal 2011, 17, 10–12, doi:10.14806/ej.17.1.200.

20. Callahan, B.J.; McMurdie, P.J.; Rosen, M.J.; Han, A.W.; Johnson, A.J.A.; Holmes, S.P. DADA2: High-Resolution Sample Inference from Illumina Amplicon Data. Nat. Methods 2016, 13, 581–583, doi:10.1038/nmeth.3869.
21. Quast, C.; Pruesse, E.; Yilmaz, P.; Gerken, J.; Schweer, T.; Yarza, P.; Peplies, J.; Glöckner, F.O. The SILVA Ribosomal RNA Gene Database Project: Improved Data Processing and Web-Based Tools. Nucleic Acids Res. 2013, 41, D590-596, doi:10.1093/nar/gks1219.
22. Rognes, T.; Flouri, T.; Nichols, B.; Quince, C.; Mahé, F. VSEARCH: A Versatile Open Source Tool for Metagenomics. PeerJ 2016, 4, e2584, doi:10.7717/peerj.2584.
23. Edgar, R.C. Accuracy of Taxonomy Prediction for 16S rRNA and Fungal ITS Sequences. PeerJ 2018, 6, e4652, doi:10.7717/peerj.4652.
24. Liu, C.; Cui, Y.; Li, X.; Yao, M. Microeco: An R Package for Data Mining in Microbial Community Ecology. FEMS Microbiol. Ecol. 2021, 97, fiaa255, doi:10.1093/femsec/fiaa255.
25. Chalita, M.; Kim, Y.O.; Park, S.; Oh, H.-S.; Cho, J.H.; Moon, J.; Baek, N.; Moon, C.; Lee, K.; Yang, J.; et al. EzBioCloud: A Genome-Driven Database and Platform for Microbiome Identification and Discovery. Int. J. Syst. Evol. Microbiol. 2024, 74, 006421, doi:10.1099/ijsem.0.006421.
26. Kowalska-Krochmal, B.; Dudek-Wicher, R. The Minimum Inhibitory Concentration of Antibiotics: Methods, Interpretation, Clinical Relevance. Pathogens 2021, 10, 165, doi:10.3390/pathogens10020165.
27. Ebada, S.S.; Edrada, R.A.; Lin, W.; Proksch, P. Methods for Isolation, Purification and Structural Elucidation of Bioactive Secondary Metabolites from Marine Invertebrates. Nat. Protoc. 2008, 3, 1820–1831, doi:10.1038/nprot.2008.182.
28. Ahn, M.-R.; Kumazawa, S.; Hamasaka, T.; Bang, K.-S.; Nakayama, T. Antioxidant Activity and Constituents of Propolis Collected in Various Areas of Korea. J. Agric. Food Chem. 2004, 52, 7286–7292, doi:10.1021/jf048726s.
29. Shindo, A.; Kusano, M.; Sakagami, H.; Amano, S.; Inomata, M.; Abe, M.; Okazawa, M.; Ooka, T. Comparison of UVC Sensitivity and Dectin-2 Expression Between Malignant and Non-Malignant Cells. In Vivo 2022, 36, 2116–2125, doi:10.21873/invivo.12937.
30. Bolger, A.M.; Lohse, M.; Usadel, B. Trimmomatic: A Flexible Trimmer for Illumina Sequence Data. Bioinforma. Oxf. Engl. 2014, 30, 2114–2120, doi:10.1093/bioinformatics/btu170.
31. Babraham Bioinformatics - FastQC A Quality Control Tool for High Throughput Sequence Data Available online: https://www.bioinformatics.babraham.ac.uk/projects/fastqc/ (accessed on 11 July 2024).
32. Arkin, A.P.; Cottingham, R.W.; Henry, C.S.; Harris, N.L.; Stevens, R.L.; Maslov, S.; Dehal, P.; Ware, D.; Perez, F.; Canon, S.; et al. KBase: The United States Department of Energy Systems Biology Knowledgebase. Nat. Biotechnol. 2018, 36, 566–569, doi:10.1038/nbt.4163.
33. Bankevich, A.; Nurk, S.; Antipov, D.; Gurevich, A.A.; Dvorkin, M.; Kulikov, A.S.; Lesin, V.M.; Nikolenko, S.I.; Pham, S.; Prjibelski, A.D.; et al. SPAdes: A New Genome Assembly Algorithm and Its Applications to Single-Cell Sequencing. J. Comput. Biol. 2012, 19, 455–477, doi:10.1089/cmb.2012.0021.
34. Yoon, S.-H.; Ha, S.-M.; Kwon, S.; Lim, J.; Kim, Y.; Seo, H.; Chun, J. Introducing EzBioCloud: A Taxonomically United Database of 16S rRNA Gene Sequences and Whole-Genome Assemblies. Int. J. Syst. Evol. Microbiol. 2017, 67, 1613–1617, doi:10.1099/ijsem.0.001755.
35. Overbeek, R.; Olson, R.; Pusch, G.D.; Olsen, G.J.; Davis, J.J.; Disz, T.; Edwards, R.A.; Gerdes, S.; Parrello, B.; Shukla, M.; et al. The SEED and the Rapid Annotation of Microbial Genomes Using Subsystems Technology (RAST). Nucleic Acids Res. 2014, 42, D206–D214, doi:10.1093/nar/gkt1226.
36. Hochart, C.; Paoli, L.; Ruscheweyh, H.-J.; Salazar, G.; Boissin, E.; Romac, S.; Poulain, J.; Bourdin, G.; Iwankow, G.; Moulin, C.; et al. Ecology of Endozoicomonadaceae in Three Coral Genera across the Pacific Ocean. Nat. Commun. 2023, 14, 3037, doi:10.1038/s41467-023-38502-9.
37. Hernández-Zulueta, J.; Díaz-Pérez, L.; Echeverría-Vega, A.; Nava-Martínez, G.G.; García-Salgado, M.Á.; Rodríguez-Zaragoza, F.A. An Update of Knowledge of the Bacterial Assemblages Associated with the Mexican Caribbean Corals Acropora Palmata, Orbicella Faveolata, and Porites Porites. Diversity 2023, 15, 964, doi:10.3390/d15090964.
38. Lewis, K.; Epstein, S.; D'Onofrio, A.; Ling, L.L. Uncultured Microorganisms as a Source of Secondary Metabolites. J. Antibiot. (Tokyo) 2010, 63, 468–476, doi:10.1038/ja.2010.87.
39. Stewart, E.J. Growing Unculturable Bacteria. J. Bacteriol. 2012, 194, 4151–4160, doi:10.1128/jb.00345-12.

40. Schultz, J.; Modolon, F.; Rosado, A.S.; Voolstra, C.R.; Sweet, M.; Peixoto, R.S. Methods and Strategies to Uncover Coral-Associated Microbial Dark Matter. mSystems 2022, 7, e00367-22, doi:10.1128/msystems.00367-22.
41. Shnit-Orland, M.; Sivan, A.; Kushmaro, A. Antibacterial Activity of Pseudoalteromonas in the Coral Holobiont. Microb. Ecol. 2012, 64, 851–859, doi:10.1007/s00248-012-0086-y.
42. Ushijima, B.; Richards, G.P.; Watson, M.A.; Schubiger, C.B.; Häse, C.C. Factors Affecting Infection of Corals and Larval Oysters by Vibrio Coralliilyticus. PLOS ONE 2018, 13, e0199475, doi:10.1371/journal.pone.0199475.
43. Huang, D.; Licuanan, W.Y.; Baird, A.H.; Fukami, H. Cleaning up the "Bigmessidae": Molecular Phylogeny of Scleractinian Corals from Faviidae, Merulinidae, Pectiniidae and Trachyphylliidae. BMC Evol. Biol. 2011, 11, 37, doi:10.1186/1471-2148-11-37.
44. Ushijima, B.; Gunasekera, S.P.; Meyer, J.L.; Tittl, J.; Pitts, K.A.; Thompson, S.; Sneed, J.M.; Ding, Y.; Chen, M.; Jay Houk, L.; et al. Chemical and Genomic Characterization of a Potential Probiotic Treatment for Stony Coral Tissue Loss Disease. Commun. Biol. 2023, 6, 1–13, doi:10.1038/s42003-023-04590-y.
45. Varasteh, T.; Hamerski, L.; Tschoeke, D.; Lima, A.S.; Garcia, G.; Cosenza, C.A.N.; Thompson, C.; Thompson, F. Conserved Pigment Profiles in Phylogenetically Diverse Symbiotic Bacteria Associated with the Corals Montastraea Cavernosa and Mussismilia Braziliensis. Microb. Ecol. 2021, 81, 267–277, doi:10.1007/s00248-020-01551-4.
46. Kusmita, L.; Mutiara, E.V.; Nuryadi, H.; Pratama, P.A.; Wiguna, A.S.; Radjasa, O.K. Characterization of Carotenoid Pigments from Bacterial Symbionts of Soft-Coral Sarcophyton Sp. from North Java Sea. Int. Aquat. Res. 2017, 9, 61–69, doi:10.1007/s40071-017-0157-2.
47. Abdel-Razek, A.S.; El-Naggar, M.E.; Allam, A.; Morsy, O.M.; Othman, S.I. Microbial Natural Products in Drug Discovery. Processes 2020, 8, 470, doi:10.3390/pr8040470.
48. Alam, K.; Mazumder, A.; Sikdar, S.; Zhao, Y.-M.; Hao, J.; Song, C.; Wang, Y.; Sarkar, R.; Islam, S.; Zhang, Y.; et al. Streptomyces: The Biofactory of Secondary Metabolites. Front. Microbiol. 2022, 13, doi:10.3389/fmicb.2022.968053.
49. Mohamed, A.R.; Ochsenkühn, M.A.; Kazlak, A.M.; Moustafa, A.; Amin, S.A. The Coral Microbiome: Towards an Understanding of the Molecular Mechanisms of Coral–Microbiota Interactions. FEMS Microbiol. Rev. 2023, 47, fuad005, doi:10.1093/femsre/fuad005.
50. Mahmoud, H.M.; Kalendar, A.A. Coral-Associated Actinobacteria: Diversity, Abundance, and Biotechnological Potentials. Front. Microbiol. 2016, 7, doi:10.3389/fmicb.2016.00204.
51. Hughes, T.P.; Kerry, J.T.; Baird, A.H.; Connolly, S.R.; Dietzel, A.; Eakin, C.M.; Heron, S.F.; Hoey, A.S.; Hoogenboom, M.O.; Liu, G.; et al. Global Warming Transforms Coral Reef Assemblages. Nature 2018, 556, 492–496, doi:10.1038/s41586-018-0041-2.
52. van Keulen, G.; Dyson, P.J. Production of Specialized Metabolites by Streptomyces Coelicolor A3(2). Adv. Appl. Microbiol. 2014, 89, 217–266, doi:10.1016/B978-0-12-800259-9.00006-8.
53. Lee, S.D.; Yang, H.L.; Kim, I.S. Four New Microbacterium Species Isolated from Seaweeds and Reclassification of Five Microbacterium Species with a Proposal of Paramicrobacterium Gen. Nov. under a Genome-Based Framework of the Genus Microbacterium. Front. Microbiol. 2023, 14, 1299950, doi:10.3389/fmicb.2023.1299950.
54. Raina, J.-B.; Tapiolas, D.; Motti, C.A.; Foret, S.; Seemann, T.; Tebben, J.; Willis, B.L.; Bourne, D.G. Isolation of an Antimicrobial Compound Produced by Bacteria Associated with Reef-Building Corals. PeerJ 2016, 4, e2275, doi:10.7717/peerj.2275.
55. Meunier, F.; van der Heijden, G.M.F.; Schnitzer, S.A.; De Deurwaerder, H.P.T.; Verbeeck, H. Lianas Significantly Reduce Aboveground and Belowground Carbon Storage: A Virtual Removal Experiment. Front. For. Glob. Change 2021, 4, doi:10.3389/ffgc.2021.663291.
56. Feling, R.H.; Buchanan, G.O.; Mincer, T.J.; Kauffman, C.A.; Jensen, P.R.; Fenical, W. Salinosporamide A: A Highly Cytotoxic Proteasome Inhibitor from a Novel Microbial Source, a Marine Bacterium of the New Genus Salinospora. Angew. Chem. Int. Ed. 2003, 42, 355–357, doi:10.1002/anie.200390115.
57. Jensen, P.R.; Williams, P.G.; Oh, D.-C.; Zeigler, L.; Fenical, W. Species-Specific Secondary Metabolite Production in Marine Actinomycetes of the Genus Salinispora. Appl. Environ. Microbiol. 2007, 73, 1146–1152, doi:10.1128/AEM.01891-06.
58. Mincer, T.J.; Jensen, P.R.; Kauffman, C.A.; Fenical, W. Widespread and Persistent Populations of a Major New Marine Actinomycete Taxon in Ocean Sediments. Appl. Environ. Microbiol. 2002, 68, 5005–5011, doi:10.1128/AEM.68.10.5005-5011.2002.

La borsa di dottorato è stata cofinanziata con risorse del Programma Operativo Nazionale Ricerca e Innovazione 2014-2020, risorse FSE REACT-EU Azione IV.4 "Dottorati e contratti di ricerca su tematiche dell'innovazione" e Azione IV.5 "Dottorati su Tematiche Green"